Design, Synthesis and Characterisation of Porphyrin, Fullerene and Naphthalene Diimide Conjugates of Tröger's Base

Md. Imam Ansari

Master of Science Medicinal Chemistry- NIPER Mohali

This thesis is submitted in partial fulfilment of the requirements for the degree of

Doctor of Philosophy

Department of Molecular Sciences

Faculty of Science

MACQUARIE University

Sydney, Australia

December 2017

Preface

The work described herein was carried out in the Department of Molecular Sciences at Macquarie University between June 2014 – December 2017 under the supervision of Associate Professor Andrew Try and Professor Peter Karuso.

Sections of this Thesis were presented in following conferences:

Conference Presentations

- Poster presented at the Royal Australian Chemical Institute Organic Chemistry Group 38th annual one-day symposium, The University of Sydney, Sydney Nov 2017; Title: Synthesis of a rigid and V-shaped porphyrin-Tröger's base-C_{60} dyads

- Poster presented at the Royal Australian Chemical Institute Centenary Congress, Melbourne July 2017; Title: Photo-responsive Λ-shaped novel non-conjugated porphyrin dyads

- Poster presented at the Royal Australian Chemical Institute Centenary Congress, Melbourne July 2017; Title: Design, synthesis and photophysical properties of *bis*-naphthalene diimide conjugates of Tröger's Base and Hünlich's Base

- Poster presented at the Royal Australian Chemical Institute Organic Chemistry Group 36th annual one-day symposium, Macquarie University, Sydney Dec 2015; Title: Synthesis of novel fullerene-C_{60} Tröger's Base analogue

Declaration

I certify that the work in this thesis entitled " Design, Synthesis and Characterisation of Porphyrin, Fullerene and Naphthalene Diimide Conjugates of Tröger's Base" is a presentation of my original work. No part of this thesis has been presented to any other university or institution for any award. To the best of my knowledge and belief, the thesis contains no material previously published or written by another person except where due references are made.

Md Imam Ansari

December 2017

Acknowledgements

First of all, I would like to thank Almighty Allah for everything in my life, without his blessings and guidance I would never be able to accomplish anything in my whole life.

This thesis is the result of more than three and a half years of work during which I have been supported by many people. My first thanks must go to my supervisors Assoc. Prof. Andrew Try and Prof. Peter Karuso for the opportunity to conduct my research in their lab. Without their support, supervision, advice, and encouragement the completion of my degree would not have been possible. I have learned a lot with their enthusiasm, vocabulary and vast knowledge of chemistry.

Thanks to the past members, of my research group. I would like to give a special mention to Dr Rajesh Raut, Dr Mohammad Hashemi Karouei Dr. Michael Howden, Ketan, Kavita, Nirmal, Jason, Tahnim, Murali and Rashid Javaid for their help, support and guidance over my time at Macquarie University.

Thanks to the Staff and Students of the Department of Molecular Sciences, especially, Anthony Gurlica, Dr Erika Davies, Tareq, Aneesh, Shahjahan, Kalpesh, Shalini, Ishan, Amol, Minakshi, Nandani, Pragati, Fuyan and Dr. Kartik Kamath.

I am very grateful to my family and friends for their encouragement and support. Special mention must go to my Mum and Dad. Without you there was no way I would have survived.

List of Abbreviations and Symbols

TB	Tröger's base
D	Donor
A	Acceptor
D-B-A	Donor-bridge-acceptor
LHCs	Light harvesting complexes
PET	Photoinduced electron transfer
EtOAc	Ethyl acetate
DCM	Dichloromethane
NDI	Naphthalene diimide
NMI	Naphthalene monoimide
DMF	Dimethyl formamide
C_{60}	Fullerene-C_{60}
PRC	Photosynthetic Reaction Centre
DDQ	2,3-Dichloro-5,6-dicyano-1,4-benzoquinone
BF_3	Boron trifluoride
TFA	Trifluoroacetic acid
μ	micro
ArH	aromatic hydrogen
^{t}Bu	*tertiary*-butyl
°C	degree Celsius
$CDCl_3$	deutero-chloroform
d	doublet
DCM	dichloromethane
dd	double of doublets

DMSO-d_6	dimethyl sulfoxide-d_6
equiv	equivalent
FT-IR	Fourier transform infrared spectroscopy
HRESIMS	High-resolution electron-spray ionization mass spectrometry
g	grams
h	hour
J	coupling constant
K	kelvin
m	multiplet
M	molar (moles/litre)
m	*meta*
mg	milligram
min	minute
mmol	millimole
m.p.	melting point
NMR	Nuclear Magnetic Resonance
Hz	Hertz
ppm	parts per million
MHz	Megahertz
o	*ortho*
Ph	phenyl
p	*para*
q	quartet
s	singlet
t	triplet

Bu*t*	tertiary butyl
THF	tetrahydrofuran
TLC	thin layer chromatography
UV	ultraviolet
λ_{abs}	absorption wavelength
λ_{ex}	excitation wavelength
λ_{em}	emission wavelength
ICT	Internal charge transfer
DNA	Deoxyribonucleic acid
XRD	X-ray powder diffraction

Abstract

Porphyrins, naphthalene diimide and fullerene-C_{60} are particularly important chromophores that have been used in light-energy conversion research and the design and synthesis of artificial photosynthetic systems. The electron donor (porphyrins) and electron acceptors (naphthalene diimide or fullerene-C_{60}) play key roles in mimicking the photosynthetic antenna-reaction centre of plants. The main aim of this thesis is to provide further insight into the construction of donor-acceptor compounds separated by a well-defined V-shaped bridging molecule. Various linear and conjugated porphyrin arrays have been developed to better understand structure-electronic properties relationship between the two chromophores but the emphasis of this thesis is the development of synthetic methods for the construction of these donor-acceptor systems. In particular, we focus on Tröger's base as a V-shaped bridge molecule between two chromophores.

This thesis first describes the synthesis of new Tröger's bases with the desired functional groups such as nitro, amino, ester, alcohol and aldehyde then post-modification of Tröger's base to append chromophores.

Novel architectures were made such as symmetric porphyrin dyads using two different types of porphyrin and hybrid porphyrin-Tröger's base-naphthalene diimide and porphyrin-Tröger's base-C_{60} dyads. In addition, bis-naphthalene diimide Tröger's base and Tröger's base-C_{60} were made in order to develop methodology for post-modification of TB to append NDI and C_{60}, respectively. Preliminary photophysical characterisation (fluorescence and UV/Vis) is presented but charge transfer properties of selected compounds will be studied by cyclic voltammetry and transient absorbent spectroscopy in the future. All Tröger's base compounds made are racemic.

Key words: Organic synthesis, porphyrin, Tröger's base, fullerene-C_{60}, zinc(II), naphthalene diimide, donor-acceptor complexes, artificial photosynthesis.

Chapter Two

Chapter Three

Chapter Four

Account of Research Progress Linking the Research Papers and Chapters

The relationship between the progression of research to the preparation of papers for publication is explained in the flow diagram below. This flow diagram also shows how the individual chapters in this thesis relate to the extension of ideas and research results.

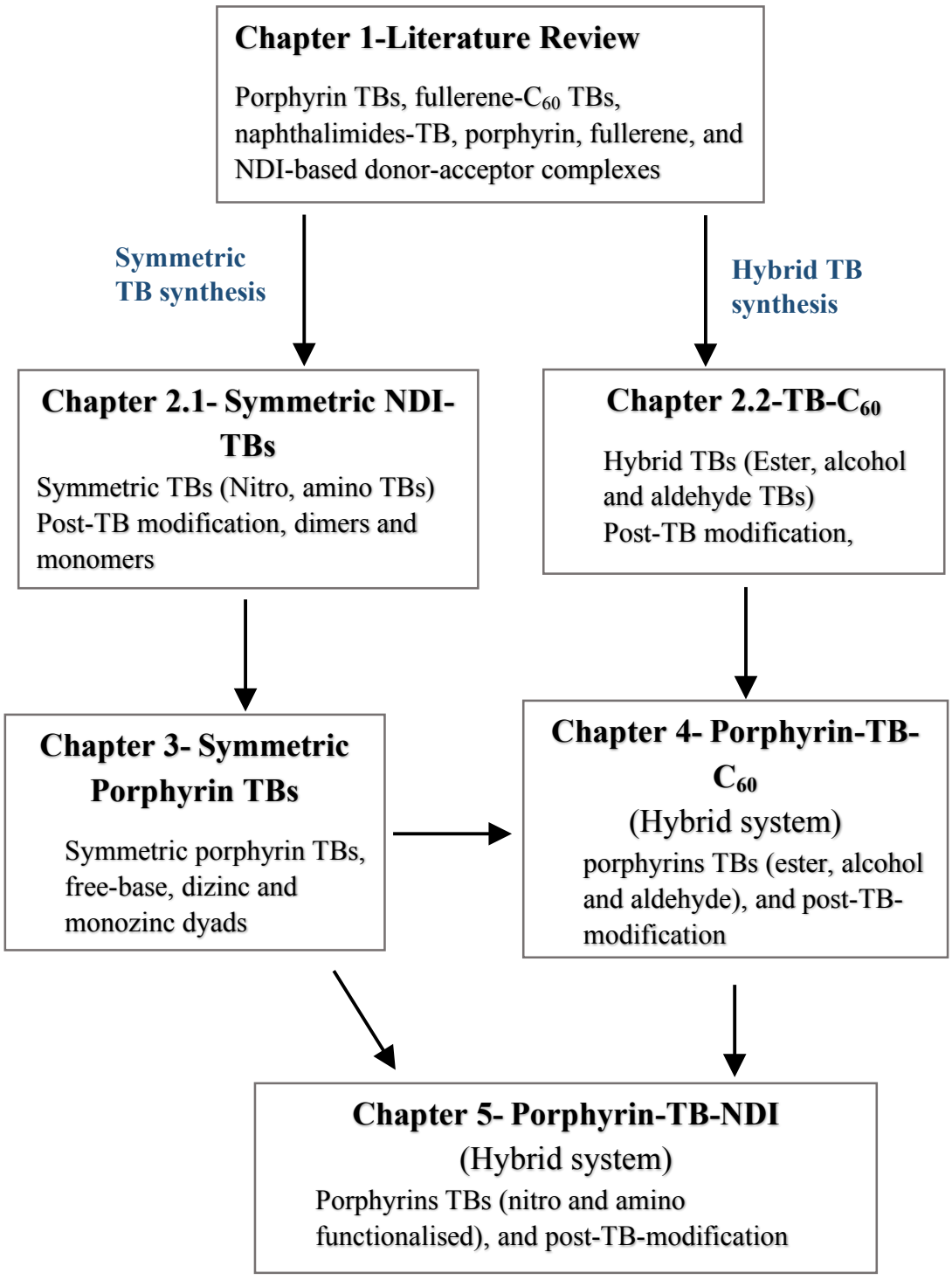

Fig. i. The flow of research progress and the relationship between research papers and chapters in this thesis.

Notes for Readers

This thesis is purely based on the synthesis of Tröger's base conjugates not any photophysical characterisation. In future, selected compounds will be sent to collaborators for electron transfer studies. All TB analogues synthesised and drawn in this thesis are racemic.

Research Problem Investigated

Porphyrins and related compounds are fundamentals to all living things on our planet and are responsible for harvesting energy from light (photosynthesis). Photosynthetic antenna arrays found in plants funnel energy into the reaction centre through chromophores that are held at defined geometries with respect to one another. Attempts have been made to synthesise artificial photosynthetic antenna so that the energy-transfer processes can be understood. Recently, Tröger's base has emerged as a rich area of chemical research due to a unique set of structural features (rigidity, V-shaped and C_2 symmetry). This rigid scaffold can hold two chromophores in close proximity to each other and thus allow through-space intramolecular interactions. Several porphyrin Tröger's bases are known and conjugates make a starting point for our further investigation of the system. The goal of this research is to employ a simple scaffold (Tröger's base) as the framework for the attachment of chromophores that are commonly used by researchers in the development of photosynthetic reaction centre mimics.

Chapter One
Literature Review

1.1 A Brief History of Tröger's Base Chemistry

The history of Tröger's base (TB) began in 1887 when Carl Julius Ludwig Tröger reported his work on condensation of *p*-toluidine with formaldehyde in a mixture of hydrochloric acid and ethanol.[1] Tröger isolated an unexpected product from the reaction mixture and determined the correct molecular formula ($C_{16}H_{18}N_2$), though, he was not able to determine the structure and it took nearly half a century (1935) before the correct chemical structure was assigned by Spielman as racemic 2,8-dimethyl-6*H*,12*H*-5,11-methanodibenzo[*b*,*f*]diazocine [(±)-**1**] (Figure 1.1) as result of degradation studies.[2] In 1986, the confirmation of structure was finally provided by way of an X-ray crystal structure reported by Larson and Wilcox.[3] This definitive proof of the structure also showed that the two aromatic rings are constrained in an approximately perpendicular arrangement with respect to one another. Wagner proposed a potential reaction sequence in the formation of Tröger's base **1** (Fig. 1.1). The central bicyclic aliphatic unit fused with the two benzene rings making TB a rigid V-shaped molecule possessing a hydrophobic cavity (Fig. 1.2). In addition, TB **1** is a C_2-symmetric chiral amine and it was the first compound whose chirality is due solely to asymmetric nitrogen atoms. The methylene bridge precludes pyramidal inversion of the nitrogen atoms, making them configurationally stable stereogenic centres.

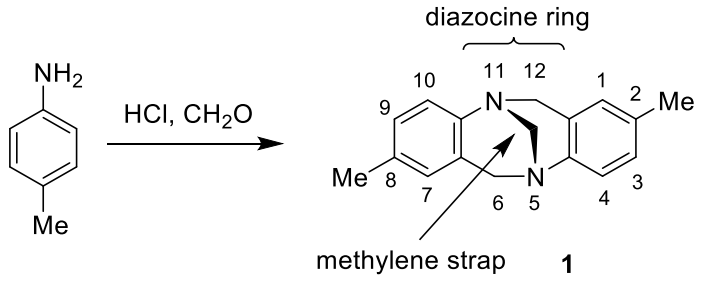

Fig. 1.1. Synthesis of TB **1** using the conditions of Tröger,[1] important features of TB and the numbering scheme.

These unique set of structural features (rigidity, C_2 symmetry, and folded geometry with the planes of aromatic rings making both aromatic ring almost perpendicular to each other) attracted many researchers to investigate its applications in molecular recognition,[4] gas separation,[5-6] functional materials[7] and supramolecular chemistry.[8-9] Since the initial discovery many diverse TB derivatives and synthetic strategies have been reported, although the synthesis generally involves an aromatic amine, a methylene source (formaldehyde) and an acid catalyst.[9-16]

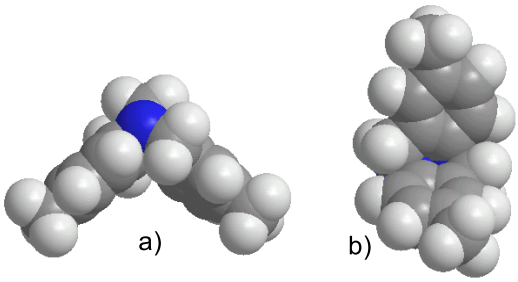

Fig. 1.2. Three-dimensional representations of 2,8-dimethyl TB **1** showing a) the cleft type structure and (b) into the cavity.

As the stereogenic nitrogen atoms are bridgehead atoms, only the enantiomers of either the *R,R* or *S,S* configuration are possible. All TB analogues synthesised and drawn in this Thesis are racemic.

In revolutionary work in 1985, Wilcox reported the XRD structure of Tröger's base with the synthesis of several unprecedented TB analogues.[17] This initiated further developments in the synthesis of TB analogues and over 250 research papers dealing with TB chemistry are currently found to be in the literature over the last two decade.[16] Review articles and book chapters comprehensively covering TB chemistry have been published frequently in the past decades.[18-22] In the following overview, selected areas of TB research, particularly relevant to the context of this Thesis are discussed, namely synthesis and the mechanism of formation, aryl functionalisation of TB.

1.2 Synthesis and the Mechanism of Tröger's Base Formation

1.2.1 Synthesis of Symmetric Tröger's Base Analogues

The first TB synthesis involved the condensation of *p*-toluidine and methylal in aqueous hydrochloric acid.[1] The various approaches used for the synthesis of TB analogous are just deviations of the original conditions, in which a synthetic equivalent of methylal (formaldehyde or a precursor, such as paraformaldehyde or hexamethyltetramine) is treated with a suitably substituted aniline derivative under acidic conditions (usually TFA or hydrochloric acid solutions, acetic acid or methanesulfonic acid).[10, 18, 20, 23] Condensations based on this common method have established high sensitivity, both towards the electronic properties of the substituents and towards the substitution patterns of the aniline components. It was long believed that the substituents on the aromatic ring should be of an electron-donating nature, to avoid the low-yielding, slow reactions witnessed with electron-withdrawing groups.[24-25] Additionally, it was also understood that a substituent in the *para*-position might be needed to avoid polymerisation. In 2001, the Wärnmark group developed of a condensation protocol for the synthesis of halogenated TB analogues, that led to a synthetic breakthrough in TB chemistry.[11] The use of paraformaldehyde and TFA overwhelmed the longstanding drawback of electron-withdrawing substituents and gave access to TB analogues substituted with halogen atoms in virtually any positions on the aromatic rings. This procedure has become the most commonly used method of all the known variations.[26] The mechanism of formation was first investigated by Wagner,[23, 27] and then afterward both Wagner and Farrar[28] re-examined this work, which led to the proposed mechanism for the formation of methano[1,5]diazocine skeleton. As a basis for their study, two synthetic routes were investigated, one of the study utilised most commonly used conditions of *p*-toluidine, paraformaldehyde and trifluoroacetic acid

(TFA), whereas the other employed hexamethylenetetramine as the methylene source, also in the presence of *p*-toluidine and TFA. For both sets of conditions, the major intermediates involved in the reactions were identical.

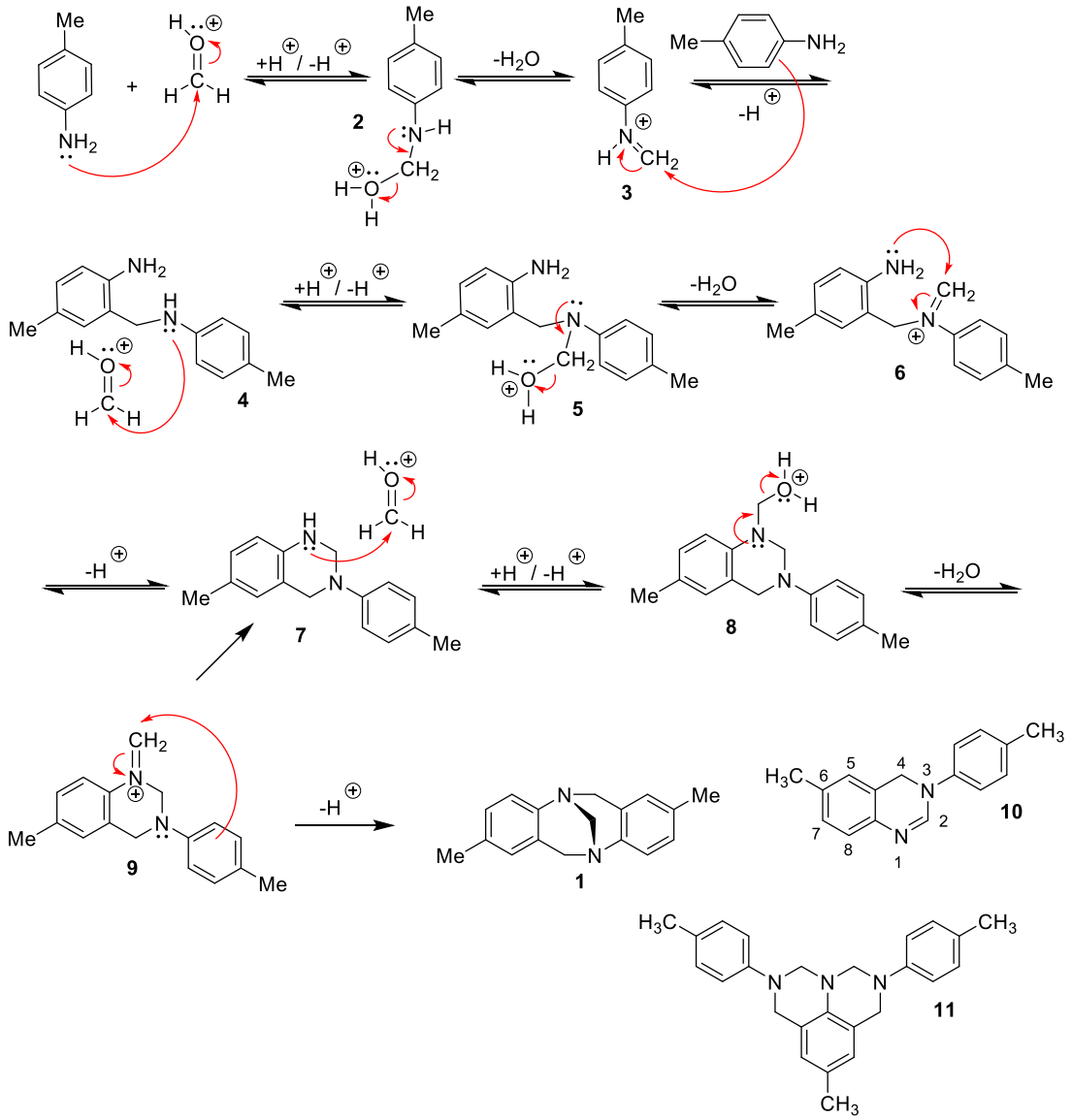

Fig. 1.3. The proposed mechanism for the formation of racemic TB **1** proposed by Wagner and Farrar.

The formation involves a series of electrophilic aromatic substitutions as key steps and undertakes the four substantial intermediates (**3**,**4**,**7** and **9** Fig. 1.3). The first step of the mechanism involves an acid catalysed condensation between *p*-toluidine and

formaldehyde to form iminium ion **3**, which reacts with second equivalent of aniline to give precursor **4**. Two sequential methylene additions accompanied by cyclisation yield TB through intermediates **7** and **9**. Furthermore, by-products such as 3,4-dihydroquinazoline **10** and **11** have been isolated and characterised from Tröger's base reactions.[29]

1.2.2 Synthesis of Hybrid Tröger's Base Analogues

The Wilcox group was the first to prepare Tröger's base bearing different substituents on each of the two benzene rings, compounds that are referred to in the remainder of this thesis as "hybrid" TB analogues. Webb and Wilcox suggested the rational synthesis of such analogues through the tethering of two different substituted aniline derivatives through a methylene unit followed by cyclisation with formaldehyde (Scheme 1.1).[15, 30]

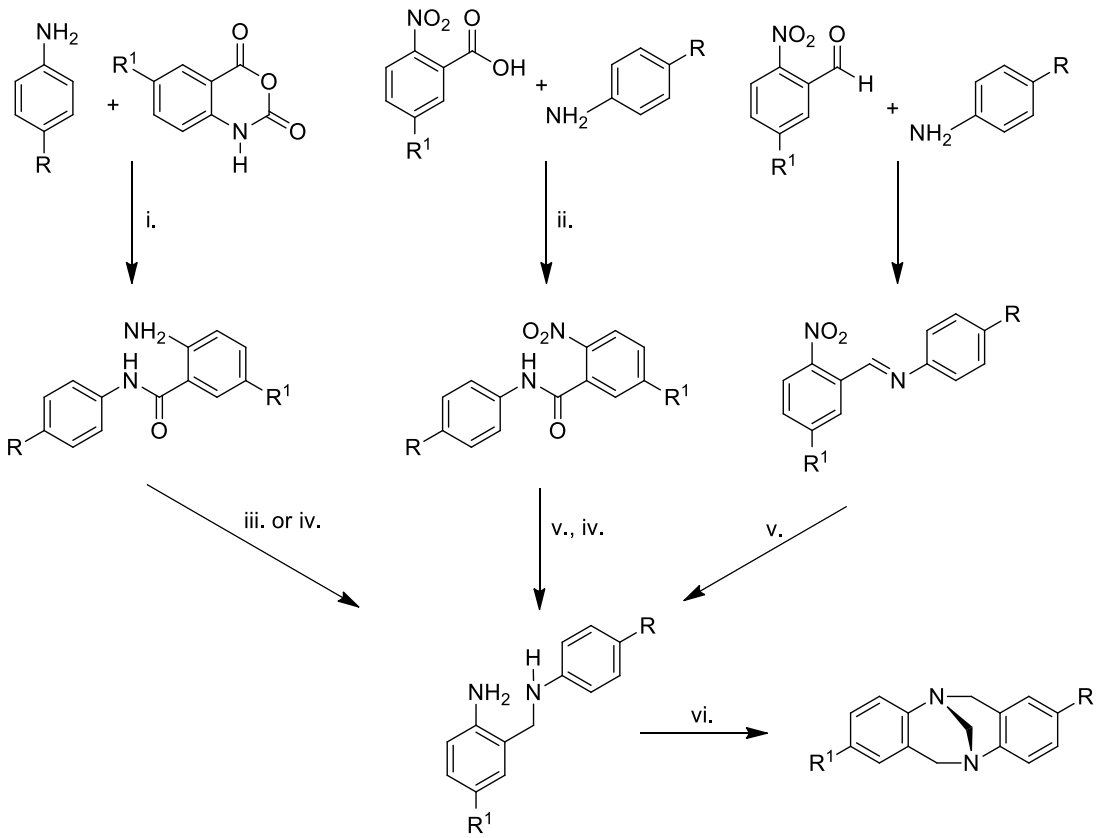

Scheme 1.1. i. EtOH, reflux. ii. DCC, DMF. iii. BH_3-THF, THF, reflux. iv. PtO_2, H_2, MeOH. v. $LiAlH_4$, THF, reflux. vi. H_2CO, HCl.

Importantly, this approach allows for the synthesis of TB compounds with one aryl ring bearing an electron-withdrawing group. The Try group published the simple one-step reaction of two anilines derivatives to form a statiscal mixture of TB analogues in a ratio of 1:2:1 yields (Fig. 1.4).[31] This protocol allows to formed three different TB analogues, and the desired hybrid has an R_f value in between two symmetric forms. As a result, separation of the hybrid is dependent upon on the polarity differences between the all three TBs.[31]

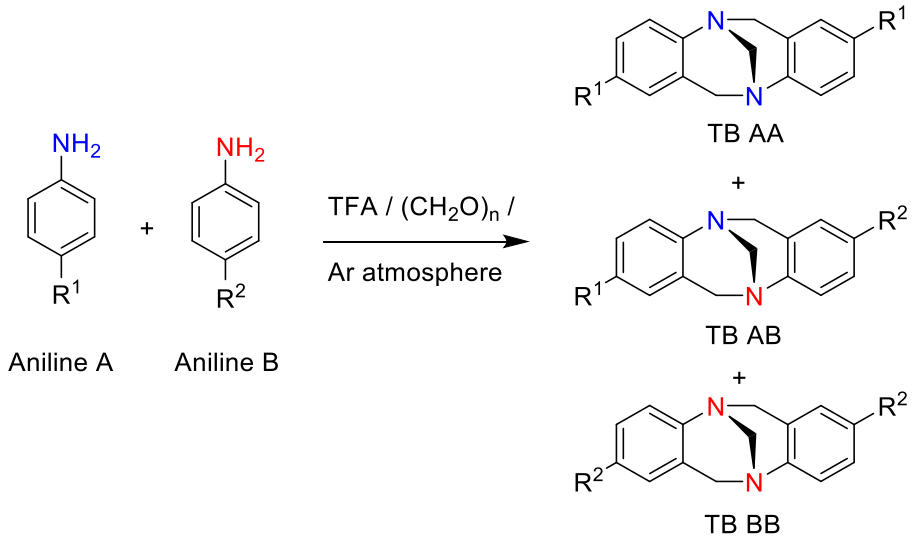

Fig. 1.4. One step preparation of hybrid TB analogues.

1.3 Porphyrins

The porphyrins are naturally occurring macrocyclic compounds which consist of four pyrrole moieties linked *via* methine bridges, and have garnered increasing interest in host-guest chemistry in the last two decades. Porphyrin macrocycles provide an extremely versatile synthetic base for a variety of materials applications.[32] The properties of the porphyrin molecule are due to its structure wherein the porphyrin ring comprises 26 π electrons which participate in a delocalised aromatic system.[33] As a result, due to the large aromatic system they are strong chromophores.

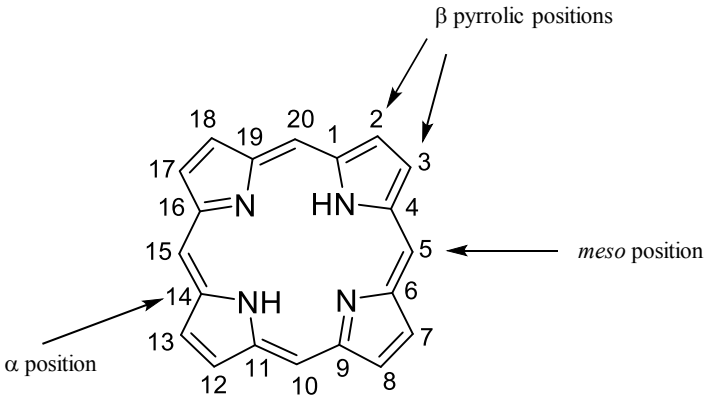

Fig. 1.5. The structure of porphyrin and the IUPAC numbering system.

The porphyrin ring current causes shielding of NH protons (–1 to –4 ppm) and deshielding of *meso* protons (8 to 10 ppm) as can be evidenced from NMR spectroscopy. Positions 5,10,15,20 are usually referred to as the *meso* positions while positions 2,3,7,8,12,13,17,18 are usually referred to as the β-pyrrolic positions (Fig. 1.5). Reducing one peripheral bond on the pyrrole results in a chlorin, or two bonds on opposite pyrroles makes bacteriochlorin. Both of these show strong visible absorption and does not break aromaticity (Fig. 1.6).[33]

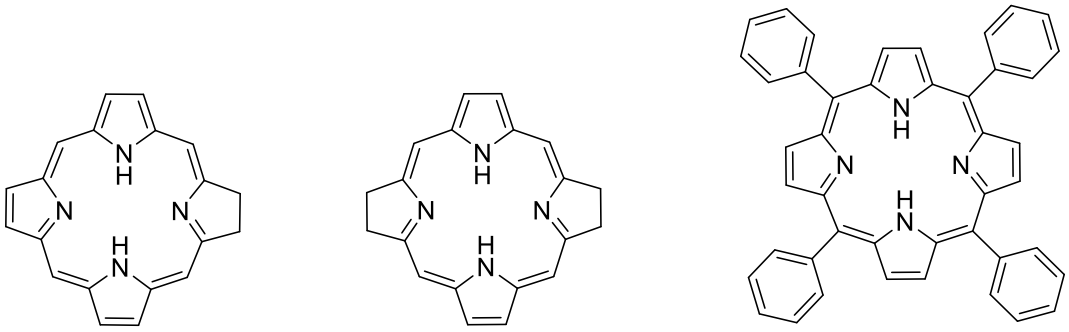

Fig. 1.6. Chemical structures of porphyrin-related heterocycles: the chlorin family, the bacteriochlorin family and 5,10,15,20-tetraphenylporphyrin, an example of a tetra-arylporphyrin.

In the porphyrin macrocycle, two pyrrole rings are in an oxidised state due to their nitrogen atoms being of the pyridine type, with the unshared electron pairs oriented towards the inside of the macrocycle. Hence, a highly symmetrical dianion is formed if both NH bonds in the porphyrin molecule are ionised, in this case all four nitrogen atoms become equal due to the delocalisation of the negative charges. The ionic radii of several metals especially dications allow them to fit within this cavity and the metal can be fixed in space by coordinating the bonds with the four porphyrin nitrogen atoms.

Likewise, the porphyrin ring can act as an acid and as a base. The strong bases remove the two nitrogen protons to form a dianion, while the protonation of "free" nitrogen atoms is easily achieved in acids. Moreover, porphyrins with extended conjugated π-systems have been reported to exhibit favourable charge-transfer kinetics and metallo-porphyrins undergo facile redox reactions.[34-35] Interestingly, porphyrins undergo minimal structural changes during electron transfer reactions and the photo-physical properties of the porphyrins can be tailored by changing metal ion chelation and / or peripheral substitution.[36] Another interesting feature of porphyrins is the number of sites available for functionalisation. For example, substitution of porphyrin at the β and the *meso* positions is possible, enabling to function as a versatile platform for numerous applications, for example in the field of molecular electronics or functional materials.

1.3.1 UV/Visible Absorption of Porphyrins

The electronic absorption spectrum of a 5,10,15,20-tetrakis(3,5-di-*tert*-butylphenyl)porphyrin which is a typical free-base porphyrin (Fig. 1.7) consists of two distinct regions. In the first UV region (360 to 430 nm) there is an intense absorption known as the Soret band or B band, which corresponds to a strong transition from ground state to the second excited state ($S_0 \rightarrow S_2$), and a weaker transition to the first excited state ($S_0 \rightarrow S_1$) is seen at about 500 to 700 nm (Fig. 1.8).

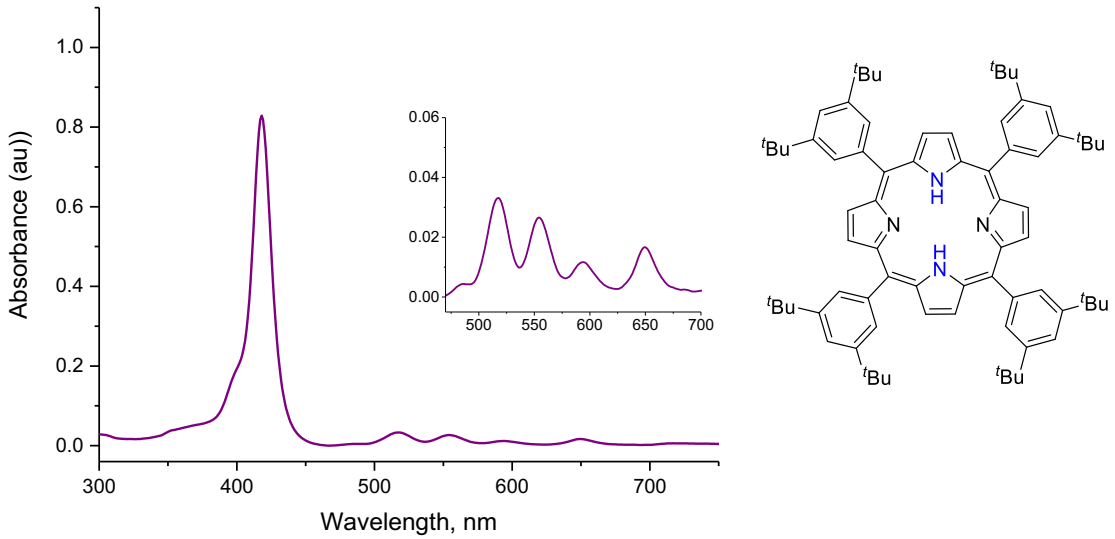

Fig. 1.7. UV/Vis spectra of 5,10,15,20-tetrakis(3,5-di-*tert*-butylphenyl)porphyrin in CH_3CN.

When the molecule is excited from the ground state S_0 to any singlet excited state S_x leads to fast radiationless decay to the lowest excited singlet state S_1. The molecule can exhibit either radiationless decay (at the rate $k_{1)}$ or emit fluorescence ($S_1 \rightarrow S_0$) (at the rate k_f) or can internally convert to the lowest triplet $S_1 \rightarrow T_1$ (at a rate k_2).[37] The molecule can emit phosphorescence $T_1 \rightarrow S_0$ at the rate k_p from T_1, or radiationless decay $T_1 \rightarrow S_0$ at the rate k_3 or can be excited again ($T_1 \rightarrow S_1$) at the rate k_{-2}. As a result, only the relaxation process from S_1 to S_0 and $T_1 \rightarrow S_0$ can emit fluorescence. According to this theory, as reported in Fig. B, the absorption bands in porphyrin systems arise from transitions between two HOMOs and two LUMOs. The HOMOs were calculated to be an a_{1u} and an a_{2u} orbital, while the LUMOs were calculated to be a degenerate set of e.g. orbitals. Transitions between these orbitals gave rise to two excited states. Orbital mixing splits these two states in energy, creating a higher energy state with greater oscillator strength, giving rise to the Soret band, and a lower energy state with less oscillator strength, giving rise to the Q-bands.[32-33]

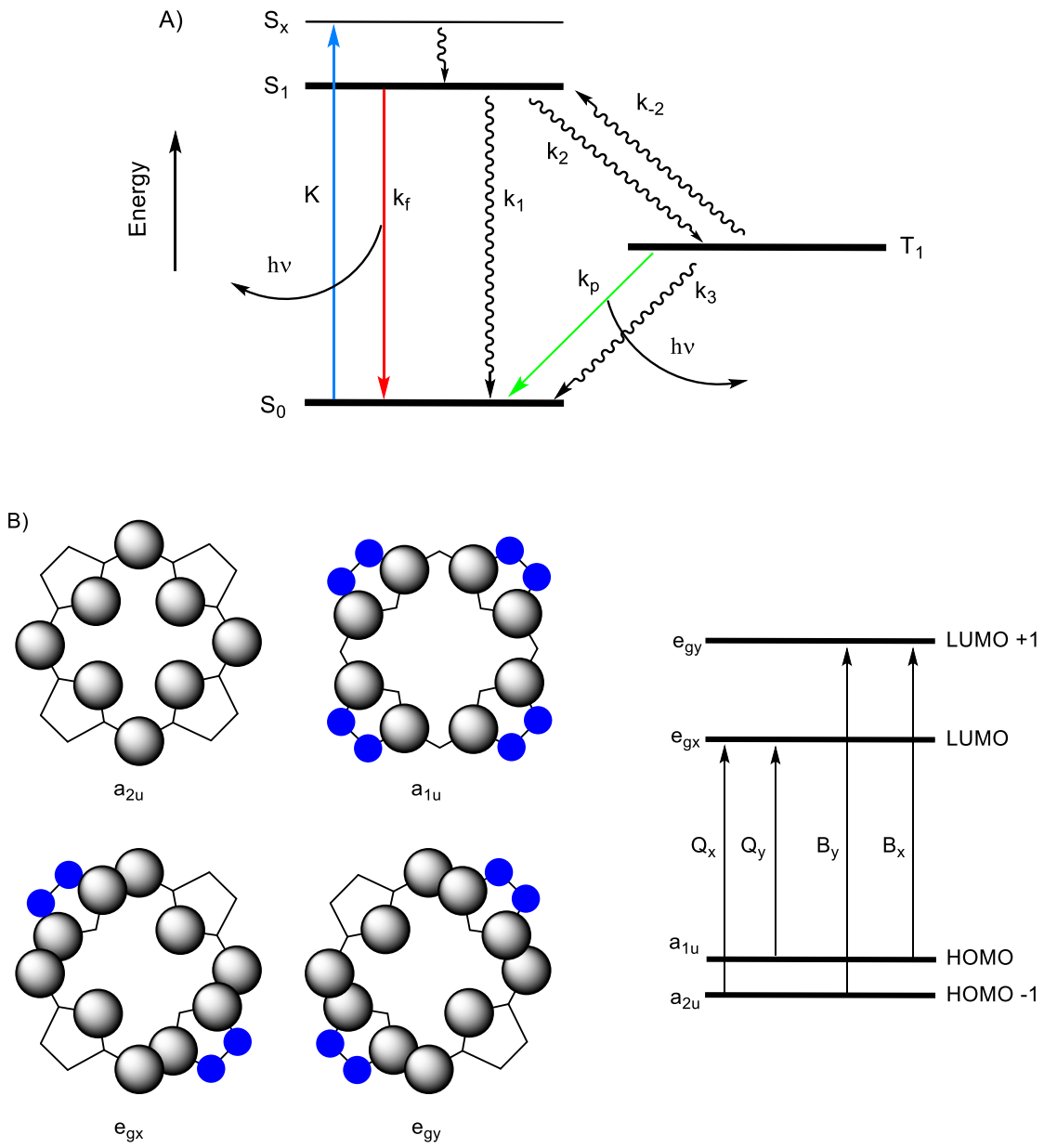

Fig. 1.8. A) Jablonski diagram shows decay scheme for singlet and triplet relaxation. The radiationless processes are shown as wavy lines and radiation processes are shown by straight lines (blue-absorption, red-fluorescence and green-phosphorescence). B) Porphyrin HOMOs and LUMOs. (left) Representation of the four Gouterman orbitals in porphyrins. (right) Drawing of the energy levels of the four Gouterman orbitals upon symmetry lowering from *D4h* to *C2V*. The set of e.g. orbitals gives rise to Q and B bands.

1.3.2 Porphyrin Synthesis

The most famous and readily accessible synthetic porphyrins involve reaction between pyrrole and benzaldehyde for the synthesis of tetraphenylporphyrin.[38] This procedure was developed by Rothemund in 1935,[39] later modified by Alder-Longo[40-41] and co-workers (using equimolar mixture of pyrrole and aryl aldehyde in propanoic acid (Fig. 1.9). However, the reason for the low yields is the competition between macrocyclisation and polymerisation (main product in most porphyrin synthesis). Calvin and co-workers discovered that adding metal salts to the reaction mixture, such as zinc acetate, increased the yield of the free-base porphyrin around 4-5%.[42]

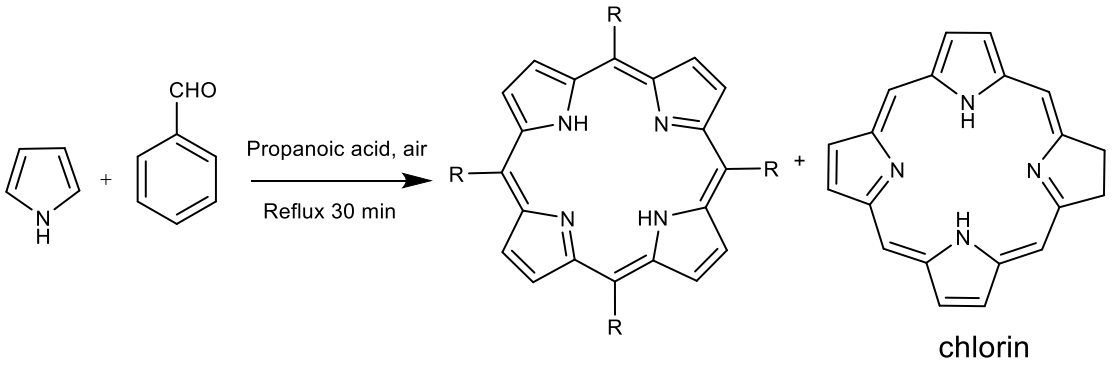

Fig. 1.9. Adler-Longo method for preparing *meso*-substituted porphyrins.

Over the period 1979-1986, Lindsey developed a new and innovative method (equimolar mixture of pyrrole and aryl aldehydes in dichloromethane or chloroform, TFA or BF_3-etherate as a catalyst, DDQ or *p*-chloranil as oxidant) with room temperature reaction conditions and the wide-ranging scope of aldehydes.[43-44] A drawback of this method is the need to evaporate large volumes of solvent if the reaction is done on moderate to large scale and the use of chromatography to obtain the pure product.

For certain applications, compounds in which not all *meso* aryl units are the same may be desired. In such cases a stepwise methodology is sometimes

advantageous. For instance, access to *trans*-A_2B_2 porphyrins is made possible through initial formation of 5-substituted dipyrrolomethanes (*via* acid-catalysed condensation of an aldehyde with an excess of pyrrole), followed by condensation of the dipyrrolomethane with a second aldehyde (Fig. 1.10). However, scrambling of the preformed dipyrrolomethane units (*via* cleavage of the *meso*-carbon-β-pyrrolic bonds and recombination with the other reaction components) is known to occur, to varying degrees.[45]

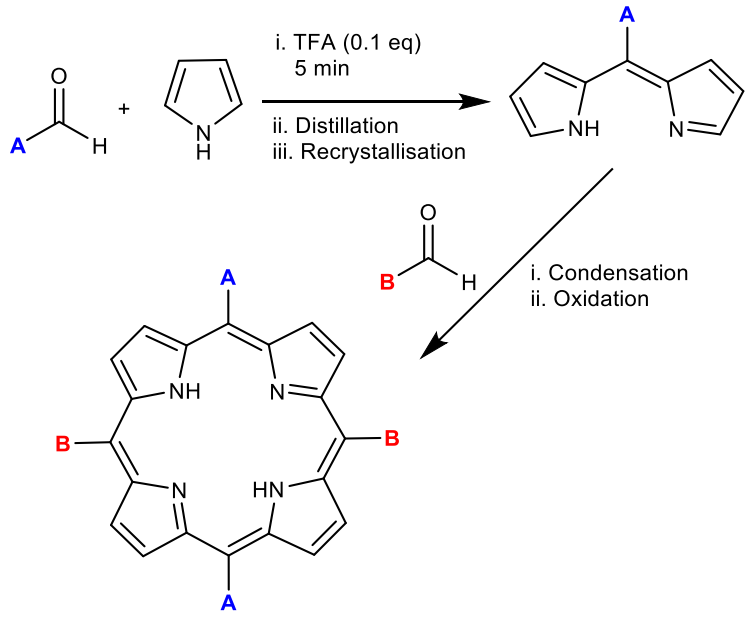

Fig. 1.10 Synthetic route to *trans*-A_2B_2 porphyrins.

As expected for all aromatic compounds, porphyrins undergo the electrophilic substitution reactions typical of the aromatic compounds such as nitration, sulphonation, halogenation, acylation and formylation. In particular, there are two different sites (*meso* and β–pyrrolic positions) on the porphyrin macrocycle where electrophilic substitution takes place owing to different reactivity.[46] These sites activation depends on the porphyrin's electronegativity, which can be controlled by choosing appropriate metal to coordinate the central nitrogen atoms. The *meso*-

positions of porphyrins were nitrated using nitric acid in either sulphuric acid or acetic acid, NO_2BF_4[47] or with nitrate salts such as $[Cu(NO_3)_2]$.[48] The resulting nitroporphyrins were reduced to the corresponding amines by reduction with sodium borohydride and Pd/C in methanol. Moreover the porphyrin macrocycle also undergoes nucleophilic substitution reactions.[49-50]

Introduction to Multicomponent Arrays That Contain Porphyrins and / or Tröger's Base

In the last two decades, synthetic chemists have constructed artificial photosynthetic models to mimic the light harvesting processes of plants and bacteria by designing multiporphyrin dyads or triads. Numerous strategies have been employed to synthesise covalent and / or supramolecular assemblies that comprise porphyrin chromophores. A detailed account of these methodologies are beyond the scope of this brief literature review; however, an overview of some of the most popular porphyrin-based assemblies with and without Tröger's base framework will be discussed.

1.3.3 Porphyrin Analogues of Tröger's Base

Most synthetic models for artificial photosynthesis have been based on the linkage of two porphyrin units but generally they have been linked by a flexible bridge due to which inter macrocycle distance was not controlled. Hence, the elegant porphyrin dyads or dimer with a rigid bridge and fixed distance between the two porphyrins may overcome the limitations of the previous systems. A simple synthetic strategy was reported to assemble to porphyrins separated by a rigid bridging molecule. For instance, porphyrin Tröger's base analogue **12** was first synthesised by Crossley *et al*., who reported the resolution of the dizinc(II) bisporphyrin Tröger's base analogues and host-guest interactions of porphyrin with histidine and lysine esters (Fig. 1.11).[10]

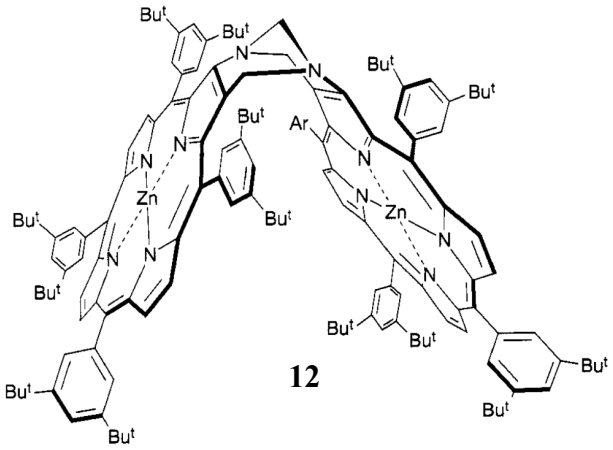

Fig. 1.11. Dizinc bis-porphyrin joined by diazocine bridge.

In the following year, Crossley and co-workers synthesised quinoxalinoporphyrins Tröger's base **13** where two porphyrins are connected *via* quinoxaline TB (Fig. 1.12). The reported synthetic models not only had remarkably similar edge-edge and centre-centre distances to those found in the photosynthetic reaction centre (PRC); they also had a constrained geometry.[51]

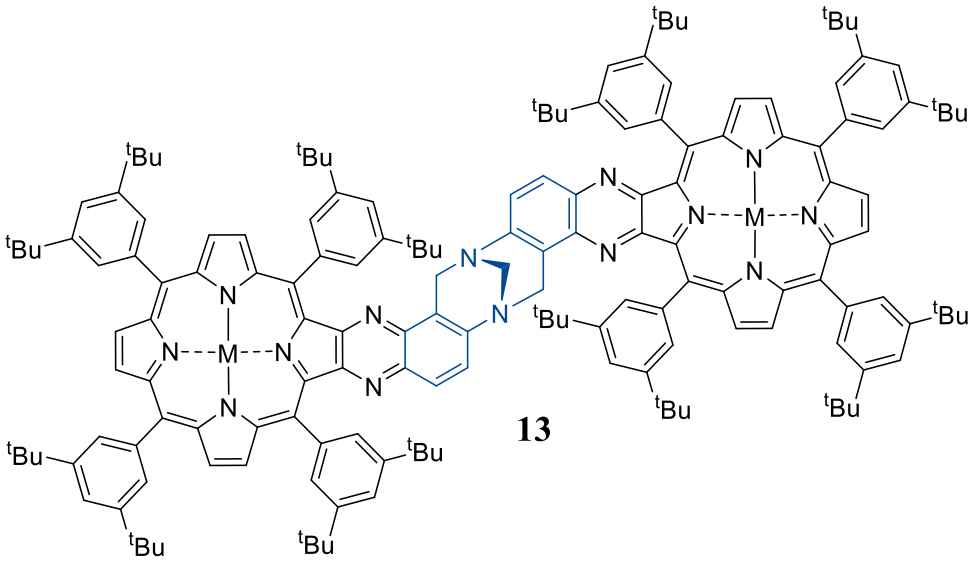

Fig. 1.12. Quinoxalinoporphyrins fused Tröger's base.

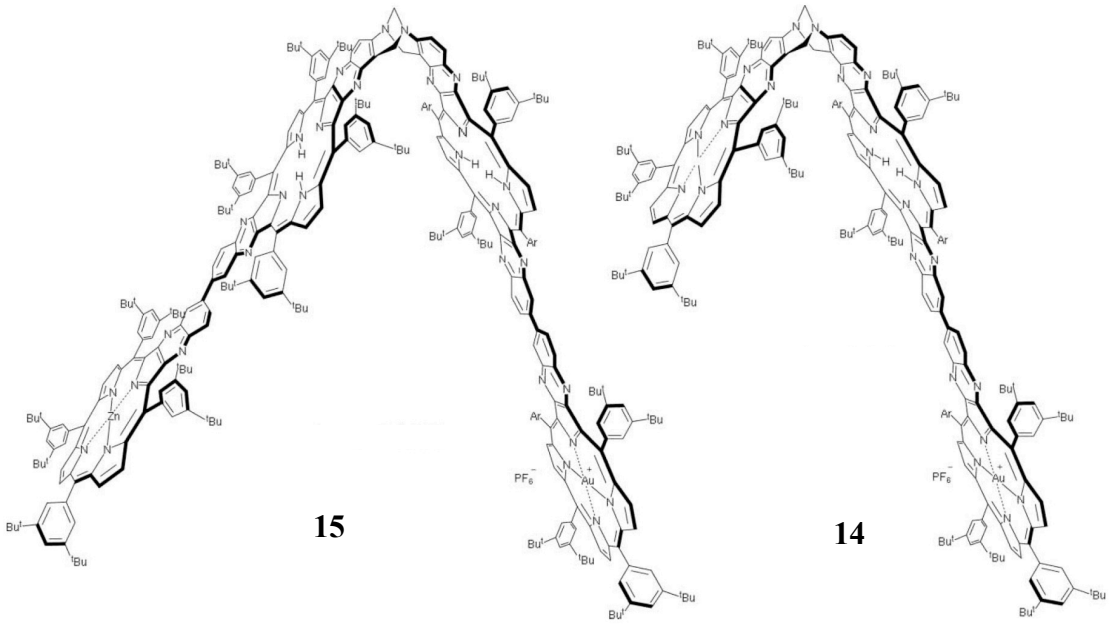

Fig. 1.13. The gigantic porphyrin Tröger's base studied by the Crossley's group.

More recently, Crossley *et al*. reported large multiporphyrins complexes with a Tröger's base core to serve as an artificial photosynthetic model or as a donor-acceptor dyad (Fig. 1.13). For instance, the tetrakis-porphyrin and tris-porphyrin arrays **14** and **15** function as models for the arrangement of the chromophores that constitute PRCs. The use of gold(III) and zinc(II) chelation creates an energy gradient for photoinduced electron transfer in each compound. They utilised the same synthetic strategy as for **13**. Photophysical analysis indicated that long-range photoinduced electron and energy transfer processes occurred in the extended arrays. Step-wise electron transfer was evidenced between zinc(II) chelated and gold(II) chelated porphyrin chromophores in polar solvents representing charge transfer across 35 Å for dyad **14** and 50 Å for dyad **15**.[52]

Exploiting Crossley's work on porphyrin Tröger's base, in 2014, Dolensky *et al.* reported the synthesis and enantioselective binding studies of a new chiral cobalt(II)porphyrin Tröger's base conjugate **16** as a potential receptor for methyl esters

of several amino acids (Fig. 1.14). Here, the conjugate was prepared as a racemic mixture which was then resolved *via* preparative high-performance liquid chromatography (HPLC) on a chiral column. Complexation and UV/Vis spectroscopy revealed that the pure enantiomers have a high affinity for histidine, lysine and proline methyl esters. Circular dichroism spectroscopic studies confirmed the highest enantioselectivity for lysine methyl esters.[53]

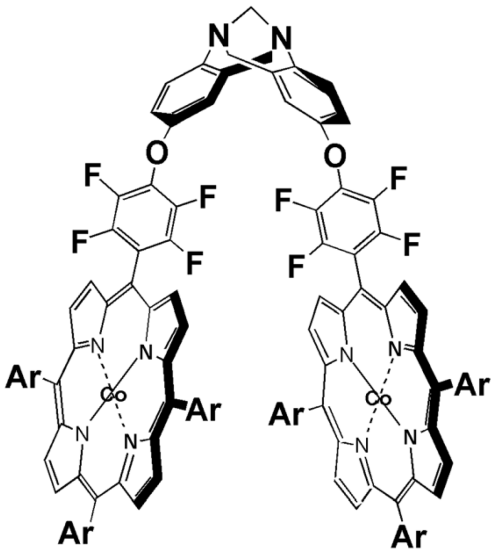

16 Ar = perfluorophenyl

Fig. 1.14. Cobalt(II)porphyrin Tröger's base.

1.4 Naphthalene Diimide and Naphthalimides

Naphthalene diimide (NDI) is a versatile aromatic compound that possesses high electron affinity, excellent thermal and oxidative stability and good charge mobility. Furthermore, NDIs are electron deficient and capable of being appended to large multicomponent assemblies through intercalations.[54] These attractive features of NDIs make them promising candidates for photovoltaic devices, organic electronics and semiconductor materials (Fig. 1.15).[55-56]

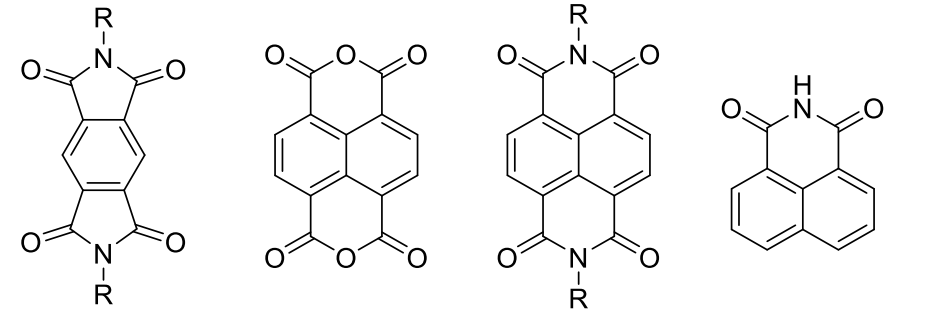

Fig. 1.15. Aromatic diimide structures with self-assembly and functional properties.

The poorly soluble **NDA** (1,4,5,8-naphthalenetetracarboxylic acid dianhydride) is the main precursor for the synthesis of functionalised NDI, and it can be readily functionalised with arylamino or alkylamino groups at anhydride positions. The NDIs have emerged as excellent functional materials (e.g. in rotaxanes and catenanes) owing to their superior spectroscopic properties over pyromellitic diimide dyes.[57] The 1,8-naphthalimide derivatives have been used in diverse applications such as the development of luminescent sensors for biologically relevant molecules,[58-59] fluorescent logic gates[60] and molecular switches.[61] Recently, they have also been reported as potential DNA targeting agents[62-64] and luminescent probes for selective staining of living cells.[65-66] Hence, NDIs constitute a proven candidate that can specifically be used as an electron acceptor component for constructing donor-acceptor complexes.

1.4.1 General Synthesis and Reactivity

The synthesis of symmetric NDI compounds is simple, efficient and a one-step reaction from commercially available **NDA** (1,4,5,8-naphthalenetetracarboxylic dianhydride). For example, **NDA** can be condensed with an alkylamine or arylamine in a high boiling solvent (usually DMF or toluene) (Scheme 1.2). In general, the NDI product obtained in high yield.[57] This procedure allows a variety of primary anilines to be used that can be substituted at the imide position, and hence, a diverse range of functionalised NDI

can be prepared. For certain applications, unsymmetrical or monoimide derivatives may be desired. In this case, naphthalene diimides bearing two different substitutions on the diimide nitrogens can be prepared using Ghadiri's method, with the proviso that pH is carefully controlled (Scheme 1.2).[67] Imide-functionalised NDIs have shown potential in charge transfer complexes[68] and are particularly useful for the construction of self-assembled architectures, high conductivity materials,[69] artificial photosynthetic models[70-73] and donor-acceptor systems.[68]

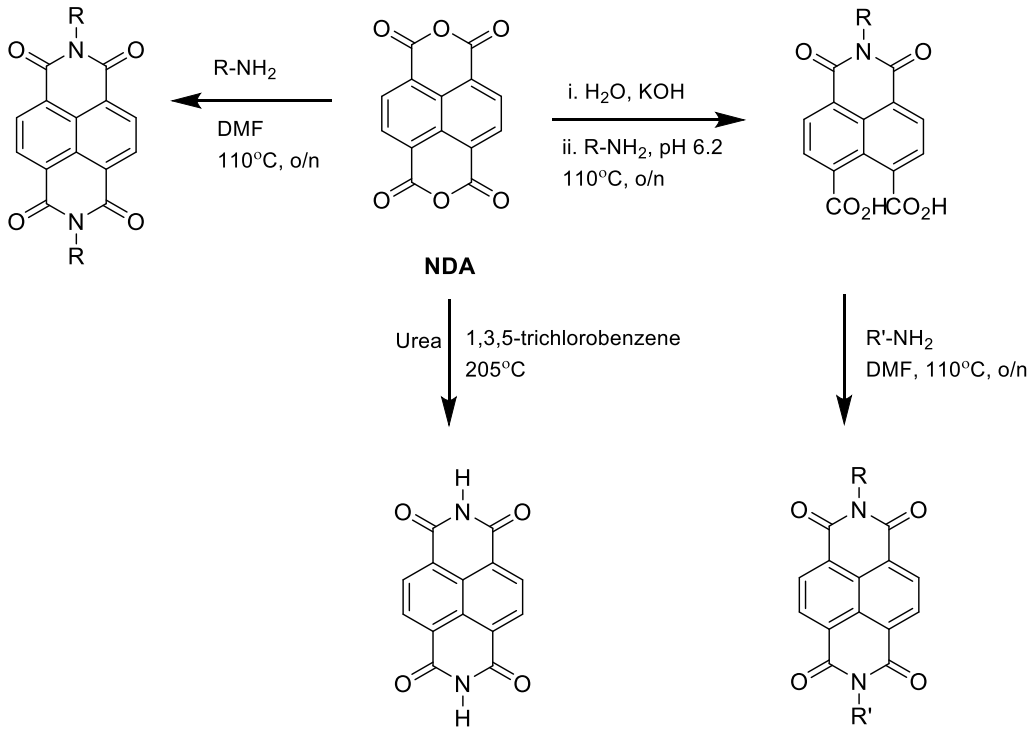

Scheme 1.2. Synthetic route for preparing symmetric and non-symmetric NDI.

1.4.2 Naphthalimides Analogues of Tröger's Base

To date, only naphthalimides Tröger's base have been reported and their applications as fluorescent probes for DNA targeting and to the best of our knowledge there are no reports on naphthalene diimide TBs. For instance, Lewis and Brown's research group spent several years investigating the synthesis and properties of naphthalimides; predominantly they worked with amino-substituent in the 4-position.[74]

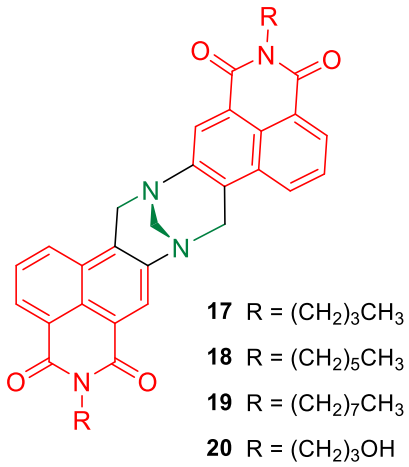

Fig. 1.16. Chemical structures of fluorescent Tröger's base.[74]

In 2005, they reported the synthesis and fluorescence properties of naphthalimides-containing Tröger's base **17-20** with medium-dependant fluorescence emission intensity (Fig. 1.16).[74]

Recently, Gunnlaugsson and Vaele reported on 4-amino-1,8-naphthalimide-based Tröger's base as high affinity DNA targeting fluorescent supramolecular scaffolds.[75] They described the synthesis and photophysical and biological investigation of naphthalimides conjugated TB **21-23** (Fig. 1.16).[75-76]These compounds bind strongly to DNA in competitive media at pH 7.4 with concomitant modulation of their fluorescence emissions.

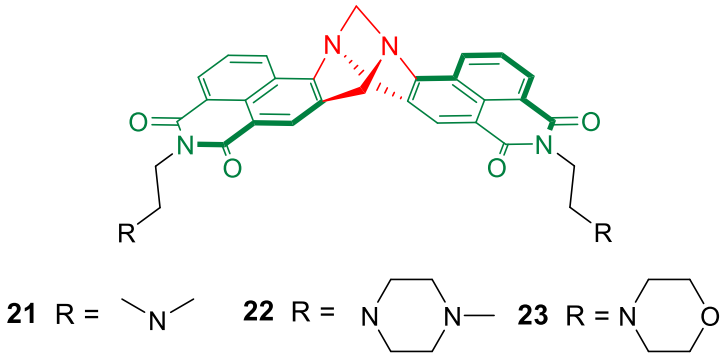

Fig. 1.16. Naphthalimide-based Tröger's base as high affinity DNA targeting fluorescent supramolecular scaffolds.[75-76]

Importantly, these compounds also undergo rapid cellular uptake and are cytotoxic against human HL60 and K562 cell lines.[75]

Likewise, for the development of functional materials, supramolecular self-assembly chemistry offers an interesting platform that can be utilised in diverse applications.[77-80] For example, Shanmugaraju and Gunnlaugsson reported on the supramolecular Tröger's base derived coordination zinc polymer for fluorescent sensing of phenolic-nitroaromatic explosives in water (Fig. 1.17).[81]

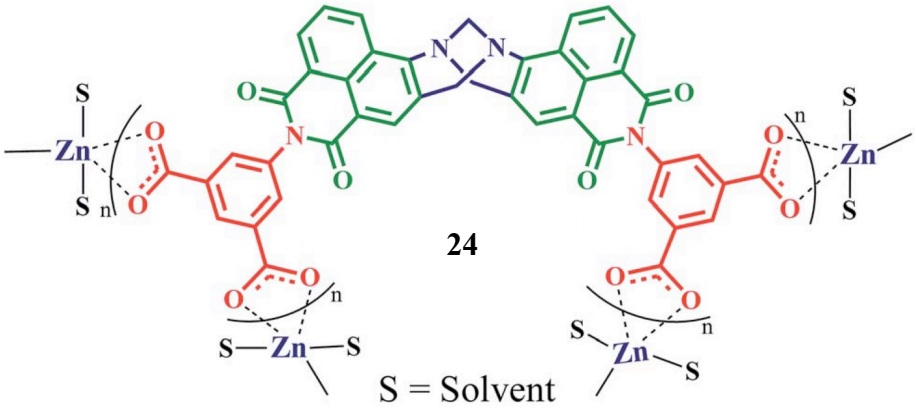

Fig. 1.17. A supramolecular Tröger's base for fluorescent sensing of phenolic-nitroaromatic explosives in water.[81]

Compound **24** showed strong green fluorescence (λ_{em} 520 nm) due to ICT formation with electron acceptors such as picric acid (lod 26.3 ppb).[81]

1.5 Fullerene-C_{60}

Fullerene-C_{60} is a carbon allotrope discovered by H. Kroto, R. Curl and R. Smalley (Fig. 1.18)[82-83] and led to them being awarded the Nobel Prize in Chemistry in 1996.[84] Over the last two decades, a lot of attention has been devoted to fullerene as an electron acceptor in intramolecular photoinduced electron transfer (PET) reactions, owing to its favourable reduction potential and small reorganisation energy.[85-89]

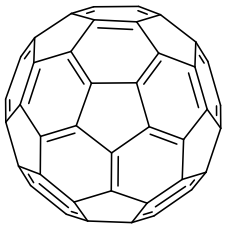

Fig. 1.18. Structure of fullerene-C_{60} molecule.

As a consequence, fullerene promotes charge separation (CS), but retards the charge recombination (CR) process, resulting in the formation of much desired long-lived charge-separated states.[90-96] These features makes C_{60} useful for the construction of electron donor-acceptor dyads or Light Harvesting Complexes (LHCs). These applications rely on the specific functionalization of C_{60}.

The fullerene molecule can be functionalised *via* several methods for example, using active methylene group of malonates (Bingle functionalization) or Diels-Alder Reaction with cyclic sulfones[97-98] which takes place under mild conditions. One of the most successful approaches has been the reaction between an aryl aldehyde, *N*-methyl glycine (sarcosine) and fullerene-C_{60}, known as the Prato reaction. This derivatisation of fullerene is based on a 1,3-dipolar cycloaddition of the ylide generated from the condensation of sarcosine with an aldehyde with C_{60} (Fig. 1.19).[99]

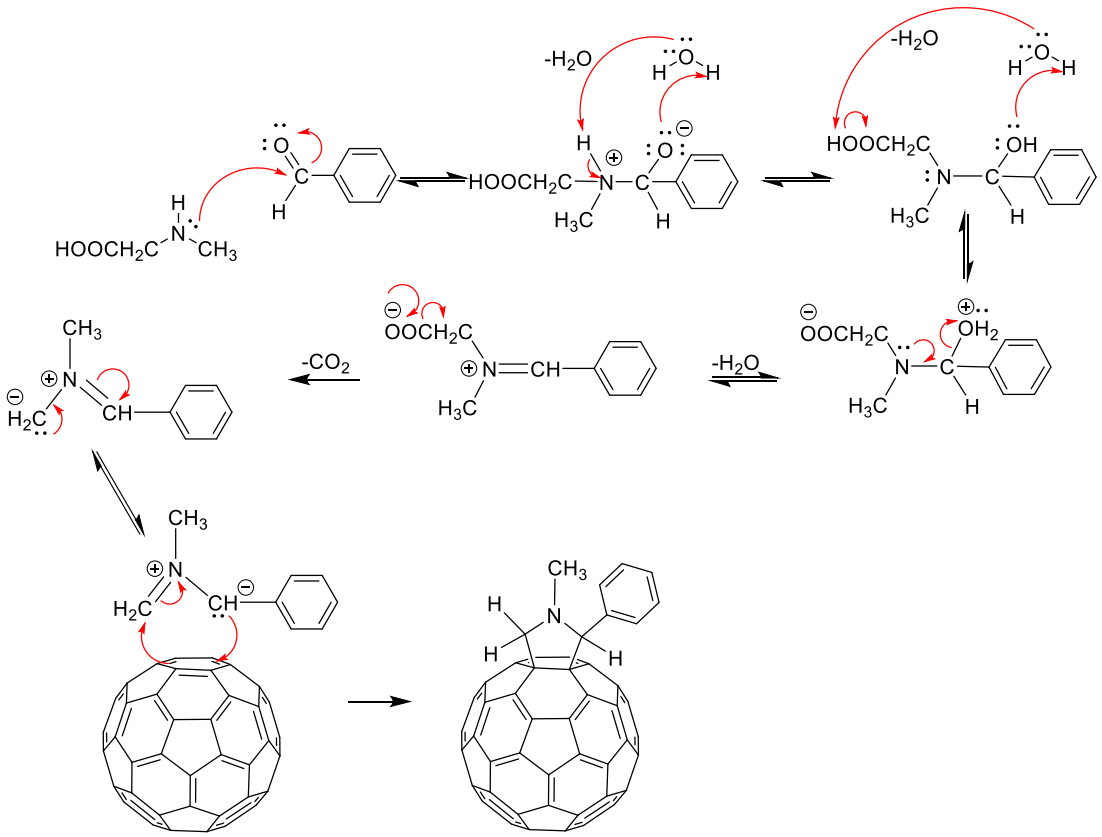

Fig. 1.19. The mechanism of Prato reaction.

1.5.1 Fullerene Analogues of Tröger's Base

In 2004, Diederich and Sergeyev demonstrated the first example of regio- and stereo-selective functionalization of C_{60} with a Tröger's base (Fig. 1.20).[100]

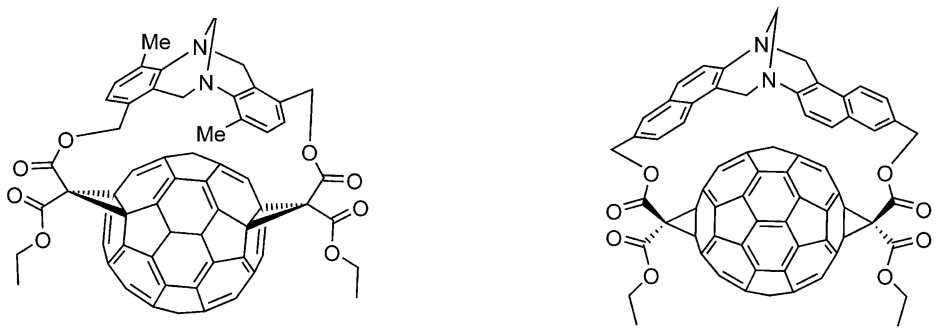

(±)-**25** (*C*$_1$, *trans*-4), 38% (±)-**26** (*C*$_2$, *trans*-1), 58%

Fig. 1.20. Bisadducts of fullerene-C_{60} with the structural motif of Tröger's base.

The following year Saigo and co-workers reported the synthesis of four kinds of bismalonates tethered with a Tröger's base and used this for the double Bingle reaction of C_{60} (Fig. 1.21).[97] The regio- and distereoselectivities of the reaction was dependent on the structure of the Tröger's base. They tested various Tröger's base derivatives but only some of them showed a good to excellent regio- and diastereo-selectivities.[97]

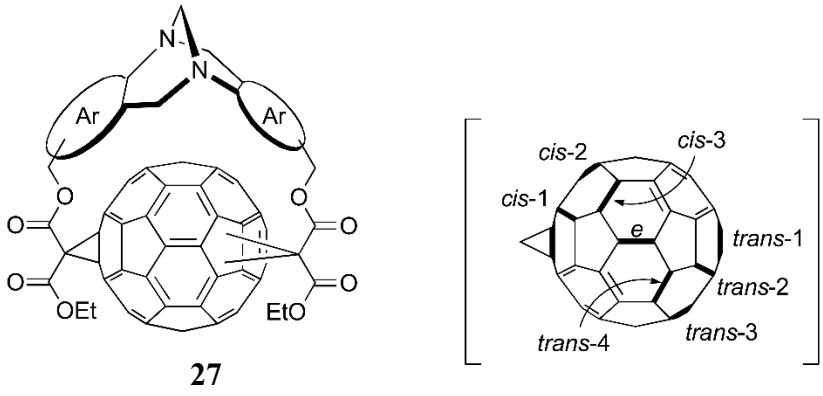

27

Fig. 1.21. Example of four kinds of bismalonates with a Tröger's base structural motif.

However, the methodology presented by Diederich and Saigo, limits appending any other chromophore (e.g. porphyrin or NDI) as both aryl rings of the TB are connected to C_{60}. Consequently, they are not useful for the construction of donor-acceptor complexes. To the best of our knowledge, there are no examples of fullerene-C_{60} onto the TB frameworks structural motif constructed a *via* Prato reaction.

1.6 Porphyrin-based Dyads and Triads

Numerous porphyrin dyads have been synthesised and studied however, only selected and relevant work has been covered in the following section.

1.6.1 bis-Porphyrin Conjugates

As noted in the preceding section, like Crossley's bis-porphyrin system, in 2001, Ono and co-workers reported the synthesis of "gable" bis-porphyrins linked with a bicyclo[2.2.2]octadiene ring and its transformation into a conjugated planar bis-porphyrin (Fig. 1.22).[101]

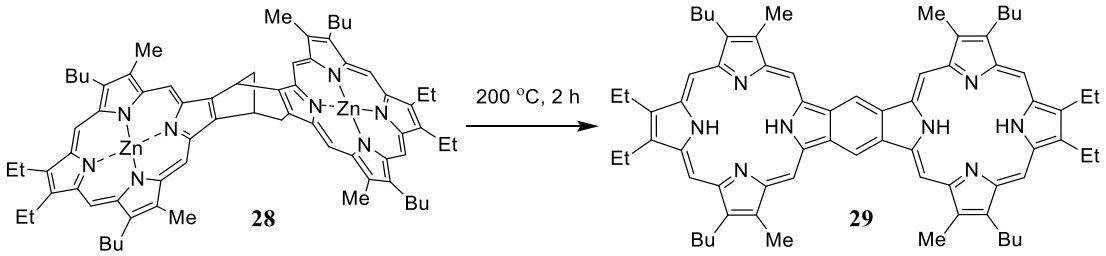

Fig. 1.22. Synthesis of gable porphyrin.

Here, a soluble non-conjugated porphyrin dimer was converted into an insoluble conjugated porphyrin dimer by heating under vacuum at 200 °C for 2 h. The planar molecule **29** was formed *via* retro-Diels-Alder reaction and essentially insoluble due to the strong π-π stacking. This retro-Diels-Alder process provides a powerful strategy for the fabrication of electronic devices from π-extended compounds.[101]

On the other hand, Arnold and co-workers first synthesised dyads like **30**, which consists of a simple bis-porphyrin system linked *via* a butadiyne bridge that allows electron transfer between the macrocycles *via* the conjugated bridge (Fig. 1.23).[102]

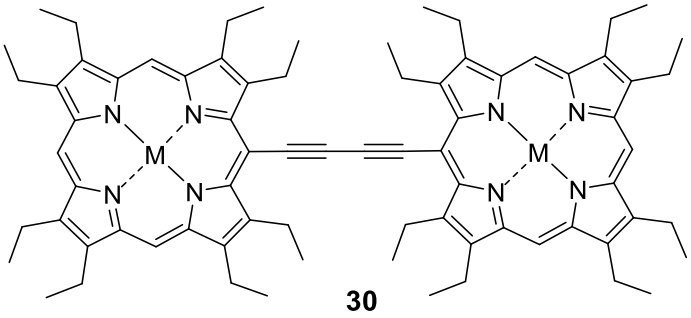

Fig. 1.23. Porphyrin dimers linked *via* butadiyne bridge.

Since the initial report a variety of *meso-meso*, *meso*-β and β-β alkyne linked porphyrin dimers have been synthesised.[103-106] The *meso-meso* linked dyads had better π-overlap compared to the meso-β and β-β linked dimers.

In 2011, Senge and co-workers reported carbazole-linked dimers for organic light emitting diode applications (Fig. 1.24).[107] They synthesised porphyrin dimers *via* Suzuki coupling reactions between bromoporphyrins and borylated carbazoles.

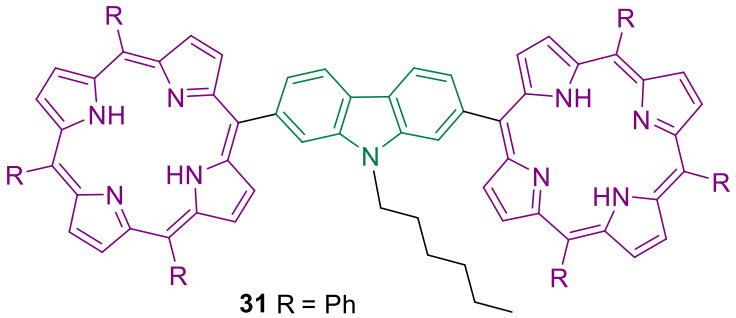

31 R = Ph

32 R = methylphenyl

Fig. 1.24. Porphyrin dimers linked *via* carbazole bridge.

Single layer organic light emitting diodes (OLEDs) were created to demonstrate the optical properties of these materials. Light emission from **31** and **32** showed better results compared to previously reported porphyrin with better electroluminescence.[107]

In recent reports, Bakar and co-workers synthesised dimers and trimers of a fluorenone-appended porphyrin *via* Lindsey optimised Sonogashira coupling reaction (Fig. 1.25).[108] The photophysical properties of compound **33** were investigated upon excitation of the fluorenone arms which act as donors.[109] Interestingly, the emission profiles of the covalently linked porphyrin indicated that the diphenyleneacetylene bonds are important for effective intramolecular energy transfer between the porphyrin units.[108]

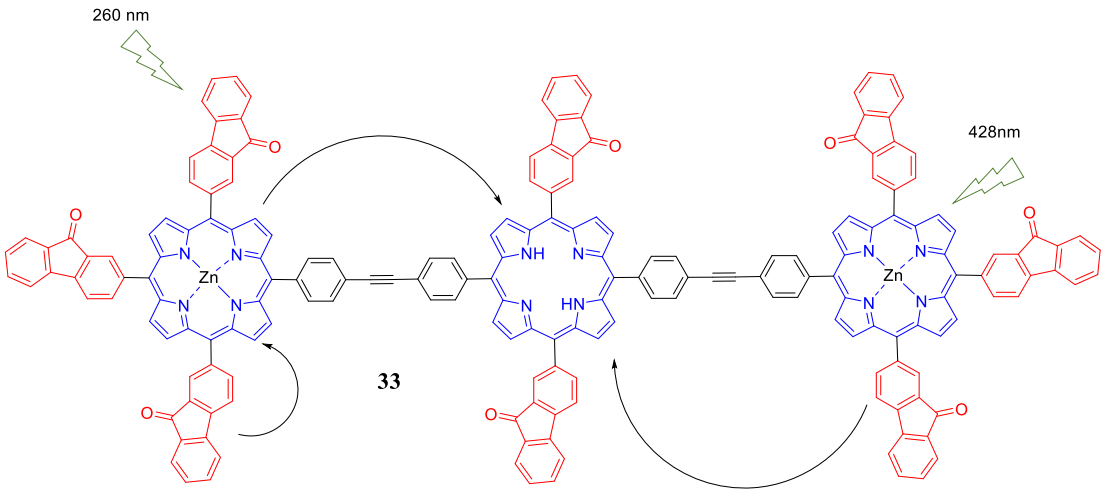

Fig. 1.25. Example of possible energy donors (fluorenone) and acceptors (porphyrin free-base and zinc) synthesised *via* Sonogashira coupling. Lightning bolts indicate photoexcitation and arrows shows possible electron transfer pathways.[108]

1.6.2 Porphyrin-Fullerene-C_{60} Dyads

Porphyrin and fullerene components are commonly used in the design and synthesis of donor-acceptor (D-A) molecular frameworks for artificial photosynthetic models, LHCs, and supramolecular assemblies.[36, 85-86, 90, 110-111] Fullerene-C_{60} shows small reorganisation energy associated with the electron transfer process which is a prerequisite for attaining relatively long-lasting photoinduced charge separated (CS) states in dyad and triad complexes.[112-117]

Also, the introduction of a molecular bridge or spacer between the D-A chromophores where the aim is to achieve long-lived CS states may strongly alter the electronic coupling has been the subject of intensive investigation in recent years.[118-119] The bridging molecule between donor-acceptor units, control their mutual orientation and determine the distance between the donor and the acceptor chromophore which affects the electronic coupling between D-A and thus rate of electron transfer. Moreover, most commonly reported D-A dyads and triads are separated by either linear bridge molecules or conjugated systems.[89, 120] For instance, a recent report from Tsuji,

Guldi, Nakamura[89] and co-workers demonstrated the electron transfer through rigid molecular wires enhanced by electronic and electron-vibration coupling (Fig. 1.26). The investigation revealed photoinduced electron transfer using donor-bridge-acceptor molecules, in which π-conjugated wires were employed as bridges. They demonstrated that the carbon-bridge oligo-*p*-phenylenevinylene (COPV) **34**, a rigid and flat structure, shows an 840-fold increase in electron transfer rate compared to **35** which has a flexible non-conjugated molecular bridge.[89]

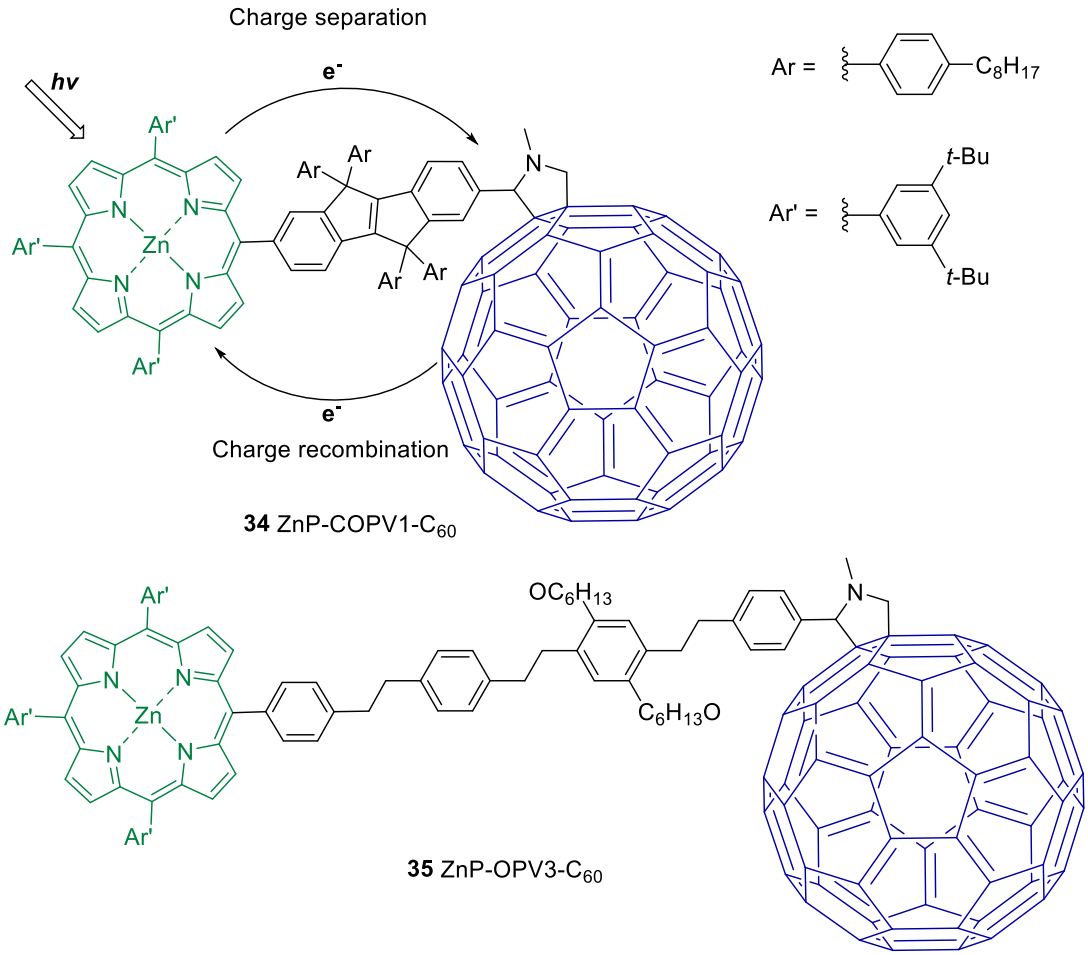

Fig. 1.26. Zinc porphyrin-fullerene-C_{60} conjugates linked by carbon-bridged oligo-*p*-phenylvinylenes (COPVs) that possess a rigid and planar structure (top) and zinc porphyrin-fullerene-C_{60} conjugates linked by OPVs, with flexible linker (green-porphyrin serve as an electron donor, blue-C_{60} as an electron acceptor).[89]

This type of nonlinear effect demonstrates the flexibility and potential practical utility of COPVs in molecular device applications. Covalently linked porphyrin-fullerene dyads have afforded extensive insights into the electron transfer mechanism of the natural photosynthetic processes and promising examples to mimic these natural processes have also been developed in recent years. Unfortunately, the synthesis of such molecular systems includes tedious, challenging and low-yielding multistep synthetic strategies and therefore limiting their practical applications. However, a constant effort to develop such molecular systems is of critical importance since an affordable and reliable artificial photosynthetic model must be discovered to ensure future energy needs.[85, 87, 121]

Much interest has been shown by Crossley, Reimers and Fukuzumi in the mimicry of photoinduced electron transfers. Recently, they reported on synthetically tuneable biomimetic artificial photosynthetic reaction centres that closely resemble the natural system in purple bacteria[122] which overcome the deficiencies of previous photosynthetic models. In the latest model, they introduced the modified photosynthetic mimics **$(MP)_2Q$-Q_2HP-C_{60}** (Fig. 1.27) (M = Zn or 2H) to remove these differences. The inclusion of a "special pair" is not vital in the artificial system and most compounds in current use are more like their previous designs.[122]

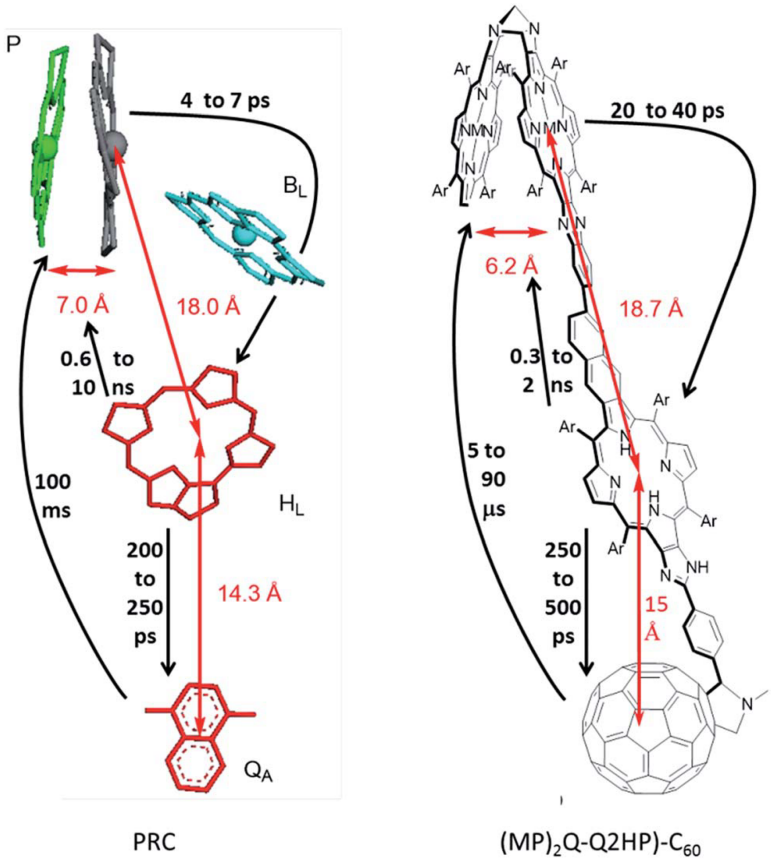

M = Zn(II) or 2H, Ar = 3,5-di-*tert*-butylphenyl

Fig. 1.27. Schematic representation of the chromophores in the PRC from *Rhodopseudomonas viridis,* with inter-chromophoric distances and process rates shown (Left). Crossley's artificial photosynthetic model, **$(MP)_2Q$-Q_2HP-C_{60})**, with inter-chromophoric distances and analogues rates shown. BL = auxiliary bacteriochlorophyll, P = 'special pair', HL = primary-acceptor bacteriophytin, and QA = secondary-acceptor menaquinone.[122]

A detailed investigation of electron transfer mechanism using femtosecond and nanosecond transient absorption spectroscopy was conducted, wherein all models showed picosecond-timescale charge separations and the final singlet charge-separation with microsecond-timescale. The rigid, synthetically flexible molecule provides a close mimic to the natural photosynthetic reaction centre. It also opens the way for the

construction of light harvesters with controllable redox, kinetic and absorption properties.[122]

1.6.3 Porphyrin-Naphthalene Diimide Dyads

Apart from the fullerene C_{60} as an electron acceptor discussed above, the use of naphthalene diimide as an electron acceptor component for the construction of donor-acceptor complexes has attracted considerable interest in the last two decade.[57, 68] Due to the favourable properties of NDI such as high electron affinity, good charge carrier mobility, and excellent thermal and oxidative stability, these features enhance their use in construction of donor-acceptor dyads.[123-126] In 2010, Bhosale and Vauthey reported on the excited dynamics of strongly coupled porphyrin core substituted naphthalene diimide dyads (Fig. 1.28).[127]

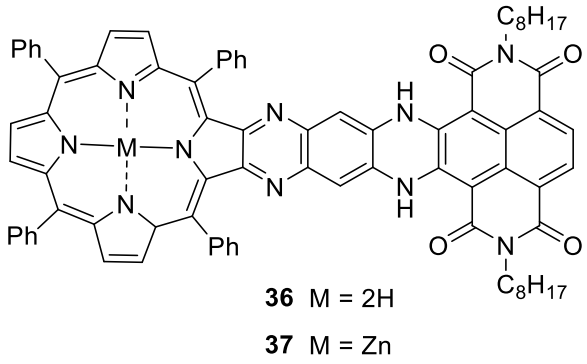

Fig. 1.28. Porphyrin-naphthalene diimide dyads linked *via* quinoxaline bridge.

The dyads **36** and **37** were synthesised by the condensation of the *ortho*-diamine functionalised NDI with tetraphenylporphyrin-2,3-dione in high yield. The rigid aromatic diaza bridge core substituted NDI dyads were studied using femtosecond-resolved spectroscopy to investigate the excited state properties of free-base and zinc dyads. They found that the excited state dynamics of **36** and **37** are strongly solvent dependent with a fluorescence lifetime that shortens by a factor of 500-1000 when

going from nonpolar to polar solvent.[127] This impressive outcome is due to strong electronic coupling between the electron donor and acceptor unit.

In another report,[128] the same authors reported excited state dynamics of two triads consisting of NDI substituted at the core position by two zinc porphyrins or free-base porphyrins (Fig. 1.29). Ultrafast fluorescence decay was measured in THF and benzonitrile, demonstrating charge separation from the excited porphyrin to the NDI took place with ~1 ps time constants in **39** and ~25 ps time constants in **38**.

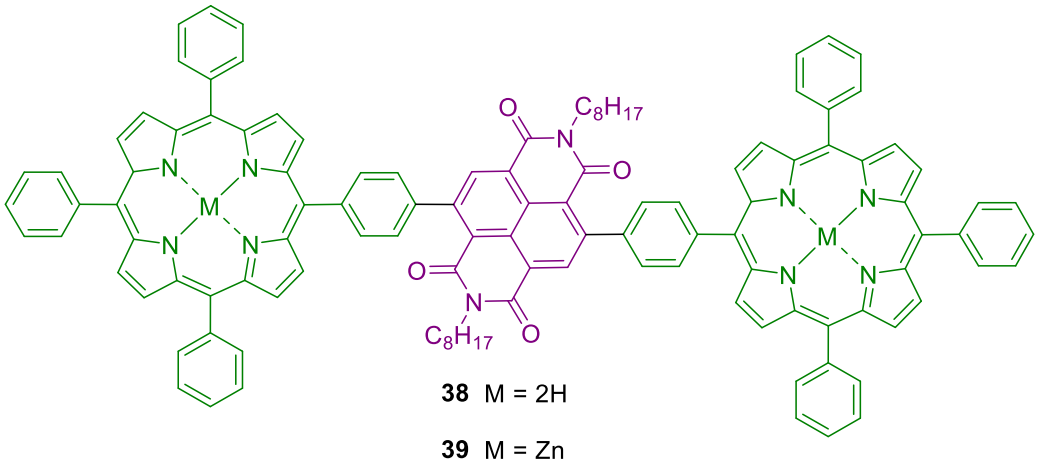

38 M = 2H

39 M = Zn

Fig. 1.29. bis-Tetraphenylporphyrin triad bridged by naphthalene diimide.

Wasielewski and co-workers recently reported the synthesis and photoinduced electron transfer properties of a series of self-assembling cyclic tetramers using chlorophyll-based donor-acceptor building blocks (Fig. 1.30).[124]

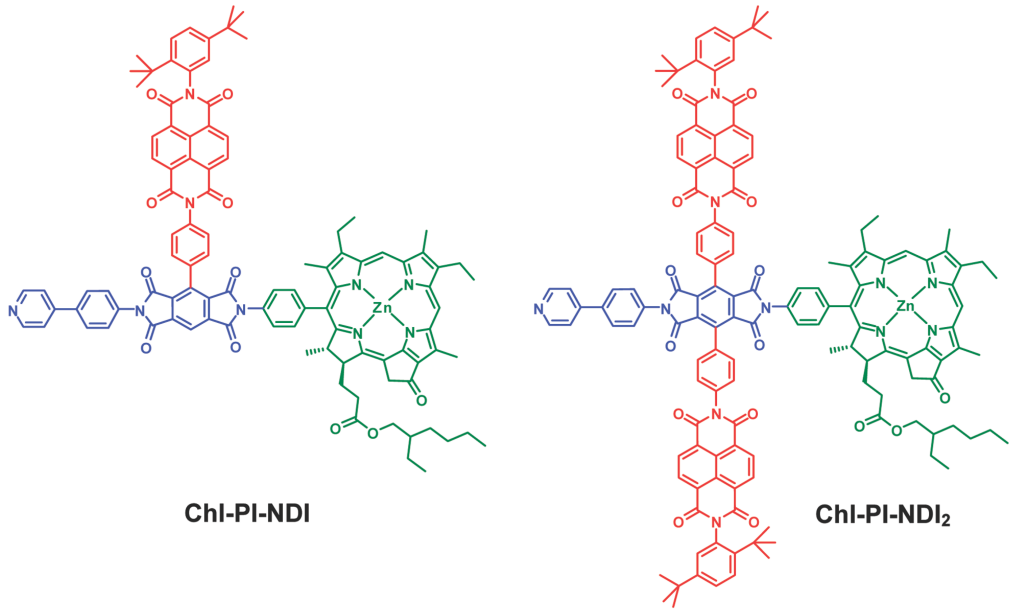

Fig. 1.30. Porphyrin–pyrromellitimide–naphthalene diimide donor-acceptor triad structures.

They converted chlorophyll *a* into zinc methyl 3-ethylpyrochlorophyllide *a* (Chl) and then further modified at its 20-position to append a pyrromellitimide (PI) acceptor bearing a pyridine ligand and one or two NDI units as a secondary electron acceptor to give **Chl-PI-NDI** and **Chl-PI-NDI$_2$**. Hence, investigation by femtosecond and nanosecond transient absorption analysis of dyads revealed charge recombination in the **Chl-PI-NDI2** cyclic tetramer (τ_{CR} = 30 ± 1 ns) was slower by a factor of 3 relative the monomeric building blocks. This indicates that the self-assembly of these building blocks into the cyclic tetramers alters their structure in a way that extends their charge separation lifetimes, which is beneficial for the design of artificial photosynthetic systems.

1.7 Overall Aims of the Projects

The overall aims of this work is to employ a Tröger's base as a rigid linker for the attachment of chromophores (e.g. porphyrin, fullerene-C_{60} and naphthalene diimide) that are commonly used in the development of photosynthetic reaction centre mimics

(PRC) or light harvesting complexes (LHCs). The scaffold is essentially two aromatic rings that are held in a rigid V-shaped arrangement as a result of non-conjugated diazocine bridging unit. In terms of PRCs and LHCs, the overwhelming majority of previous work has involved conjugated linkers. However, development of supramolecular donor-acceptor complexes with through-space charge transfers rather than through bond between the two chromophores is unknown. As the connection between the donor and the acceptor molecule is based on supramolecular interactions (weaker, reversible and non-covalent), this often produces ambiguous photophysical results. Non-conjugated and a rigid bridging molecules between the donor and the acceptor chromophore is of prime importance in order to achieve our stated goals. It is a major aim of this work to explore the synthesis of rigid donor-acceptor dyads separated by bent non-conjugated linker that could be potentially useful for electron transport investigation through-space.

1.7.1 Specific Aims of the Study

- To investigate and synthesise symmetric and hybrid Tröger's bases
- To investigate and optimise methodologies for the preparation of synthetically useful, soluble and easy functionalisable porphyrin Tröger's base conjugates in gram quantities.
- To investigate and synthesise bis-NDI Tröger's base *via* post-modification of TB
- To utilise hybrid Tröger's base to append C_{60}.
- To utilise the porphyrins and porphyrin-Tröger's bases building blocks for the synthesis of dyads, for example,
    - 1) Porphyrin-TB-porphyrin dyads
    - 2) Porphyrin-TB-fullerene dyads

- 3) Porphyrin-TB-NDI dyads.

- Characterise the structural, spectroscopic and electronic properties of all compounds mentioned above by
  - ^{1}NMR spectroscopy
  - IR spectroscopy
  - Mass spectroscopy
  - UV/Visible spectroscopy
  - Fluorescence spectroscopy

1.8 References

1. Tröger, J., *J. Prakt. Chem.* **1887**, *36*, 225-245.
2. Spielman, M. A., *J. Am. Chem. Soc.* **1935**, *57*, 583-585.
3. Larson, S. B.; Wilcox, C. S., *Acta Crystallogr., Sect. C: Cryst. Struct. Commun.* **1986**, *42*, 224-227.
4. Cowart, M. D.; Sucholeiki, I.; Bukownik, R. R.; Wilcox, C. S., *J. Am. Chem. Soc.* **1988**, *110*, 6204-6210.
5. Wang, Z. G.; Wang, D.; Jin, J., *Macromolecules* **2014**, *47*, 7477-7483.
6. Wang, Z. G.; Wang, D.; Zhang, F.; Jin, J., *Acs Macro Lett.* **2014**, *3*, 597-601.
7. Neogi, I.; Jhulki, S.; Ghosh, A.; Chow, T. J.; Moorthy, J. N., *Acs Appl. Mater. Interfaces* **2015**, *7*, 3298-3305.
8. Kim, E.; Paliwal, S.; Wilcox, C. S., *J. Am. Chem. Soc.* **1998**, *120*, 11192-11193.
9. Wilcox, C. S.; Adrian, J. C.; Webb, T. H.; Zawacki, F. J., *J. Am. Chem. Soc.* **1992**, *114*, 10189-10197.
10. Crossley, M. J.; Hambley, T. W.; Mackay, L. G.; Try, A. C.; Walton, R., *J. Chem. Soc., Chem. Commun.* **1995**, 1077-1079.
11. Jensen, J.; Wärnmark, K., *Synthesis* **2001**, 1873-1877.

12. Periasamy, M.; Suresh, S.; Satishkumar, S., *Tetrahedron: Asymmetry* **2012**, *23*, 108-116.

13. Satishkumar, S.; Periasamy, M., *Tetrahedron: Asymmetry* **2006**, *17*, 1116-1119.

14. Li, Z.; Xu, X. Y.; Peng, Y. Q.; Jiang, Z. X.; Ding, C. Y.; Qian, X. H., *Synthesis* **2005**, 1228-1230.

15. Webb, T. H.; Wilcox, C. S., *J. Org. Chem.* **1990**, *55*, 363-365.

16. Runarsson, O. V.; Artacho, J.; Wärnmark, K., *Eur. J. Org. Chem.* **2012**, 7015-7041.

17. Wilcox, C. S., *Tetrahedron Lett.* **1985**, *26*, 5749-5752.

18. Bag, B. G., *Curr. Sci.* **1995**, *68*, 279-288.

19. Sergeyev, S., *Helv. Chim. Acta* **2009**, *92*, 415-444.

20. Dolensky, B.; Elguero, J.; Kral, V.; Pardo, C.; Valik, M., *Adv Heterocycl. Chem.* **2007**, *93*, 1-56.

21. Valik, M.; Cejka, J.; Havlik, M.; Kral, V.; Dolensky, B., *Chem. Commun.* **2007**, 3835-3837.

22. Valik, M.; Dolensky, B.; Herdtweck, E.; Kral, V., *Tetrahedron: Asymmetry* **2005**, *16*, 1969-1974.

23. Miller, T. R.; Wagner, E. C., *J. Am. Chem. Soc.* **1941**, *63*, 832-836.

24. Cerrada, L.; Cudero, J.; Elguero, J.; Pardo, C., *J. Chem. Soc., Chem. Commun.* **1993**, 1713-1714.

25. Cudero, J.; Pardo, C.; Ramos, M.; GutierrezPuebla, E.; Monge, A.; Elguero, J., *Tetrahedron* **1997**, *53*, 2233-2240.

26. Hansson, A.; Jensen, J.; Wendt, O. F.; Wärnmark, K., *Eur. J. Org. Chem.* **2003**, 3179-3188.

27. Wagner, E., *J. Org. Chem.* **1954**, *19*, 1862-1881.

28. Farrar, W., *J. App. Chem.* **1964**, *14*, 389-399.

29. Johnson, R. A.; Gorman, R. R.; Wnuk, R. J.; Crittenden, N. J.; Aiken, J. W., *J. Med. Chem.* **1993**, *36*, 3202-3206.

30. Didier, D.; Sergeyev, S., *Eur. J. Org. Chem.* **2007**, 3905-3910.

31. Faroughi, M.; Zhu, K. X.; Jensen, P.; Craig, D. C.; Try, A. C., *Eur. J. Org. Chem.* **2009**, 4266-4272.

32. Smith, K. M., *Porphyrins and metalloporphyrins*. Elsevier Amsterdam: 1975; Vol. 9.

33. Kadish, K. M.; Smith, K. M.; Guilard, R., *The Porphyrin Handbook: Multiporphyrins, multiphthalocyanines, and arrays*. Academic Press: 2003; Vol. 18.

34. Eu, S.; Hayashi, S.; Umeyama, T.; Matano, Y.; Araki, Y.; Imahori, H., *J. Phy. Chem., C* **2008**, *112*, 4396-4405.

35. Liao, M. S.; Scheiner, S., *J. Chem. Phy.* **2002**, *117*, 205-219.

36. Tkachenko, N. V.; Lemmetyinen, H.; Sonoda, J.; Ohkubo, K.; Sato, T.; Imahori, H.; Fukuzumi, S., *J. Phys. Chem. A* **2003**, *107*, 8834-8844.

37. Zheng, W.; Shan, N.; Yu, L.; Wang, X., *Dyes Pigm.* **2008**, *77*, 153-157.

38. Atwood, J. L.; Suslick, K. S.; Lehn, J.-M., *Comprehensive supramolecular chemistry: Supramolecular reactivity and transport: bioinorganic systems. Vol. 5*. Elsevier: 1996; Vol. 4.

39. Rothemund, P., *J. Am. Chem. Soc.* **1935**, *57*, 2010-2011.

40. Adler, A. D.; Longo, F. R.; Finarelli, J. D.; Goldmacher, J.; Assour, J.; Korsakoff, L., *J. Org. Chem.* **1967**, *32*, 476-476.

41. Adler, A. D.; Longo, F. R.; Kampas, F.; Kim, J., *J. Inorg. Nucl. Chem.* **1970**, *32*, 2443-2445.

42. Calvin, M.; Ball, R.; Aronoff, S., *J. Am. Chem. Soc.* **1943**, *65*, 2259-2259.

43. Lindsey, J. S.; Hsu, H. C.; Schreiman, I. C., *Tetrahedron lett.* **1986**, *27*, 4969-4970.

44. Lindsey, J. S.; Schreiman, I. C.; Hsu, H. C.; Kearney, P. C.; Marguerettaz, A. M., *J. Org. Chem.* **1987**, *52*, 827-836.

45. Littler, B. J.; Ciringh, Y.; Lindsey, J. S., *J. Org. Chem.* **1999**, *64*, 2864-2872.

46. Milgrom, L., The Colours of Life: An Introduction to the Chemistry of Porphyrins and Related Compounds OUP. Oxford: 1997.

47. Smith, N. W.; Dzyuba, S. V., *Arkivoc* **2010**, *7*, 10-18.

48. Chauhan, S.; Kumar, A.; Srinivas, K., *Synth. commun.* **2004**, *34*, 2673-2680.

49. Smith, K. M.; Barnett, G. H.; Evans, B.; Martynenko, Z., *J. Am. Chem. Soc.* **1979**, *101*, 5953-5961.

50. Dolphin, D.; Muljiani, Z.; Rousseau, K.; Borg, D.; Fajer, J.; Felton, R., *Ann. N. Y. Acad. Sci.* **1973**, *206*, 177-200.

51. Crossley, M. J.; Try, A. C.; Walton, R., *Tetrahedron Lett.* **1996**, *37*, 6807-6810.

52. Crossley, M. J.; Sintic, P. J.; Hutchison, J. A.; Ghiggino, K. P., *Org. Biomol. Chem.* **2005**, *3*, 852-865.

53. Tatar, A.; Valík, M.; Novotná, J.; Havlík, M.; Dolenský, B.; Král, V.; Urbanová, M., *Chirality* **2014**, *26*, 361-367.

54. Stewart, W. W., *Nature* **1981**, *292*, 17-21.

55. Wurthner, F.; Stolte, M., *Chem. Commun.* **2011**, *47*, 5109-5115.

56. Jones, B. A.; Facchetti, A.; Wasielewski, M. R.; Marks, T. J., *J. Am. Chem. Soc.* **2007**, *129*, 15259-15278.

57. Bhosale, S. V.; Jani, C. H.; Langford, S. J., *Chem. Soc. Rev.* **2008**, *37*, 331-342.

58. Duke, R. M.; Veale, E. B.; Pfeffer, F. M.; Kruger, P. E.; Gunnlaugsson, T., *Chem. Soc. Rev.* **2010**, *39*, 3936-3953.

59. Veale, E. B.; Tocci, G. M.; Pfeffer, F. M.; Kruger, P. E.; Gunnlaugsson, T., *Org. Biomol. Chem.* **2009**, *7*, 3447-3454.

60. Wang, H.; Wu, H.; Xue, L.; Shi, Y.; Li, X., *Org. Biomol. Chem.* **2011**, *9*, 5436-5444.

61. Zheng, S.; Lynch, P. M.; Rice, T. E.; Moody, T. S.; Gunaratne, H. N.; de Silva, A. P., *Photochem. Photobiol. Sci.* **2012**, *11*, 1675-1681.

62. Ryan, G. J.; Quinn, S.; Gunnlaugsson, T., *Inorg. Chem.* **2008**, *47*, 401-403.

63. Banerjee, S.; Kitchen, J. A.; Bright, S. A.; O'Brien, J. E.; Williams, D. C.; Kelly, J. M.; Gunnlaugsson, T., *Chem. Commun.* **2013**, *49*, 8522-8524.

64. Banerjee, S.; Kitchen, J. A.; Gunnlaugsson, T.; Kelly, J. M., *Org. Biomol. Chem.* **2013**, *11*, 5642-5655.

65. Qian, X.; Xiao, Y.; Xu, Y.; Guo, X.; Qian, J.; Zhu, W., *Chem. Commun.* **2010**, *46*, 6418-6436.

66. Calatrava-Pérez, E.; Bright, S. A.; Achermann, S.; Moylan, C.; Senge, M. O.; Veale, E. B.; Williams, D. C.; Gunnlaugsson, T.; Scanlan, E. M., *Chem. Commun.* **2016**, *52*, 13086-13089.

67. Horne, W. S.; Ashkenasy, N.; Ghadiri, M. R., *Chemistry* **2005**, *11*, 1137-44.

68. Kobaisi, M. A.; Bhosale, S. V.; Latham, K.; Raynor, A. M.; Bhosale, S. V., *Chem. Rev.* **2016**, *116*, 11685-11796.

69. Chen, Z.; Lohr, A.; Saha-Moller, C. R.; Wurthner, F., *Chem. Soc. Rev.* **2009**, *38*, 564-584.

70. Borgström, M.; Shaikh, N.; Johansson, O.; Anderlund, M. F.; Styring, S.; Åkermark, B.; Magnuson, A.; Hammarström, L., *J. Am. Chem. Soc.* **2005**, *127*, 17504-17515.

71. Iengo, E.; Pantos, G. D.; Sanders, J. K. M.; Orlandi, M.; Chiorboli, C.; Fracasso, S.; Scandola, F., *Chem. Sci.* **2011**, *2*, 676-685.

72. Debreczeny, M. P.; Svec, W. A.; Wasielewski, M. R., *Science* **1996**, *274*, 584-587.

73. Handayani, M.; Gohda, S.; Tanaka, D.; Ogawa, T., *Chem. Eur. J.* **2014**, *20*, 7655-7664.

74. Deprez, N. R.; McNitt, K. A.; Petersen, M. E.; Brown, R. G.; Lewis, D. E., *Tetrahedron lett.* **2005**, *46*, 2149-2153.

75. Veale, E. B.; Frimannsson, D. O.; Lawler, M.; Gunnlaugsson, T., *Org. Lett.* **2009**, *11*, 4040-4043.

76. Veale, E. B.; Gunnlaugsson, T., *J. Org. Chem.* **2010**, *75*, 5513-5525.

77. Banerjee, D.; Hu, Z.; Li, J., *Dalton Trans.* **2014**, *43*, 10668-10685.

78. Ayme, J.-F.; Beves, J. E.; Leigh, D. A.; McBurney, R. T.; Rissanen, K.; Schultz, D., *Nat. Chem.* **2012**, *4*, 15-20.

79. You, L.; Zha, D.; Anslyn, E. V., *Chem. Rev.* **2015**, *115*, 7840-7892.

80. Lloyd, G. O.; Steed, J. W., *Nat. Chem.* **2009**, *1*, 437-442.

81. Shanmugaraju, S.; Dabadie, C.; Byrne, K.; Savyasachi, A. J.; Umadevi, D.; Schmitt, W.; Kitchen, J. A.; Gunnlaugsson, T., *Chem. Sci.* **2017**, *8*, 1535-1546.

82. Kroto, H. W.; Allaf, A. W.; Balm, S. P., *Chem. Rev.* **1991**, *91*, 1213-1235.

83. Kroto, H. W.; Heath, J. R.; O'Brien, S. C.; Curl, R. F.; Smalley, R. E., *Nature* **1985**, *318*, 162-163.

84. Hirsch, A., *Nat. Mater.* **2010**, *9*, 868-871.

85. Guldi, D. M., *Chem. Soc. Rev.* **2002**, *31*, 22-36.

86. Wasielewski, M. R., *Chem. Rev.* **1992**, *92*, 435-461.

87. D'Souza, F.; Ito, O., *Coord. Chem. Rev.* **2005**, *249*, 1410-1422.

88. Coropceanu, V.; Cornil, J.; da Silva Filho, D. A.; Olivier, Y.; Silbey, R.; Brédas, J.-L., *Chem. Rev.* **2007**, *107*, 926-952.

89. Sukegawa, J.; Schubert, C.; Zhu, X.; Tsuji, H.; Guldi, D. M.; Nakamura, E., *Nat. Chem.* **2014**, *6*, 899-905.

90. Fukuzumi, S.; Guldi, D. M., *Electron transfer in chemistry* **2000**, 270-337.

91. Imahori, H.; Fukuzumi, S., *Adv. Funct. Mater.* **2004**, *14*, 525-536.

92. Hasobe, T.; Imahori, H.; Kamat, P. V.; Ahn, T. K.; Kim, S. K.; Kim, D.; Fujimoto, A.; Hirakawa, T.; Fukuzumi, S., *J. Am. Chem. Soc.* **2005**, *127*, 1216-1228.

93. Imahori, H.; Sekiguchi, Y.; Kashiwagi, Y.; Sato, T.; Araki, Y.; Ito, O.; Yamada, H.; Fukuzumi, S., *Chem. Eur. J.* **2004**, *10*, 3184-3196.

94. Fukuzumi, S.; Ohkubo, K.; Imahori, H.; Shao, J.; Ou, Z.; Zheng, G.; Chen, Y.; Pandey, R. K.; Fujitsuka, M.; Ito, O., *J. Am. Chem. Soc.* **2001**, *123*, 10676-10683.

95. Imahori, H.; Tamaki, K.; Guldi, D. M.; Luo, C.; Fujitsuka, M.; Ito, O.; Sakata, Y.; Fukuzumi, S., *J. Am. Chem. Soc.* **2001**, *123*, 2607-2617.

96. Imahori, H.; Tamaki, K.; Araki, Y.; Sekiguchi, Y.; Ito, O.; Sakata, Y.; Fukuzumi, S., *J. Am. Chem. Soc.* **2002**, *124*, 5165-5174.

97. Ishida, Y.; Ito, H.; Mori, D.; Saigo, K., *Tetrahedron lett.* **2005**, *46*, 109-112.

98. Khan, S. I.; Oliver, A. M.; Paddon-Row, M. N.; Rubin, Y., *J. Am. Chem. Soc.* **1993**, *115*, 4919-4920.

99. Maggini, M.; Scorrano, G.; Prato, M., *J. Am. Chem. Soc.* **1993**, *115*, 9798-9799.

100. Sergeyev, S.; Diederich, F., *Angew. Chem. Int. Ed. Engl.* **2004**, *43*, 1738-1740.

101. Ito, S.; Nakamoto, K.-i.; Uno, H.; Murashima, T.; Ono, N., *Chem. Commun.* **2001**,, 2696-2697.

102. Arnold, D. P.; Hartnell, R. D., *Tetrahedron* **2001**, *57*, 1335-1345.

103. Drobizhev, M.; Stepanenko, Y.; Rebane, A.; Wilson, C. J.; Screen, T. E. O.; Anderson, H. L., *J. Am. Chem. Soc.* **2006**, *128*, 12432-12433.

104. Drobizhev, M.; Stepanenko, Y.; Dzenis, Y.; Karotki, A.; Rebane, A.; Taylor, P. N.; Anderson, H. L., *J. Am. Chem. Soc.* **2004**, *126*, 15352-15353.

105. Winters, M. U.; Dahlstedt, E.; Blades, H. E.; Wilson, C. J.; Frampton, M. J.; Anderson, H. L.; Albinsson, B., *J. Am. Chem. Soc.* **2007**, *129*, 4291-4297.

106. Grozema, F. C.; Houarner-Rassin, C.; Prins, P.; Siebbeles, L. D. A.; Anderson, H. L., *J. Am. Chem. Soc.* **2007**, *129*, 13370-13371.

107. Ryan, A.; Tuffy, B.; Horn, S.; Blau, W. J.; Senge, M. O., *Tetrahedron* **2011**, *67*, 8248-8254.

108. Tan, K. X.; Lintang, H. O.; Maniam, S.; Langford, S. J.; Bakar, M. B., *Tetrahedron* **2016**, *72*, 5402-5413.

109. Paul-Roth, C. O.; Simonneaux, G., *Tetrahedron lett.* **2006**, *47*, 3275-3278.

110. Das, S. K.; Song, B.; Mahler, A.; Nesterov, V. N.; Wilson, A. K.; Ito, O.; D'Souza, F., *J. Phys. Chem. C* **2014**, *118*, 3994-4006.

111. Iehl, J.; Vartanian, M.; Holler, M.; Nierengarten, J.-F.; Delavaux-Nicot, B.; Strub, J.-M.; Van Dorsselaer, A.; Wu, Y.; Mohanraj, J.; Yoosaf, K.; Armaroli, N., *J. Mater. Chem.* **2011**, *21*, 1562-1573.

112. Imahori, H.; Tkachenko, N. V.; Vehmanen, V.; Tamaki, K.; Lemmetyinen, H.; Sakata, Y.; Fukuzumi, S., *J. Phys. Chem. A* **2001**, *105*, 1750-1756.

113. Hartnett, P. E.; Mauck, C. M.; Harris, M. A.; Young, R. M.; Wu, Y. L.; Marks, T. J.; Wasielewski, M. R., *J. Am. Chem. Soc.* **2017**, *139*, 749-756.

114. Bill, N. L.; Ishida, M.; Kawashima, Y.; Ohkubo, K.; Sung, Y. M.; Lynch, V. M.; Lim, J. M.; Kim, D.; Sessler, J. L.; Fukuzumi, S., *Chem. Sci.* **2014**, *5*, 3888-3896.

115. Bandi, V.; Gobeze, H. B.; Karr, P. A.; D'Souza, F., *J. Phys. Chem. C* **2014**, *118*, 18969-18982.

116. Bill, N. L.; Ishida, M.; Bahring, S.; Lim, J. M.; Lee, S.; Davis, C. M.; Lynch, V. M.; Nielsen, K. A.; Jeppesen, J. O.; Ohkubo, K.; Fukuzumi, S.; Kim, D.; Sessler, J. L., *J. Am. Chem. Soc.* **2013**, *135*, 10852-10862.

117. Tachibana, Y.; Vayssieres, L.; Durrant, J. R., *Nat. Photonics* **2012**, *6*, 511-518.

118. Fukuzumi, S.; Ohkubo, K.; Suenobu, T., *Acc. Chem. Res.* **2014**, *47*, 1455-1464.

119. Ricks, A. B.; Brown, K. E.; Wenninger, M.; Karlen, S. D.; Berlin, Y. A.; Co, D. T.; Wasielewski, M. R., *J. Am. Chem. Soc.* **2012**, *134*, 4581-4588.

120. Numata, T.; Murakami, T.; Kawashima, F.; Morone, N.; Heuser, J. E.; Takano, Y.; Ohkubo, K.; Fukuzumi, S.; Mori, Y.; Imahori, H., *J. Am. Chem. Soc.* **2012**, *134*, 6092-6095.

121. Kang, B.; Yang, W.; Lee, S.; Mukherjee, S.; Forstater, J.; Kim, H.; Goh, B.; Kim, T.-Y.; Voelz, V. A.; Pang, Y., *Sci. Rep.* **2017**, *7*.

122. Lee, S. H.; Blake, I. M.; Larsen, A. G.; McDonald, J. A.; Ohkubo, K.; Fukuzumi, S.; Reimers, J. R.; Crossley, M. J., *Chem. Sci.* **2016**, *7*, 6534-6550.

123. Ghiggino, K. P.; Hutchison, J. A.; Langford, S. J.; Latter, M. J.; Lee, M. A.-P.; Takezaki, M., *Aust. J. Chem.* **2006**, *59*, 179-185.

124. Gunderson, V. L.; Smeigh, A. L.; Kim, C. H.; Co, D. T.; Wasielewski, M. R., *J. Am. Chem. Soc.* **2012**, *134*, 4363-4372.

125. Jaggi, M.; Schmid, B.; Liu, S.-X.; Bhosale, S. V.; Rivadehi, S.; Langford, S. J.; Decurtins, S., *Tetrahedron* **2011**, *67*, 7231-7235.

126. Villamaina, D.; Bhosale, S. V.; Langford, S. J.; Vauthey, E., *Phys. Chem. Chem. Phys.* **2013**, *15*, 1177-1187.

127. Banerji, N.; Bhosale, S. V.; Petkova, I.; Langford, S. J.; Vauthey, E., *Phys. Chem. Chem. Phys.* **2011**, *13*, 1019-1029.

128. Villamaina, D.; Bhosale, S. V.; Langford, S. J.; Vauthey, E., *Phys. Chem. Chem. Phys.* **2013**, *15*, 1177-1187.

Chapter Two

2.1 Synthesis of Naphthalene Diimide Analogues of Tröger's Base and Hünlich's Base

2.2 Synthesis of a Halogen Functionalised Tröger's Base-C_{60} Analogue

Statement of Contribution

The research presented in this manuscript is based on work done by myself (M.I.A) except high-resolution mass spectra that were obtained commercially at Australian Proteome Analysis Facility (APAF), Macquarie University. The manuscript was written by the author and checked and edited by the principal supervisor (P.K).

Synthesis of Naphthalene Diimide Analogues of Tröger's Base and Hünlich's Base

Md Imam Ansari, Andrew Try, and Peter Karuso*

Department of Molecular Sciences, Macquarie University, Sydney NSW 2109, Australia

* Corresponding author. Tel.: +612-9850-8290 fax: +612-9850-8313, e-mail: peter.karuso@mq.edu.au

Abstract

Naphthalene diimide (NDI) has been used in the construction of a variety of donor-acceptor complexes and organic semiconductors. We report here synthesis and characterisation of V-shaped NDI-dimers separated by rigid and non-conjugated bringing molecule (Tröger's base). The synthesis is highly modular as the NDI is incorporated in the last step of the reaction. Appending the NDI unit after post-Tröger's base reaction, allows preparation of Tröger's base-NDI monomers. Although the dimers and monomers showed similar UV/Vis spectra, dimers are potential candidate to investigate through-space charge transfer between the two chromophores. Research on functional NDI architectures will in any case contribute to research on energy conversion and electron transport.

Introduction

Naphthalene diimide (NDI) is an attractive functional unit because of its high electron affinity, good charge carrier mobility, and excellent photochemical and thermal stability. These features make it suitable for fundamental investigations of photoinduced electron and energy transfer processes.[1-3] Over the past two decades, impressive efforts have been devoted to the development of NDI-based electron donor-acceptor dyads for various applications, such as optoelectronics and artificial photosynthetic models.[1, 4] Most dyads are separated by a conjugated bridging molecule between the two chromophores and thus electron and energy transfer phenomena investigated in conjugated molecular systems. However, development of supramolecular donor-acceptor complexes made available for through-space charge transfers rather than through bond between the two chromophores. As the connection between the donor and the acceptor molecule is based on supramolecular interaction (weaker, reversible and non-covalent), this often produces

ambiguous photophysical results. Therefore, non-conjugated and rigid bridging molecules between the donor and acceptor chromophores is of prime importance in order to achieve our stated aims. On the other hand, Tröger's base (TB) is a rigid, a C_2 symmetric and V-shaped, molecule that can accommodate two chromophores at a well-defined distance (Fig. 1).[5-6]

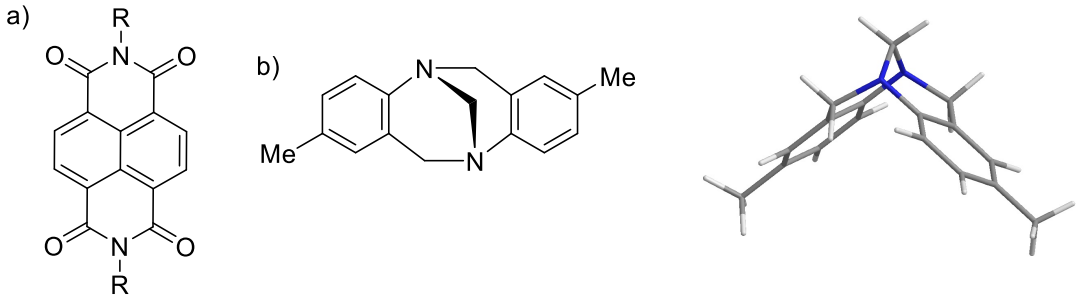

Fig. 1 Structural formula of a) NDI and b) Tröger's base and its V-shape geometry.

Crossley and co-workers synthesised porphyrin dyads bridged by non-conjugated and a rigid molecule.[6-7] Efforts to combine NDIs and TB into one framework have attracted a great deal of recent attention.[8-9] For instance, Lewis and co-workers reported the synthesis and fluorescence properties of naphthalimides-containing Tröger's base with medium-dependant fluorescence emission intensity.[10] Recently, Gunnlaugsson research group reported similar TB frameworks based on 4-amino-1,8-naphthalimide-based Tröger's base as high affinity DNA targeting fluorescent supramolecular scaffolds.[11] To the best of our knowledge, only 1,8-bis-naphthalimides Tröger's base have previously been prepared using commercially available compounds such as 4-nitro-1,8-naphthalic anhydride which can be reduced to an amino derivative for use in Tröger's base synthesis.[8, 11] Another important aspect is that the reported methodology can only provide symmetric TB product that limits the possibility to append another chromophore of interest. Although, the greater

efforts have been devoted to investigate their fluorescence properties, hybrid NDI-porphyrin frameworks have also been developed. Hybrid NDI-porphyrin associates have been built up by π-π intereactions.[12-13]

In contrast, post-modification of TB compounds will allow us to append either one or two NDI units onto the TB scaffold. Tröger's base with one NDI unit could be potentially useful to incorporate a second chromophore of interest. To investigate usefulness of post-modification of TB, symmetric dinitro TB and diamino TB were prepared as building blocks. Subsequently, Tröger's base- and Hünlich's base-NDI were prepared *via* a post-TB syntheses strategy. Successful incorporation of the NDI unit in the TB system encouraged us to apply this strategy to hybrid porphyrin Tröger's bases that are more complex and larger. These will be reported in due course (Chapter 5).

Results and discussion

Synthesis of amino functionalised Tröger's base

The dinitro Tröger's base **1**, was prepared as a racemic mixture by the condensation of commercially available 2-methyl-4-nitroaniline with paraformaldehyde in TFA.[14] The crude product was purified by column chromatography and reduced (H_2, 10% Pd/C) to afford **2** (Scheme 1). On the other hand, Hünlich's base **3** was prepared by the protocol of Gianins and co-workers,[15] using commercially available 2,4-diaminotoluene with dropwise addition of formaldehyde (37%) in the presence of H_2SO_4 (Scheme 2).[15] The TB compounds **1**, **2** and **3** were characterised by proton NMR with consistent data reported in the literature.[14-15]

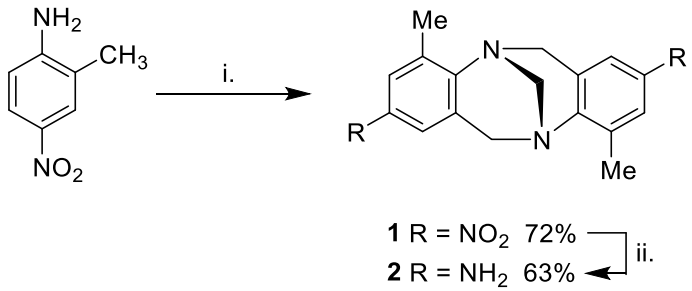

Scheme 1. i. TFA, $(CH_2O)_n$, Ar, rt, 5 days; ii. Pd (10% on carbon), ethanol, 3 days, under H_2 atmosphere.

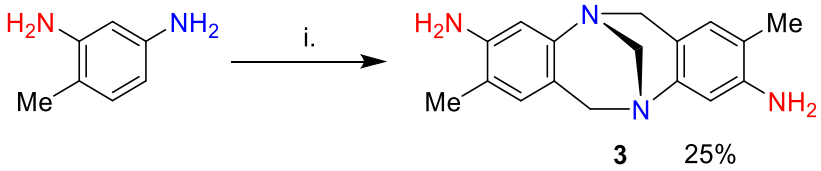

Scheme 2. Synthesis of Hünlich's base i. Formaldehyde (37% in H_2O), H_2SO_4 (5% in H_2O).

In order to append the NDI unit onto the TB framework, compound **4** was prepared according to the protocol of Wasielewski and Stoddart[2] by using commercially available 1,4,5,8-naphthalenetetracarboxylic dianhydride (**NDA**) and 1 equiv of *n*-hexylamine at 125 °C in DMF overnight. The desired monoimide **4**, was isolated in 25% yield after column chromatography (Scheme 3).

In spite of the advantages of **NDA** in organic molecular electronics, the major drawback as with many flat aromatic system is its lack of solubility. We envisioned using *n*-hexylamine in order to increase the disorder and thus solubility of the target compounds, leading to easier purification by column chromatography. This has been proven in the synthesis and isolation of our target compounds **6-9** that demonstrated comparatively better solubility than other NDI derivatives.

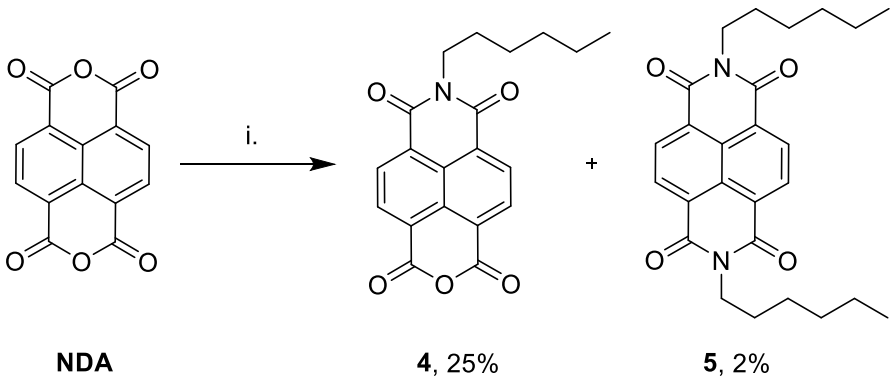

Scheme 3. i. Dry dimethylformamide, *n*-hexylamine, at 125 °C o/n Ar atmosphere.

Synthesis and characterisation of mono and bis-NDI Tröger's base and Hünlich's base

Next, employing the same approach of NDI functionalisation as shown in Scheme 3, we were able to react amino TB **2** and **4** (Scheme 4). The solvent was removed in *vacuo* and the crude compound was purified by column chromatography to give Tröger's base-NDI dimer **6** in 42% yield and Tröger's base-NDI monomer **7** in 28% yield. Similarly, the Hünlich's base-NDI dimer **8**, and monomer **9** were prepared under the same condition and purified by column chromatography to yield 30% and 15% respectively (Scheme 4). All the compounds were fully characterised by ^{1}H NMR and ^{13}C NMR spectroscopies (Supplementary Information). The ^{1}H NMR spectrum supports the identity of **6-9** by the presence of peaks between 3.90 and 5.00 ppm corresponding to the methylene bridges of TB and also reflecting the C_2 symmetry of compounds **6-9** (Fig. S1, S5, S9, S13). The HRMS of dimer **6** and dimer **8** correspond to molecular formula of $C_{57}H_{51}N_6O_8$ (Δmmu +0.8) and $C_{57}H_{51}N_6O_8$ (Δmmu −1.65), respectively (Fig.. S3, S11, HR-ESI). The presence of diimides in **6** and **8** was supported by IR spectroscopy ν_{max} 1663 and 1661, respectively (Fig. S4, S12).[8]

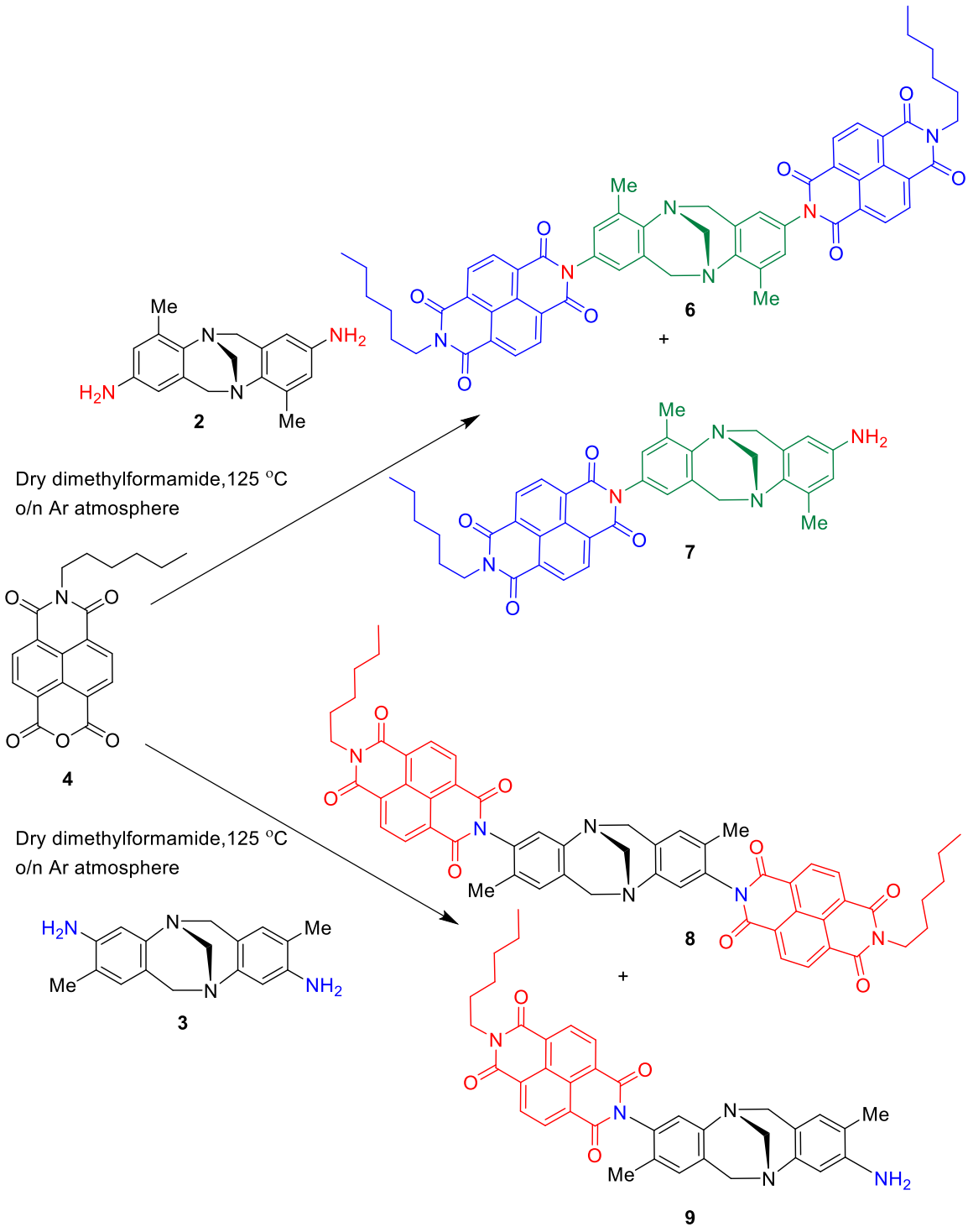

Scheme 4. Synthesis of Tröger's base-NDIs and Hünlich's base-NDIs.

UV/Visible Properties

The electronic properties of **6-9** with their controls **2-4** were investigated by UV/Vis absorption spectroscopy in acetonitrile (Figs 2, 3). These spectra showed typical vibronically saturated spectra with two well resolved sharp absorption peaks at 376 and 356 nm along with a shoulder peak at 337 nm, which is a characteristic of the $S_1 \leftarrow S_0$ transition with the electric dipole moment polarised along the long axis of the NDI core.[16] The absorption spectra of **6** and **7** differ from their controls (**2** and **4**) and display a slight red-shift (Fig. 2) and large variation is due to leading to an absorptive ICT. The rigid V-shaped Tröger's base bridge in dimer **6** likely allows some electronic interaction upon appending the NDI moieties.

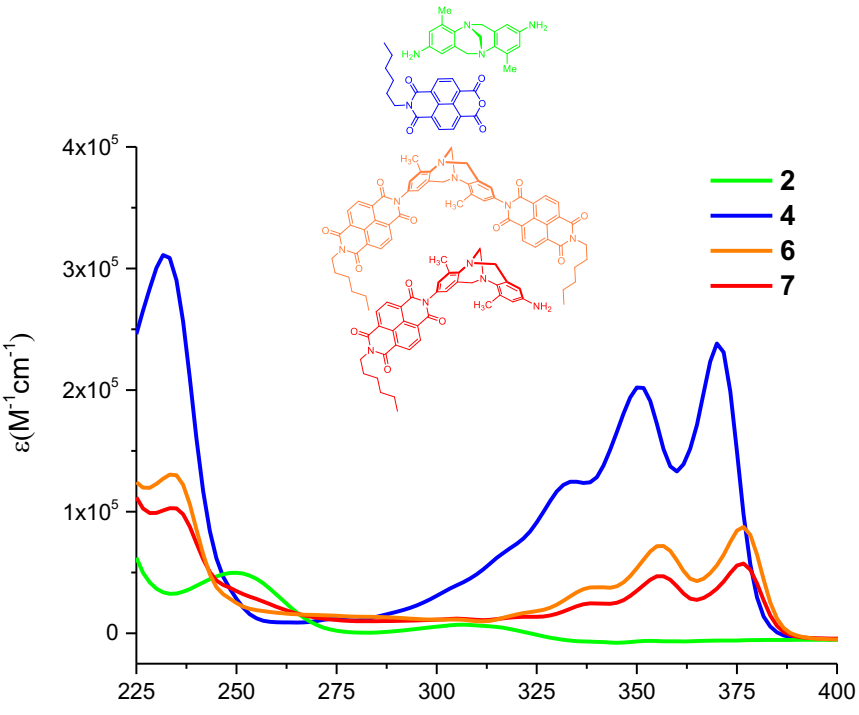

Fig. 2 UV/Vis spectra of **2** (green), **4** (blue), **6** (orange), and **7** (red) in acetonitrile. The concentration of each compound was 2.5×10^{-6} M.

Only a hyperchromic effect and little red-shift was observed in the case of dimer **6** compared to monomer **7**. Similar spectra were obtained in the case of dimer **8** and monomer **9** (Fig. 3).

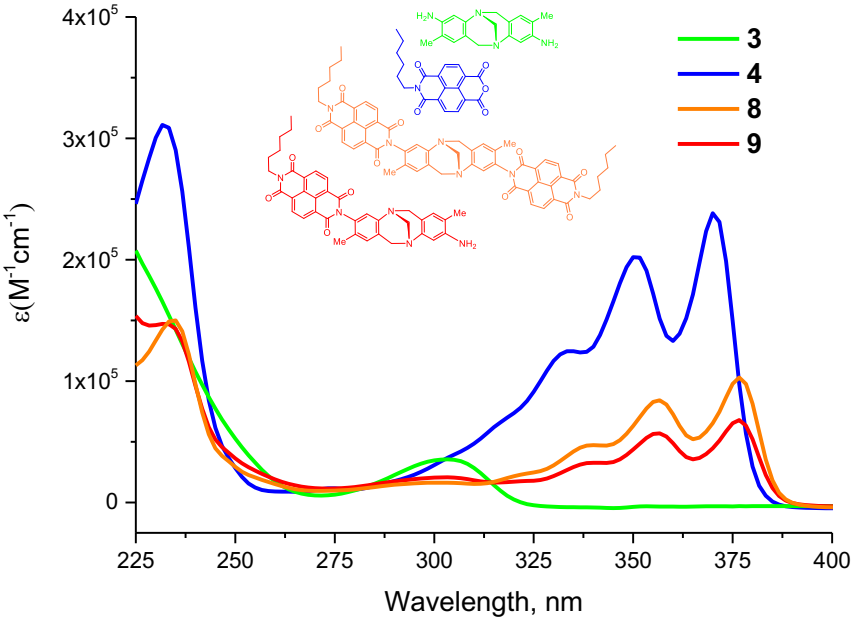

Fig. 3 UV/Vis spectra of **3** (green)**, 4** (blue), **8** (orange), and **9** (red) in acetonitrile. The concentration of each compound was 2.5×10^{-6} M.

Conclusion

Four distinct sets of host materials based on the Tröger's base scaffold were synthesised. The rigid and non-conjugated TB framework holds the two NDI units in close proximity due to the V-type configuration, resulting in through-space electronic interaction between the two NDIs. Although, the dimers showed similar spectra compared to monomers, a hyperchromic effect and little red-shift was observed. Simple synthetic protocols made ready access to these materials possible. Post-modification of TB permits easy access to Tröger's base- and Hünlich's base-NDI monomers in which further exploration could

improve access to more complex NDI-based architectures. For example, attachment of another chromophore of interest is possible in monomers. Research on functional NDI architectures will in any case contribute to research on energy conversion and electron transport. On the other hand, this successful incorporation of NDI units onto the TB framework encouraged us to construct more complex hybrid multimodular system such as porphyrin-TB-naphthalene diimide dyad which will be reported on in due course (Chapter 5).

Acknowledgements

This work was supported by Macquarie University (Sydney, Australia). We would also like to thank India@75 and Macquarie University for the award of an iMQRES PhD scholarship to M.I.A.

Experimental

General information: Reagents were purchased from Sigma-Aldrich and Alfa Aesar and used without purification unless otherwise stated.

^{1}H NMR and ^{13}C NMR spectra were recorded in Aldrich 5 mm NMR tubes on a Bruker DRX 400 NMR spectrometer (400 MHz) at 300 K unless otherwise stated, processed using Topspin 3.5, and referenced to residual solvent peak ($CDCl_3$ δ_H 7.26 and δ_C 77.01 ppm; DMSO-d_6 δ_H 2.49 and δ_C 39.5 ppm). The following abbreviations for multiplicity are used: s, singlet; d, doublet; t, triplet; m, multiplet; and dd, doublet of doublets. Column chromatography was carried out using the gravity feed column techniques on a Merck silica gel type 9385 (230-400 mesh) with the stated solvent systems. Analytical thin layer chromatography (TLC) analyses were performed on Merck silica gel 60 F254 sheets (0.2 mm). Visualisation of compounds was achieved by illumination under ultraviolet light

(254 nm). Charcoal and celite were pre-washed with MeOH and water before being used. HRMS (ESI) were performed at the Australian Proteome Analysis Facility (APAF), Macquarie University, Australia using a Q Exactive Plus hybrid quadrupole-orbitrap mass spectrometer (Thermo Scientific, Bremen, Germany). ESI-MS spectra were recorded using an Agilent 6130 single quadrupole mass spectrometer (Agilent Corp.). The IR spectra were taken on a Thermo Scientific Nicolet iS10 ATR FTIR spectrometer at 298 K. UV-visible absorbances were recorded on a Varian Cary 1Bio UV-visible spectrophotometer. All commercial solvents were of HPLC grade and used without further purification. Where solvent mixtures are used, the portions are given by volume. Chloroform used for photophysical experiments were HPLC grade purchased from Sigma-Aldrich (amylene stabilised).

4,10-Dimethyl-2,8-dinitro-6*H*,12*H*-5,11-methanodibenzo[*b*,*f*][1,5]diazocine 1

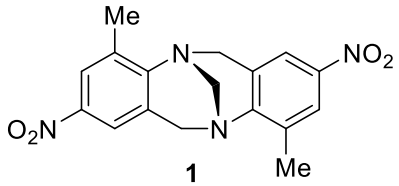

1

2-Methyl-4-nitroaniline (2.01 g, 13.1 mmol) and paraformaldehyde (828 mg, 27.4 mmol) were dissolved in trifluoroacetic acid (30 mL) and the mixture was stirred in the dark for 5 days. The reaction mixture was then poured onto ice (300 g), basified by the addition of sodium hydroxide (6 M; ~200 mL) and extracted with dichloromethane (3 × 100 mL). The organic layers were combined, washed with brine (200 mL), dried over anhydrous magnesium sulfate, filtered and evaporated to dryness to give yellow solid. The crude compound was purified by column chromatography (silica gel, 30% ethyl acetate/70% hexane) to afford 4,10-dimethyl-2,8-dinitro-6*H*,12*H*-5,11-

methanodibenzo[*b,f*][1,5]diazocine, (**1**) as a yellow solid (1.60 g, 72%). ^{1}H NMR (400 MHz, $CDCl_3$) δ 7.96 (d, *J* = 2.0 Hz, 2H, ArH), 7.72 (d, *J* = 2.0 Hz, 2H, ArH), 4.72 (d, *J* = 17.1, 2H, CH_2), 4.34 (s, 2H, CH_2), 4.12 (d, *J* = 17.1 Hz, 2H, CH_2), 2.51 (s, 6H, 2 × CH_3).These data are consisted with those reported from our lab.[14]

4,10-Dimethyl-6*H*,12*H*-5,11-methanodibenzo[*b,f*][1,5]diazocine-2,8-diamine 2

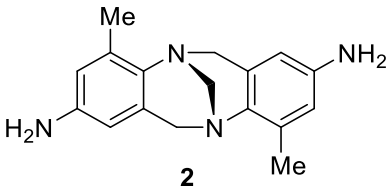

2

4,10-Dimethyl-2,8-dinitro-6*H*,12*H*-5,11-methanodibenzo[*b,f*][1,5]diazocine, (**1**) (1.01 g, 2.9 mmol) was dissolved in ethanol (20 mL). Palladium on carbon (10%; 80 mg) was added, and the reaction stirred under an atmosphere of hydrogen in the dark for 3 days. The reaction mixture was then filtered through celite and the solvent evaporated to dryness to afford a viscous brownish liquid crude. The crude compound was chromatographed (silica gel, 60% ethyl acetate/40% hexane) to afford diamino TB **2** as an off-white solid (500 mg, 61%); FTIR (neat) ν_{max} 3414, 3317, 3199, 2950, 2893, 1615, 1476, 1373, 1323, 1257, 1213, 1123, 1073. 992, 950, 917, 849, 805, 651 cm^{-1}. ^{1}H NMR (400 MHz, $CDCl_3$) δ 6.42 (d, *J* = 2.3 Hz, 2H, ArH), 6.09 (d, *J* = 2.3 Hz, 2 H, ArH), 4.45 (d, *J* = 16.7 Hz, 2H, CH_2), 4.28 (s, 2H, CH_2), 3.81 (d, *J* = 16.7 Hz, 2H, CH_2), 3.37 (br s, 4H, NH_2), 2.31 (s, 6H, CH_3). These data are consisted with those reported in literature.[17]

2,8-Dimethyl-6*H*,12*H*-5,11-methanodibenzo[*b*,*f*][1,5]diazocine-3,9-diamine (Hünlich's base) 3

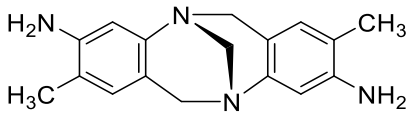

3

Formaldehyde (37% in H_2O; 1.1 mL, 14.6 mmol,) was added dropwise to a solution of 2,4-diaminotoluene (3.66 g, 30.0 mmol; 2.1 eq.) in aqueous sulphuric acid (5%; 100 mL). After the reaction was stirred for 36 h ammonia (25% in H_2O; 30 ml) was added and the precipitated crude product was separated by filtration. Purification was achieved by dissolving the raw material in hot methanol (15 mL) and slow addition of hot water (3-4 mL) then filtration to affod Hünlich's base **3** (1.01 g, 25%) as light brown solid. UV (CH_3CN) λ_{max} (log ε) 303 (3.87) nm; FTIR (neat) ν_{max} 3403, 3335, 2889, 2846, 1620, 1573, 1499, 1442, 1369, 1333, 1281, 1183, 1085, 1042, 995, 955, 913, 870, 670 cm^{-1}; ^1H NMR (400 MHz, DMSO-d_6) δ 6.42 (s, 2H, ArH), 6.25 (s, 2H, ArH), 4.55 (br s, 4H, 2 × NH_2), 4.35 (d, J = 16.0 Hz, 2H, CH_2), 4.02 (s, 2H, CH_2), 3.76 (d, J = 16.0 Hz, 2H, CH_2), 1.89 (s, 6H, 2 × CH_3).[15]

Compound 4

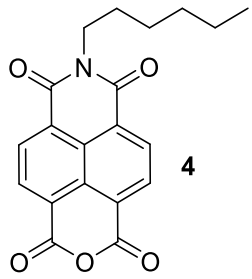

4

Naphthalene dianhydride (3.01 g, 11.2 mmol) was suspended in anhydrous dimethylformamide (30 mL) and heated to 125 ^oC under an argon atmosphere and stirred

at 125 °C to afford a brown slurry. 1-Hexylamine (1.1 mL, 8.9 mmol) was added dropwise over 30 min to aid the preferential formation of desired monoimide product, at which point a homogenous solution was obtained. The reaction was continued at 125 °C in an argon atmosphere overnight. Afterwards, the solution was cooled to room temperature and the solvent removed by rotary evaporation. The resulting residue was re-dissolved in dichloromethane, washed with water (2 × 50 mL) and the organic layer dried over anhydrous magnesium sulfate, filtered and evaporated to dryness. The brown crude product was then subjected to column chromatography (silica:dichloromethane) to afford the desired monoimide **4** as a white solid (1.01 g, 25%). UV/Vis (CH_3CN) λ_{max} (log ε) 233 (4.92), 351 (4.73), 370 (4.81) nm; ^{1}H NMR (400 MHz, $CDCl_3$) δ 8.82 (s, 4H, ArH), 4.20 (t, J = 7.6 Hz, 2H, CH_2), 1.68-1.79 (m, 2H, CH_2), 1.38-1.48 (m, 2H, CH_2), 1.26-1.38 (m, 4H, CH_2), 0.90 (t, J = 7.1 Hz, 3H, CH_3).[2]

4,10-Dimethyl 2,8-*bis*-(naphthalene diimide) Tröger's Base 6

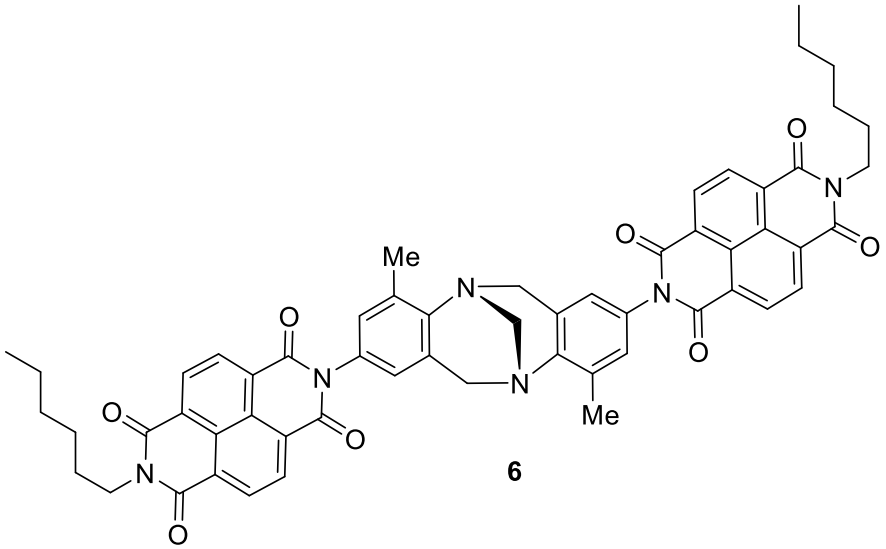

6

Compound **4** (250 mg, 0.71 mmol) was dissolved in dry dimethylformamide (30 ml) with diamino TB **2** (100 mg, 0.36 mmol) under an argon atmosphere. The reaction mixture was

stirred at 125 °C under an argon atmosphere overnight. The reaction progress was followed by TLC (chloroform 95% and 5% methanol), upon consumption of the starting material the reaction was stopped and cooled down to room temperature. Dimethylformamide was removed in *vacuo* and crude was chromatographed (silica gel, chloroform 95% and 5% methanol) to afford Tröger's base–NDI dimer **6** as a light orange solid (140 mg, 42%). UV/Vis (CH_3CN) λ_{max} (log ε) 233 (4.97), 357 (4.71), 377 (4.80) nm; FTIR (neat) ν_{max} 2957, 1707, 1663, 1578, 1450, 1333, 1244, 1187, 1081, 971, 880, 764, 725 cm^{-1}; ^1H NMR (400 MHz, $CDCl_3$) δ 8.78 (m, 8H, 2 × NDI ArH), 7.02 (d, J = 1.5 Hz, 2H, ArH), 6.80 (d, J = 1.5 Hz, 2H, ArH), 4.71 (d, J = 17.1 Hz, 2H), 4.38 (s, 2H, TB-bridge CH_2), 4.21 (t, J = 7.5 Hz, 4H, 2 × NDI N-CH_2), 4.16 (d, J = 17.1 Hz, 2H, TB-bridge-CH_2), 1.71-1.82 (m, 4H, 2 × CH_2), 2.46 (s, 6H, 2 × Ar-CH_3), 1.75 (m, 4H) 1.31-1.50 (m, 12H, 6 × CH_2), 0.90 (t, J = 7.0 Hz, 6H, 2 × CH_3); ^{13}C NMR (100 MHz, $CDCl_3$) δ 163.11, 162.79, 146.88, 135.00, 131.35, 131.01, 123.00, 129.27, 128.60, 127.01, 126.93, 126.81, 126.72, 124.11, 66.97, 54.46, 41.05, 31.48, 28.03, 26.74, 22.54, 17.26, 14.01; HRMS (ESI) (*m/z*): calcd for $C_{57}H_{51}N_6O_8$ 947.3768; found 947.3776 $[M+H]^+$.

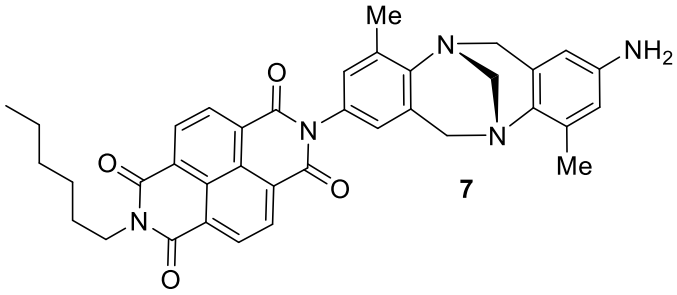

7

A second compound eluted (Tröger's base-NDI monomer **7**) as a dark green solid (30 mg, 28%). UV/Vis (CH_3CN) λ_{max} (log ε) 233 (4.67), 357 (4.34), 377 (4.43) nm; FTIR (neat) ν_{max} 3365, 2951, 1703, 1662, 1581, 14756, 1452, 1371, 1331, 1247, 1211, 1192, 1075, 991, 951, 919, 846, 762, 725, 649 cm^{-1}; ^1H NMR (400 MHz, $CDCl_3$) δ 8.70-8.80 (m, 4H,

NDI-ArH), 6.98 (d, J = 2.0 Hz, 1H, ArH), 6.74 (d, J = 2.0 Hz, 1H, ArH), 6.42 (d, J = 2.3 Hz, 1H, ArH), 6.12 (d, J = 2.3 Hz, 1H, ArH), 4.57 (t, J = 17.6 Hz, 2H), 4.32 (s, 2H, bridge CH_2), 4.20 (t, J = 7.6 Hz, 2H, NDI N-CH_2), 3.98 (d, J = 4.0 Hz, 1H, CH_2), 3.95 (d, J = 4.0 Hz, 1H, CH_2), 3.40 (br s, 2H, NH_2), 2.45 (s, 3H, Ar-CH_3), 2.30 (s, 3H, Ar-CH_3), 1.71-1.82 (m, 2H, CH_2), 1.23-1.50 (m, 6H, 3 × CH_2), 0.90 (t, J = 7.0 Hz, 3H, CH_3); ^{13}C NMR (100 MHz, $CDCl_3$) δ 163.11, 162.79, 146.88, 135.00, 131.35, 131.01, 123.00, 129.27, 128.60, 127.01, 126.93, 126.81, 126.72, 124.11, 66.97, 54.46, 41.05, 31.48, 28.03, 26.74, 22.54, 17.26, 14.01; HRMS (ESI) (*m/z*): calcd for $C_{37}H_{36}N_5O_4$ 614.2767; found 614.2753 $[M+H]^+$.

2,8-Dimethyl 3,9-bis-NDI-Hünlich's Base 8

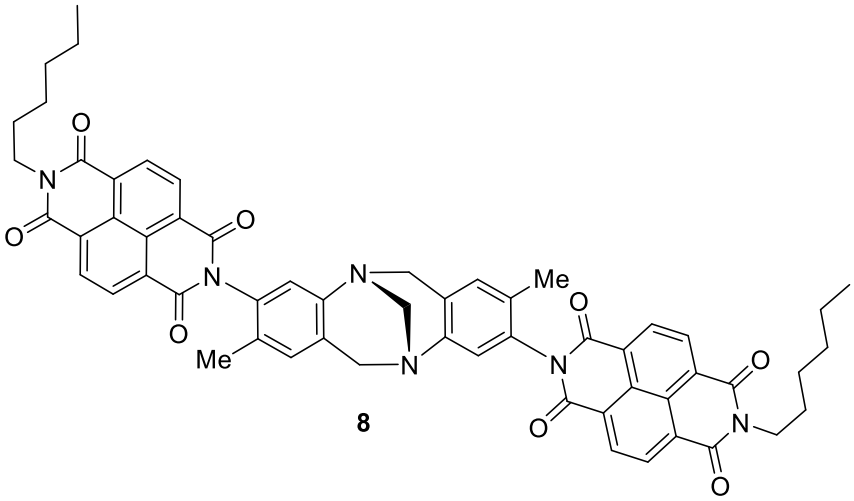

8

Compound **4** (250 mg, 0.71 mmol) was dissolved in dry dimethylformamide with Hünlich's base **3** (100 mg, 0.36) mmol under an argon atmosphere. The reaction mass was stirred at 125°C overnight. The reaction progress was followed by TLC and upon consumption of the starting material, the reaction was stopped and cooled down to room temperature. DMF was removed in *vacuo* and the dark brown crude solid was chromatographed (silica gel, chloroform 95% and 5% methanol) to afford Hünlich's base-NDI dimer **8** as a light brown solid (105 mg, 30%). UV/Vis (CH_3CN) λ_{max} (log ε) 377

(4.87), 357 (4.78), 233 (5.03) nm; FTIR (neat) ν_{max} 2961, 1707, 1663, 1578, 1495, 1450, 1370, 1333, 1244, 1190, 1082, 965, 917, 878, 826, 764, 659 cm^{-1}; ^1H NMR (400 MHz, $CDCl_3$) δ 8.74-8.81 (m, 8H, 2 × NDI-ArH), 7.04 (s, 2H, ArH), 6.97 (s, 2H, ArH), 4.70 (d, *J* = 17.0 Hz, 2H), 4.33 (s, 2H, bridge CH_2), 4.24 (d, *J* = 17.0 Hz, 2H, TB-bridge-CH_2), 4.21 (t, *J* = 7.5 Hz, 4H, 2 × N-CH_2), 2.05 (s, 6H, 2 × Ar-CH_3), 1.69-1.80 (m, 4H, 2 × CH_2), 1.25-1.50 (m, 12H, 6 × CH_2), 0.90 (t, *J* = 7.0 Hz, 6H, 2 × CH_3); ^{13}C NMR (100 MHz, $CDCl_3$) δ 163.11, 162.79, 146.88, 135.00, 131.35, 131.01, 123.00, 129.27, 128.60, 127.01, 126.93, 126.81, 126.72, 124.11, 66.97, 54.46, 41.05, 31.48, 28.03, 26.74, 22.54, 17.26, 14.01; HRMS (ESI) (*m/z*): calcd for $C_{57}H_{51}N_6O_8$ 947.37684; found 947.37528 $[M+H]^+$.

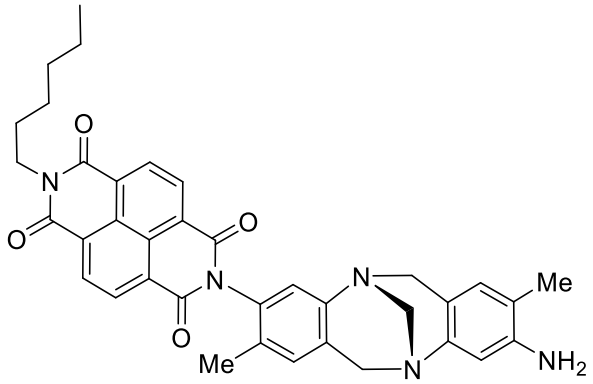

9

A second compound eluted **(**Hünlich's base-NDI monomer **9**) as a light brown solid (16 mg, 15%). UV/Vis (CH_3CN) λ_{max} (log ε) 303 (3.98), 357 (4.42), 377 (4.50) nm; FTIR (neat) ν_{max} 3671, 2958, 1708, 1665, 1577, 1494, 1449, 1370, 1334, 1244, 1191, 1085, 956, 917, 856, 763, 728, 656 cm^{-1}; ^1H NMR (400 MHz, $CDCl_3$) δ 8.75-8.83 (m, 4H, NDI-ArH), 6.93 (s, 1H, ArH), 6.97 (s, 1H, ArH), 6.58 (s, 1H, ArH), 6.47 (s, 1H, ArH), 4.68 (d, *J* = 16.2 Hz, 1H, bridge CH_2) 4.57 (d, *J* = 16.2 Hz, 1H, bridge CH_2), 4.29 (s, 2H, bridge CH_2), 4.18-4.27 (m, 3H, N-CH_2 and bridge CH_2), 4.04 (d, *J* = 16.2 Hz, 1H, bridge CH_2), 3.54 (br s, 2H, NH_2), 2.06 (s, 3H, Ar-CH_3), 2.03 (s, 3H, Ar-CH_3), 1.71-1.81 (m, 2H, CH_2), 1.30-

1.52 (m, 6H, 3 × CH_2), 0.90 (t, J = 7.0 Hz, 3H, CH_3); ^{13}C NMR (100 MHz, $CDCl_3$) δ 162.76, 162.56, 162.51, 147.45, 146.63, 143.87, 132.55, 131.42, 131.29, 131.00, 130.93, 130.74, 129.55, 129.30, 128.61, 127.16, 126.95, 126.93, 126.84, 126.59, 124.91, 119.56, 117.38, 110.46, 66.69, 58.33, 58.23, 41.02, 31.46, 28.01, 26.70, 22.51, 17.03, 16.81, 14.01; HRMS (ESI) (*m/z*): calcd for $C_{37}H_{36}N_5O_4$ 614.2767; found 614.2756 $[M+H]^+$.

References

1. Kobaisi, M. A.; Bhosale, S. V.; Latham, K.; Raynor, A. M.; Bhosale, S. V., *Chem. Rev.* **2016**, *116*, 11685-11796.
2. Avestro, A. J.; Gardner, D. M.; Vermeulen, N. A.; Wilson, E. A.; Schneebeli, S. T.; Whalley, A. C.; Belowich, M. E.; Carmieli, R.; Wasielewski, M. R.; Stoddart, J. F., *Angew. Chem., Int. Ed.* **2014**, *53*, 4442-9.
3. Bhosale, S. V.; Jani, C. H.; Langford, S. J., *Chem. Soc. Rev.* **2008**, *37*, 331-342.
4. Gunderson, V. L.; Smeigh, A. L.; Kim, C. H.; Co, D. T.; Wasielewski, M. R., *J. Am. Chem. Soc.* **2012**, *134*, 4363-4372.
5. Crossley, M. J.; Hambley, T. W.; Mackay, L. G.; Try, A. C.; Walton, R., *J. Chem. Soc., Chem. Commun.* **1995**,, 1077-1079.
6. Yeow, E. K. L.; Sintic, P. J.; Cabral, N. M.; Reek, J. N. H.; Crossley, M. J.; Ghiggino, K. P., *Phys. Chem. Chem. Phys.* **2000**, *2*, 4281-4291.
7. Crossley, M. J.; Hambley, T. W.; Mackay, L. G.; Try, A. C.; Walton, R., *J. Chem. Soc., Chem. Commun.* **1995**, 1077-1079.
8. Shanmugaraju, S.; Dabadie, C.; Byrne, K.; Savyasachi, A. J.; Umadevi, D.; Schmitt, W.; Kitchen, J. A.; Gunnlaugsson, T., *Chem. Sci.* **2017**, *8*, 1535-1546.

9. Shanmugaraju, S.; McAdams, D.; Pancotti, F.; Hawes, C. S.; Veale, E. B.; Kitchen, J. A.; Gunnlaugsson, T., *Org. Biomol. Chem.* **2017**, *15*, 7321-7329.

10. Deprez, N. R.; McNitt, K. A.; Petersen, M. E.; Brown, R. G.; Lewis, D. E., *Tetrahedron lett.* **2005**, *46*, 2149-2153.

11. Veale, E. B.; Frimannsson, D. O.; Lawler, M.; Gunnlaugsson, T., *Org. Lett.* **2009**, *11*, 4040-4043.

12. Villamaina, D.; Bhosale, S. V.; Langford, S. J.; Vauthey, E., *Phys. Chem. Chem. Phys.* **2013**, *15*, 1177-1187.

13. Villamaina, D.; Kelson, M. M. A.; Bhosale, S. V.; Vauthey, E., *Phys. Chem. Chem. Phys.* **2014**, *16*, 5188-5200.

14. Bhuiyan, M. D. H.; Mahon, A. B.; Jensen, P.; Clegg, J. K.; Try, A. C., *Eur. J. Org. Chem.* **2009**, 687-698.

15. Rigol, S.; Beyer, L.; Hennig, L.; Sieler, J.; Giannis, A., *Org. Lett.* **2013**, *15*, 1418-1420.

16. Rogers, J. E.; Weiss, S. J.; Kelly, L. A., *J. Am. Chem. Soc.* **2000**, *122*, 427-436.

17. Kiehne, U.; Weilandt, T.; Lützen, A., *Org. Lett* **2007**, *9*, 1283-1286.

SUPPORTING INFORMATION

Synthesis of Naphthalene Diimide Analogues of Tröger's Base and Hünlich's Base

Md Imam Ansari, Andrew Try, and Peter Karuso*

Department of Molecular Sciences, Macquarie University, Sydney NSW 2109, Australia

* Corresponding author. Tel.: +612-9850-8290 fax: +612-9850-8313, e-mail: peter.karuso@mq.edu.au

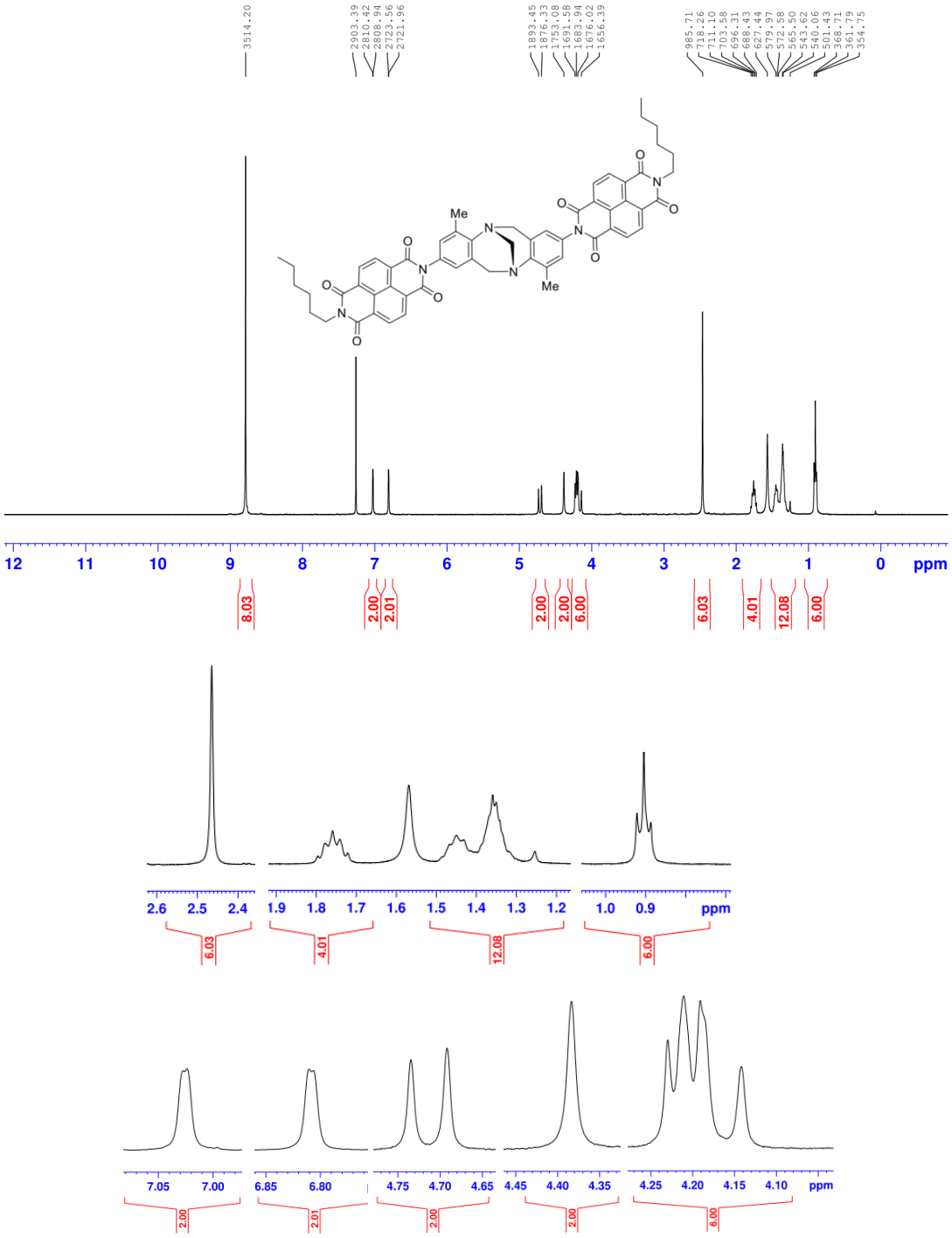

Fig. S1 ^{1}H NMR spectrum (400 MHz) of **6** in $CDCl_3$.

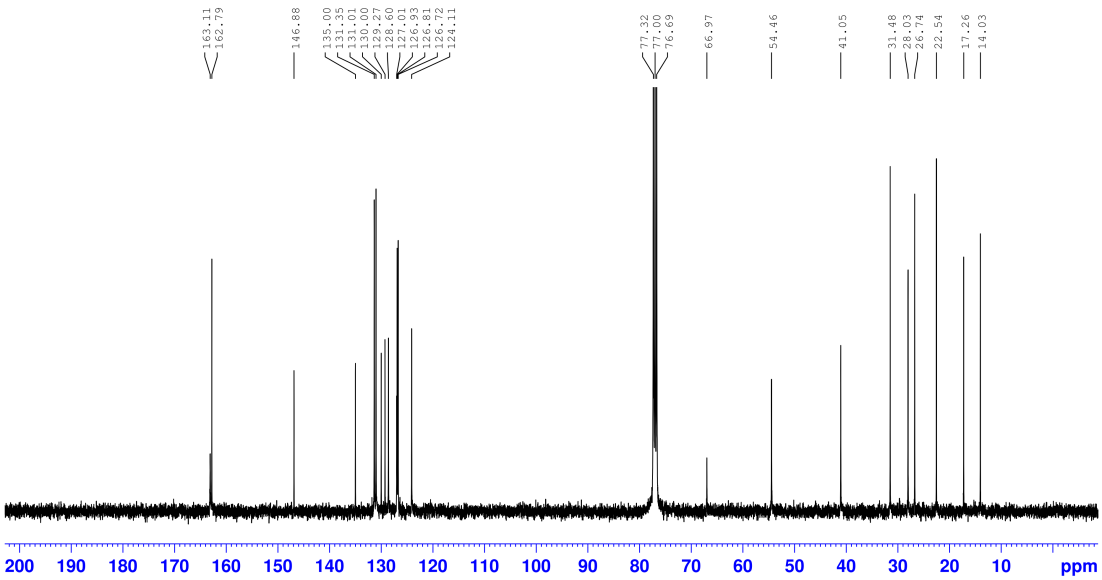

Fig. S2 ^{13}C NMR spectrum (100 MHz) of **6** in $CDCl_3$.

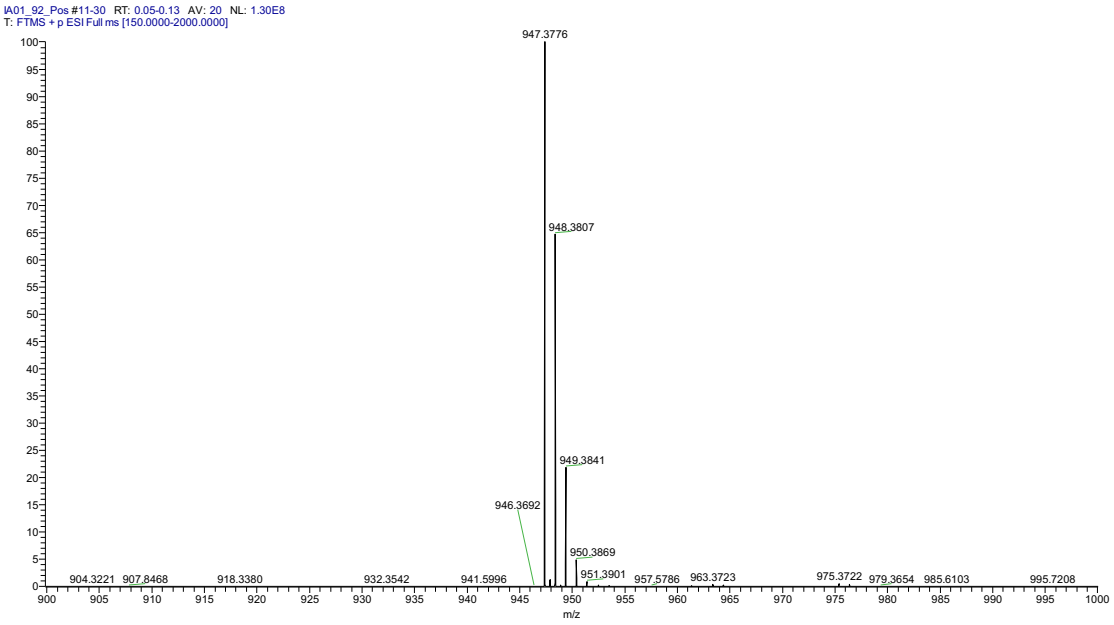

Fig. S3 High resolution mass spectrum of **6**.

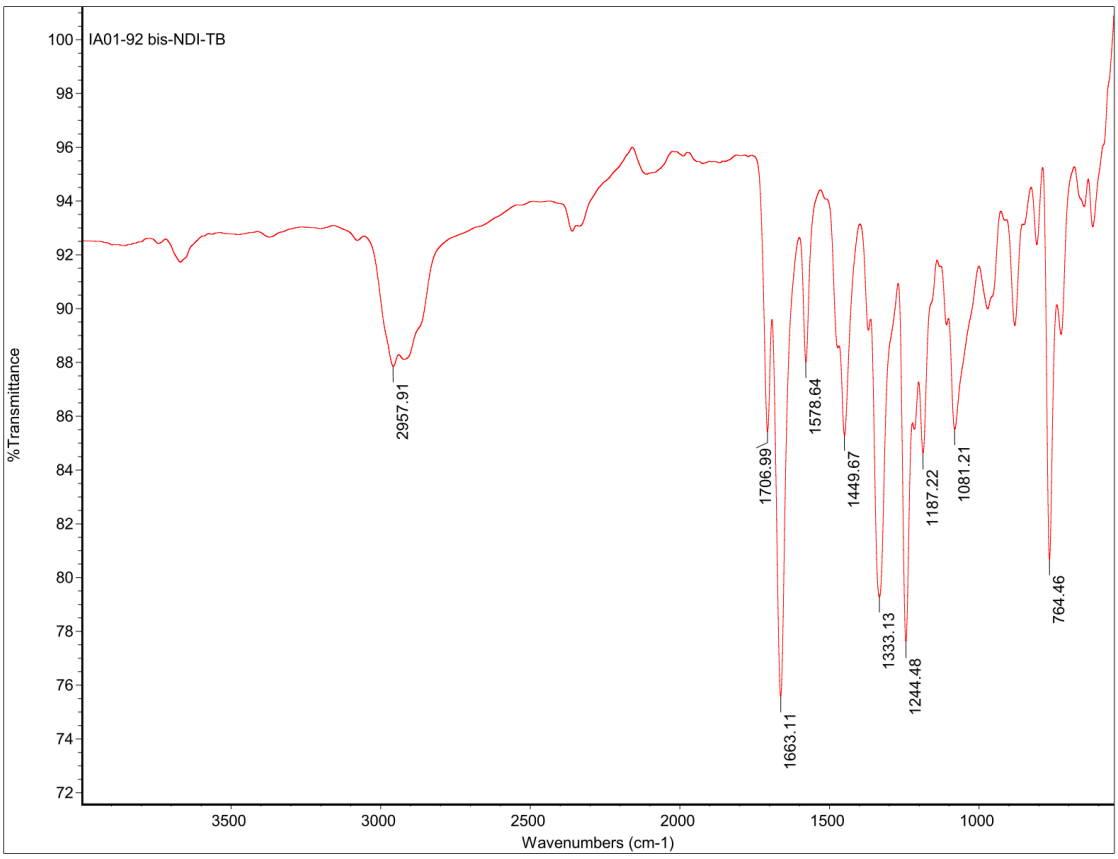

Fig. S4 Fourier transform infrared (FTIR) spectrum of **6**.

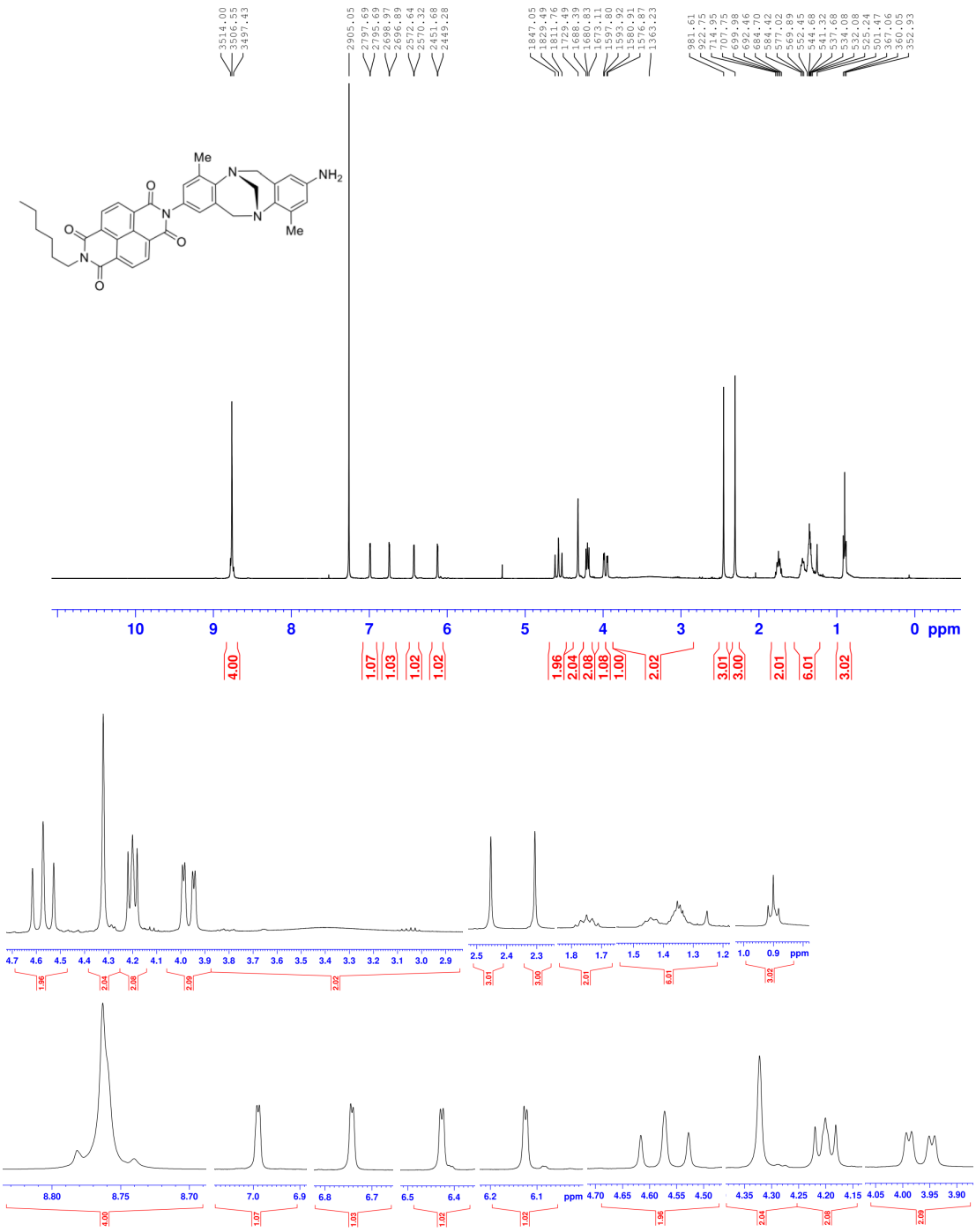

Fig. S5 ^{1}H NMR spectrum (400 MHz) of **7** in $CDCl_3$.

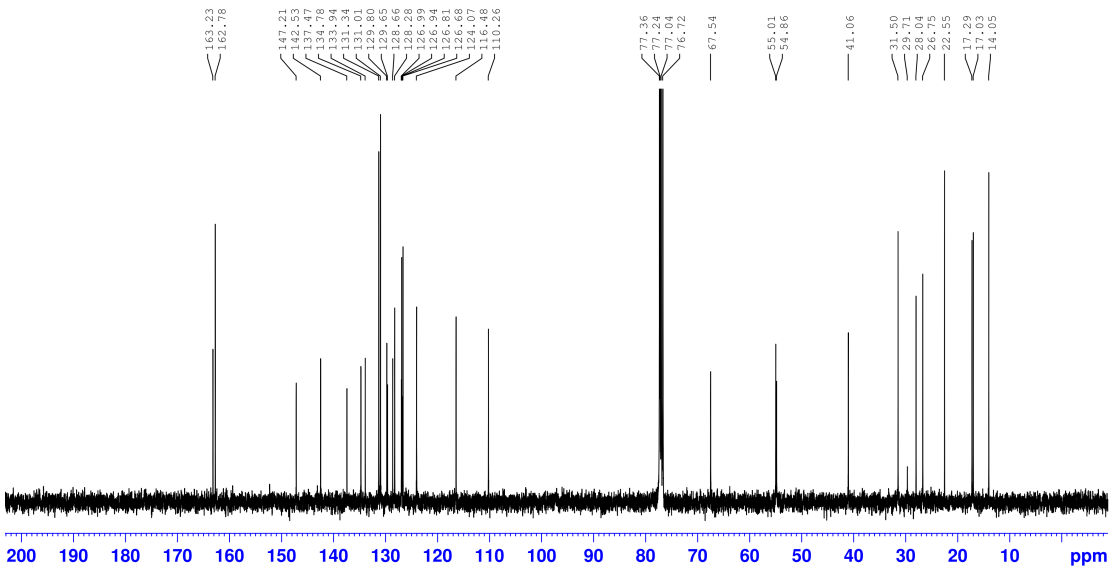

Fig. S6 ^{13}C NMR spectrum (100 MHz) of **7** in $CDCl_3$.

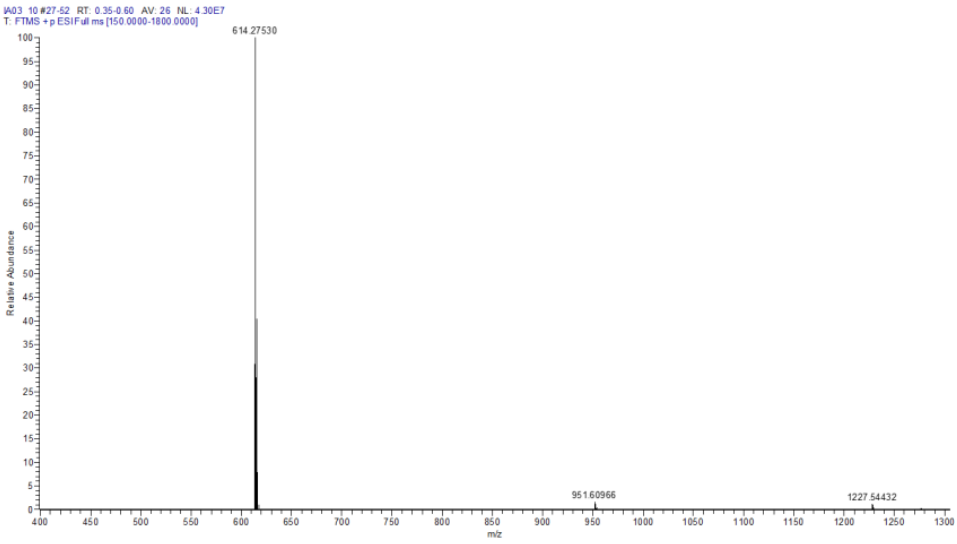

Fig. S7 High resolution mass spectrum of **7**.

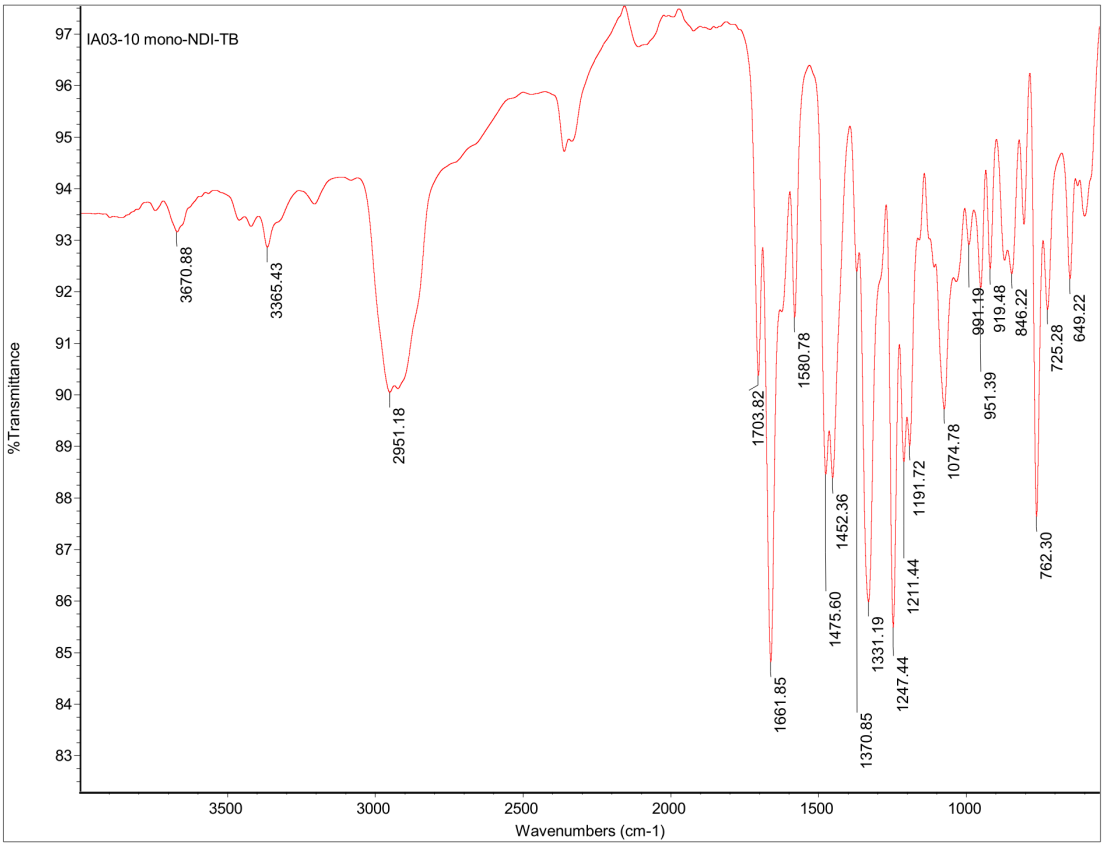

Fig. S8 Fourier transform infrared (FTIR) spectrum of **7**.

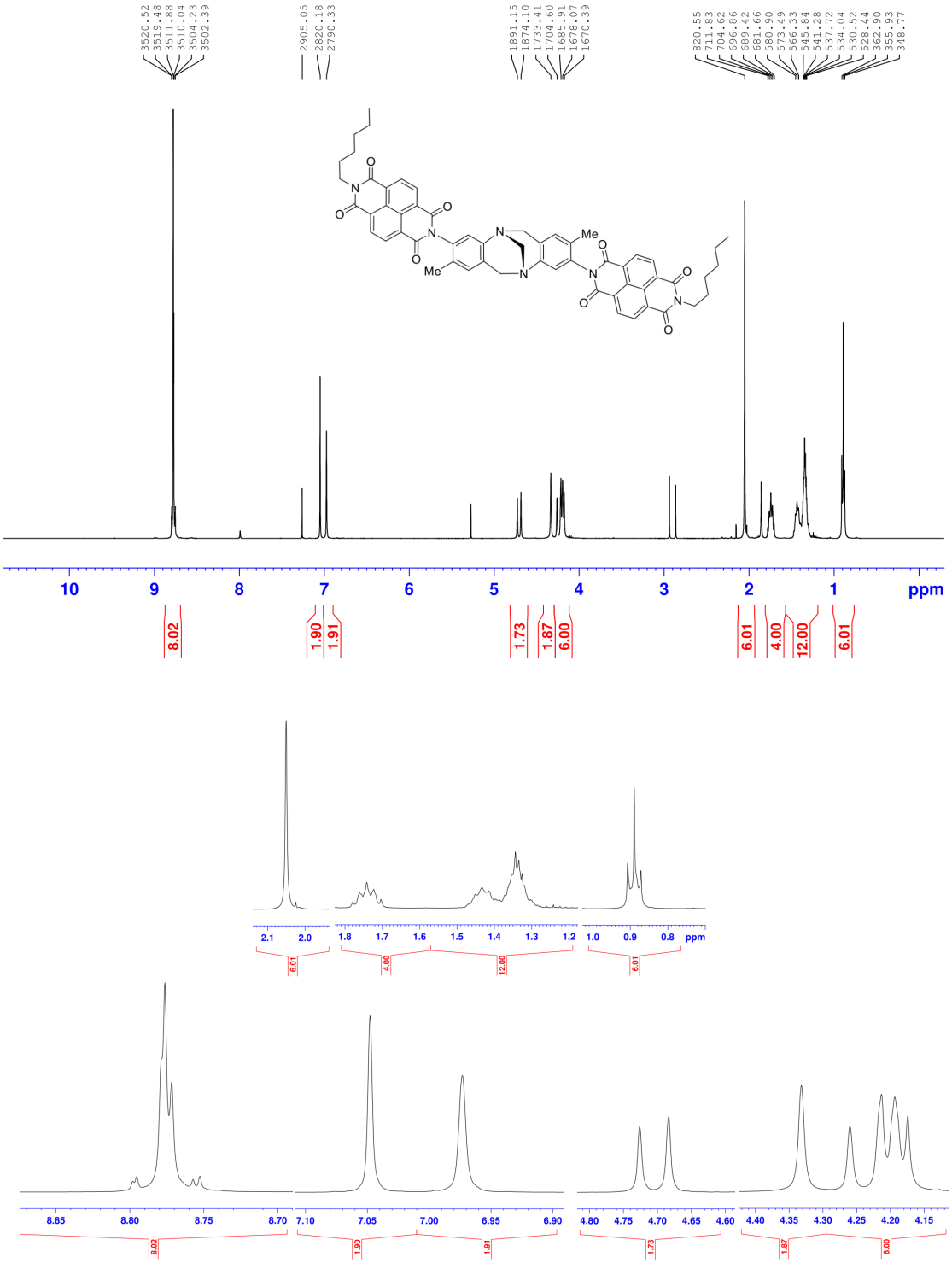

Fig. S9 ^{1}H NMR spectrum (400 MHz) of **8** in $CDCl_3$.

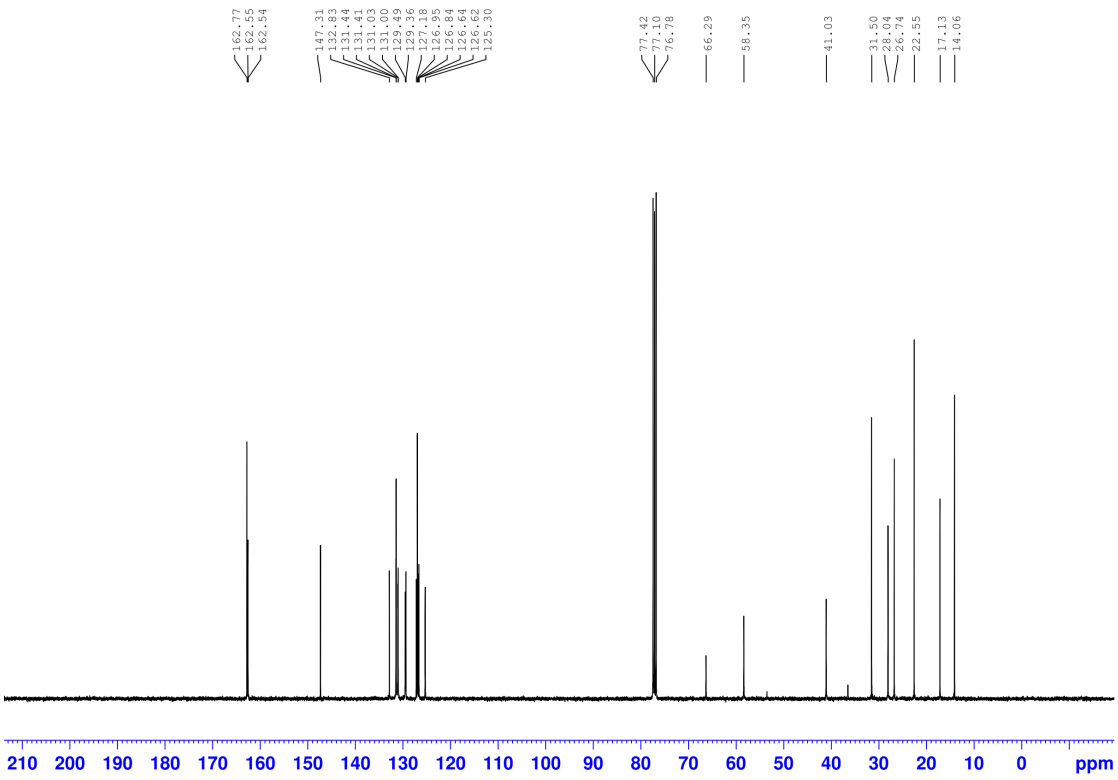

Fig. S10 ^{13}C NMR spectrum (100 MHz) of **8** in $CDCl_3$.

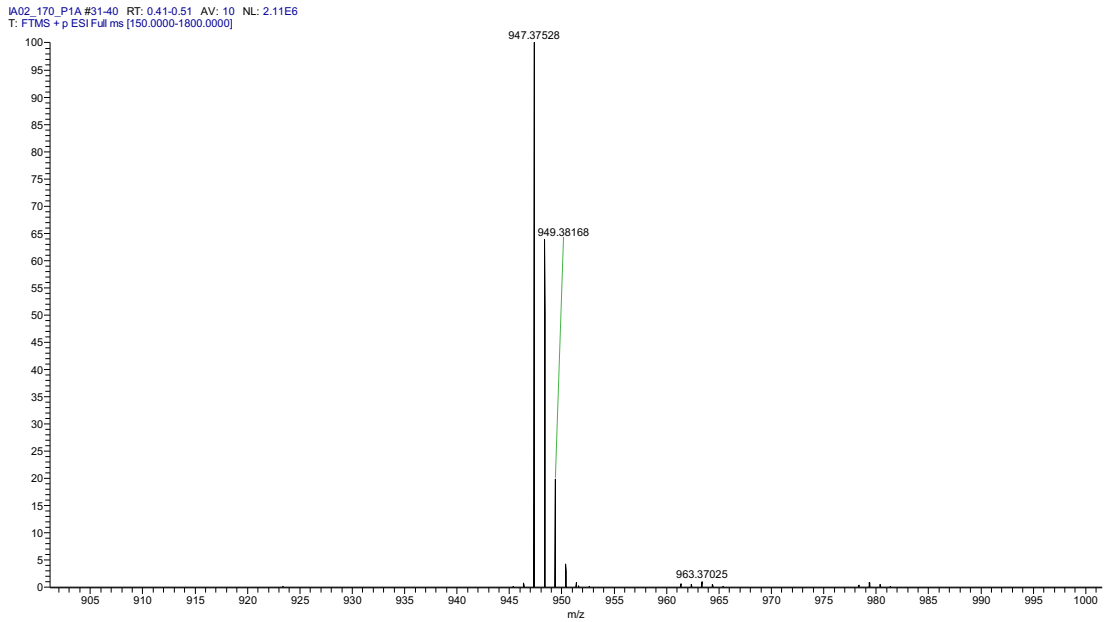

Fig. S11 High resolution mass spectrum of **8**.

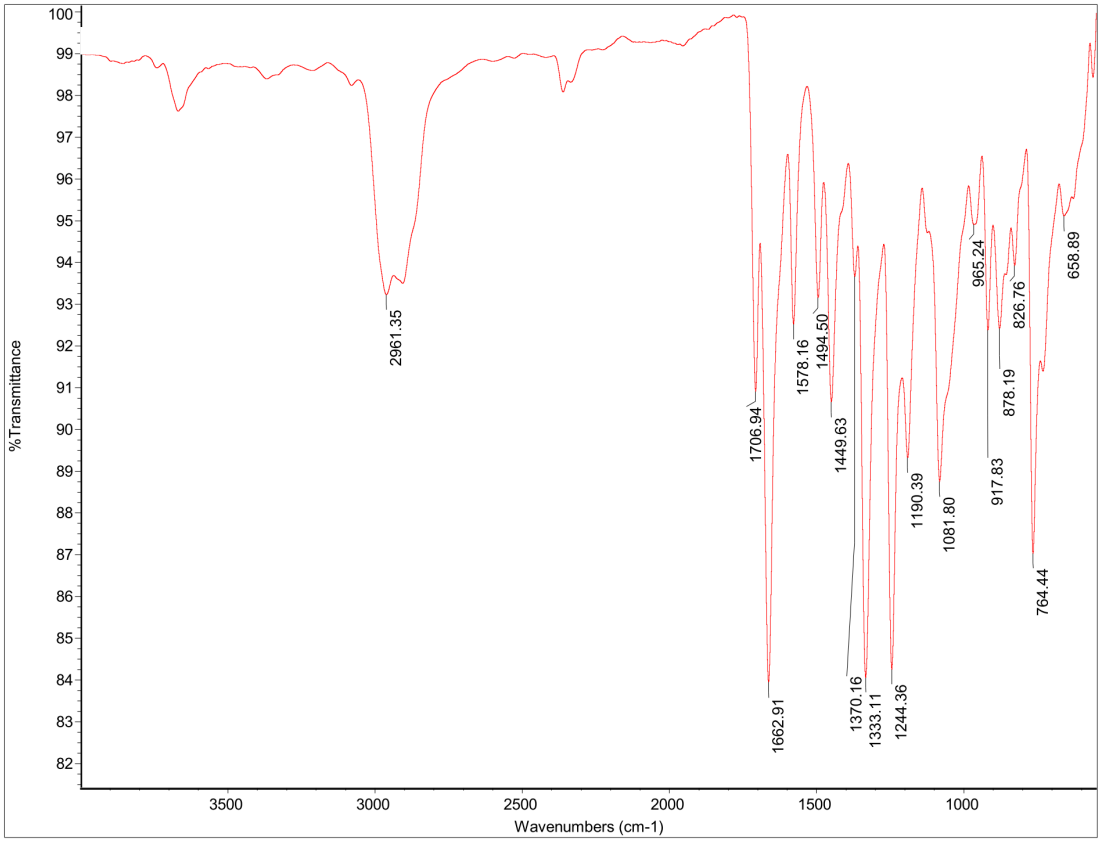

Fig. 12 Fourier transform infrared (FTIR) spectrum of **8**.

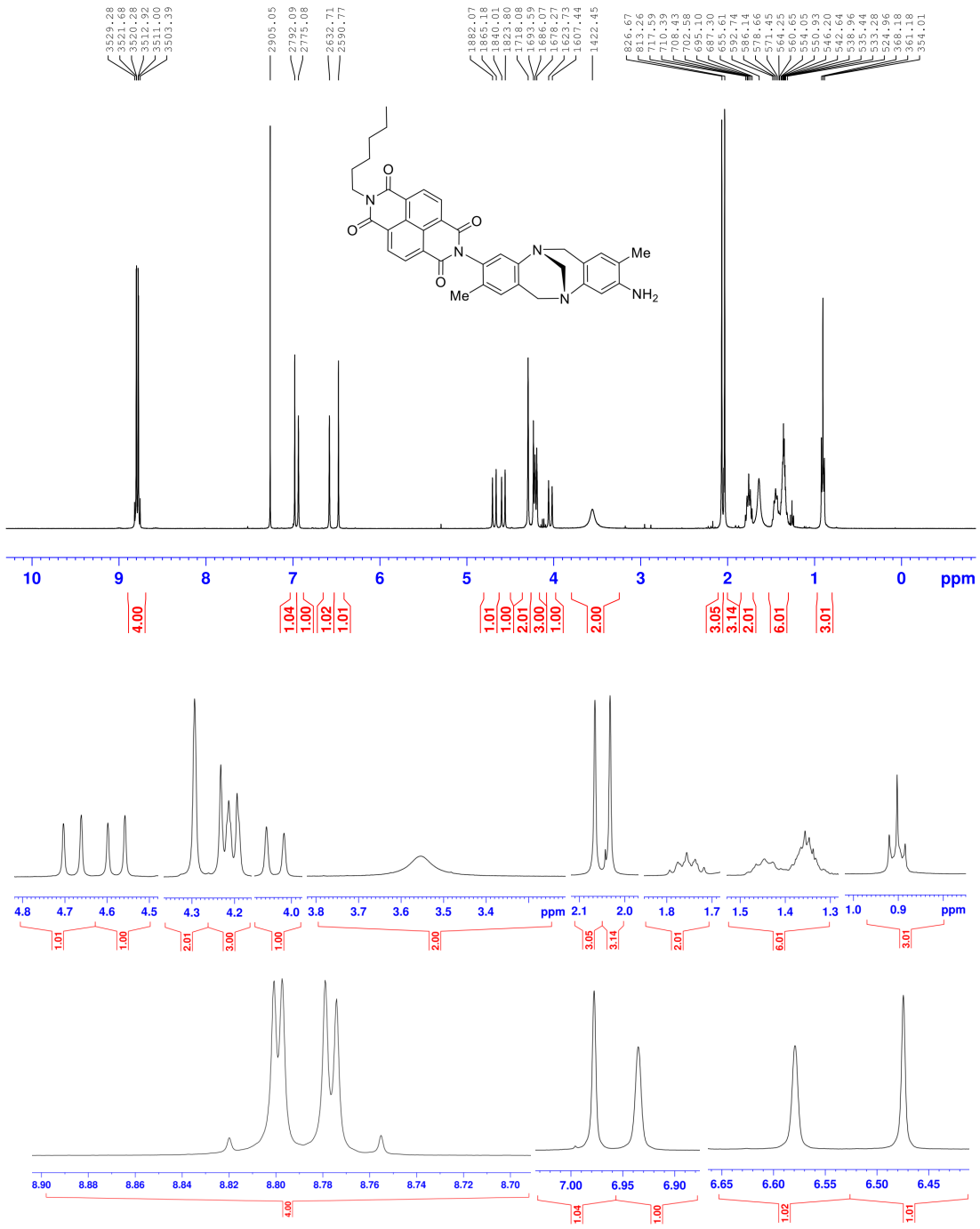

Fig. S13 ^{1}H NMR spectrum (400 MHz) of **9** in $CDCl_3$.

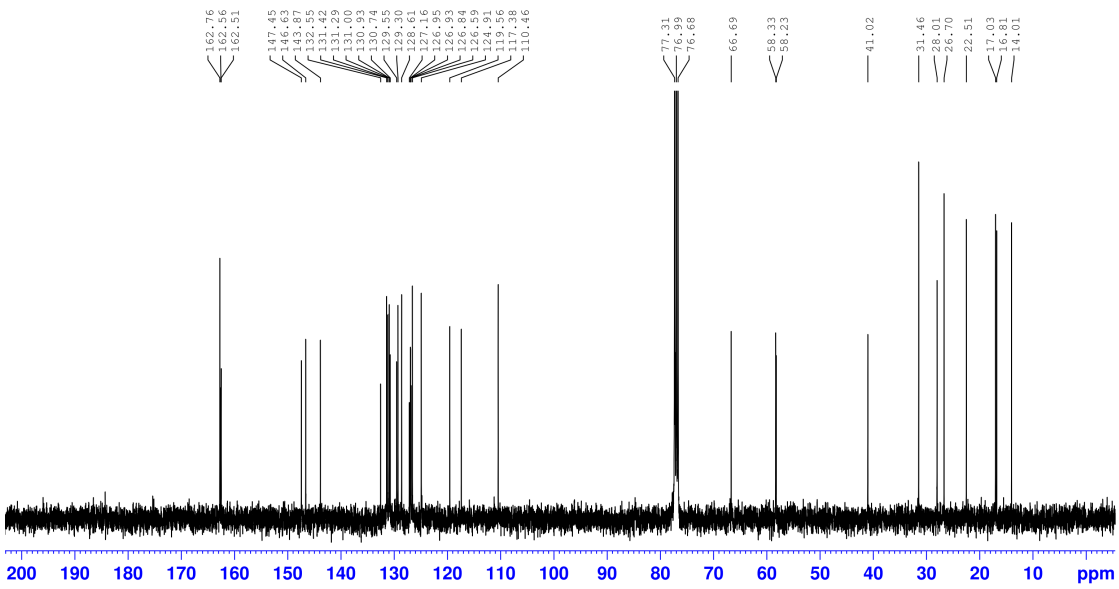

Fig. S14 ^{13}C NMR spectrum (100 MHz) of **9** in $CDCl_3$.

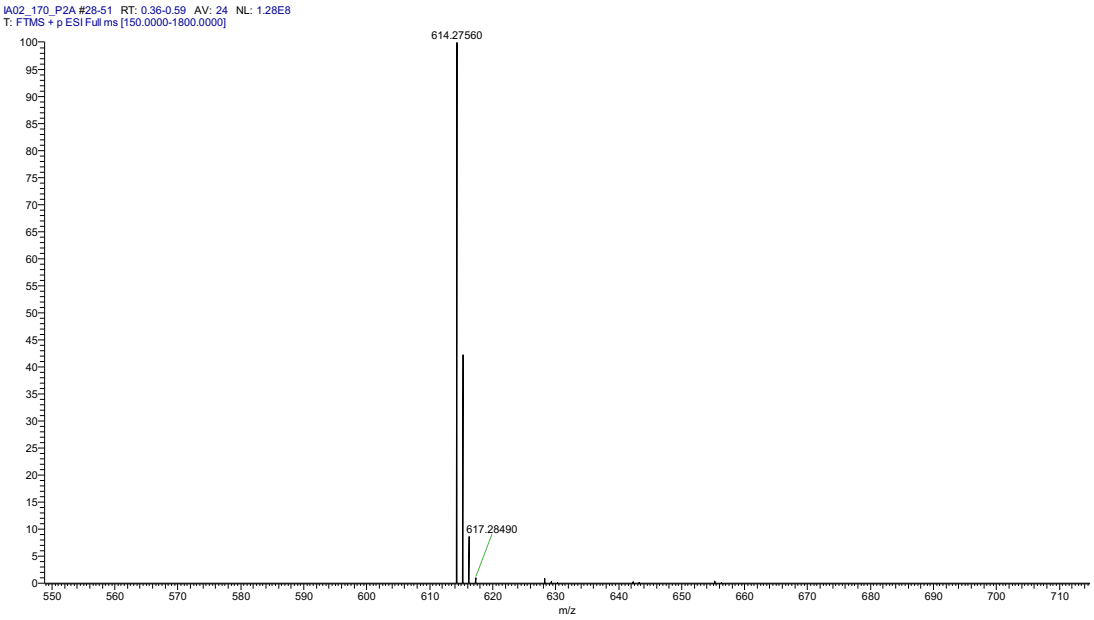

Fig. S15 High resolution mass spectrum of **9**.

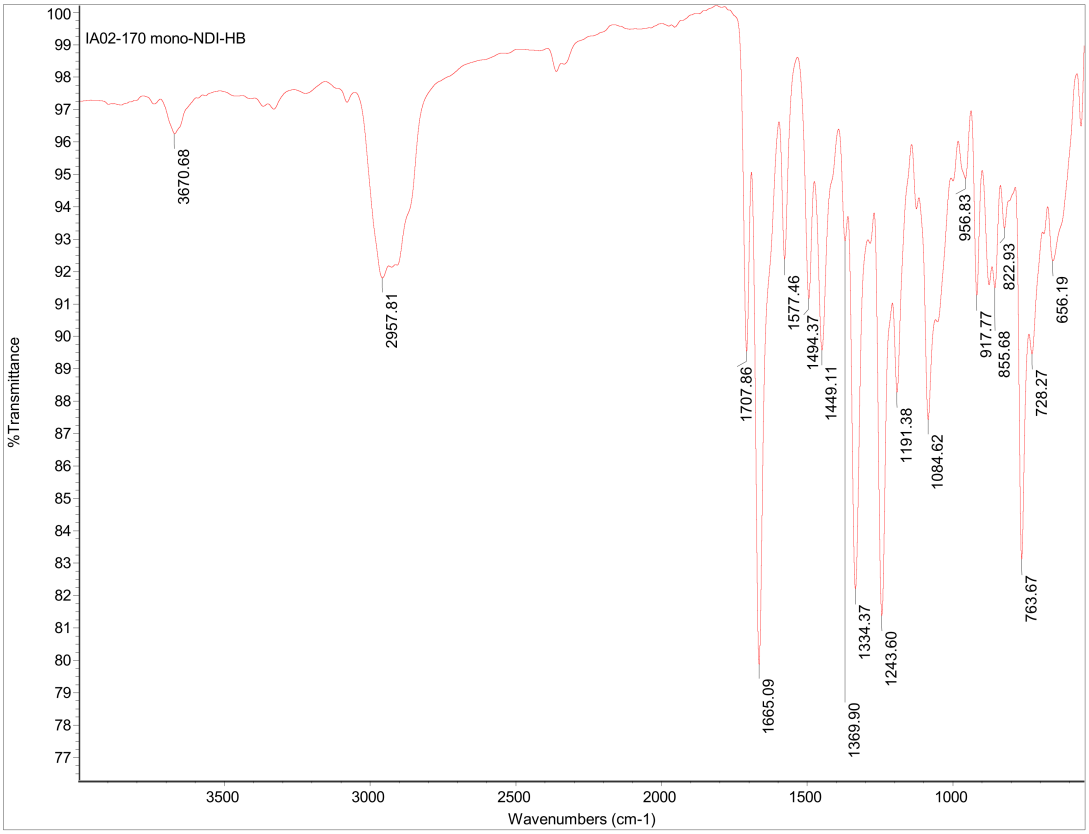

Fig. S16 Fourier transform infrared (FTIR) spectrum of **9**.

Synthesis of a Halogen Functionalised Tröger's Base-C_{60} Analogue

Md Imam Ansari, Andrew Try, and Peter Karuso*

Department of Molecular Sciences, Macquarie University, Sydney NSW 2109, Australia

* Corresponding author. Tel.: +612-9850-8290 fax: +612-9850-8313, e-mail: peter.karuso@mq.edu.au

Abstract Fullerene-C_{60} derivatives as a functional materials have attracted considerable interest because of their potential applications in developing artificial photosynthetic models. We report on the synthesis of a novel halogen functionalised Tröger's base-C_{60} analogue as a building block in the development of fullerene-based molecular architectures. The synthesis is highly modular and efficient, since the fullerene moiety is introduced in the last step. This method opens up the possibility for the synthesis of complex donor-acceptor systems separated by virtue of a well-defined V-shaped molecule between the two chromophores. Additionally, we report the synthesis of three novel halogenated hybrid Tröger's base (TB) compounds (ester, alcohol and aldehyde functionalised TBs) *via* mixed aniline condensation.

Introduction

Fullerene-C_{60} has a cage–like fused-ring structure[1] with potential applications in the area of solar cell technology,[2-5] organic semiconductors[6-7] and artificial photosynthesis.[5, 8-10] C_{60}-based electron donor-acceptor dyads separated by bridging molecule have been developed in the past two decade.[11-12] Although, the majority of fullerene-based dyads involved linear and conjugated linkers for electron and energy transfer, supramolecular dyads also have been reported.[13-15] However, construction of non-conjugated but rigid dyads has been hampered by the lack of scaffolding materials. The incorporation of a rigid and non-conjugated linker between the two chromophores needs to be investigated. In contrast, Tröger's base (TB **1**); is a molecule of great interest due to its V-shaped structure.[16] It was first isolated by Tröger in 1887 and characterised by Spielman in 1935 (Fig. 1).[17]

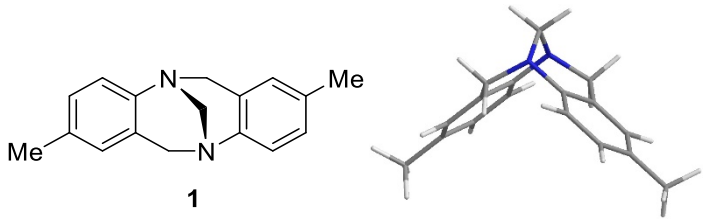

1

Fig. 1 Tröger's base (**1**), and the three-dimensional representation of (**1**) looking side-on showing V-shaped geometry.

TB has found many applications in chemistry, for example gas separation,[18-19] supramolecular chemistry[20] and optoelectronics.[16] The TB scaffold can be used as bridging molecule to separate two chromophores. Consequently, unique properties of Tröger's base (C_2 symmetry and rigidity)[21] has attracted considerable attention in the past decade for the construction of artificial photosynthetic models.[22-23] TB analogues can be synthesised with functional groups at almost any position on the aryl rings, including halogens,[24] ethers, esters[25] and nitro groups.[26] Asymmetric TB analogues may be prepared *via* mixed condensation reaction involving two different anilines.[16, 24] Efforts to append C_{60} onto a TB framework have also been reported.[21, 27-28] For instance, fullerene-C_{60} moiety has been employed for the first time onto the TB framework by Diederich and co-workers by regio- and stereo-selective tethered-directed remote functionalisation.[21, 27] However, this limit appending any additional chromophore because C_{60} is attached to both aryl rings of TB. On the other hand, Prato and co-workers discovered that aromatic aldehydes with sarcosine can be used for the functionalisation of C_{60}.[29] We envisioned appending C_{60} to TB framework *via* the Prato method to only one of the aryl rings. This allows addition of a second chromophore to the other aryl ring of TB and more complex C_{60}-based architectures to be accessed. Recently it has been shown that halogenated TB compounds can undergo Suzuki-Miyara and Buchwald-Hartwig cross-coupling reactions.[30] The utility of halogen

functionalised novel Tröger's base-C_{60} could be in ever-increasing demand to access new and more challenging targets in the field of ligand design.

In this paper, we describe our efforts to expand the chemistry of hybrid Tröger's base by appending C_{60} to only one of the aryl rings of TB.

Results and Discussion

One-step mixed aniline approaches to the synthesise of hybrid Tröger's base have been reported from our lab.[24] In the present context, the reaction of two *para*-substituted different anilines affords a mixture of three possible Tröger's base products: two symmetric compounds and a hybrid. In this way, our initial target was a bromo-ester functionalised hybrid Tröger's base **3** (Scheme 1). Reaction of 4-bromoaniline and ethyl-4-amino-3-methyl benzoate with paraformaldehyde yield **3** (36%) along with the two symmetrical TBs **2** and **4** that we easily separated by column chromatography on silica. The first compound eluted was the symmetric diester TB **2** followed by the desired TB **3**, and last, the symmetric dibromo TB **4** (Scheme 1). In this case, the hybrid, not surprisingly, has an R_f value that lies between the two symmetric compounds (**2** and **4**). If the symmetric products would have similar R_f values, the isolation of the hybrid by chromatographic techniques would be problematic. The symmetric dibromo[31] **4** and diester[25] **2** have been reported previously but the mixed TB **3** is new. Next, TB **3** was reduced to the alcohol ($LiAlH_4$) to afford **5** in excellent yield, and oxidation to **6** was achieved with MnO_2 (Scheme 2). The molecular formula of **3** ($C_{19}H_{20}BrN_2O_2$) was confirmed by HRMS (Δmmu −0.3). The ^1H NMR spectrum, confirmed the identity of **3** due to the presence of a well-separated doublet peaks between 3.90 and 4.8 ppm corresponding to the methylene protons of the TB diazocine bridge, also reflecting the C_2 symmetry of **3** (Fig. 2).

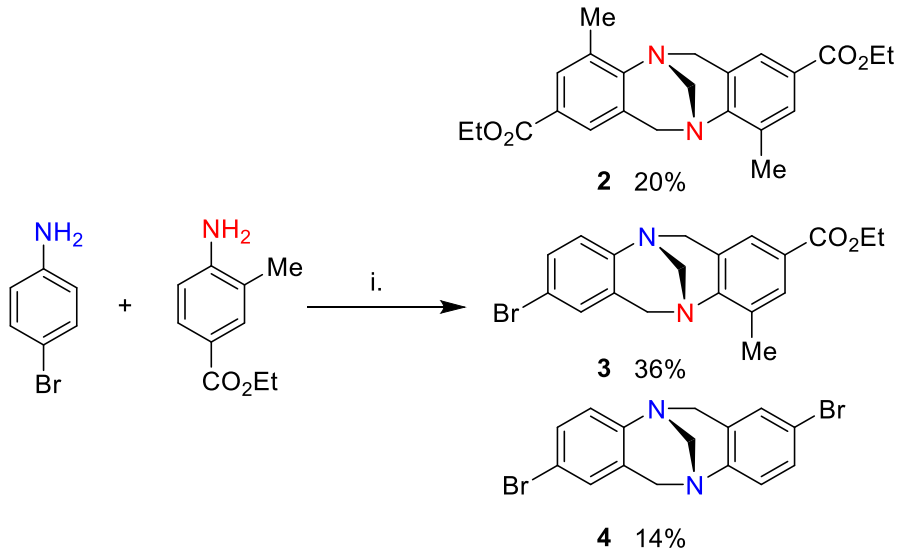

Scheme 1. Synthesis of Tröger's base hybrid. i. TFA, $(CH_2O)_n$, argon atmosphere, rt, 7 days.

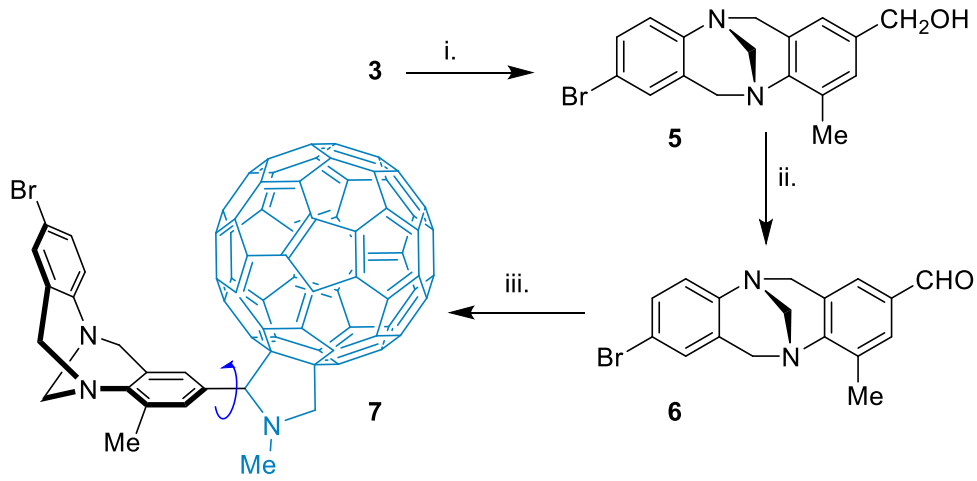

Scheme 2. Synthesis of fullerene-C_{60} Tröger's base analogue; i. $LiAlH_4$, dry THF, 4 h, rt, argon atmosphere; ii. MnO_2, CH_2Cl_2, rt, overnight; iii. Sarcosine, C_{60}, toluene, 110 °C, overnight.

The aldehyde functionality on TB **6** serves as an attachment point for fullerene-C_{60} *via* a Prato reaction (Scheme 2). We then turned our attention to appending the fullerene-C_{60} chromophore onto aldehyde TB **6** by following the protocol of Prato *et al.*[29] In this way, the Tröger's base-C_{60} analogue was prepared by the 1,3-dipolar cycloaddition of

an ylide, resulting from the aldehyde TB **6** and sarcosine, in the presence of C_{60} afforded **7** in 20% yield (Scheme 2).

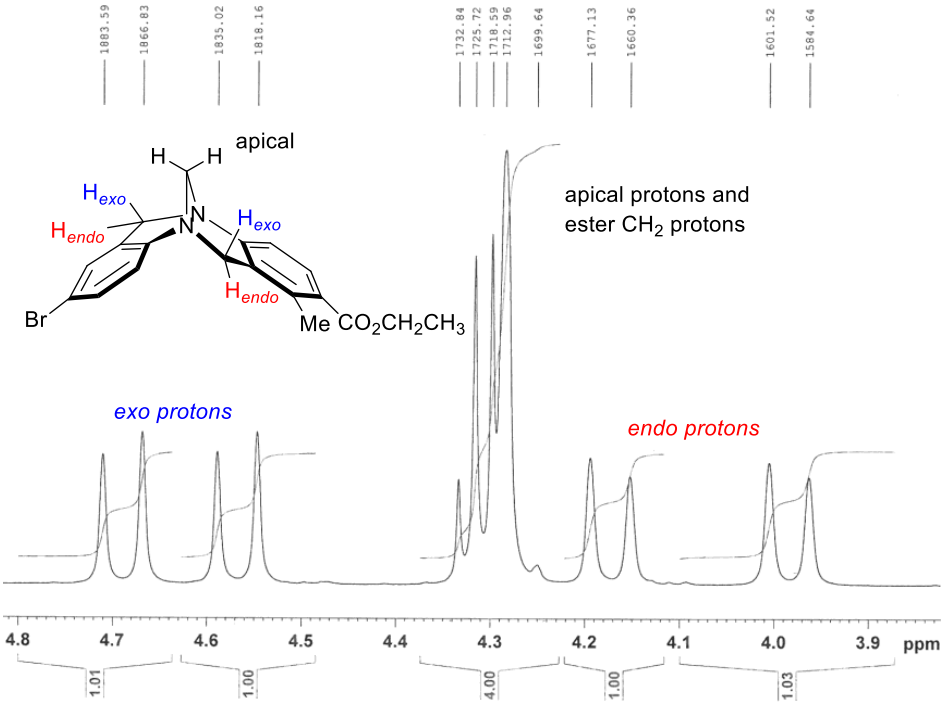

Fig. 2 400 MHz ^{1}H NMR spectrum (298 K, $CDCl_3$) of the bridge region of hybrid TB **3**.

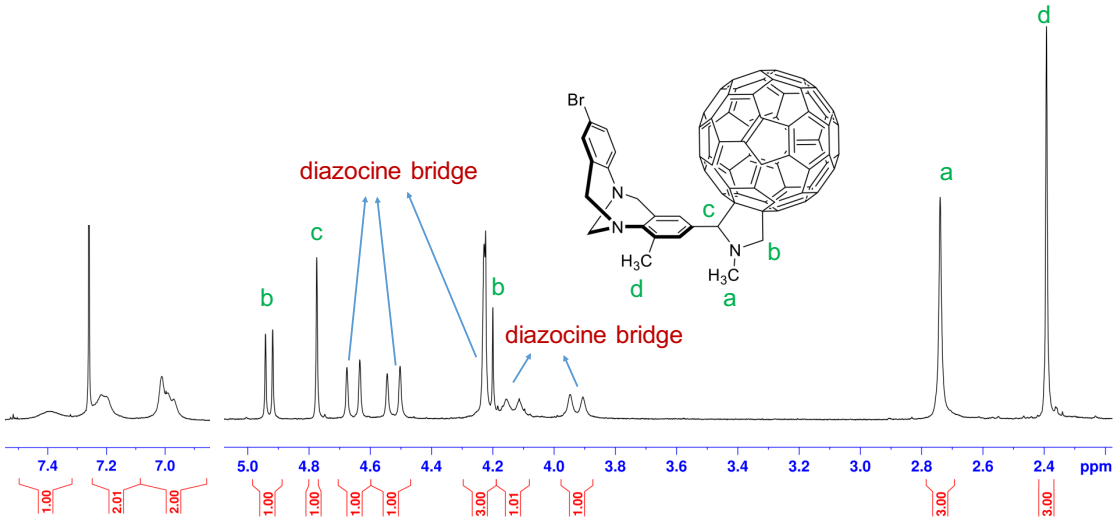

Fig. 3 Expansion of 400 MHz ^{1}H NMR (298 K, $CDCl_3$) spectra of **7** shows important features of Tröger's base region and pyrrolidine functionalised fullerene-C_{60}. The peak

marked with ***a***, ***b*** and ***c*** display the protons for *N*-methylpyrrolidine and ***d*** represents aromatic CH_3.

Purification was achieved with Biotage flash chromatography (silica gel, 10% ethyl acetate/90% chloroform). In the ^{1}H NMR spectrum of **7**, signals of the aromatic region are broadened and shifted upfield (Fig. 3) with respect to the resonances of **6**, indicative of shielding of these protons by fullerene. We tried to resolve aromatic signals of **7** by VT NMR and by increasing the number of scans in proton NMR experiments without success. These features are consistent with the C_{60} unit "residing" in the cavity of the TB scaffold (*endo* conformation) with the associated π-system shielding the aryl protons. However, DFT calculation done for porphyrin-TB-C_{60} (Chapter 4) showed there is no difference in the ground state energy of the *endo* or *exo*-forms. At −60 °C all the ^{1}H NMR signals were split into two with a ratio of 2:1(Fig. 4) which is a reasonable agreement with DFT calculations that suggested a 1.4 KJ/mol difference between the *exo*- and *endo*- forms. Variable temperature (VT) effects on the dynamics of this system were investigated (Fig. 4). Heating the system led to an increase in its kinetic energy and, thus the pyrrolidinofullerene moiety started to rotate across the TB-pyrrolidine bond. As a consequence of heating, all the diazocine bridge protons and pyrrolidinic protons were equally affected by delocalised electrons of C_{60}, changing the apparent symmetry of the systems in the diazocine bridge region and reducing the complexity of the proton spectrum. The activation energy ($\Delta G^{\#}$) across the TB-pyrrolidine bond was obtained from the coalescence temperature (Tc) of the methylene bridge protons (blue bar) using the following procedure. First we calculated the rate constant (k_c) of the AB system according to equation (1) where $\Delta\nu_o$ is the separation in Hz between the two signals in the absences of rotation and $\Delta\nu_e$ is their

mutual coupling constant which were measured was $\Delta\nu_o$ = 49 Hz and $\Delta\nu_e$ = 16.6 Hz, respectively.

$$k_c = \frac{\pi}{\sqrt{2}}[\Delta v_{o^2} - \Delta v_{e^2}]^{1/2} \quad (1)$$

$$k_c = 46\ Hz$$

k_c = rate constant, T_c = coalescence temperature K = 273 K, h = Planck's constant, k = Boltzman constant, ln(k/h) = 23.760, R = gas constant (1.987 cal K^{-1} mol^{-1}).

$\Delta G^{\#}$ was calculated using the k_c value and equation (2) derived from the Erying equation.[32] The rotational barrier was estimated to be ca. 13.8 kcal.mol^{-1}

$$\Delta G^{\#} = -RT_c \ln\frac{k_c h}{kT_c} \quad (2)$$

$$\Delta G^{\#} = 1.987\ T_c\ [23.760 + \ln(T_c/k_c)]\text{k.cal}.mol^{-1}$$

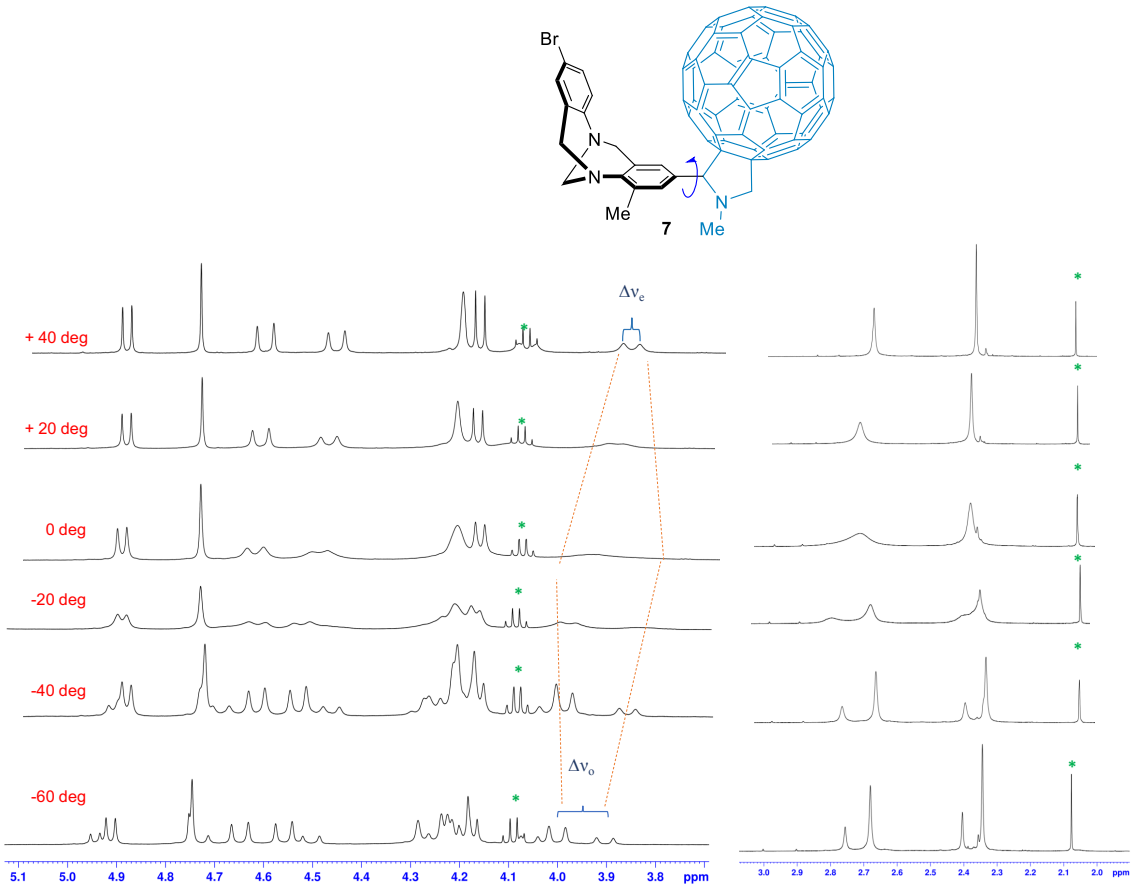

Fig. 4 (400 MHz) ^{1}H NMR of variable temperature experiments of **7** in $CDCl_3$.

* Indicates solvent peak (ethyl acetate).

UV/Vis Properties

Compound **7** shows absorption of typical fullerene-C_{60} at 330 nm (Fig. 5) indicating no interaction between fullerene-C_{60} and Tröger's base framework. This could be advantageous for the construction of donor-acceptor complexes as any communication between donor and acceptor chromophores would not confused by interaction with TB.

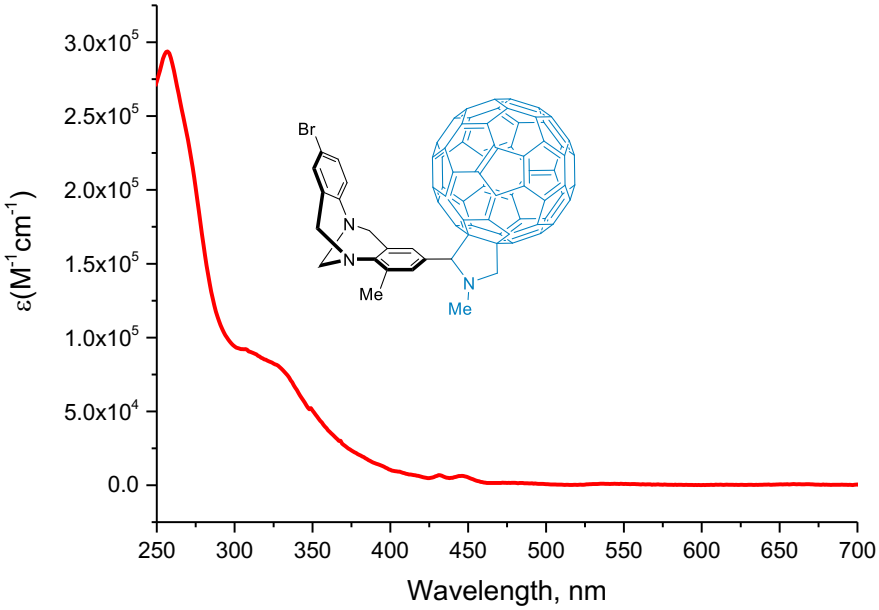

Fig. 5 UV/Vis spectrum of **7** in $CHCl_3$. The concentration of compound was 2.5×10^{-6} M.

Conclusion

We successfully prepared and characterise three hybrid Tröger's bases and have developed an efficient synthetic route to a novel Tröger's base fullerene-C_{60} conjugates. The reaction of two different *para*-substituted anilines afforded ester functionalised TB which was reduced to alcohol and then oxidised to aldehyde prior to reacting with C_{60}. Previous approaches to appending C_{60} onto the TB framework are limited by the inability to attach a second chromophore. Consequently, halogenated Tröger's base-C_{60}

was prepared using Prato*'s* method which is now set up for undergo Suzuki-Miyara or Buchwald-Hartwig cross-coupling reactions. This, opens up the possibility of constructing complex C_{60} Tröger's base architectures. The variable temperature NMR analysis revealed that C_{60} moiety rotate across the TB-pyrrolidine bond and that the *exo*-conformer is only slightly more stable than the *endo*-conformer. At room temperature these two forms are interchanging.

Acknowledgements

This work was supported by Macquarie University (Sydney, Australia). We would also like to thank India@75 and Macquarie University for the award of an iMQRES PhD scholarship to M.I.A.

Experimental Section

General information: Reagents were purchased from Sigma-Aldrich and Alfa Aesar and used without purification unless otherwise stated.

^{1}H NMR and ^{13}C NMR spectra were recorded in Aldrich 5 mm NMR tubes on a Bruker DRX 400 NMR spectrometer (400 MHz) at 300 K unless otherwise stated, processed using Topspin 3.5, and referenced to residual solvent peak ($CDCl_3$ δ_H 7.26 and δ_C 77.01 ppm; DMSO-d_6 δ_H 2.49 and δ_C 39.5 ppm). The following abbreviations for multiplicity are used: s, singlet; d, doublet; t, triplet; m, multiplet; and dd, doublet of doublets. Column chromatography was carried out using the gravity feed column techniques on a Merck silica gel type 9385 (230-400 mesh) with the stated solvent systems. Analytical thin layer chromatography (TLC) analyses were performed on Merck silica gel 60 F254 sheets (0.2 mm). Visualisation of compounds was achieved by illumination under ultraviolet light (254 nm). Charcoal and celite were pre-washed with MeOH and water before being used. HRMS (ESI) were performed at the Australian Proteome Analysis

Facility (APAF), Macquarie University, Australia using a Q Exactive Plus hybrid quadrupole-orbitrap mass spectrometer (Thermo Scientific, Bremen, Germany). ESI-MS spectra were recorded using an Agilent 6130 single quadrupole mass spectrometer (Agilent Corp.). The IR spectra were taken on a Thermo Scientific Nicolet iS10 ATR FTIR spectrometer at 298 K. UV-visible absorbances were recorded on a Varian Cary 1Bio UV/Visible spectrophotometer. All commercial solvents were of HPLC grade and used without further purification. Where solvent mixtures are used, the portions are given by volume. Chloroform used for photophysical experiments were HPLC grade purchased from Sigma-Aldrich (amylene stabilised).

Compound 3

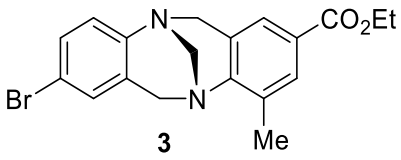

3

4-Bromoaniline (2.00 g, 11.6 mmol), ethyl 4-amino-3-methylbenzoate (2.10 g, 11.6 mmol) and paraformaldehyde (1.10 g, 37.2 mmol) were dissolved in trifluoroacetic acid (50 mL), and the mixture was stirred in the dark for 7 days. The reaction mixture was then basified with a solution of concentrated ammonia (120 mL) and water (120 mL). The crude material was then extracted with dichloromethane (2 × 200 mL). The combined organic layers were washed with brine, dried over magnesium sulfate, filtered and evaporated to dryness to afford a light yellow solid. The crude material was chromatographed (silica gel, 10% ethyl acetate/70% hexane/10% dichloromethane), and the first compound eluted from column was symmetric diester TB **2** (850 mg, 20%) as an off-white solid. ^{1}H NMR (400 MHz, $CDCl_3$) δ 7.74 (app s, 2H, ArH), 7.49 (app s, 2H, ArH), 4.65 (d, J = 16.8 Hz, 2H, CH_2), 4.35 (s, 2H, CH_2), 4.30 (q, J = 7.1 Hz, 4H, CH_2), 4.08 (d, J = 16.8 Hz, 2H, CH_2), 2.45 (s, 6H, CH_3), 1.34 (t, J = 7.1 Hz, 6H, CH_3), ppm.[25]

The second compound eluted was the desired hybrid TB **3** (1.60 g, 36%) as a white solid. m.p. 138-140 °C; ^{1}H NMR (400 MHz, $CDCl_3$) δ 7.73 (s, 1H, ArH), 7.47 (s, 1H, ArH), 7.26 (dd, *J* = 8.6, 1H, 2.0 Hz, ArH), 7.05 (d, *J* = 2.0 Hz, 1H, ArH), 7.02 (d, *J* = 8.6 Hz, 1H, ArH), 4.69 (d, *J* = 16.8 Hz, 1H, CH_2), 4.57 (d, *J* = 16.9 Hz, 1H, CH_2), 4.25-4.35 (m, 4H, apical CH_2 and $OC\underline{H}_2CH_3$), 4.17 (d, *J* = 16.8 Hz, 1H, CH_2), 3.98 (d, *J* = 16.9 Hz, 1H, CH_2), 1.34 (t, *J* = 7.1 Hz, 3H, CH_3), 2.42 (s, 3H, CH_3) ppm. HRMS (ESI) *m/z*: 387.0707 $[M+H]^+$ (calcd for $C_{19}H_{20}{}^{79}BrN_2O_2$, 387.0708; *m/z*: 389.0685 $[M+H]^+$ (calcd for $C_{19}H_{20}{}^{81}BrN_2O_2$, 389.0687).

The third compound eluted from the same column was symmetric dibromo TB **4** (600 mg, 14%) as a white solid. ^{1}H NMR (400 MHz, $CDCl_3$) δ 7.27 (dd, *J* = 2.2, 8.6 Hz, 2H, ArH), 7.05 (d, *J* = 2.2 Hz, 2H, ArH), 6.99 (d, *J* = 8.6 Hz, 2H, ArH), 4.64 (d, *J* = 16.8 Hz, 2H, CH_2), 4.24 (s, 2H, CH_2), 4.09 (d, *J* = 16.8 Hz, 2H, CH_2) ppm.[31]

Compound 5

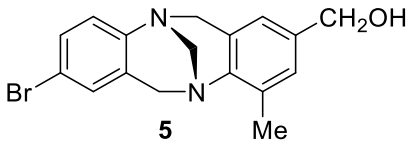

5

Lithium aluminium hydride (593 mg, 15.6 mmol, 6 equiv) was added to dry tetrahydrofuran (40 mL) and the mixture was stirred under an argon atmosphere in an ice bath for 30 min. Compound **3** (1.00 g, 2.6 mmol) was dissolved in dry tetrahydrofuran (15 mL) and added to the reaction mixture. The mixture was stirred at 0 °C for 2 h and then allowed to warm at room temperature overnight. Water (3 mL) and sodium hydroxide solution (15%; 6 mL) were added dropwise to the reaction mixture. Then more water (10 mL) was added to provide an inorganic precipitate. The reaction mixture was then rinsed with dichloromethane (2 × 200 mL) and the inorganic precipitate was filtered. The collected organic layers were washed with brine (100 mL),

dried over anhydrous magnesium sulfate, filtered and evaporated to dryness to afford **5** as a white solid (890 mg, 98%) m.p. 105-110 °C; FTIR ν_{max} 3372(br), 3225(br), 1669(s), 1011(s), 966(s), 894(s), 736(s), 725(s) cm^{-1}; ^{1}H NMR (400 MHz, $CDCl_3$) δ 7.22-7.28 (m, 1H, ArH), 7.02-7.06 (m, 2H, ArH), 7.01 (d, *J* = 8.7 Hz, 1H, ArH), 6.74 (app s, 1H, ArH), 4.64 (d, *J* = 16.8 Hz, 1H, CH_2), 4.51 (s, 2H, $C\underline{H}_2OH$), 4.47 (d, *J* = 16.9 Hz, 1H, CH_2), 4.24 (app s, 2H, apical CH_2), 4.09 (d, *J* = 16.8 Hz, 1H, CH_2), 3.93 (d, *J* = 16.9 Hz, 1H, CH_2), 2.38 (s, 3H, CH_3) ppm. ^{13}C NMR (100 MHz, $CDCl_3$) δ 147.05, 144.85, 136.37, 133.04, 130.33, 130.22, 129.69, 128.19, 127.42, 126.80, 123.09, 116.60, 67.03, 64.91, 58.71, 54.53, 17.11 ppm. HRMS (ESI) *m/z*: 345.0602 $[M+H]^+$ (calcd for $C_{17}H_{18}{}^{79}BrN_2O$, 345.0602); *m/z*: 347.0580 $[M+H]^+$ (calcd for $C_{17}H_{18}{}^{81}BrN_2O$, 347.0582).

Compound 6

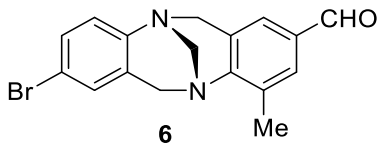

6

Manganese(IV)oxide (8.00 g, 92.0 mmol) was added to a solution of **5** (640 mg, 1.8 mmol) in dichloromethane (80 mL) at 0 °C and stirred for 30 min with a drying tube attached. The reaction mixture was allowed to warm at room temperature overnight. The mixture was then filtered through celite, and the solvent was evaporated to dryness to afford **6** (0.45 g, 70%) as a white solid. m.p. 145-146 °C; FTIR ν_{max} 2955(br), 2902(br), 1717(w), 1591(m), 1419(m), 1278(s), 1138(s), 949(s), 713(s), cm^{-1}; ^{1}H NMR (400 MHz, $CDCl_3$) δ 9.82 (s, 1H, CHO), 7.57 (app s, 1H, ArH), 7.25-7.32 (m, 2H, ArH), 7.06 (d, *J* = 1.9 Hz, 1H, ArH), 7.03 (d, *J* = 8.6 Hz, 1H, ArH), 4.72 (d, *J* = 16.8 Hz, 1H, CH_2), 4.60 (d, *J* = 16.8 Hz, 1H, CH_2), 4.20 (d, *J* = 16.8 Hz, 1H, CH_2), 4.29 (d, *J* = 13.5 Hz, 2H, apical CH_2), 4.01 (d, *J* = 16.8 Hz, 1H, CH_2), 2.45 (s, 3H, CH_3) ppm;

^{13}C NMR (100 MHz, $CDCl_3$) δ 191.39, 151.92, 146.73, 133.77, 132.03, 130.63, 130.38, 129.78, 129.63, 128.18, 126.85, 126.60, 116.80, 66.86, 58.51, 54.49, 17.23, ppm. HRMS (ESI) *m/z*: 343.0444 $[M+H]^+$ (calcd for $C_{17}H_{16}{}^{79}BrN_2O$, 343.0446); *m/z*: 345.0423 $[M+H]^+$ (calcd for $C_{17}H_{16}{}^{81}BrN_2O$, 345.0425).

Compound 7

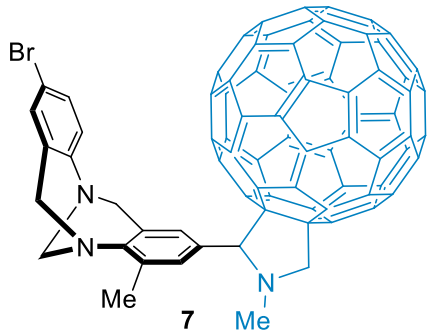

7

A mixture of **6** (144 mg, 0.42 mmol), fullerene-C_{60} (200 mg, 0.28 mmol) and *N*-methylglycine (40 mg, 0.45 mmol) in toluene (250 mL) was heated to reflux under an argon atmosphere overnight. The reaction mixture was allowed to cool to room temperature and solvent was removed under reduced pressure to afford a dark brown solid. Flash column chromatography (silica gel, 10% ethyl acetate/90% chloroform) yielded **7** as a dark brown solid in 20% yield; FTIR (neat) ν_{max} 2961, 2914, 2847, 2777, 2359, 1734, 1643, 1472, 1428, 1258, 1208, 1179, 1078, 1014, 943, 867, 794, 705, 598, 573 cm^{-1}; ^{1}H NMR (400 MHz, $CDCl_3$) δ 7.39 (br s, 1H), 7.21 (br s, 1H, ArH), 6.91-7.06 (m, 2H, ArH), 4.93 (d, *J* = 9.3 Hz, 1H, pyrrolidine H), 4.77 (s, 1H, pyrrolidine H), 4.65 (d, *J* = 16.8 Hz, 1H, TB CH_2), 4.52 (d, *J* = 16.8 Hz, 1H, TB CH_2), 4.28 (s, 2H, TB CH_2), 4.21 (d, *J* = 9.3 Hz, 1H, pyrrolidine H), 4.13 (d, *J* = 17 Hz, 1H, TB CH_2), 3.92 (d, *J* = 167 Hz, 1H, TB CH_2), 2.73 (s, 3H, pyrrolidine H), 2.39 (s, 3H, CH_3); HRMS (ESI) *m/z*: 1090.0905 $[M+H]^+$ (calcd for $C_{79}H_{21}{}^{79}BrN_3$, 1090.0919); *m/z*: 1092.0902 $[M+H]^+$ (calcd for $C_{79}H_{21}{}^{81}BrN_3$, 1092.0898).

References

1. Kroto, H. W.; Heath, J. R.; O'Brien, S. C.; Curl, R. F.; Smalley, R. E., *Nature* **1985**, *318*, 162-163.
2. Imahori, H.; Tamaki, K.; Araki, Y.; Sekiguchi, Y.; Ito, O.; Sakata, Y.; Fukuzumi, S., *J. Am. Chem. Soc.* **2002**, *124*, 5165-5174.
3. Imahori, H.; Fukuzumi, S., *Adv. Funct. Mater.* **2004**, *14*, 525-536.
4. Fukuzumi, S.; Saito, K.; Ohkubo, K.; Khoury, T.; Kashiwagi, Y.; Absalom, M. A.; Gadde, S.; D'Souza, F.; Araki, Y.; Ito, O.; Crossley, M. J., *Chem. Commun.* **2011**, *47*, 7980-7982.
5. Gust, D.; Moore, T. A.; Moore, A. L., *Acc. Chem. Res.* **2001**, *34*, 40-48.
6. Coropceanu, V.; Cornil, J.; da Silva Filho, D. A.; Olivier, Y.; Silbey, R.; Brédas, J.-L., *Chem. Rev.* **2007**, *107*, 926-952.
7. Jones, B. A.; Facchetti, A.; Wasielewski, M. R.; Marks, T. J., *J. Am. Chem. Soc.* **2007**, *129*, 15259-15278.
8. Guldi, D. M., *Chem. Soc. Rev.* **2002**, *31*, 22-36.
9. Benniston, A. C.; Harriman, A., *Mater. Today* **2008**, *11*, 26-34.
10. D'Souza, F.; Wijesinghe, C. A.; El-Khouly, M. E.; Hudson, J.; Niemi, M.; Lemmetyinen, H.; Tkachenko, N. V.; Zandler, M. E.; Fukuzumi, S., *Phys. Chem. Chem. Phys.* **2011**, *13*, 18168-18178.
11. Curiel, D.; Ohkubo, K.; Reimers, J. R.; Fukuzumi, S.; Crossley, M. J., *Phys. Chem. Chem. Phys.* **2007**, *9*, 5260-5266.
12. D'Souza, F.; Maligaspe, E.; Karr, P. A.; Schumacher, A. L.; El Ojaimi, M.; Gros, C. P.; Barbe, J. M.; Ohkubo, K.; Fukuzumi, S., *Chem. Eur. J.* **2008**, *14*, 674-681.
13. D'Souza, F.; Ito, O., *Coord. Chem. Rev.* **2005**, *249*, 1410-1422.

14. Davis, C. M.; Ohkubo, K.; Lammer, A. D.; Kim, D. S.; Kawashima, Y.; Sessler, J. L.; Fukuzumi, S., *Chem. Commun.* **2015**, *51*, 9789-9792.

15. Moreira, L.; Calbo, J.; Aragó, J.; Illescas, B. M.; Nierengarten, I.; Delavaux-Nicot, B.; Ortí, E.; Martín, N.; Nierengarten, J.-F., *J. Am. Chem. Soc.* **2016**, *138*, 15359-15367.

16. Runarsson, O. V.; Artacho, J.; Warnmark, K., *Eur. J. Org. Chem.* **2012**, , 7015-7041.

17. Tröger, J., *J. Prakt. Chem.* **1887**, *36*, 225-245.

18. Wang, Z. G.; Wang, D.; Jin, J., *Macromolecules* **2014**, *47*, 7477-7483.

19. Wang, Z. G.; Wang, D.; Zhang, F.; Jin, J., *Acs Macro Lett.* **2014**, *3*, 597-601.

20. Shanmugaraju, S.; Dabadie, C.; Byrne, K.; Savyasachi, A. J.; Umadevi, D.; Schmitt, W.; Kitchen, J. A.; Gunnlaugsson, T., *Chem. Sci.* **2017**, *8*, 1535-1546.

21. Sergeyev, S.; Diederich, F., *Angew. Chem. Int. Ed. Engl.* **2004**, *43*, 1738-1740.

22. Yeow, E. K. L.; Sintic, P. J.; Cabral, N. M.; Reek, J. N. H.; Crossley, M. J.; Ghiggino, K. P., *Phys. Chem. Chem. Phys.* **2000**, *2*, 4281-4291.

23. Lee, S. H.; Blake, I. M.; Larsen, A. G.; McDonald, J. A.; Ohkubo, K.; Fukuzumi, S.; Reimers, J. R.; Crossley, M. J., *Chem. Sci.* **2016**, *7*, 6534-6550.

24. Faroughi, M.; Zhu, K. X.; Jensen, P.; Craig, D. C.; Try, A. C., *Eur. J. Org. Chem.* **2009**, *2009*, 4266-4272.

25. Bhuiyan, M. D. H.; Zhu, K. X.; Jensen, P.; Try, A. C., *Eur. J. Org. Chem.* **2010**,, 4662-4670.

26. Bhuiyan, M. D. H.; Mahon, A. B.; Jensen, P.; Clegg, J. K.; Try, A. C., *Eur. J. Org. Chem.* **2009**, 687-698.

27. Sergeyev, S.; Schär, M.; Seiler, P.; Lukoyanova, O.; Echegoyen, L.; Diederich, F., *Chem. Eur. J.* **2005**, *11*, 2284-2294.

28. Ishida, Y.; Ito, H.; Mori, D.; Saigo, K., *Tetrahedron lett.* **2005**, *46*, 109-112.

29. Maggini, M.; Scorrano, G.; Prato, M., *J. Am. Chem. Soc.* **1993**, *115*, 9798-9799.

30. Pereira, R.; Cvengroš, J., *Eur. J. Org. Chem.* **2013**, *2013*, 4233-4237.

31. Jensen, J.; Strozyk, M.; Warnmark, K., *J. Heterocyclic Chem.* **2003**, *40*, 373-375.

32. Günther, H., *NMR spectroscopy: basic principles, concepts and applications in chemistry*. John Wiley & Sons: 2013.

SUPPORTING INFORMATION

Synthesis of a Halogen Functionalised Tröger's Base-C_{60} Analogue

Md Imam Ansari, Andrew Try, and Peter Karuso*

Department of Molecular Sciences, Macquarie University, Sydney NSW 2109, Australia

* Corresponding author. Tel.: +612-9850-8290 fax: +612-9850-8313, e-mail: peter.karuso@mq.edu.au

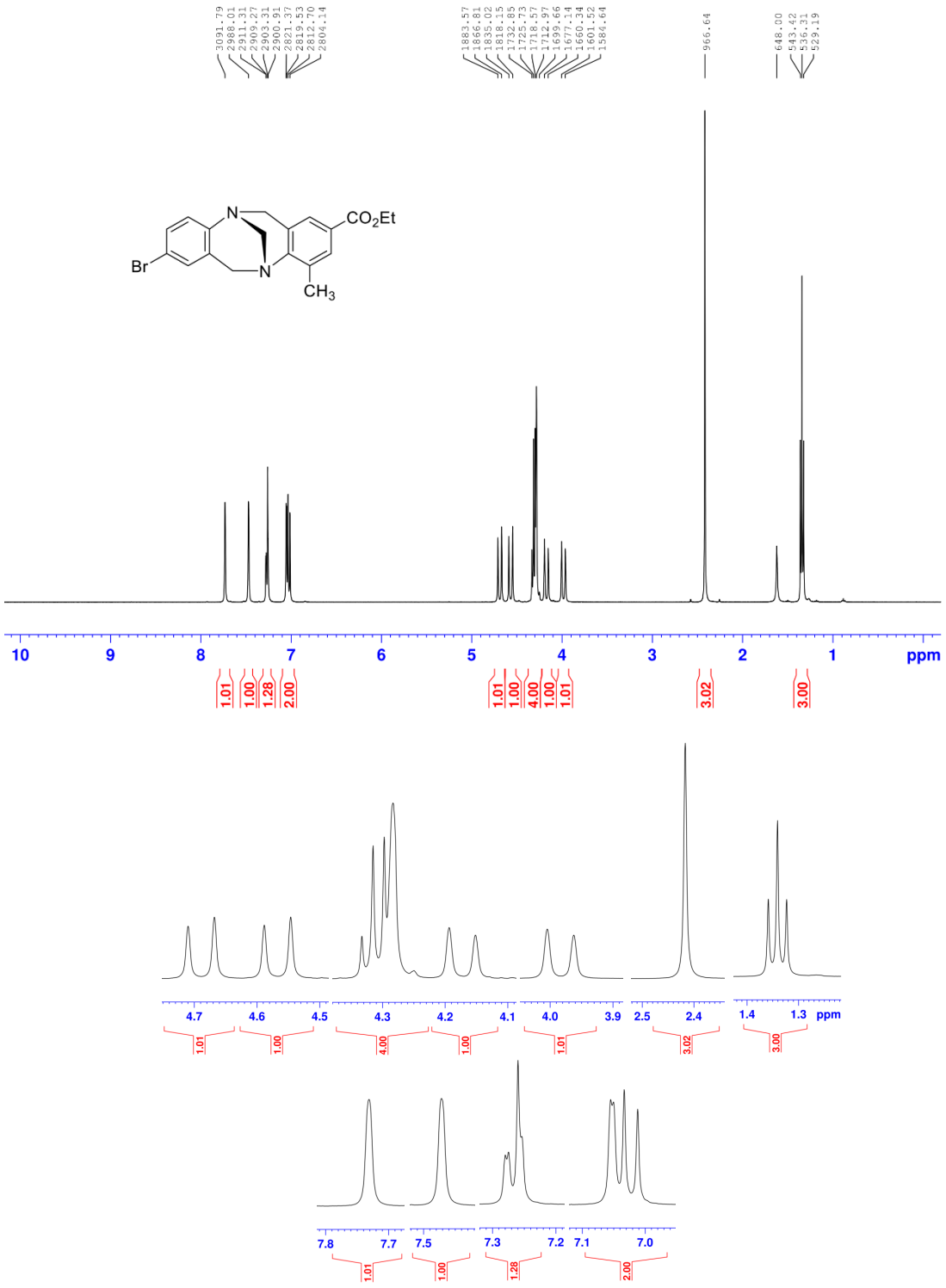

Fig. S1 ^{1}H NMR spectrum (400 MHz) of **3** in $CDCl_3$.

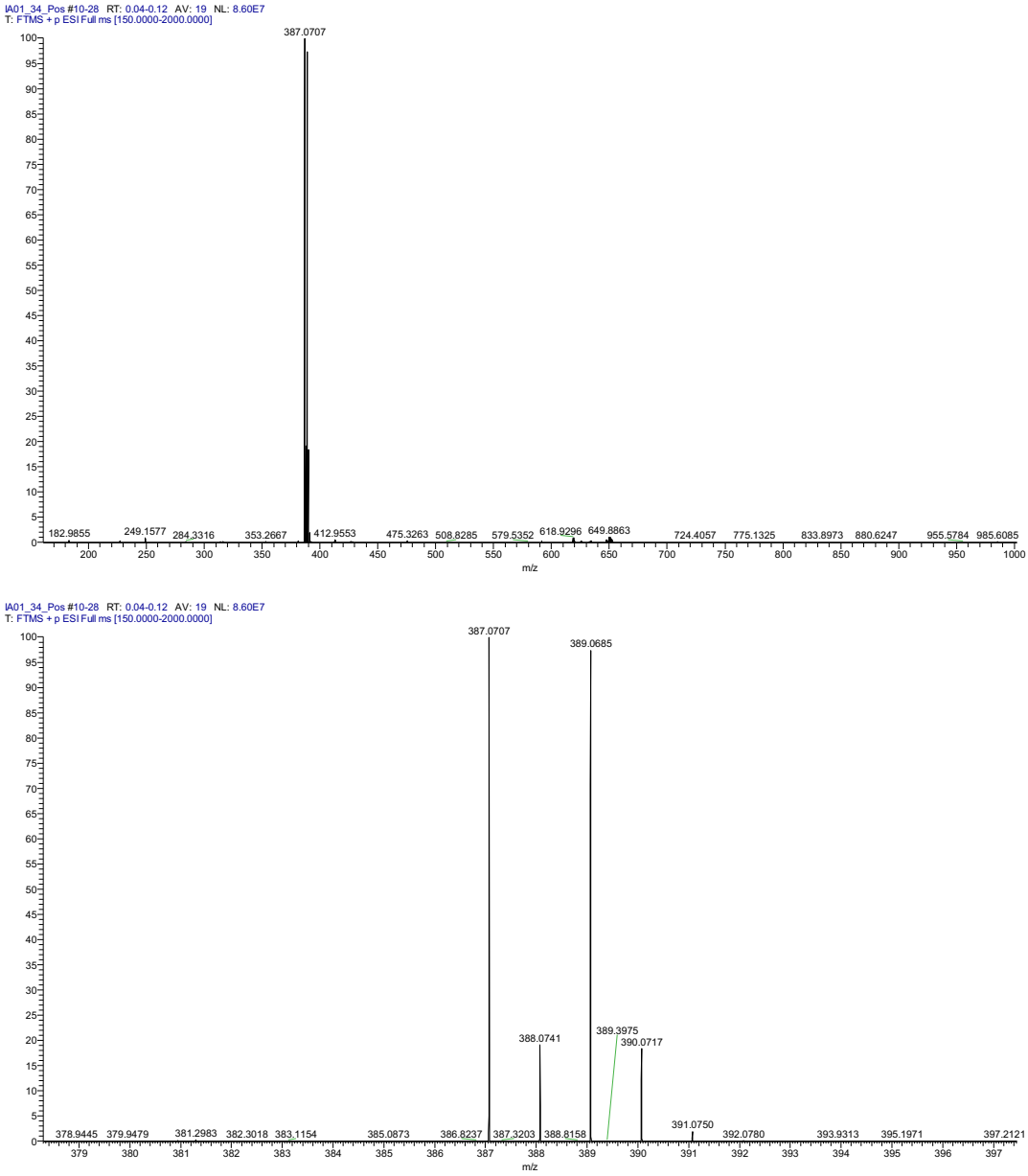

Fig. S2 High resolution mass spectrum of **3**.

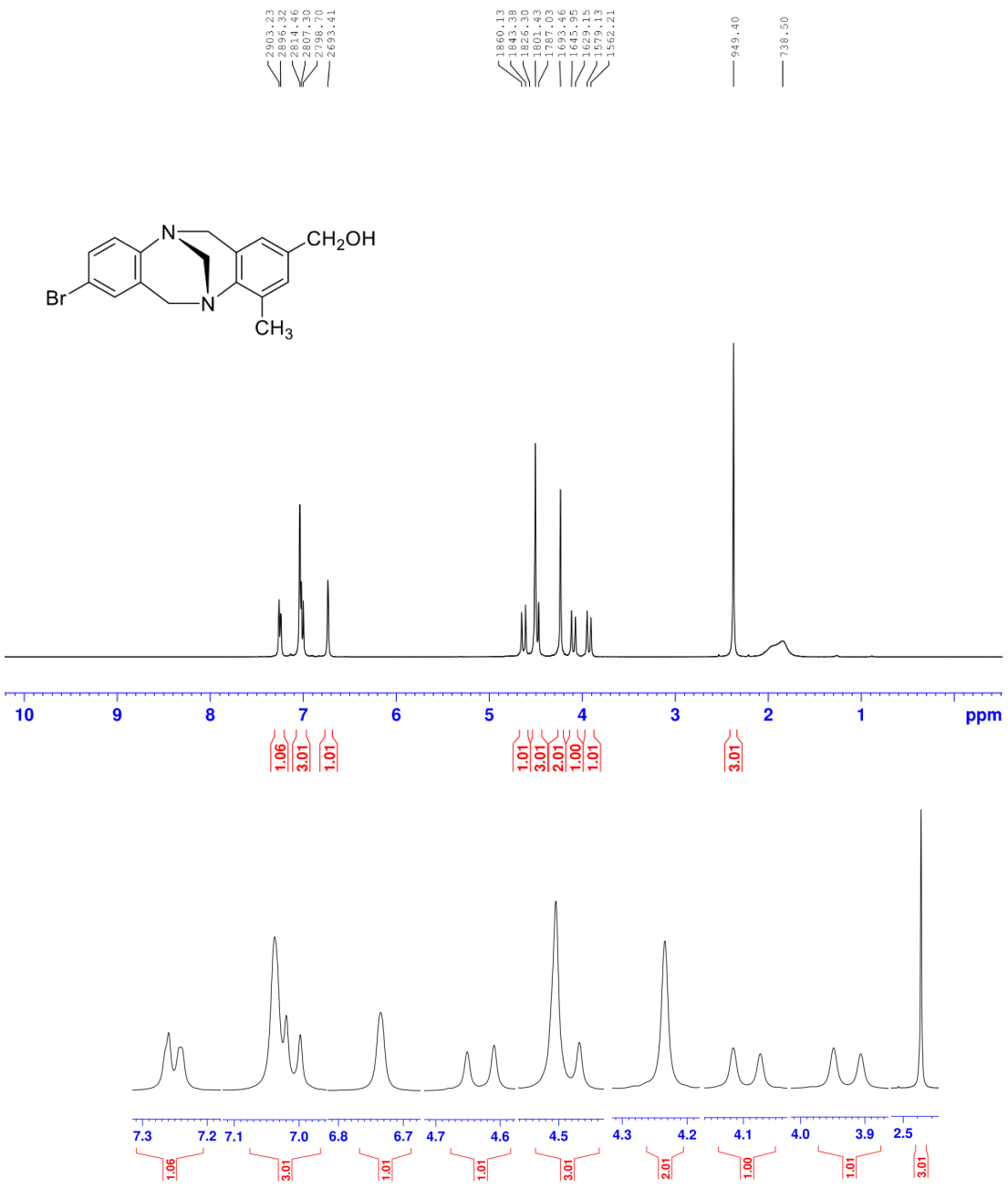

Fig. S3 ^{1}H NMR spectrum (400 MHz) of **5** in $CDCl_3$.

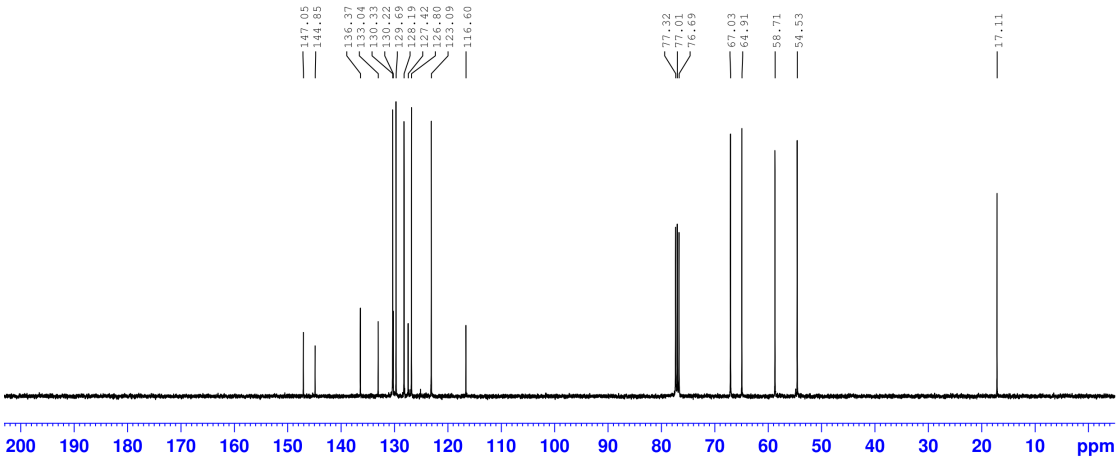

Fig. S4 ^{13}C NMR spectrum (100 MHz) of **5** in $CDCl_3$.

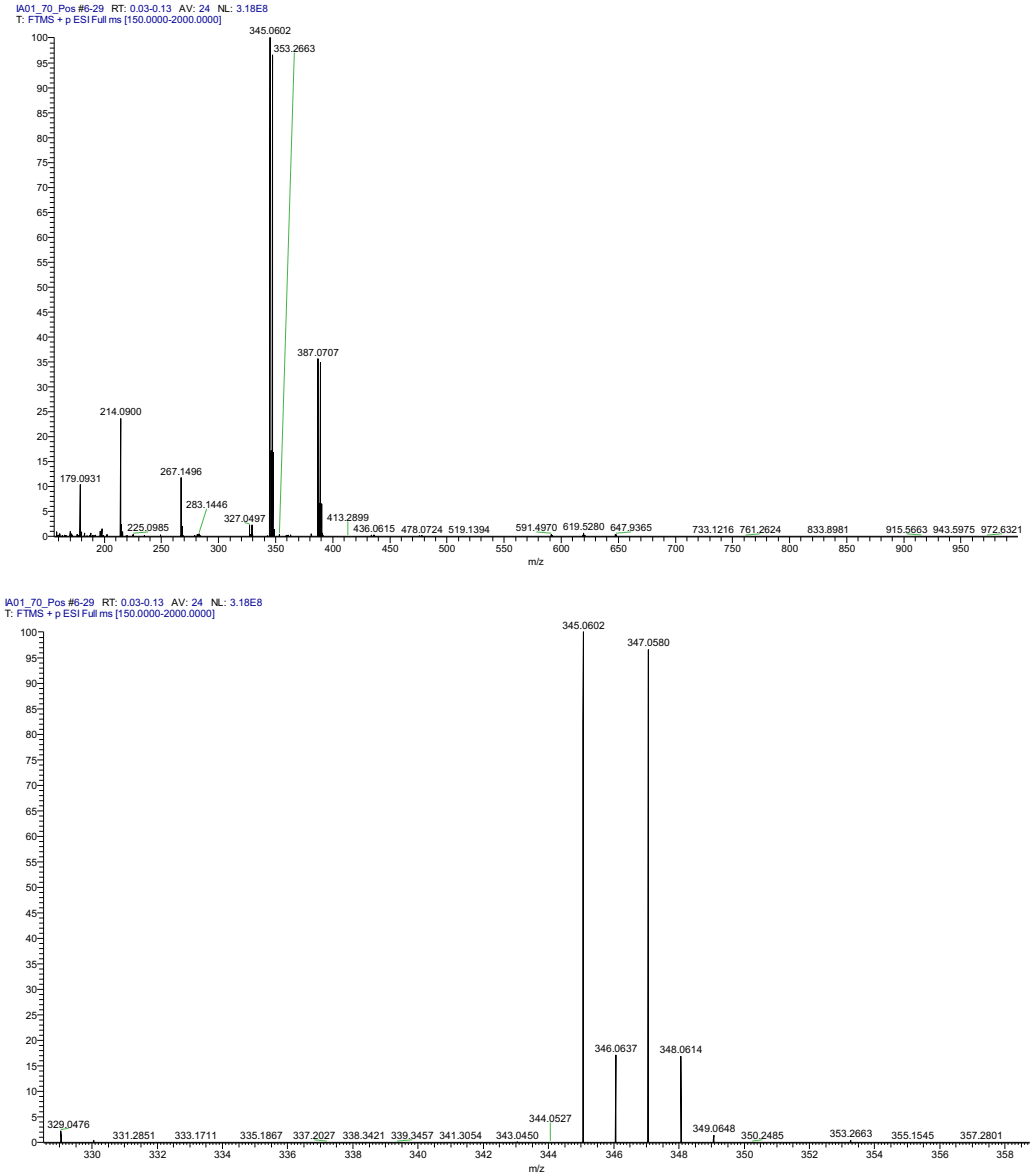

Fig. S5 High resolution mass spectrum of **5**.

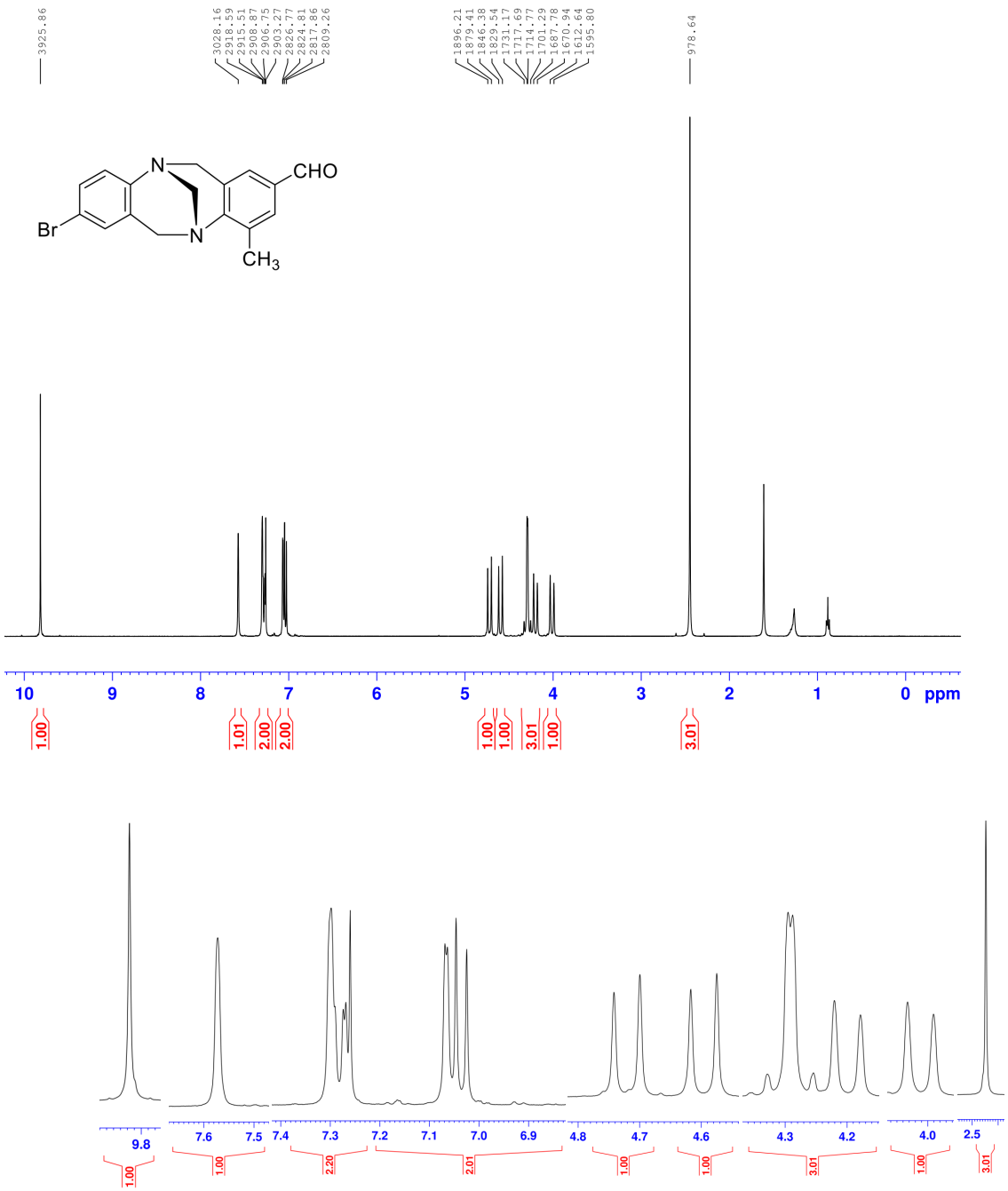

Fig. S6 ^{1}H NMR spectrum (400 MHz) of **6** in $CDCl_3$.

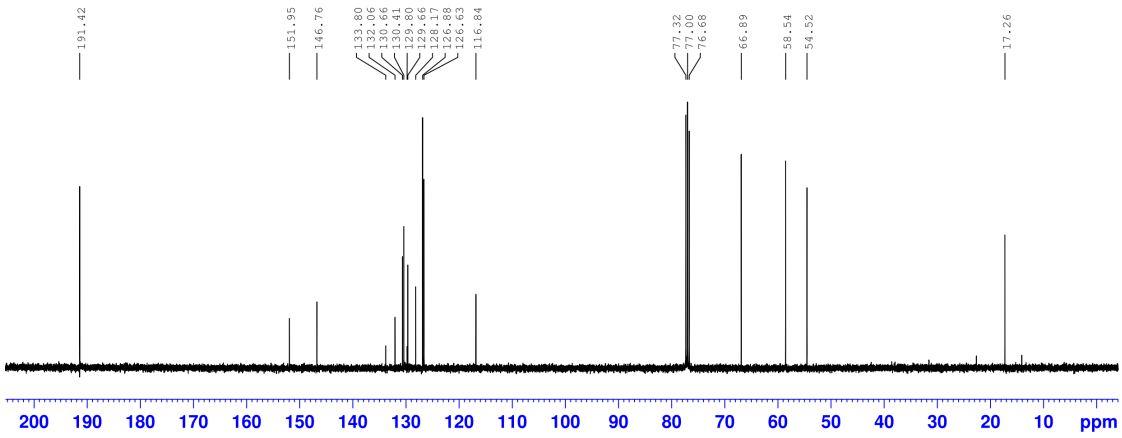

Fig. S7. ^{13}C NMR spectrum (100 MHz) of **6** in $CDCl_3$.

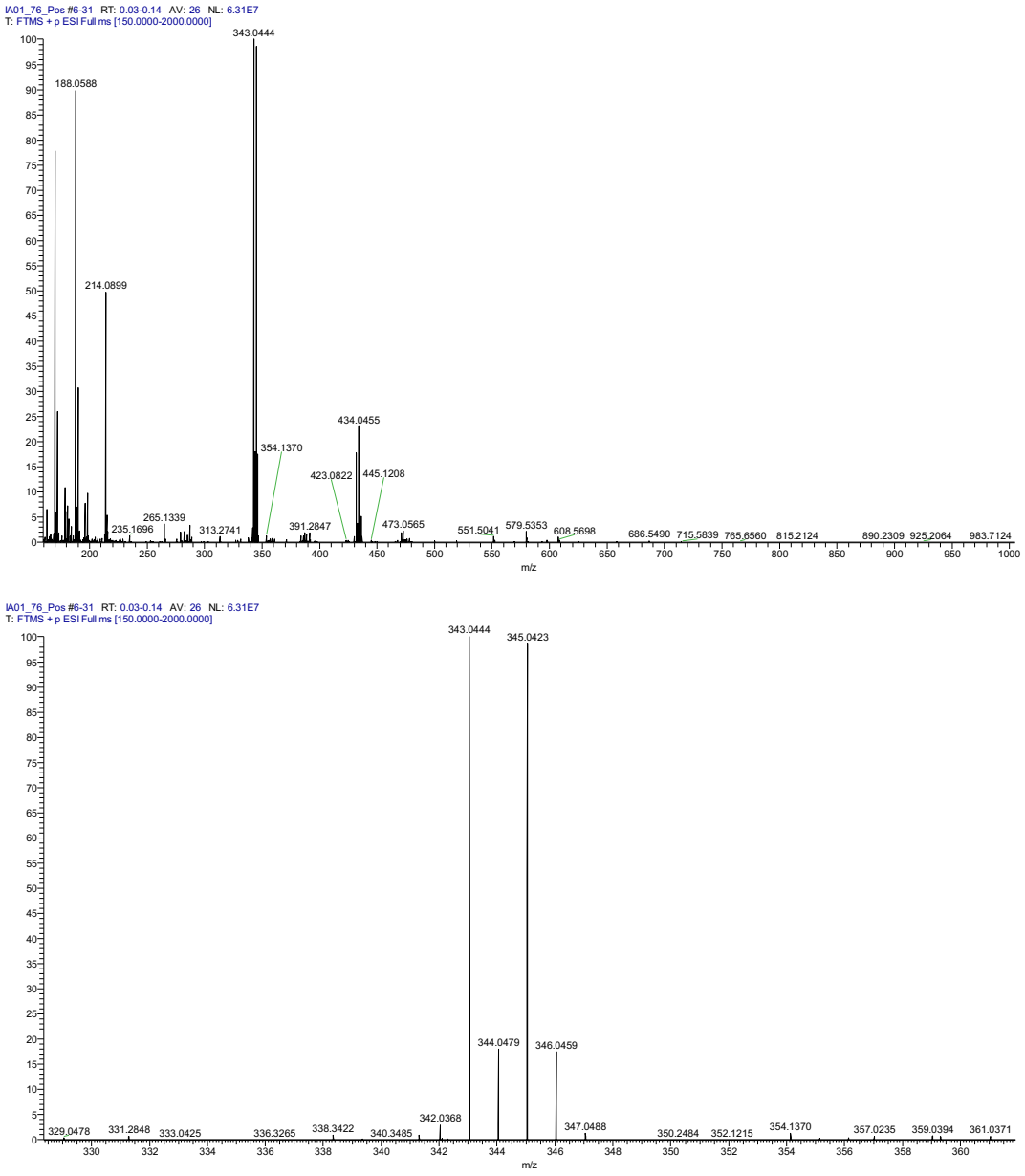

Fig. S8 High resolution mass spectrum of **6**.

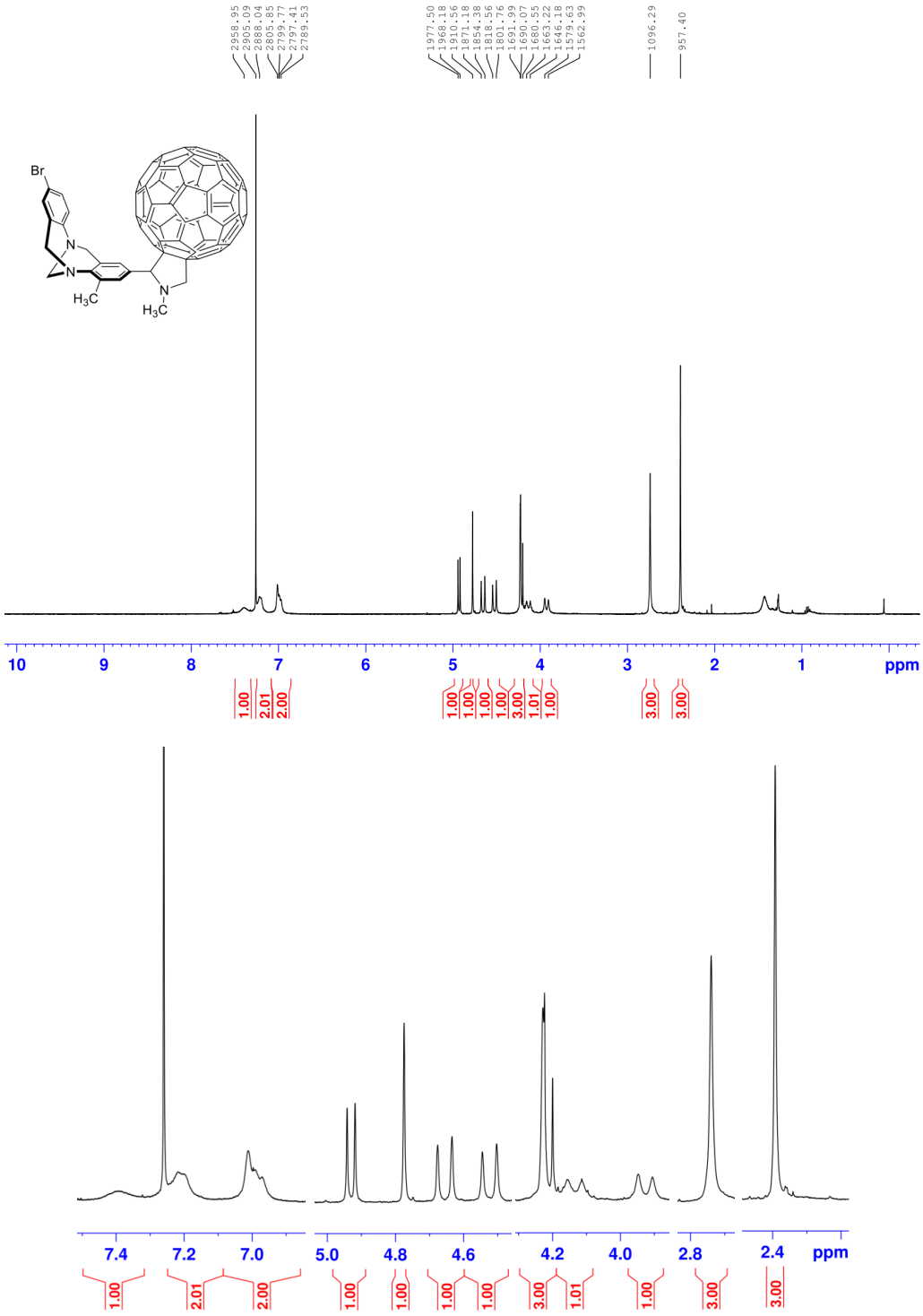

Fig. S9 ^{1}H NMR spectrum (400 MHz) of **7** at 25°C in $CDCl_3$.

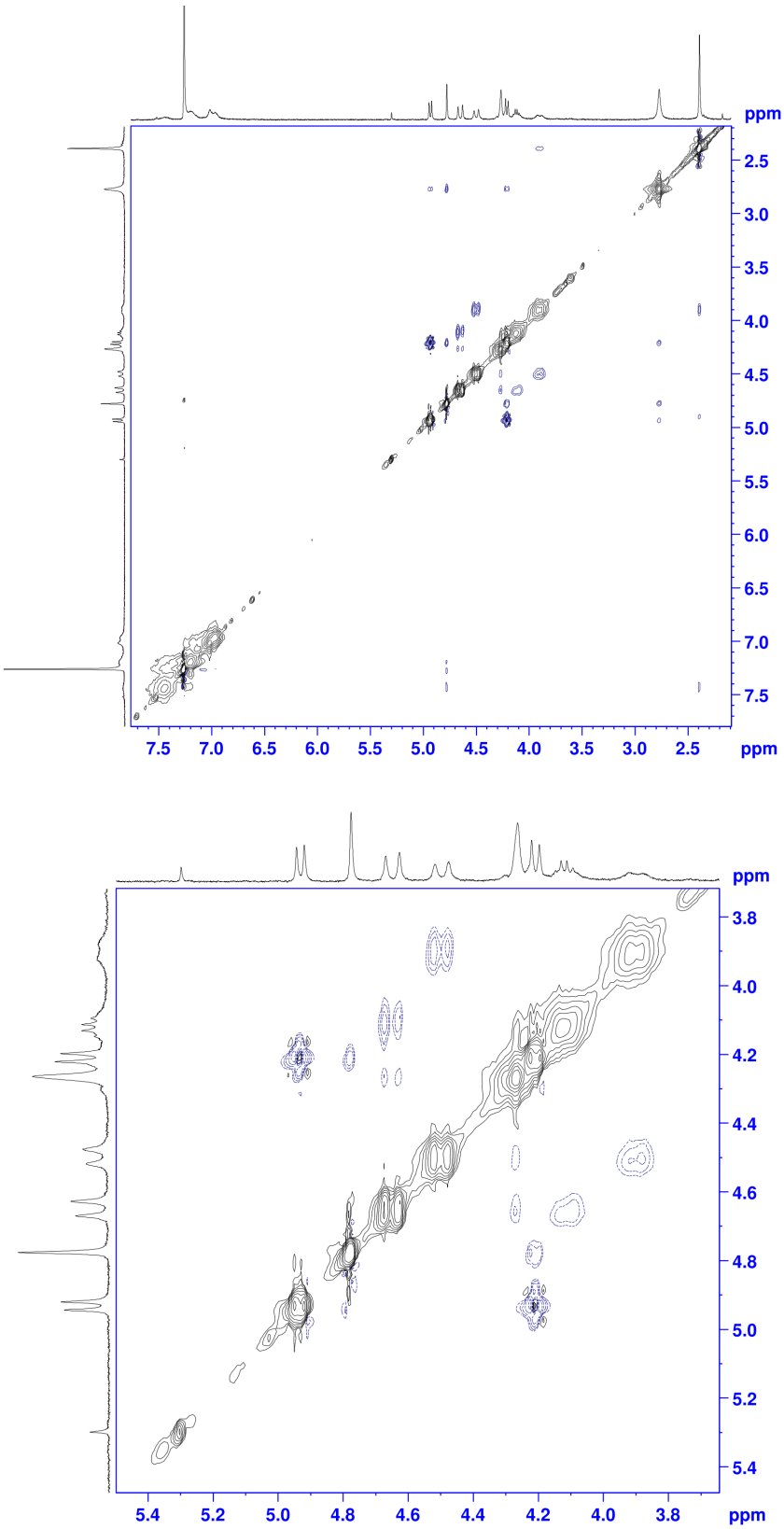

Fig. S10 ^{1}H-^{1}H NOESY spectrum (400 MHz) of **7** in $CDCl_3$. Mixing time of 100 ms used.

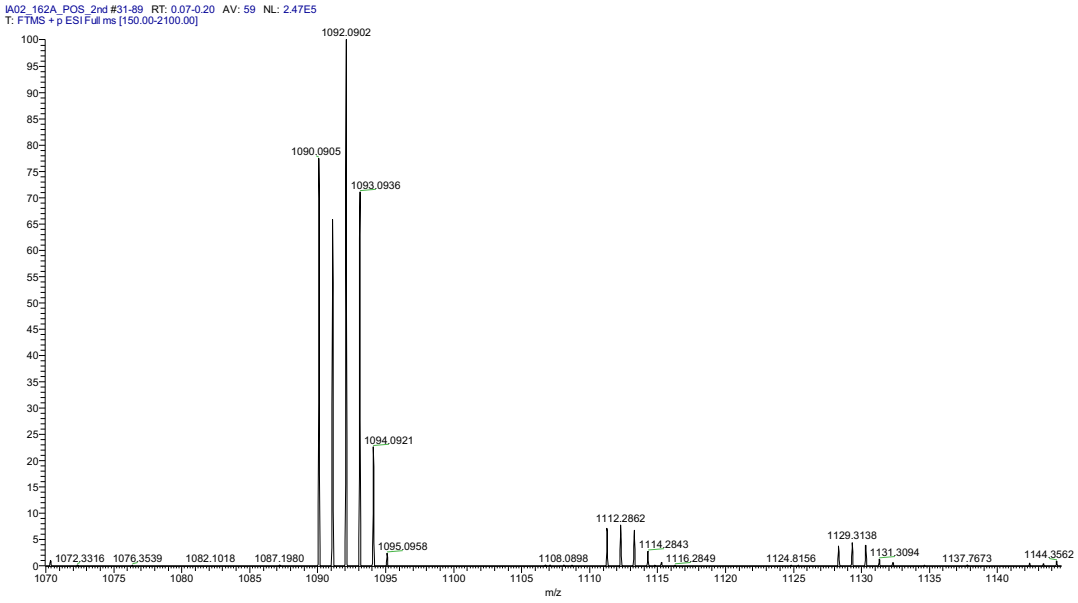

Fig. S11 High resolution mass spectrum of **7**.

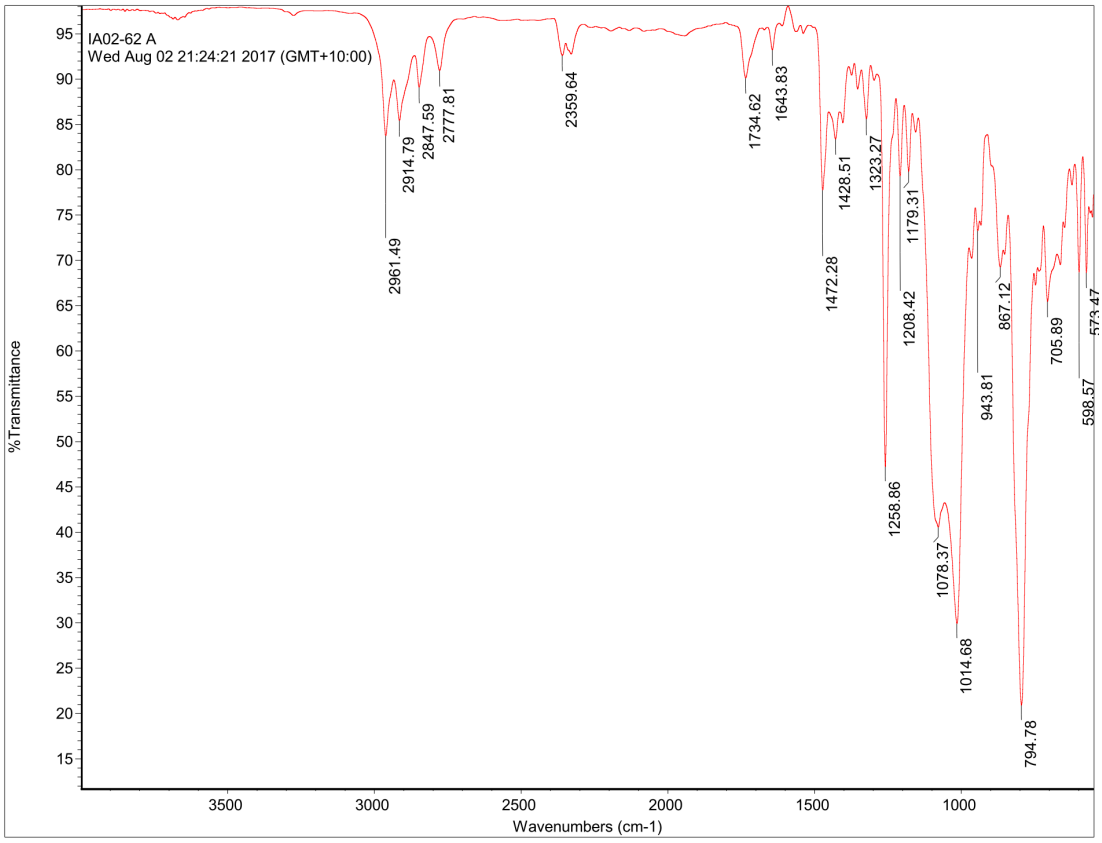

Fig. S12 Fourier transform infrared (FTIR) spectrum of **7**.

Chapter Three

Statement of Contribution

The research presented in this manuscript is based on work done by author (M.I.A) except high-resolution mass spectra which were obtained commercially at Australian Proteome Analysis Facility (APAF), Macquarie University. DFT-D3//BP86/SV(P) calculation was done by (P.K). The manuscript was written by author (M.I.A) and it was checked and edited by the principal supervisor (P.K).

Synthesis and Photophysical Properties of Λ-Shaped non-Conjugated Porphyrin Dyad

Md Imam Ansari, Andrew Try, and Peter Karuso*

Department of Molecular Sciences, Macquarie University, Sydney NSW 2109, Australia

* Corresponding author. Tel.: +612-9850-8290 fax: +612-9850-8313, e-mail: peter.karuso@mq.edu.au

Abstract Five new non-conjugated Λ-shaped porphyrin based-systems (dyads **4**, **5**, **6**, **8** and **9**) have been synthesised. The two porphyrins are connected *via* Tröger's base through *meso* phenyl positions of porphyrins. Mono and dizinc(II) derivatives can be prepared over pre-formed porphyrin Tröger's base dyads. Electronic properties have been determined by steady state UV/Visible and fluorescence spectroscopy. The designed hosts are suitable candidates towards the goal of understanding the process of photoinduced electron transfer in dyads where bridge molecule and V-type configuration are important. For comparative purpose fused-porphyrin Tröger's base (dyads **11**-**12**) were synthesised.

Introduction

During the past decades, porphyrins have attracted much attention for the design and synthesis of artificial photosynthetic systems because of their remarkable, optical, electrical and optoelectronic properties.[1, 2] Various linear and conjugated porphyrin arrays have been developed to better understand structure-electronic properties relationship between the two chromophores.[3-7] These arrays generally have the porphyrins in linear or parallel sheets but Crossley and Ghiggino reported the intramolecular electronic energy transfer (EET) between two porphyrins bridged by a quinoxaline Tröger's base where the rigid bridge was postulated to be responsible for enhanced energy transfer.[8] Elegant donor-acceptor systems have subsequently been design to study photoinduced electron transfer in these systems.[1, 2, 8-12] The construction of through-space interacting porphyrin arrays has been hampered due to lack of efficient scaffolding materials and difficulty in positioning the porphyrin entity in close proximity to another chromophore and development of such dyads still remained as a challenge.[13] All these systems have the Tröger's base fused to the porphyrin core but a different approach would be to join the two porphyrins *via* one of the *meso* positions as

a result maintaining the fixed angle between the two porphyrins offered by the Tröger's base but rotating the porphyrins by 90°. A synthetic strategy for attaching a non-conjugated Tröger's base between two porphyrins is reported for the first time along with the synthesis of five new Tröger's base bridged by porphyrins.

Tröger's base[14] (**1**) is a unique chiral amine with two stereogenic nitrogens in the diazocine bridge that was first prepared in 1887 by the acid-catalysed condensation of *p*-toluidine and formaldehyde (Fig. 1).[14] A unique set of structural features (rigidity, C_2 symmetry and Λ-shaped) make Tröger's bases useful for molecular frameworks or artificial receptors,[15-18] functional materials,[19] gas separation,[20, 21] DNA targeting fluorescent probes[22, 23] and phosphorescent organic light emitting diodes (PhOLEDs).[19, 24]

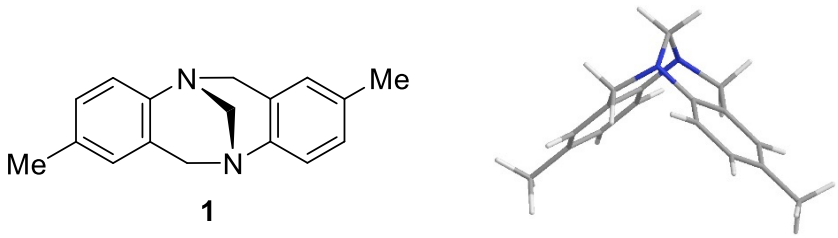

1

Fig. 1 Structural formula and optimised geometry of Tröger's base **1**.

Molecular modelling and density functional theory (DFT) calculations (Fig. 2) suggested that these novel structures would hold the two porphyrins in close proximity (~5 Å) at an angle of ~90° and a dihedral of the two porphyrin planes of ~33°. These compounds should be particularly useful for further investigation of the electronic properties of porphyrin dimers due to their rigid Λ-shape[25] and because of the chiral cavity created by the Tröger's base.[26] The bis-porphyrins dyads discussed in this paper will provide an opportunity to understand the effects of the bridging molecule in mediating energy or electron transfer due to their unique spatial orientation compared to previous bis-porphyrin dyads.[8, 27] The me*so*-*p*-nitrophenyl porphyrin **2** was

synthesised by reacting 4-nitrobenzaldehyde (1 equiv) and 3,5-di-*tert*-butyl benzaldehyde (3 equiv) with freshly distilled pyrrole (4 equiv) in chloroform with a catalytic amount of boron trifluoride diethyl etherate.[28] The tetrahydroporphyrins were oxidised *in situ* with *p*-chloroanil. TLC showed the presence of two major compounds, which were purified by column chromatography (50% dichloromethane/50% hexane) with **2** eluting as second spot in 21% yield from 4-nitrobenzaldehyde.

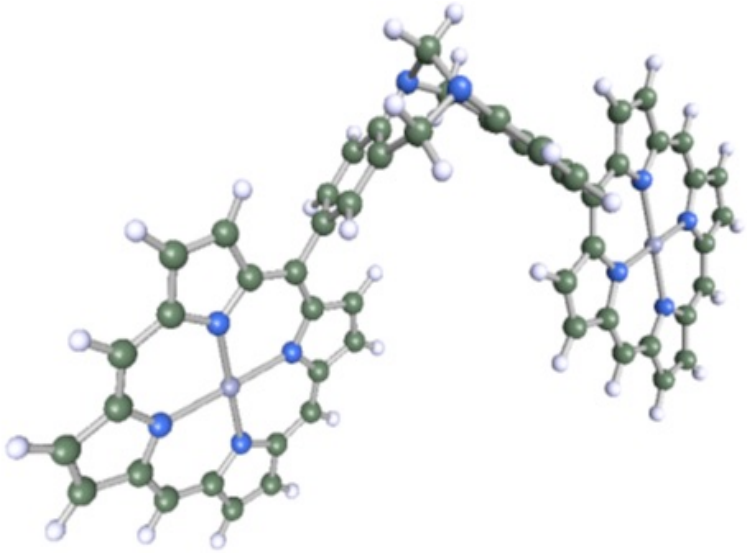

Fig. 2 Energy minimised structures of the bis-porphyrin Tröger's base (minus *meso* aryl groups) from DFT-D3//BP86/SV(P)-COSMO (for $CHCl_3$) calculations.

The nitro group of **2** was reduced ($SnCl_2$) in good yield to **3** and reacted with paraformaldehyde in the presence of TFA to provide the free-base porphyrin dyad **4** in 55% yield. Porphyrin **7** was synthesised by Luguya's procedure[29] (Supplementary Information) this was transformed into free-base porphyrin dyad **8**.

In each case, metallo derivatives can be obtained in excellent (88-94%) yield under standard conditions. The free bases and the zinc(II) porphyrin derivatives were characterised by ^{1}H NMR, FTIR and mass spectrometry (Supplementary Information).

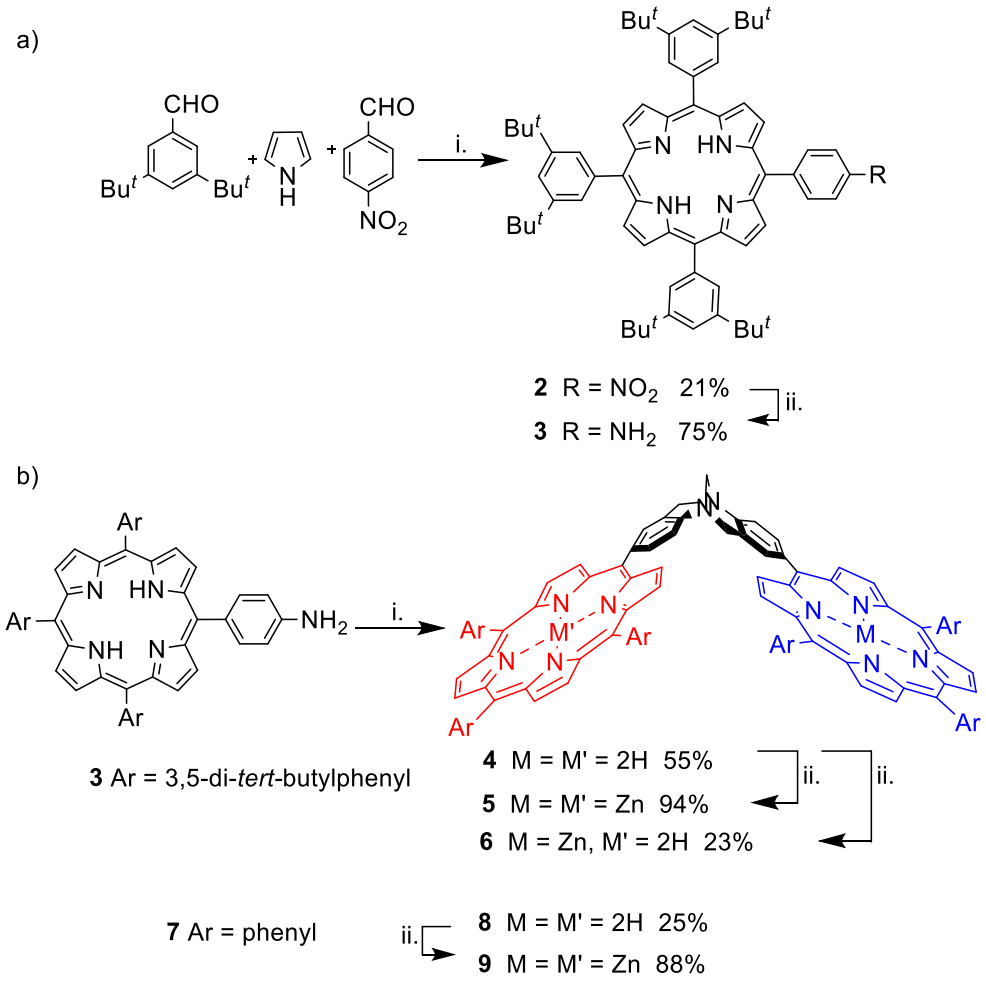

Scheme 1: a) Synthesis of porphyrin aniline **3** i. BF_3OEt_2, $CHCl_3$, rt; then *p*-chloranil, reflux; ii. $SnCl_2$, conc. HCl, CH_2Cl_2. b) Synthesis of porphyrin Tröger's base. i. TFA, $(CH_2O)_n$, Ar, rt, 7 days; ii. $Zn(OAc)_2$, $CHCl_3$, 30 min.

For comparison purposes, the known dyads **11** and **12** were synthesised using literature methods (Scheme 2).[27] In case of symmetric Tröger's base analogues,[30, 31] the most striking feature of the ^{1}H NMR spectrum lies between 4.0 and 5.5 ppm where protons of the diazocine bridge resonate (Fig. 3). The dyads **4**, **8**, **11** and **12** revealed a characteristic diazocine bridge protons; two geminally coupled doublets (J = 17-18 Hz), and the apical methylene strap appear as a singlet (Supporting Information, Figs S5, S14, S20, S21). Interestingly, the characteristic diazocine bridge protons of the

dizinc(II)porphyrins dyads **5**, **6** and **9** were very broadened (Figs S8, S11, S17) in the ^{1}H NMR spectra. The Fig. 3 indicates slow conformational change on the NMR time scale in dizinc compound. The figure provides information on metallation of two-porphyrin which are in face to face position and how the 1H NMR spectra bridge region of porphyrin TB changes from free-base to dizinc dyads. Suppression of bridge region (4-5 ppm) peaks were not observed in case of free-base dyads that indicates phenomenon is being observed due to metallation. Alternatively, this phenomenon (suppression of bridge region peaks) may be possibly due to aggregation of porphyrins. We tried to resolve bridge region peaks by using VT-NMR without any success. .

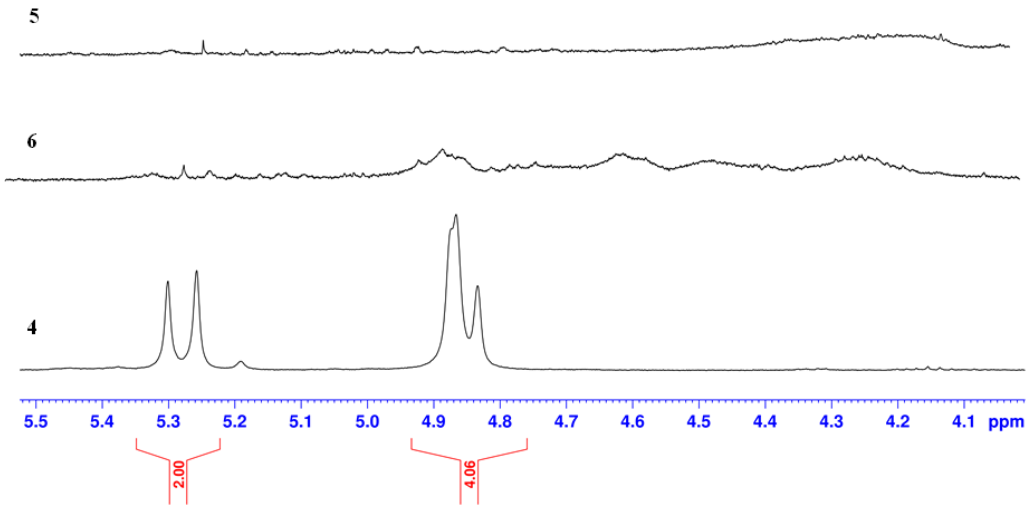

Fig. 3 Partial ^{1}H NMR spectrum of porphyrin dyads **5**, **6** and **4** in $CDCl_3$ at 298 K illustrating diazocine bridge region.

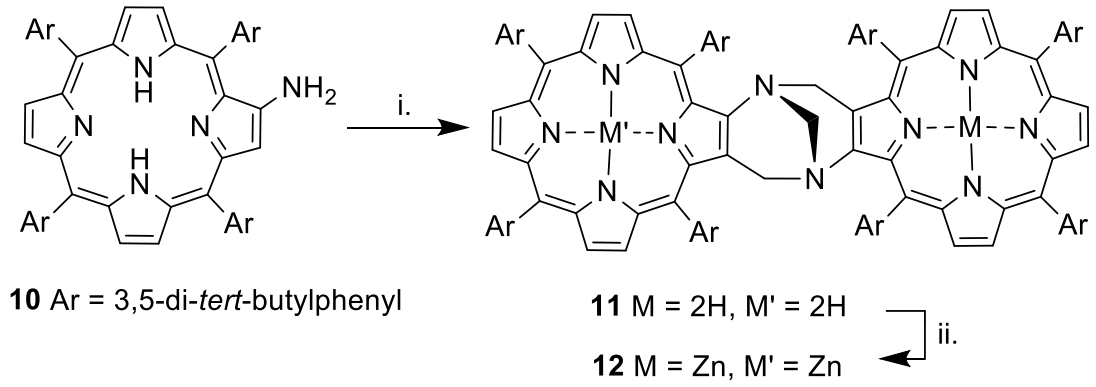

10 Ar = 3,5-di-*tert*-butylphenyl

11 M = 2H, M' = 2H

12 M = Zn, M' = Zn

Scheme 2: Synthesis of fused-porphyrin TB **11** and **12** i. Formaldehyde (37% in H_2O), THF; then 2:1 ethanol/HCl, Ar, 50-60 °C 18 h, 60%; ii. $Zn(OAc)_2$, $CHCl_3$, 30 min., 82%.[27]

Photophysical Properties

The UV/Vis absorption spectra of dyads **4**-**6** and monomeric porphyrin **3** in $CHCl_3$ are shown in Fig. 4A. The free base dyad **4** and monozinc dyad **6** exhibited a split Soret band at 422 and 451 nm, due to excitonic coupling dipole-dipole interactions between the porphyrin moieties.[32-34] In contrast, dizinc dyad **5** displayed split Soret band at 422 and 452 nm where band at 452 nm was almost collapsed. This could be due to metallation of both porphyrin rings that caused increase in symmetry and consequently this splitting was not large compared to **4** and **6**. The exact reason is still unknown. In contrast, in the case of **5**, Q-bands were essentially collapsed into one band due to increase in symmetry (D_4) upon zinc metallation. Mandoj and co-workers reported on the β-pyrazino-fused tetraphenyl porphyrins with a split Soret band indicated strong ground state interaction between the two porphyrins.[35] Comparing with these results suggest some electronic communications between the two porphyrins of **4**-**6**.

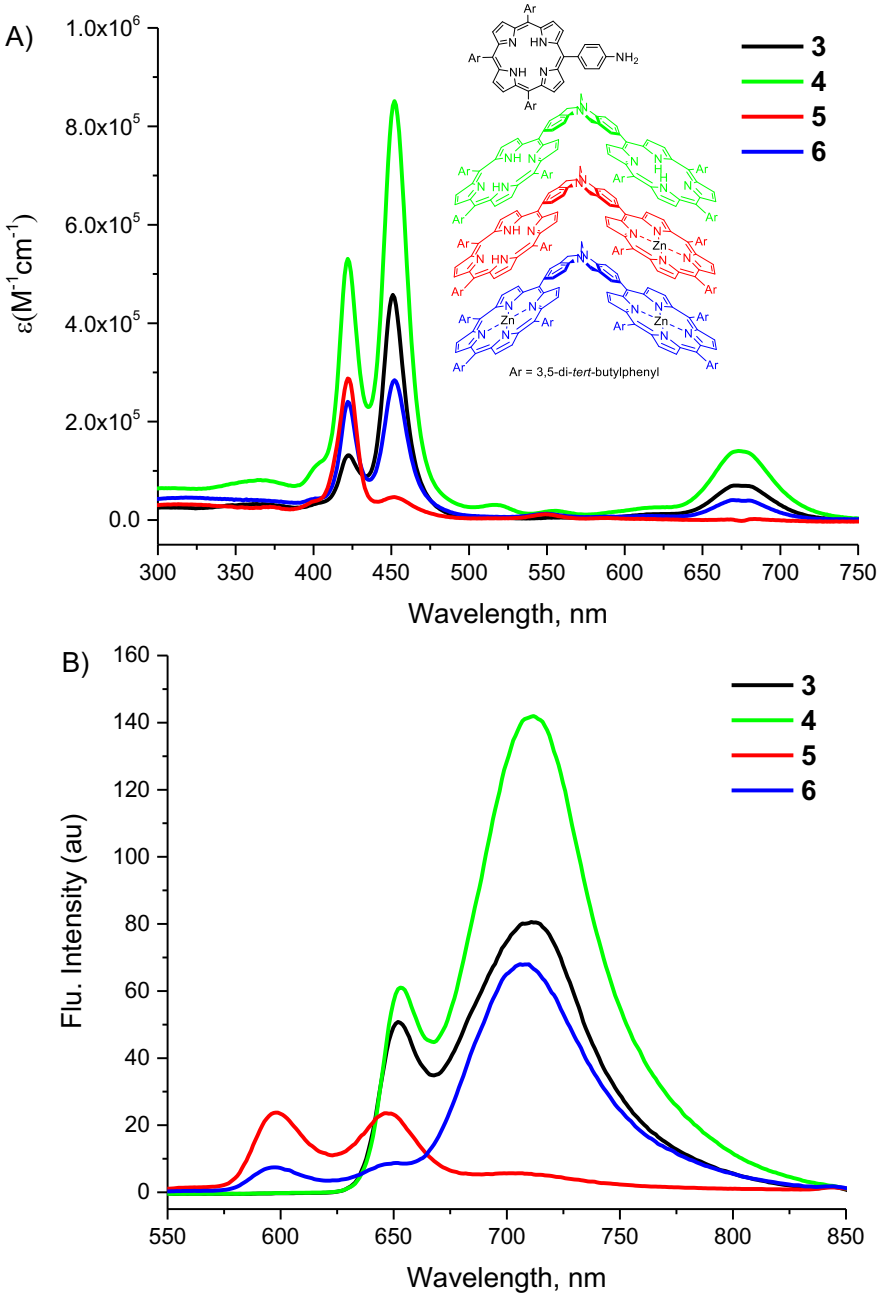

Fig. 4 A) UV/Vis spectra and B) emission spectra of **3** (black), **4** (green), **5** (red) and **6** (blue) in $CHCl_3$ at 1.6×10^{-6} M (λ_{ex} = 423 nm, λ_{abs} = 423 nm).

Fluorescence spectra of dyad **4-6** along with monomer **3** are shown in Fig. 4B. The samples were excited at 423 nm. Upon excitation, the free base porphyrin dyad **4** and the monozinc porphyrin dyad **6**, they displayed red emission at 653 nm assign to Q(0,1) and a strong emission at 720 nm which corresponds to Q(2,0) (Fig. 6).[36] In

contrast dizinc(II)porphyrin dyad **5** showed weak emission at 595 and 605 nm with broad absorption at 700 nm. Interestingly, monozinc dyad **6** revealed features of both dyads **4** and **5** with the three emission peaks instead two, referring to the combination of free base and dizinc(II)porphyrin emission bands.

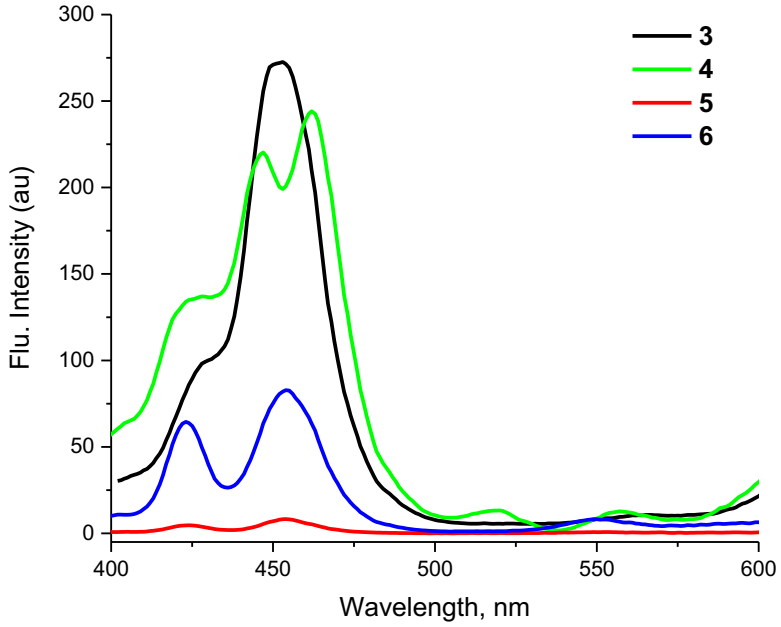

Fig. 5 Fluorescence excitation spectra of **3** (black), **4** (green), **5** (red) and **6** (blue) in $CHCl_3$ (1.6×10^{-6} M) (λ_{em} = 650 nm).

Energy transfer could be better predicted in case of dyad **6**. Upon excitation, the energy from the metallated porphyrin unit which is at higher energy is transferred to the free base porphyrin which is at low energy. The zinc porphyrin unit acts as donor and the free base acted as the acceptor. The fluorescence is quenched in dyads **5** and **6**, indicative of some energy transfer phenomena.

We monitored the fluorescence excitation spectra of dyads **4-6** to investigate preliminary information regarding electronic communication between the two porphyrin (Fig. 5). At the emission wavelength (λ_{em} 650 nm) of the free base **4** showed

a strong excitation spectrum with the three Q bands peaks. However, upon metallation dyad **5** and **6** showed a drastic decrease in excitation, suggesting some electronic communication between the two porphyrin moieties. On the other hand, in the case of triphenylporphyrin dyad **9**, the Soret band splitting was more compared to free-base dyad **8** (Fig. 6A). The dizinc(II)porphyrin dyad **9,** revealed the large splitting (419 and 447 nm) spectra due to exciton coupling,[33, 34] similar with dizinc(II) porphyrin dyad **5** (Fig. 6A). The most intense band for free-base porphyrin Tröger's base **8** was located at 448 nm, while two Q-bands were present at 610 and 668 nm. Interestingly dyad **9**, also revealed two additional weak bands (Q-bands) at 547 and 663 nm which indicates the symmetry of **9** is increased due to metallation but less symmetric compared to **5** due to the rigidifying effects of the 12 *tert*-butyl groups in **5**. Emission spectra of triphenylporphyrin dyads (**8** and **9**) have nearly identical fluorescence emissions with only a slight blue shift on metallation with zinc (**9**) (Fig. 6B). The absorption spectra of **11** and **12** showed some indication of exciton coupling with a shoulder on the emission peak (Fig. S4).

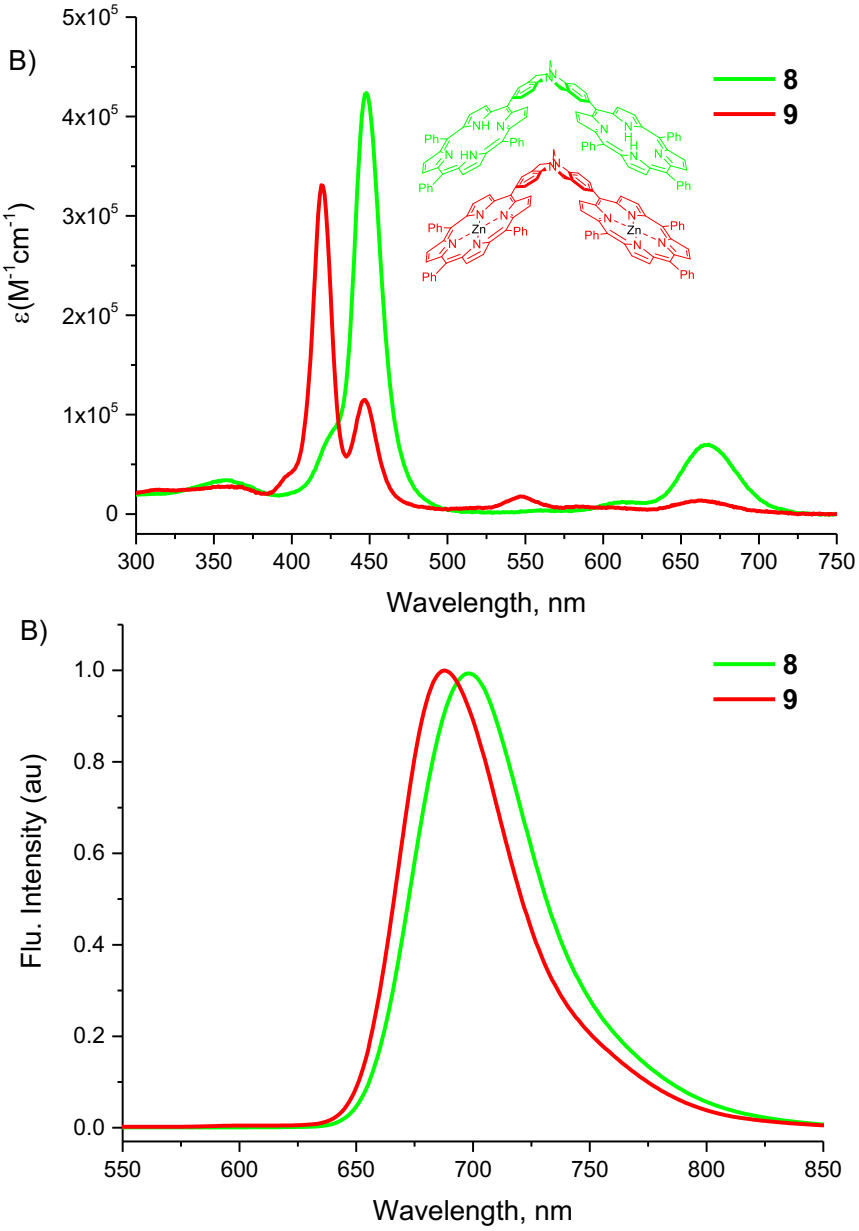

Fig. 6 A) UV/Vis spectra (top) and B) normalized emission spectra (bottom) of **8** (green), and **9** (red) in $CHCl_3$ at λ_{ex} = 451 nm. The concentration of each compound was 2.4×10^{-6} M.

In this communication, we have successfully synthesized and characterized a series of novel bis-porphyrin dyads that hold the two porphyrins in close proximity. Initial photophysical studies suggests that the existence of an exciton interaction of the

dimetallated porphyrin that is much stronger than in previously synthesised dyads based on Tröger's base. This work opens the door on a new class of supramolecular donor-acceptor dyads that could find utility molecular frameworks or artificial receptors, functional materials, fluorescent probes and phosphorescent organic light emitting diodes (PhOLEDs).

Acknowledgements

The authors thank for financial supports from Macquarie University. We also like to thank India@75 and Macquarie University for the award of an iMQRES PhD scholarship to M.I.A.

References

1. M. R. Wasielewski, *Chem. Rev.*, 1992, **92**, 435-461.
2. O. Ito and F. D'Souza, *Molecules*, 2012, **17**, 5816-5835.
3. V. Bandi, H. B. Gobeze, P. A. Karr and F. D'Souza, *J. Phys. Chem. C*, 2014, **118**, 18969-18982.
4. A. C. Benniston and A. Harriman, *Mater. Today*, 2008, **11**, 26-34.
5. P. E. Hartnett, C. M. Mauck, M. A. Harris, R. M. Young, Y. L. Wu, T. J. Marks and M. R. Wasielewski, *J. Am. Chem. Soc.*, 2017, **139**, 749-756.
6. E. Maligaspe, N. V. Tkachenko, N. K. Subbaiyan, R. Chitta, M. E. Zandler, H. Lemmetyinen and F. D'Souza, *J. Phys. Chem. A*, 2009, **113**, 8478-8489.
7. Y. Tachibana, L. Vayssieres and J. R. Durrant, *Nat. Photonics*, 2012, **6**, 511-518.
8. E. K. L. Yeow, P. J. Sintic, N. M. Cabral, J. N. H. Reek, M. J. Crossley and K. P. Ghiggino, *Phys. Chem. Chem. Phys.*, 2000, **2**, 4281-4291.

9. M. Fathalla, J. C. Barnes, R. M. Young, K. J. Hartlieb, S. M. Dyar, S. W. Eaton, A. A. Sarjeant, D. T. Co, M. R. Wasielewski and J. F. Stoddart, *Chem. Eur. J.*, 2014, **20**, 14690-14697.

10. J. J. Turner and M. M. Harding, *Supramol. Chem.*, 2005, **17**, 369-375.

11. S. A. Vail, P. J. Krawczuk, D. M. Guldi, A. Palkar, L. Echegoyen, J. P. C. Tome, M. A. Fazio and D. I. Schuster, *Chem. Eur. J.*, 2005, **11**, 3375-3388.

12. D. Curiel, K. Ohkubo, J. R. Reimers, S. Fukuzumi and M. J. Crossley, *Phys. Chem. Chem. Phys.*, 2007, **9**, 5260-5266.

13. B. Kang, W. Yang, S. Lee, S. Mukherjee, J. Forstater, H. Kim, B. Goh, T.-Y. Kim, V. A. Voelz and Y. Pang, *Sci. Rep.*, 2017, **7**.

14. J. Tröger, *J. Prakt. Chem.*, 1887, **36**, 225-245.

15. C. S. Wilcox and M. D. Cowart, *Tetrahedron Lett.*, 1986, **27**, 5563-5566.

16. M. D. Cowart, I. Sucholeiki, R. R. Bukownik and C. S. Wilcox, *J. Am. Chem. Soc.*, 1988, **110**, 6204-6210.

17. J. C. Adrian and C. S. Wilcox, *J. Am. Chem. Soc.*, 1989, **111**, 8055-8057.

18. C. Pardo, E. Sesmilo, E. Gutierrez-Puebla, A. Monge, J. Elguero and A. Fruchier, *J. Org. Chem.*, 2001, **66**, 1607-1611.

19. I. Neogi, S. Jhulki, A. Ghosh, T. J. Chow and J. N. Moorthy, *ACS Appl. Mater. Interfaces*, 2015, **7**, 3298-3305.

20. Z. G. Wang, D. Wang and J. Jin, *Macromolecules*, 2014, **47**, 7477-7483.

21. Z. G. Wang, D. Wang, F. Zhang and J. Jin, *Acs Macro Lett.*, 2014, **3**, 597-601.

22. E. B. Veale, D. O. Frimannsson, M. Lawler and T. Gunnlaugsson, *Org. Lett.*, 2009, **11**, 4040-4043.

23. E. B. Veale and T. Gunnlaugsson, *J. Org. Chem.*, 2010, **75**, 5513-5525.

24. O. V. Runarsson, J. Artacho and K. Warnmark, *Eur. J. Org. Chem.*, 2012, 7015-7041.

25. S. B. Larson and C. S. Wilcox, *Acta Crystallogr., Sect. C: Cryst. Struct. Commun.*, 1986, **42**, 224-227.

26. M. Bhaskar Reddy, M. Shailaja, A. Manjula, J. R. Premkumar, G. N. Sastry, K. Sirisha and A. V. S. Sarma, *Org. Biomol. Chem.*, 2015, **13**, 1141-1149.

27. M. J. Crossley, T. W. Hambley, L. G. Mackay, A. C. Try and R. Walton, *J. Chem. Soc., Chem. Commun.*, 1995, 1077-1079.

28. H. Imahori, K. Hagiwara, M. Aoki, T. Akiyama, S. Taniguchi, T. Okada, M. Shirakawa and Y. Sakata, *J. Am. Chem. Soc.*, 1996, **118**, 11771-11782.

29. R. Luguya, L. Jaquinod, F. R. Fronczek, A. G. H. Vicente and K. M. Smith, *Tetrahedron*, 2004, **60**, 2757-2763.

30. M. D. H. Bhuiyan, A. B. Mahon, P. Jensen, J. K. Clegg and A. C. Try, *Eur. J. Org. Chem.*, 2009, 687-698.

31. M. D. H. Bhuiyan, K. X. Zhu, P. Jensen and A. C. Try, *Eur. J. Org. Chem.*, 2010, 4662-4670.

32. M. Son, Y. M. Sung, S. Tokuji, N. Fukui, H. Yorimitsu, A. Osuka and D. Kim, *Chem. Commun.*, 2014, **50**, 3078-3080.

33. M. Kullmann, A. Hipke, P. Nuernberger, T. Bruhn, D. C. Götz, M. Sekita, D. M. Guldi, G. Bringmann and T. Brixner, *Phys. Chem. Chem. Phys.*, 2012, **14**, 8038-8050.

34. F. Koch, M. Kullmann, U. Selig, P. Nuernberger, D. C. Götz, G. Bringmann and T. Brixner, *New J. Phys.*, 2013, **15**, 025006.

35. F. Mandoj, S. Nardis, R. Pudi, L. Lvova, F. R. Fronczek, K. M. Smith, L. Prodi, D. Genovese and R. Paolesse, *Dyes Pigm.*, 2013, **99**, 136-143.

36. K. M. Kadish, K. M. Smith and R. Guilard, *The Porphyrin Handbook: Multiporphyrins, multiphthalocyanines, and arrays*, Academic Press, 2003.

SUPPORTING INFORMATION

Synthesis and Photophysical Properties of Λ-Shaped non-Conjugated Porphyrin Dyad

Md Imam Ansari, Andrew Try, and Peter Karuso*

Department of Molecular Sciences, Macquarie University, Sydney NSW 2109, Australia

Table of Contents

* Corresponding author. Tel.: +612-9850-8290 fax: +612-9850-8313, e-mail: peter.karuso@mq.edu.au

Synthetic Schemes

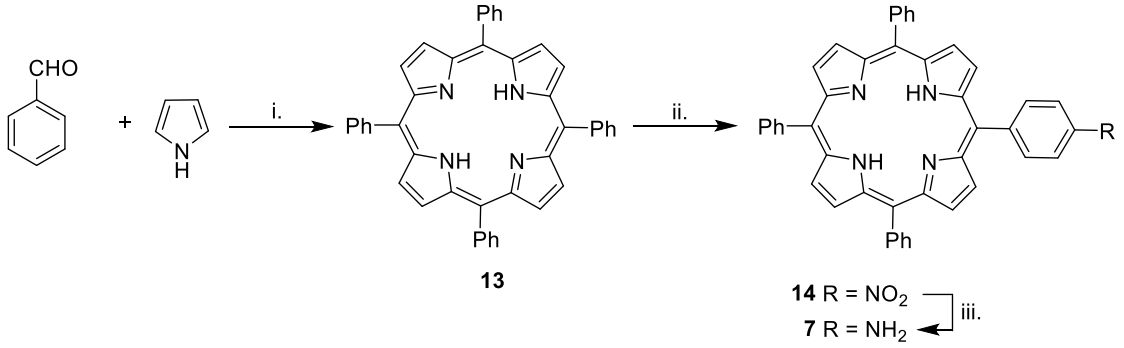

Fig. S1 Synthetic scheme for aminoporphyrin **7** i. Propanoic acid, reflux, 19%;[1] ii. $NaNO_2$, trifluoroacetic acid, 3h, 75%; iii. Anhydrous $SnCl_2$, conc. hydrochloric acid, 65 °C overnight, 67%.[2]

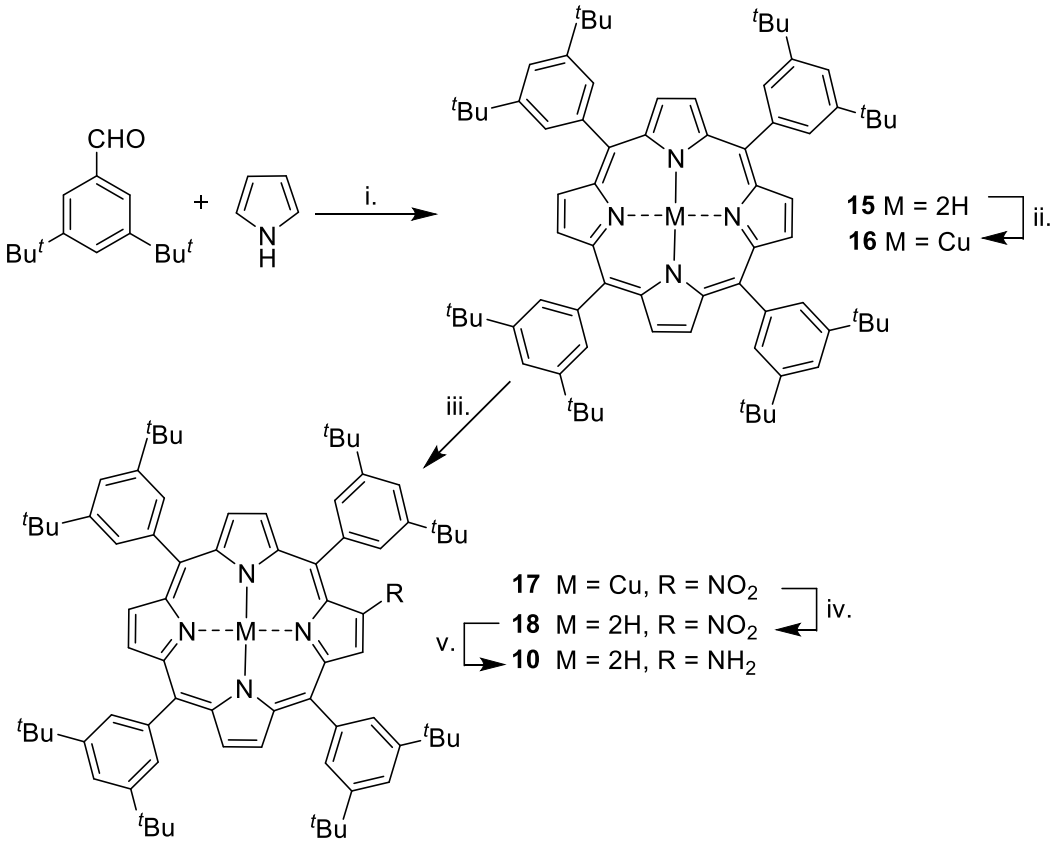

Fig. S2 Synthetic scheme for aminoporphyrin **10** i. Propanoic acid, reflux, 19%; ii. $Cu(OAc)_2$, CH_2Cl_2, reflux, 98%; iii. 0.5% (w/v) NO_2 in hexane, CH_2Cl_2, 96%; iv. conc. H_2SO_4, CH_2Cl_2, 94%;[3] v. $SnCl_2$, conc. HCl, CH_2Cl_2, 98%.[4]

General information:

Reagents were purchased from Sigma Aldrich and Alfa Aesar and used without purification unless otherwise stated.

^{1}H NMR and ^{13}C NMR spectra were recorded in Aldrich 5 mm NMR tubes on a Bruker DRX 400 NMR spectrometer (400 MHz) at 300 K unless otherwise stated, processed using Topspin 3.5, and referenced to residual solvent peak ($CDCl_3$ δ_H 7.26 and δ_C 77.01 ppm, DMSO-d_6 δ_H 2.49 and δ_C 39.5 ppm). The following abbreviations for multiplicity are used: s, singlet; d, doublet; t, triplet; m, multiplet; dd, doublet of doublets. Column chromatography was routinely carried out using the gravity feed column techniques on Merck silica gel type 9385 (230-400 mesh) with the stated solvent systems. Analytical thin layer chromatography (TLC) analyses were performed on Merck silica gel 60 F254 protected sheets (0.2 mm). Visualisation of compounds was achieved by illumination under ultraviolet light (254 nm). Charcoal and celite were pre-washed with MeOH and water before used. HRMS (ESI) were performed at the Australian Proteome Analysis Facility (APAF), Macquarie University, Australia using a Q Exactive Plus hybrid quadrupole-orbitrap mass spectrometer (Thermo Scientific, Bremen, Germany). ESI-MS spectra were recorded using an Agilent 6130 single quadrupole mass spectrometer (Agilent Corp.). The IR spectra were taken on a Thermo Scientific Nicolet iS10 ATR FTIR spectrometer at 298 K. UV/Visible absorbances were recorded on a Varian Cary 1Bio UV-visible spectrophotometer. Fluorescence emission spectra were recorded on a Cary Eclipse Fluorescence Spectrofluorometer (Agilent Technologies). All commercial solvents were HPLC grade and used without further purification. Where solvent mixtures are used, the portions are given by volume. Pyrrole was freshly distilled before use. Chloroform used for photophysical experiments were HPLC grade purchased from Sigma-Aldrich (amylene stabilised).

Experimental Section:

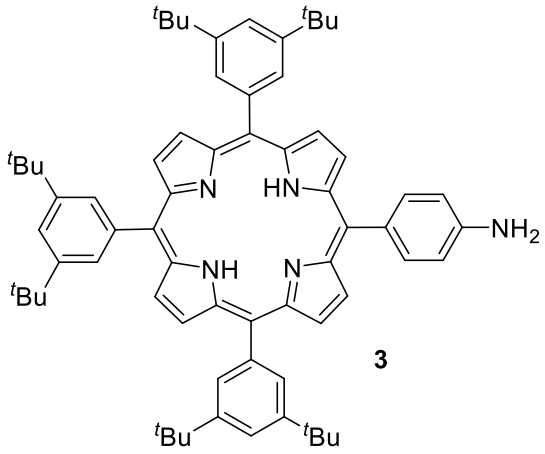

3

5-(4-Aminophenyl)-10,15,20-tris(3,5-di-*tert*-butylphenyl)porphyrin (**3**) was synthesised by the method of Imahori *et al*.[5] Briefly, a mixture of *p*-nitrobenzaldehyde (1.52 g, 10 mmol) and 3,5-di-*tert*-butylbenzaldehyde (6.56 g, 30 mmol) in chloroform (700 mL) was added freshly distilled pyrrole (2.68 g, 40 mmol) under an argon atmosphere and stirred for 15 min. A catalytic amount of boron trifluoride diethyl etherate (0.08 mL) was added dropwise and stirred for 1 h. *p*-Chloranil (7.28 g, 29.6 mmol) was then added and the reaction mixture was heated to reflux in air for 1.5 h. After chromatography (silica gel, 50% dichloromethane/50% hexane), the first compound eluted was 5,10,15,20-tetrakis(3,5-di-*tert*-butylphenyl)porphyrin (**15**) (700 mg, 9%), as purple microcrystals.^{1}H NMR (400 MHz, $CDCl_3$) δ 8.91 (br s, 8H, β-pyrrolic H), 8.10 (d, J = 1.7 Hz, 8H, ArH), 7.80 (t, J = 1.7 Hz, 4H, ArH), 1.54 (s, 72H, CH_3), −2.66 (br s, 2H, NH).

The second compound eluted was the desired mono-nitrophenyl porphyrin **2** (2.10 g, 21%) as a purple microcrystalline solid.^{1}H NMR (400 MHz, $CDCl_3$) δ9.94-8.93 (m, 6H, β-pyrrolic H), 8.78 (d, J = 4.7 Hz, 2H, β-pyrrolic H), 8.67 (d, J = 8.6 Hz, 2H, ArH), 8.46 (d, J = 8.6 Hz, 2H, ArH), 8.17-8.11 (m, 6H, ArH), 7.89-7.83 (m, 3H, ArH), 1.60-1.56 (m, 54H, CH_3), −2.63 (br s, 2H, NH).

To a mixture of mono-nitrophenyl porphyrin **2** (1.01 g, 1.03 mmol) and anhydrous stannous chloride (1.90 g, 10 mmol) in dichloromethane (100 mL), was added hydrochloric acid (10M; 5 mL) under an argon atmosphere. The reaction mixture was stirred for 3 days. The organic layer was washed with water (2 × 200 mL), sodium hydroxide (3M; 2 × 100 mL) water (100 mL), and brine (100 mL), dried over anhydrous magnesium sulfate, filtered and evaporated to dryness under vacuum. After chromatography (silica gel, 50% dichloromethane/50% hexane) aminophenyl porphyrin, **3** (720 mg, 75%) was isolated as a purple microcrystalline solid. ^{1}H NMR (400 MHz, $CDCl_3$) δ 8.94 (d, *J* = 4.7 Hz, 2H, β-pyrrolic H), 8.91-8.85 (m, 6H, β-pyrrolic H), 8.09 (d, *J* = 1.8 Hz, 4H, ArH), 8.08 (d, *J* = 1.8 Hz, 2H, ArH), 8.02 (d, *J* = 8.2 Hz, 2H, ArH), 7.83-7.77 (m, 3H, ArH), 7.06 (d, *J* = 8.2 Hz, 2H, ArH), 4.00 (br s, 2H, NH_2), 1.55-1.50 (m, 54H, CH_3), −2.66 (br s, 2H, NH). The NMR spectrum was consistent with that reported in the literature.[5]

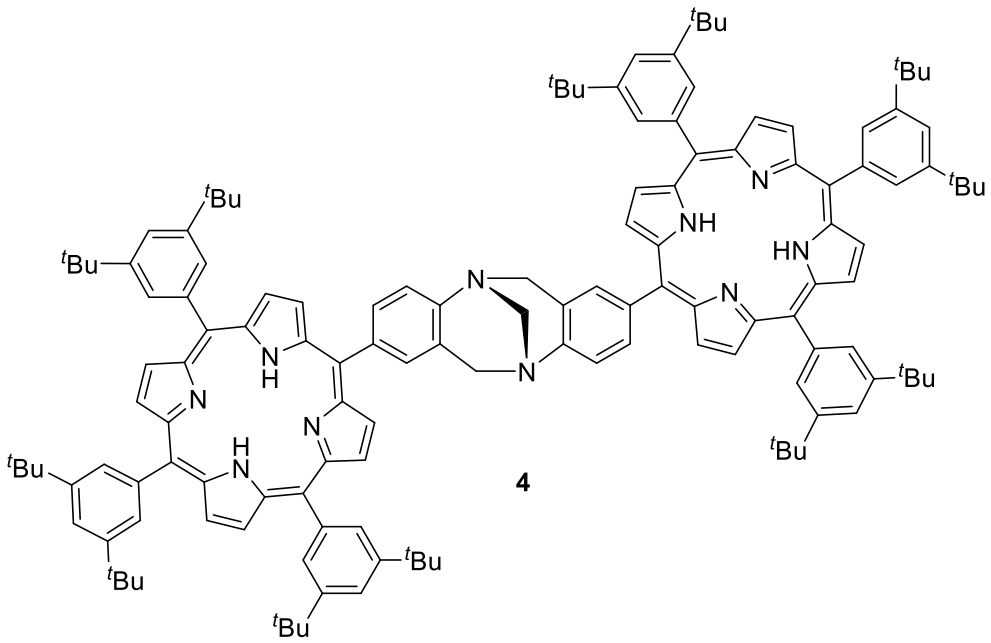

4

Free-base porphyrin dyad 4: Amino porphyrin **3** (250 mg, 0.26 mmol) and paraformaldehyde (25 mg, 0.83 mmol) were dissolved in TFA (15 mL) and the reaction mixture was stirred for 7 days under an argon atmosphere at room temperature. The

reaction mixture was then basified with a solution of concentrated ammonia (20 mL) and water (20 mL). Sodium bicarbonate (sat.; 75 mL) was added to the aqueous mixture was extracted into dichloromethane. The combined organic layers were washed with brine, dried over magnesium sulfate, filtered and evaporated to dryness. The dark brown crude material was chromatographed (silica gel, 20% ethyl acetate/80% hexane) to afford **4** as a dark purple microcrystalline solid (140 mg, 55%). UV ($CHCl_3$) λ_{max} (log ε) 240 (5.01), 362 (4.89), 452 (6.05), 674 (5.28); FTIR (neat) ν_{max} 3314, 2955, 2903, 2114, 1806, 1591, 1474, 1426, 1393, 1361, 1246, 1205, 978, 913, 880, 799, 714 cm^{-1}; ^1H NMR (400 MHz, $CDCl_3$) δ 9.12 (d, *J* = 4.7 Hz, 2H, β-pyrrolic H), 8.98 (d, *J* = 4.7 Hz, 6H, β-pyrrolic H), 8.95 (m, 8H, β-pyrrolic H), 8.23 (dd, *J* = 8, 1.7 Hz, 2H, ArH), 8.17 (s, 2H, ArH), 8.14 (d, *J* = 1.4 Hz, 8H, ArH), 8.11 (s, 2H, ArH), 8.05 (d, *J* = 1.4 Hz, 2H, ArH), 7.85 (t, *J* = 1.6 Hz, 2H, ArH), 7.80-7.89 (s, 4H, ArH), 7.69 (d, *J* = 8 Hz, 2H, ArH), 5.29 (d, *J* = 17.5 Hz, 2H, CH_2), 4.88 (s, 2H, CH_2), 4.86 (d, *J* = 16.3 Hz, 2H, CH_2), 1.48-1.63 (m, 108H, CH_3), −2.61 (br s, 4H, NH); ^{13}C NMR (100 MHz, $CDCl_3$) δ 148.7, 148.1, 141.4, 138.4, 133.9, 133.4, 131.1, 129.9, 129.7, 126.3, 123.8, 121.5, 121.4, 121.1, 120.9, 119.4, 58.8, 35.1, 31.8, 29.7; HRMS (ESI) *m/z*: 1968.2749 $[M+H]^+$ (calcd for $C_{139}H_{159}N_{10}$, 1968.2749).

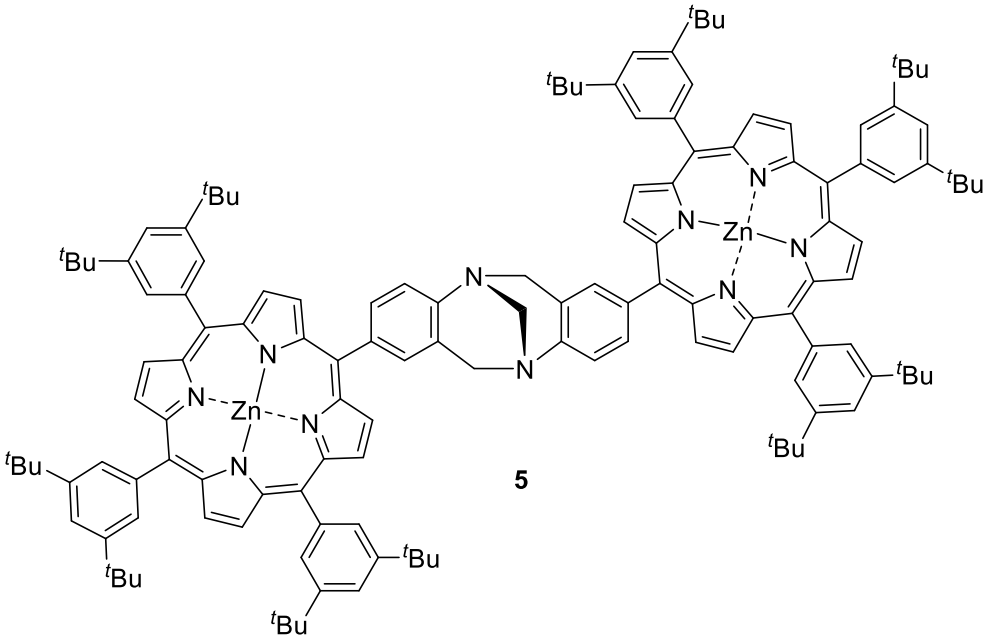

5

Dizinc(II)porphyrin dyad 5: Free-base porphyrin Tröger's base dyad **4** (15 mg, 0.01 mmol) was dissolved in chloroform (10 mL) and zinc acetate dihydrate (4 mg, 0.02 mmol, 2.5 equiv) was separately dissolved in methanol (3 mL) and then added dropwise to the stirred solution of **4**. After 30 min, the colour of the reaction mixture changed from red to pink. The reaction progress was followed by TLC (20% ethyl acetate/80% hexane) and upon consumption of the starting material, the reaction was quenched by adding chloroform (10 mL) and washing with water (2 × 10 mL), the organic layer was dried over anhydrous magnesium sulfate and filtered. The solvent was evaporated to dryness to afford pure **5** as a dark-purple microcrystalline solid (15 mg, 94%) that did not require further purification. UV ($CHCl_3$) λ_{max} (log ε) 373 (4.51), 417 (5.03), 450 (4.66); FTIR (neat) ν_{max} 2956, 2865, 2360, 2339, 1591, 1462, 1362, 1341, 1288, 1247, 1204, 1068, 1002, 929, 900, 881, 822, 797, 715 cm^{-1}; ^1H NMR (400 MHz, $CDCl_3$), δ 8.76-9.25 (m, 16H, β-pyrrolic H), 7.92-8.30 (m, 14H, ArH), 7.67-7.89 (m, 8H, ArH), 7.35-7.64 (m, 2H, ArH), 4.23-5.64 (m, 6H, CH_2), 1.38-1.58 (m, 108H, CH_3); ^{13}C NMR (100 MHz, $CDCl_3$) δ 150.4, 150.2, 148.5, 141.9, 132.3, 129.7, 129.6,

122.4, 120.8, 120.6, 35.1, 34.9, 31.8, 31.7, 29.7, 29.4, 27.2, 22.7, 14.1; HRMS (ESI) *m/z*: 1046.0459 $[M+H]^{2+}$ (calcd for $C_{139}H_{155}N_{10}Zn_2$, 1046.0510).

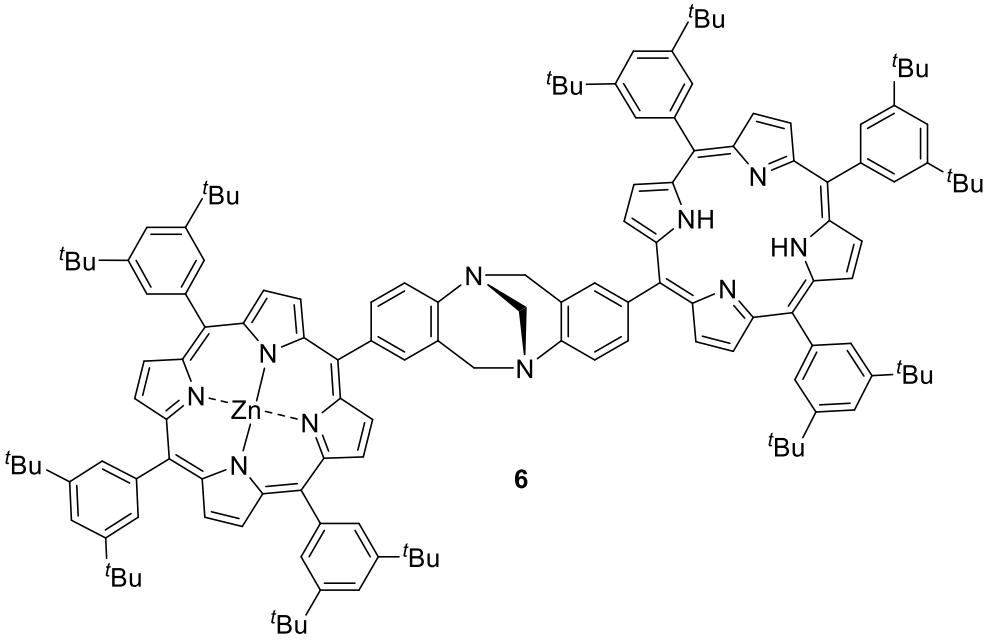

6

Monozinc(II)porphyrin dyad 6: The synthesis of **5** was repeated but with 1 equiv of zinc acetate dihydrate and dyad **4** (30 mg, 0.015 mmol). The crude was chromatographed (silica gel, 10% ethyl acetate/90% hexane). The first compound eluted was **4**, (4 mg, 13%) followed by the desired mono-zinc(II) porphyrin **6,** as a purple microcrystalline solid (7 mg, 23%). UV ($CHCl_3$) λ_{max} (log ε) 329 (4.63), 451 (5.37), 670 (4.42) nm; FTIR (neat) ν_{max} 3314, 2957, 2867, 2360, 1591, 1475, 1425, 1393, 1362, 1288, 1246, 1205, 1002, 929, 900, 880, 821, 797, 715 cm^{-1}; ^1H NMR (400 MHz, $CDCl_3$) δ 9.09 (d, *J* = 4.7 Hz, 1H, β-pyrrolic H), 9.00-9.07 (m, 7H, β-pyrrolic H), 8.95-8.99 (m, 1H, β-pyrrolic H), 8.88-8.94 (m, 6H, β-pyrrolic H), 8.72 (d, *J* = 4.7 Hz, 1H, β-pyrrolic H), 8.02-8.17 (m, 14H, ArH), 7.73-7.89 (m, 8H, ArH), 7.28-7.58 (m, 2H, ArH), 4.74-4.93 (m, 1H, CH_2), 4.43-4.69 (m, 2H, CH_2), 4.33 (br s, 1H, CH_2), 4.06 (br s, 2H, CH_2), 1.44-1.60 (m, 108H, CH_3), −2.67 (br s, 2H, NH); ^{13}C NMR (100 MHz, $CDCl_3$) δ 150.4, 148.7, 148.5, 129.7, 35.1, 31.7, 29.7; HRMS (ESI) *m/z*: 2030.1908

$[M+H]^+$ (calcd for $C_{139}H_{157}N_{10}Zn$, 2030.1884). The third compound eluted was the dizinc(II)porphyrin dyad **5** (8 mg, 25 %).

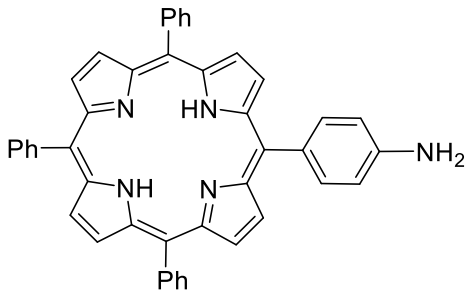

7

5-(4-Aminophenyl)-10,15,20-triphenylporphyrin (7) was synthesised by the method of Luguya *et al*. (Fig. S1).[2] Briefly, benzaldehyde (16 mL, 160 mmol) and freshly distilled pyrrole (11.2 mL, 160 mmol) were dissolved in propanoic acid (600 mL) and the reaction mixture was stirred at reflux condition for 30 min. The solution was cooled, filtered, and the precipitate washed thoroughly with methanol and then hot water, dried, and chromatographed (silica gel, 50% chloroform/50% hexane) to afford **13** (4.80 g, 19%). ^{1}H NMR (400 MHz, $CDCl_3$) δ 8.91 (s, 8H, β-pyrrolic H), 8.30-8.24 (m, 8H, ArH), 7.83-7.77 (m, 12H, ArH), −2.52 (s, 2H, NH). The NMR spectrum was consistent with that reported in the literature.[2]

To the tetraphenylporphyrin **13** (11.2 g, 18.2 mmol) in trifluoroacetic acid (200 mL), was added sodium nitrite (1.50 g, 21.7 mmol, 1.8 equiv) in 3 parts (500 mg each time at 15 min intervals). Reaction progress was followed by TLC (50% chloroform/50% hexane). The reaction mixture was neutralized with a solution concentrated ammonia (250 mL) and water (350 mL) and then extracted with chloroform (3 × 400 mL). The organic layer was washed with sodium bicarbonate (sat.) then brine, dried over magnesium sulfate and evaporated to dryness. The crude was chromatographed (silica gel, 50% chloroform/50% hexane) to afford **14** as a dark purple solid (9.01 g, 75%); ^{1}H

NMR (400 MHz, $CDCl_3$) δ 8.91 (d, *J* = 4.7 Hz, 2H, β-pyrrolic H), 8.89 (s, 4H, β-pyrrolic H), 8.75 (d, *J* = 4.7 Hz, 2H, β-pyrrolic H), 8.62 (d, *J* = 8.5 Hz, 2H, ArH), 8.38 (d, *J* = 8.5 Hz, 2H, ArH), 8.23 (m, 6H, ArH), 7.85-7.71 (m, 9H, ArH), −2.52 (s, 2H, NH).

Nitroporphyrin **14** (300 mg, 0.45 mmol) and tin(II) chloride anhydrous (680 mg, 3.61 mmol) were then dissolved in concentrated hydrochloric acid (37%, 30 mL) under an argon atmosphere. The reaction mixture was stirred at 65 °C for overnight. The reaction progress was followed by TLC (75% chloroform/25% hexane). Upon cooling, the reaction mixture was then poured onto ice (150 g) followed by addition of ammonium hydroxide solution (50 mL; ammonia:water 3:1) extracted into the chloroform (3 × 200 mL). The organic layers were combined, washed with brine (200 mL), dried over magnesium sulfate, and evaporated to dryness to afford a dark purple solid. The crude was chromatographed (silica gel, chloroform) to afford **7** as a purple solid (200 mg, 67%); ^{1}H NMR (400 MHz, $CDCl_3$) δ 8.94 (m, 2H, β-pyrrolic H), 8.83 (6H, s, β-pyrrolic H), 8.25-8.19 (m, 6H, ArH), 8.00 (d, *J* = 8.2 Hz, 2H, ArH), 7.81-7.10 (m, 9H, ArH), 7.07 (d, *J* = 8.2 Hz, 2H, ArH), 4.03 (br s, 2H, NH_2), −2.72 (s, 2H, NH). The NMR spectrum was consistent with that reported in the literature.[2]

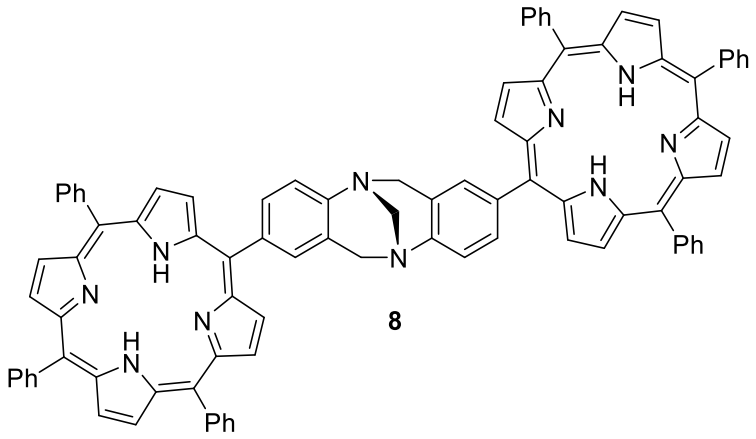

8

Free-base TPP dyad 8: 5-(4-Aminophenyl)-10,15,20-triphenylporphyrin **7** (100 mg, 0.16 mmol) and paraformaldehyde (8 mg, 0.26 mmol) were dissolved in TFA (5 mL) and the reaction mixture was stirred for 7 days under an argon atmosphere at room temperature. The reaction mass was then basified with a solution of concentrated ammonia (10 mL) and water (15 mL). Sodium bicarbonate (sat.; 50 mL) was added and the mixture extracted into dichloromethane (3 × 100 mL). The combined organic layers were washed with brine, dried over magnesium sulfate, filtered and evaporated to dryness. The dark brown crude material was chromatographed (silica gel, 5% methanol/95 % chloroform) to afford **8** as a dark purple solid (25 mg, 24%). UV ($CHCl_3$) λ_{max} (log ε) 358 (4.50), 448 (5.60), 668 (4.81) nm; FTIR (neat) ν_{max} 3313, 3046, 1710, 1595, 1557, 1471, 1439, 1401, 1348, 1318, 1203, 1153, 1070, 1031, 1001, 966, 910, 876 cm^{-1}; ^1H NMR (400 MHz, $CDCl_3$) δ 9.02 (m, 4H, β-pyrrolic H), 8.84-8.97 (m, 12H, β-pyrrolic H), 8.23-8.32 (m, 12H, ArH), 8.22 (dd, *J* = 8.0 Hz, 1.7 Hz, 2H, ArH), 7.98 (d, *J* = 1.2 Hz, 2H, ArH), 7.81 (d, *J* = 1.4 Hz, 2H, ArH), 7.77 (t, *J* = 6.9 Hz, 18 H, ArH), 7.66 (d, *J* = 8.0 Hz, 2H, ArH), 5.25 (d, *J* = 17.1 Hz, 2H, CH_2), 4.89 (s, 2H, CH_2), 4.83 (d, *J* = 17.1 Hz, 2H, CH_2), −2.65 (br s, 4H, NH); ^{13}C NMR (100 MHz, $CDCl_3$) δ 151.1, 148.1, 148.0, 146.7, 142.7, 142.6, 142.5, 138.5, 135.1, 134.8, 134.5,

134.2, 134.1, 133.6, 131.6, 130.9, 128.2, 127.2, 126.8, 126.6, 126.2, 124.1, 123.9, 120.7, 120.6, 120.4, 120.1, 67.8, 59.5; HRMS (ESI) *m/z*: 1295.5237 $[M+H]^+$ (calcd for $C_{91}H_{63}N_{10}$, 1295.5269).

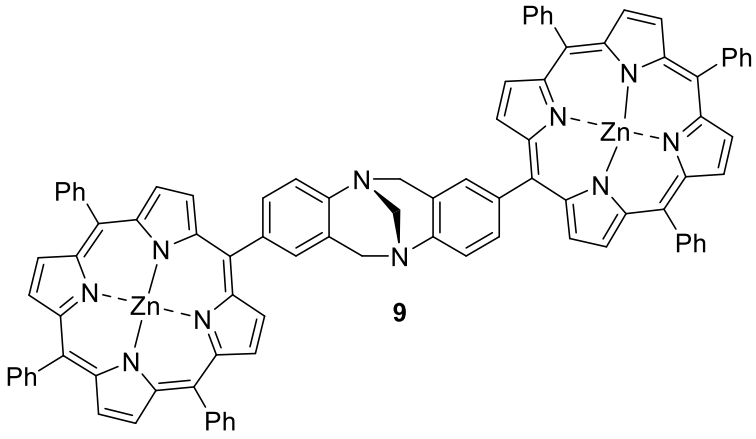

9

Dizinc(II)TPP dyad 9: Free-base porphyrin dyad **8** (15 mg, 0.01 mmol) dissolved in chloroform (10 mL) and stirred at room temperature. Zinc acetate dihydrate (7 mg, 0.03 mmol, 2.5 equiv) was separately dissolved in methanol (3 mL) and then added dropwise to the reaction mixture. After 30 min, a pink coloured solution was observed. The reaction progress was followed by TLC (90% chloroform/10% methanol) and upon consumption of all the starting material the reaction was stopped. Chloroform (10 mL) was added to the reaction mixture which was washed with water (2 × 10 mL), dried over magnesium sulfate and filtered. The solvent was evaporated to dryness to afford dizinc(II)porphyrin dyad **9** as dark-purple microcrystals (14 mg, 88%) that did not require further purification. UV ($CHCl_3$) λ_{max} (log ε) 361 (4.46), 419 (5.53), 447 (5.07), 547 (4.26), 663 (4.15), nm; FTIR (neat) ν_{max} 2921, 2851, 1660, 1522, 1484, 1439, 1338, 1259, 1203, 1067, 1001, 909, 794, 748, 718 cm^{-1}; ^1H NMR (400 MHz, $CDCl_3$), δ 8.59-9.19 (m, 16H, β-pyrrolic H), 8.45 (s, 2H, ArH), 7.97-8.39 (m, 12H, ArH), 7.35-7.89 (m, 22H, ArH), 7.03 (br s, 2H, ArH), 3.96-5.73 (m, 6H, CH_2); ^{13}C NMR (100

MHz, $CDCl_3$) δ 150.3, 142.9, 134.5, 132.1, 127.4, 126.5, 31.9, 29.7, 29.4, 22.7, 14.1; HRMS (ESI) *m/z*: 1418.3415 $[M]^+$ (calcd for $C_{91}H_{58}N_{10}Zn_2$, 1418.3428).

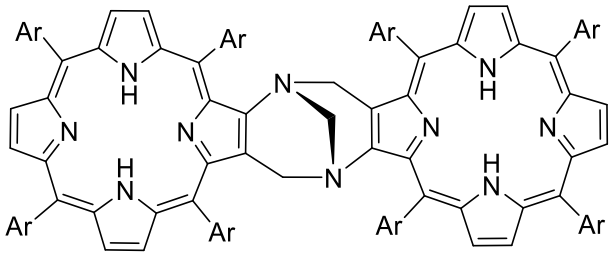

Ar = 3,5-di-*tert*-butylphenyl

11

Free-base dyad 11 was synthesised by the method of Crossley *et al*.[6] (Scheme 2). Briefly, to a stirred mixture of 3,5-di-*tert*-butylbenzaldehyde (25.0 g, 114 mmol) in propanoic acid (120 mL) was added freshly distilled pyrrole (7.68 g, 114 mmol). The reaction mixture was heated to reflux for 1 h and then stirred at room temperature overnight. The reaction mixture was then filtered and the precipitate washed with ice-cold hexane (30 mL) to afford **15** (5.10 g, 17%) as violet microcrystals that was used without further purification. ^{1}H NMR (400 MHz, $CDCl_3$) 8.91 (br s, 8H, β-pyrrolic H), 8.10 (d, *J* = 1.7 Hz, 8H, ArH), 7.80 (t, *J* = 1.7 Hz, 4H, ArH), 1.54 (s, 72H, CH_3), δ −2.66 (br s, 2H, NH); IR (neat) cm^{-1} 3315 (NH).[4]

A mixture of 5,10,15,20-tetrakis(3,5-di-*tert*-butylphenyl)porphyrin **15** (4.60 g, 4.50 mmol) and copper(II) acetate monohydrate (1.70 g, 8.50 mmol) in dichloromethane (550 mL) was heated to reflux and stirred for 1 h. Upon consumption of the starting material TLC (silica gel, 20% dichloromethane/80% hexane) the organic layer was washed with water (2 × 200 mL), brine (200 mL), dried over magnesium sulfate, filtered and evaporated under vacuum to afford **16** (4.60 g, 90%) as a purple-red microcrystalline solid. m.p. >300 °C (lit.[3] >300 °C). Compound **16** (4.60 g, 4.08 mmol)

in dichloromethane (230 mL) was added nitrogen oxide (0.5% in hexane, 325 mg in 100 mL). The reaction was followed by TLC (20% dichloromethane/80% hexane). Upon completion, the reaction mixture was filtered through a silica bed and washed with hexane to remove impurities. The organic layer was evaporated to dryness to afford **17** (4.60 g, 96%) that was used without further purification. m.p. > 300 °C; IR (neat) cm^{-1} 1525 (NO_2).[3]

To a mixture of **17** (11.0 g, 3.90 mmol) in dichloromethane (220 mL) was added sulfuric acid (18M, 22 mL) slowly. The reaction mixture was stirred for 5 min and quenched over ice (200 mL). The two layers were allowed to reach room temperature and then separated. The organic layer was washed with sodium hydroxide (3 M; 2 × 200 mL), brine (200 mL), dried over anhydrous magnesium sulfate, filtered and evaporated under vacuum to afford crude product. The crude product was purified by column chromatography (silica gel, 20% dichloromethane/80% hexane) to afford pure **18** (9.70 g, 94%). ^{1}H NMR (400 MHz, $CDCl_3$) δ 9.06-9.11 (m, 2H, β-pyrrolic H), 8.99-8.94 (m, 3H, β-pyrrolic H), 8.80 (d, *J* = 4.7 Hz, 2H, β-pyrrolic H), 8.78 (d, *J* = 4.7 Hz, 2H, β-pyrrolic H), 8.10 (d, *J* = 1.7 Hz, 2H, ArH), 8.09-8.05 (m, 6H, ArH), 7.84 (t, *J* = 1.7 Hz, 1H, ArH), 7.83-7.80 (m, 2H, ArH), 7.78 (t, *J* = 1.7 Hz, 1H, ArH), 1.56-1.53 (m, 72H, CH_3), −2.54 (br s, 2H, NH).[4]

The nitroporphyrin, **18** (500 mg, 0.45 mmol), anhydrous tin(II) chloride (700 mg, 3.70 mmol), dichloromethane (20 mL) and hydrochloric acid (10 M; 2 mL) were stirred for 24 h in the dark under an argon atmosphere. The reaction mixture was diluted with dichloromethane (150 mL) and washed with water (100 mL), sodium hydrogen carbonate (sat.; 2 × 150 mL), brine (200 mL), dried over anhydrous magnesium sulfate, filtered and evaporated to dryness to afford **10** (4.75 g, 98%) that did not require further purification. ^{1}H NMR (400 MHz, $CDCl_3$) δ 8.87-8.78 (m, 4H, β-pyrrolic H), 8.70 4H,

(d, J = 4.7 Hz, 1H, β-pyrrolic H), 8.55 (d, J = 4.7 Hz, 1H, β-pyrrolic H), 8.11-8.07 (m, 4H, ArH), 8.05-7.98 (m, 4H, ArH), 7.87-7.84 (m, 1H, ArH), 7.80-7.75 (m, 4H, ArH), 4.46 (br s, 2H, NH_2), 1.55-1.48 (m, 72H, CH_3), −2.66 (br s, 2H, NH).[4]

The aminoporphyrin, **10** (250 mg, 0.23 mmol) was dissolved in dry tetrahydrofuran (15 mL) and argon gas was bubbled through the solution for 15 min. A mixture of hydrochloric acid (10 M; 3 mL) in ethanol (6 mL) was added under an argon atmosphere. Formaldehyde solution (37%; 0.75 mL) was then added and the solution stirred under an argon atmosphere for 18 h at 50-60 °C. The organic solvents were removed and dichloromethane (50 mL) added. The mixture was then washed with water (2 × 50 mL), sodium carbonate (5%; 2 × 50 mL), water (2 × 50 mL), dried over magnesium sulfate and filtered. The solvent was evaporated to dryness and the crude solid was chromatographed over silica (40% dichloromethane/60% hexane) and a dark green major band was collected to yield the fused-porphyrin Tröger's base dyad **11** (150 mg, 60%) as a purple microcrystalline solid. UV ($CHCl_3$) λ_{max} (log ε) 447 (5.18), 680 (4.54) nm. FTIR (neat) ν_{max} 3332, 2958, 2867, 2360, 1591, 1473, 1424, 1392, 1361, 1247, 1200, 1109, 1076, 1053, 990, 920, 881, 798 cm^{-1}; ^1H NMR (400 MHz, $CDCl_3$) δ 8.91 (d, J = 4.9 Hz, 2H, β-pyrrolic H), 8.74 (d, J = 4.9 Hz, 2H, β-pyrrolic H), 8.53 (d, J = 4.5 Hz, 2H, β-pyrrolic H), 8.51 (br s, 2H, ArH), 8.38 (d, J = 4.5 Hz, 2H, β-pyrrolic H), 8.22 (d, J = 4.8 Hz, 2H, β-pyrrolic H), 8.13 (t, J = 1.6 Hz, 2H, ArH), 8.00 (d, J = 4.8 Hz, 2H, β-pyrrolic H), 7.97 (t, J = 1.6 Hz, 2H, ArH), 7.78 (t, J = 1.7 Hz, 2H, ArH), 7.77 (t, J = 1.7 Hz, 2H, ArH), 7.71 (t, J = 1.7 Hz, 2H, ArH), 7.59-7.66 (m, 4H, ArH), 7.54 (t, J = 1.7 Hz, 2H, ArH), 7.38 (br s, 2H, ArH), 7.28-7.32 (m, 2H, ArH), 7.00 (br s, 2H, ArH), 4.43 (s, 2H, CH_2), 3.95 (d, J = 17.2 Hz, 2H, CH_2), 3.44 (d, J = 17.2 Hz, 2H, CH_2), 1.18-1.86 (m, 144H, CH_3), −3.02 (br s, 2H, NH), −3.31 (br s, 2H, inner NH).[6]

The dizinc(II) dyad **12** was made from **11** by the method of Crossley *et al*.[6] The free-base fused-porphyrin TB dyad **11** (20 mg, 0.01 mmol) dissolved in chloroform (10 m L) and stirred at room temperature. Zinc acetate dihydrate (5 mg, 0.02 mmol, 2.5 equiv) was separately dissolved in methanol (3 mL) and then added dropwise to the reaction mixture. After 30 min, pink colour of solution was observed. The reaction progress was followed by TLC (40% dichloromethane/60% hexane), upon consumption of the starting material the reaction was stopped. Chloroform (10 mL) was added to the reaction mixture then washed with water (2 × 20 mL), dried over magnesium sulfate and filtered. The solvent was evaporated to dryness to afford pure **12** as dark-purple microcrystalline solid (18 mg, 82%). UV ($CHCl_3$) λ_{max} (log ε) 447 (5.06), 674 (4.28) nm. FTIR (neat) ν_{max} 2955, 2360, 1590, 1461, 1423, 1391, 1362, 1292, 1247, 1219, 1124, 1071, 1007, 933, 898, 879 cm^{-1}; ^1H NMR (400 MHz, $CDCl_3$) δ 8.96 (d, *J* = 4.7 Hz, 2H, β-pyrrolic H), 8.83 (d, *J* = 4.7 Hz, 2H, β-pyrrolic H), 8.74 (d, *J* = 4.5 Hz, 2H, β-pyrrolic H), 8.58 (d, *J* = 4.5 Hz, 2H, β-pyrrolic H), 8.22 (d, *J* = 4.7 Hz, 2H, ArH), 8.46 (s, 2H, ArH), 8.13 (t, *J* = 1.6 Hz, 2H, ArH), 8.00 (t, *J* = 1.6 Hz, 2H, ArH), 7.83 (t, *J* = 1.6 Hz, 2H, ArH), 7.80 (d, *J* = 4.7 Hz, 2H, ArH), 7.79 (t, *J* = 1.8 Hz, 2H, ArH), 7.72 (t, *J* = 1.8 Hz, 2H, ArH), 7.62 (t, *J* = 1.6 Hz, 2H, ArH), 7.60 (t, *J* = 1.8 Hz, 2H, ArH), 7.54 (t, *J* = 1.8 Hz, 2H, ArH), 7.27 (t, *J* = 1.6 Hz, 2H, ArH), 7.24 (t, *J* = 1.6 Hz, 2H, ArH), 6.51 (t, *J* = 1.6 Hz, 2H, ArH), 4.69 (s, 2H, CH_2), 4.22 (d, *J* = 17.2 Hz, 2H, CH_2), 3.89 (d, *J* = 17.2 Hz, 2H, CH_2), 1.16-1.88 (m, 144H, CH_3). The recorded spectral data was consistent with the literature.[6]

UV/Vis and Fluorescence Spectra:

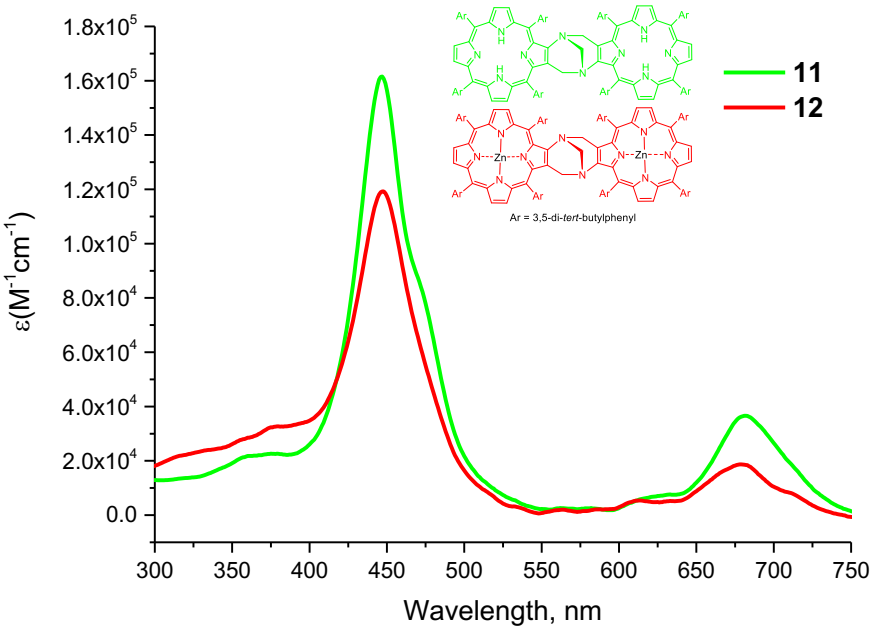

Fig. S3 UV/Vis spectrum of **11** (green) and **12** (red) in $CHCl_3$. The concentration of each compound was 1.4×10^{-6} M.

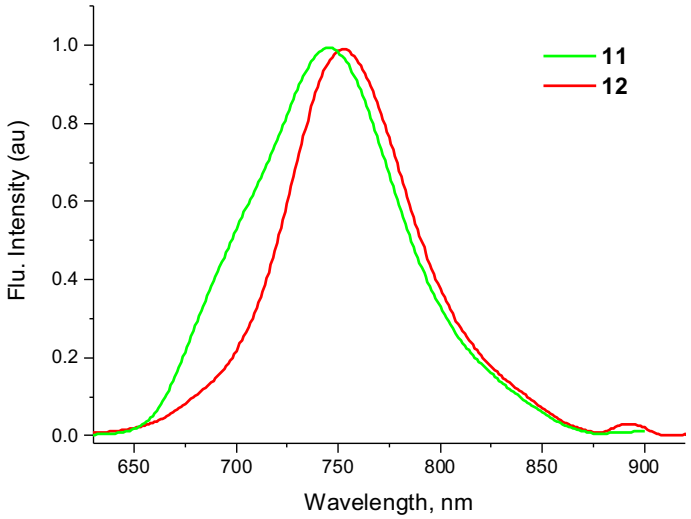

Fig. S4 Normalized fluorescence spectrum of **11** (green) and **12** (red) in $CHCl_3$ at λ_{ex} 447 nm. The concentration of each compound was 1.4×10^{-6} M.

1D NMR, HRMS and FTIR Spectra:

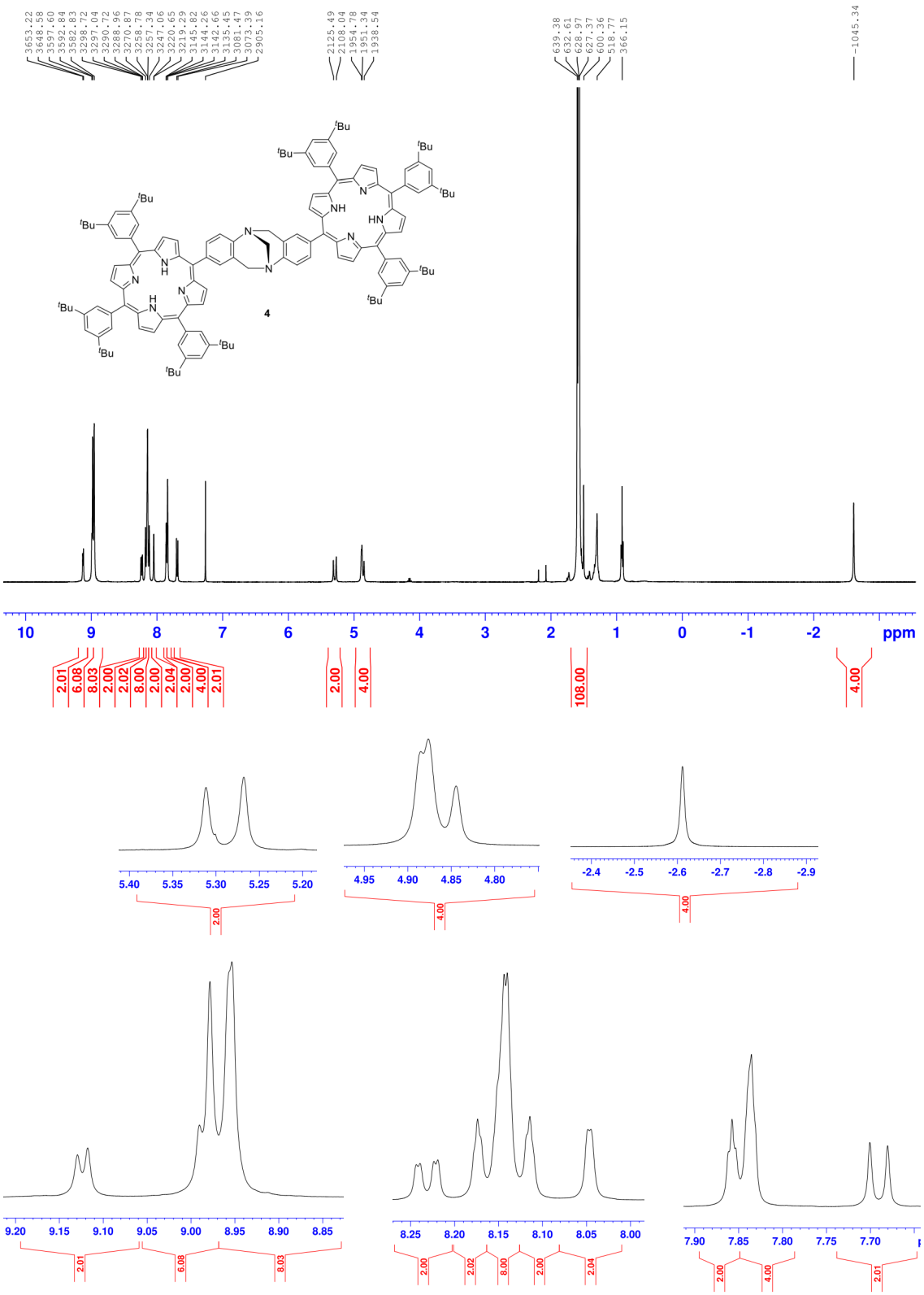

Fig. S5 ^{1}H NMR spectrum (400 MHz) of free-base porphyrin dyad **4** in $CDCl_3$.

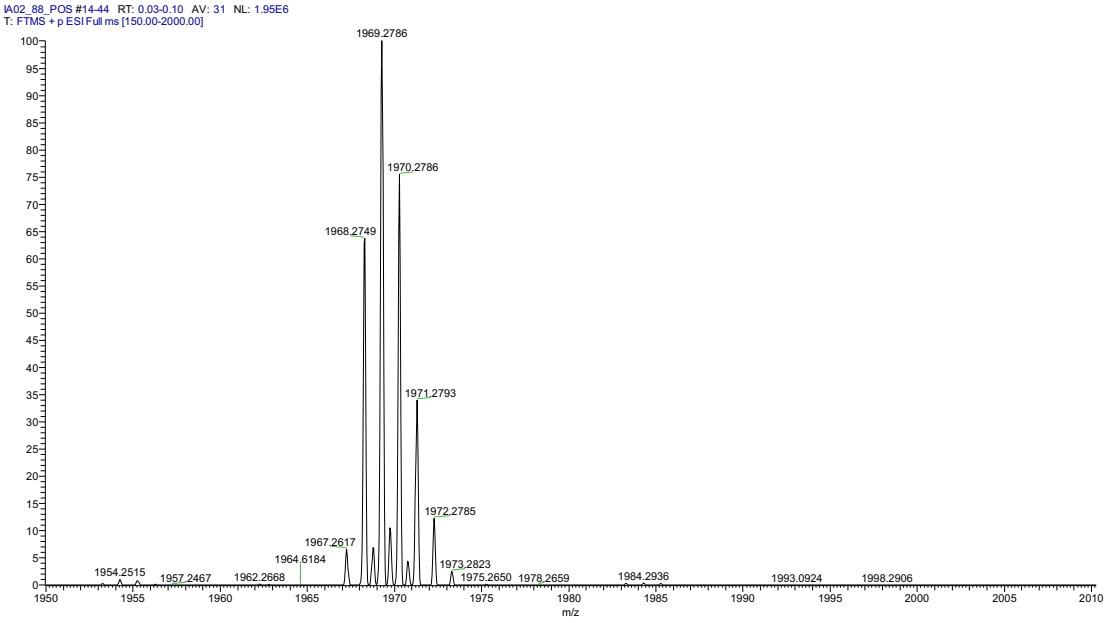

Fig. S6 High resolution mass spectrum of free-base porphyrin dyad **4**.

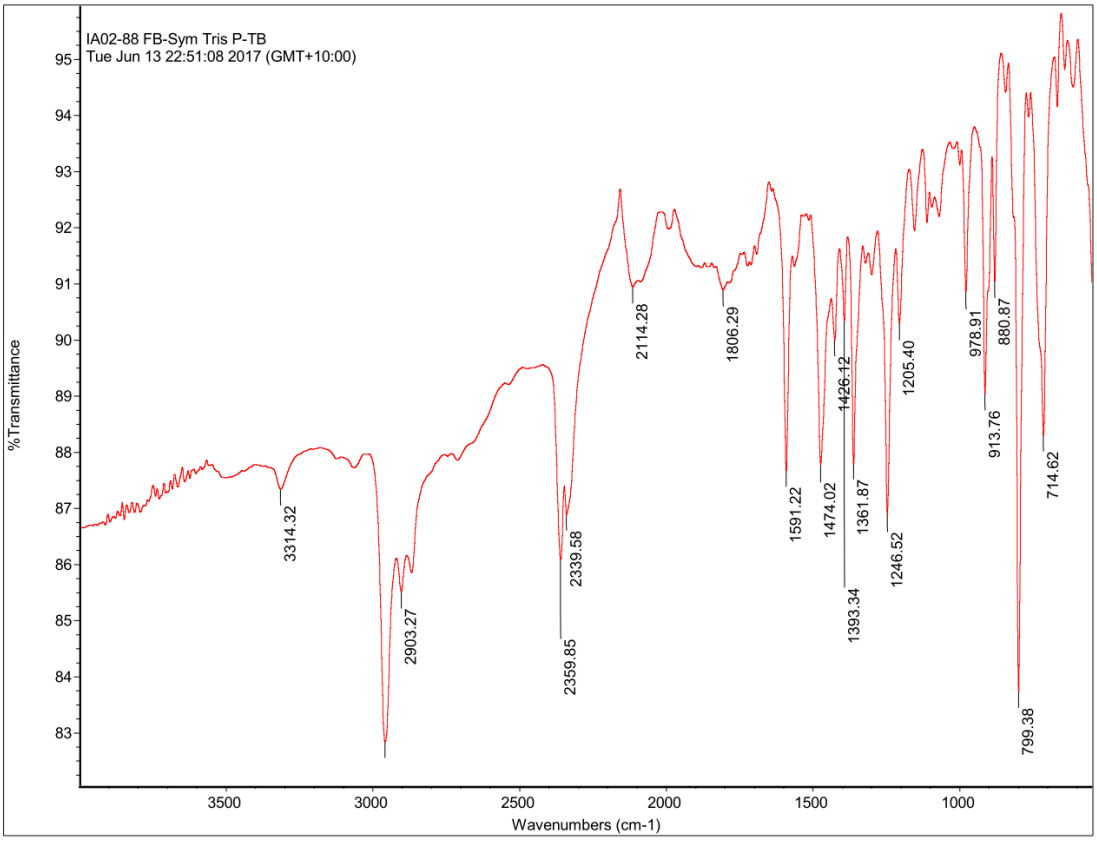

Fig. S7 Fourier transform infrared (FTIR) spectrum of free-base porphyrin dyad **4**.

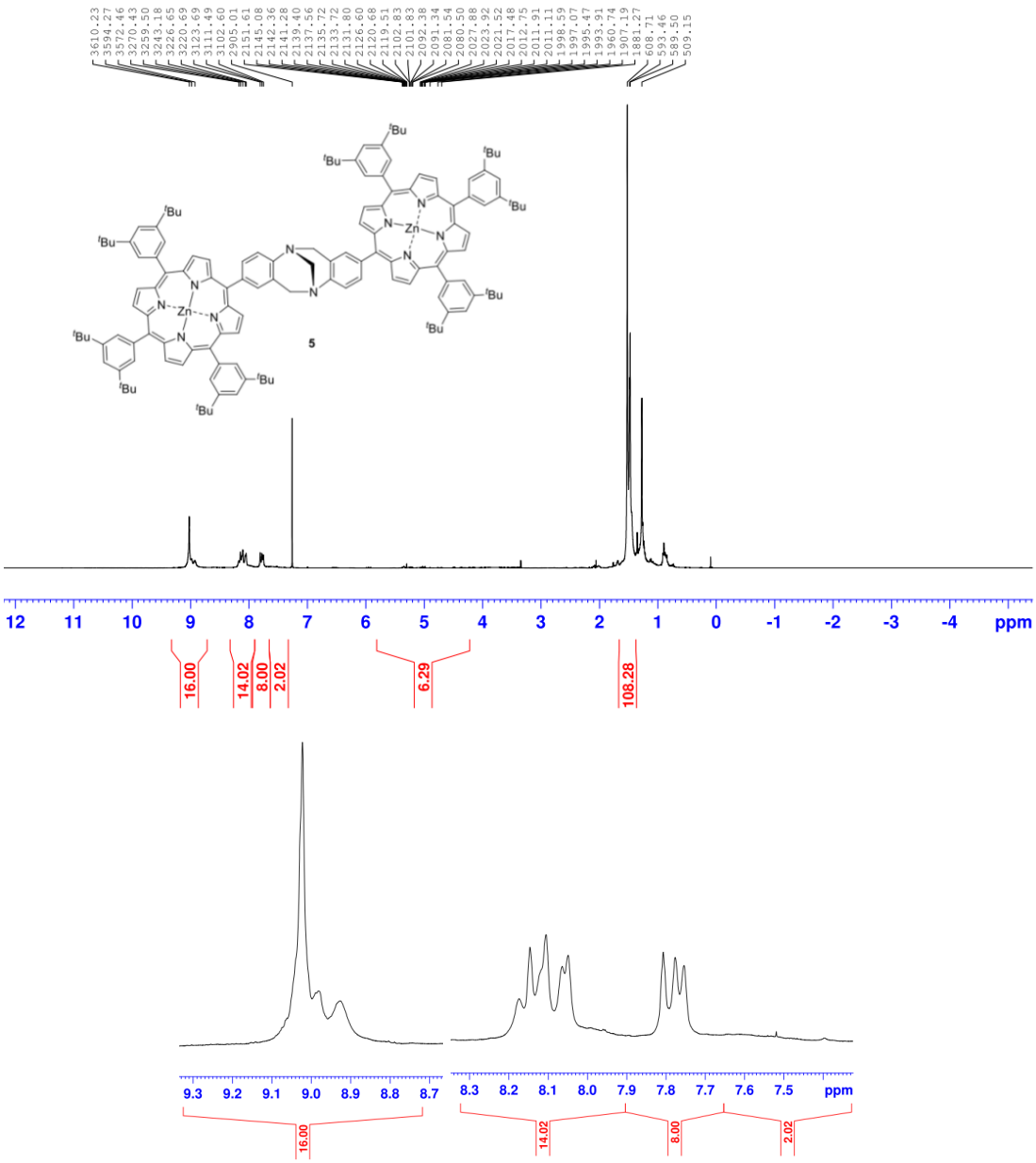

Fig. S8 ^{1}H NMR spectrum (400 MHz) of dizinc(II)porphyrin dyad **5** in $CDCl_3$.

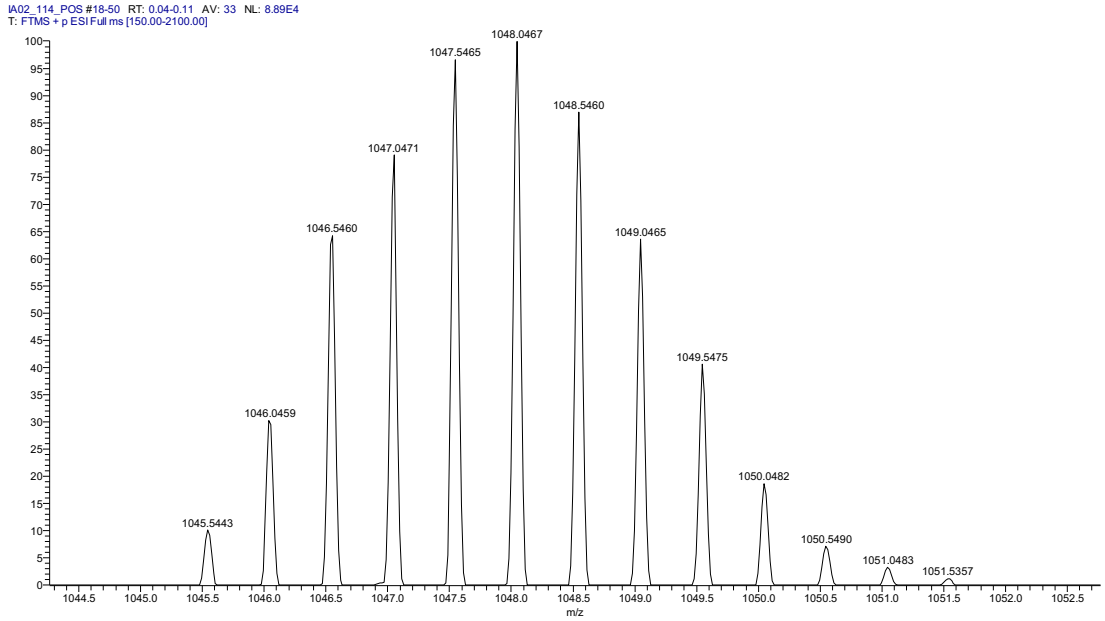

Fig. S9 High resolution mass spectrum of dizinc(II)porphyrin dyad **5**.

Fig. S10 Fourier transform infrared (FTIR) spectrum of dizinc(II)porphyrin dyad **5**.

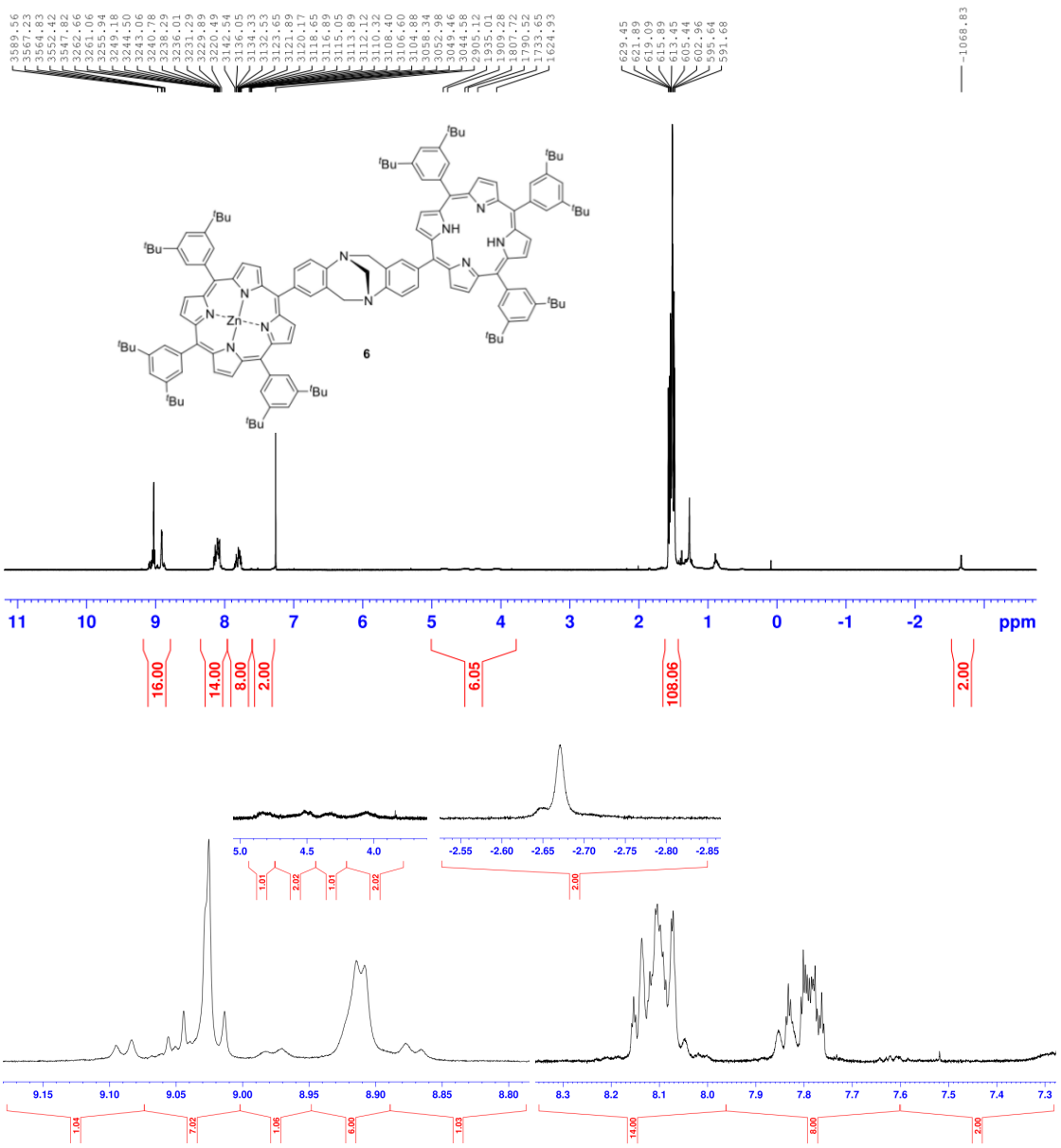

Fig. S11 ^{1}H NMR spectrum (400 MHz) of monozinc(II)porphyrin dyad **6** in $CDCl_3$.

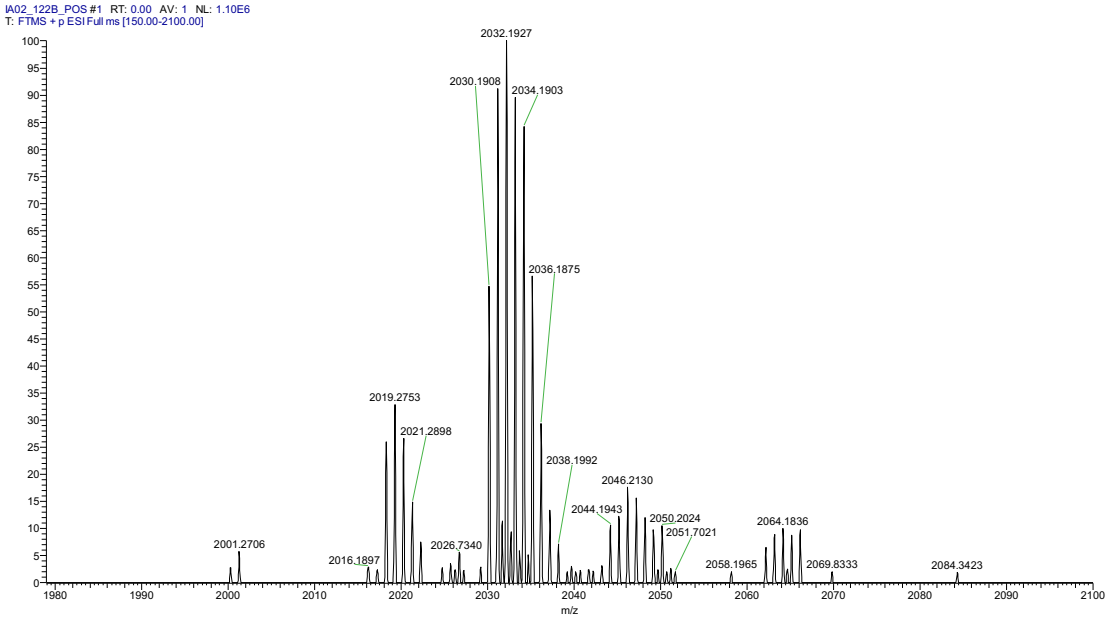

Fig. S12 High resolution mass spectrum of monozinc(II)porphyrin dyad **6**.

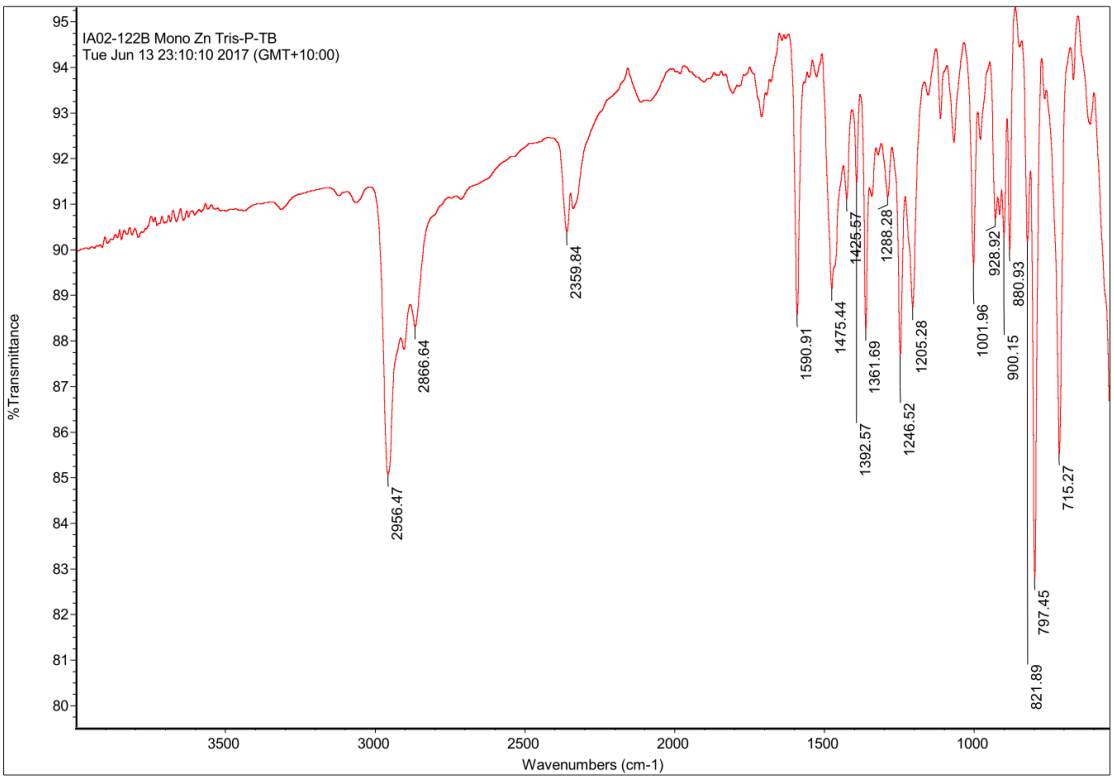

Fig. S13 Fourier transform infrared (FTIR) spectrum of monozinc(II)porphyrin dyad **6**.

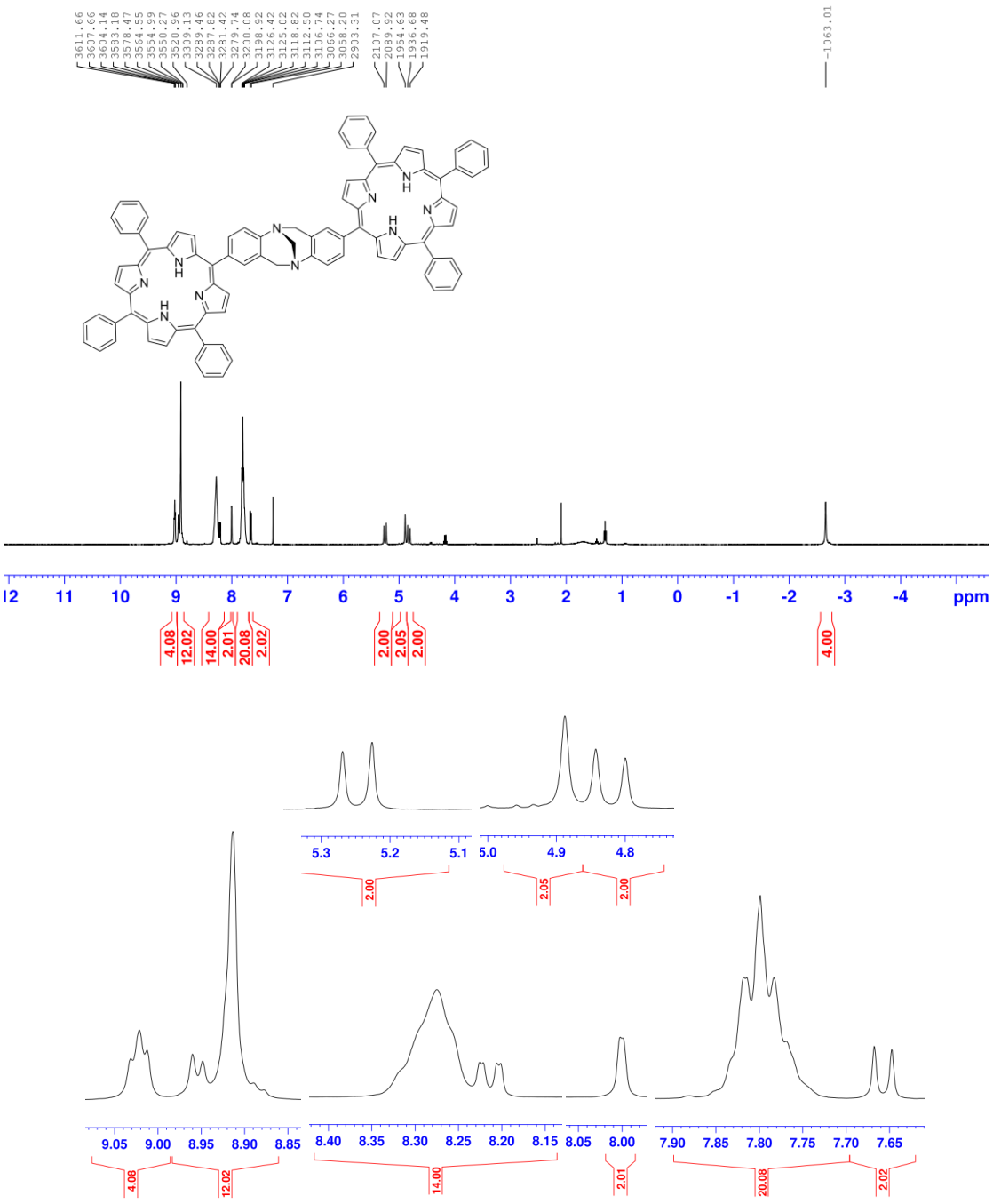

Fig. S14 ^{1}H NMR spectrum (400 MHz) of free-base porphyrin dyad **8** in $CDCl_3$.

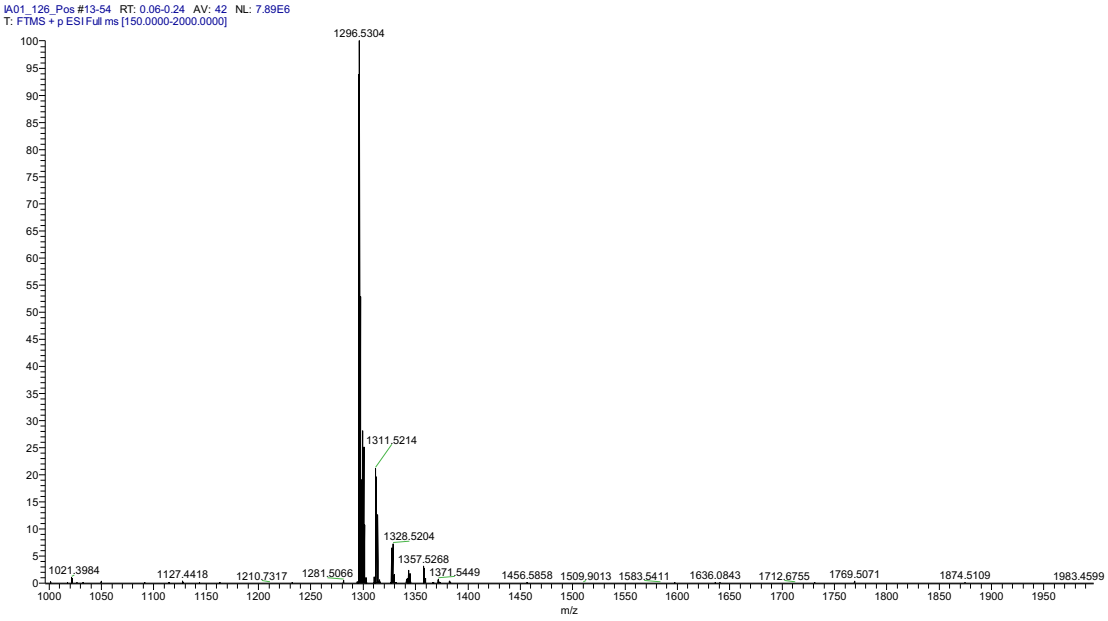

Fig. S15 High resolution mass spectrum of free-base porphyrin dyad **8**.

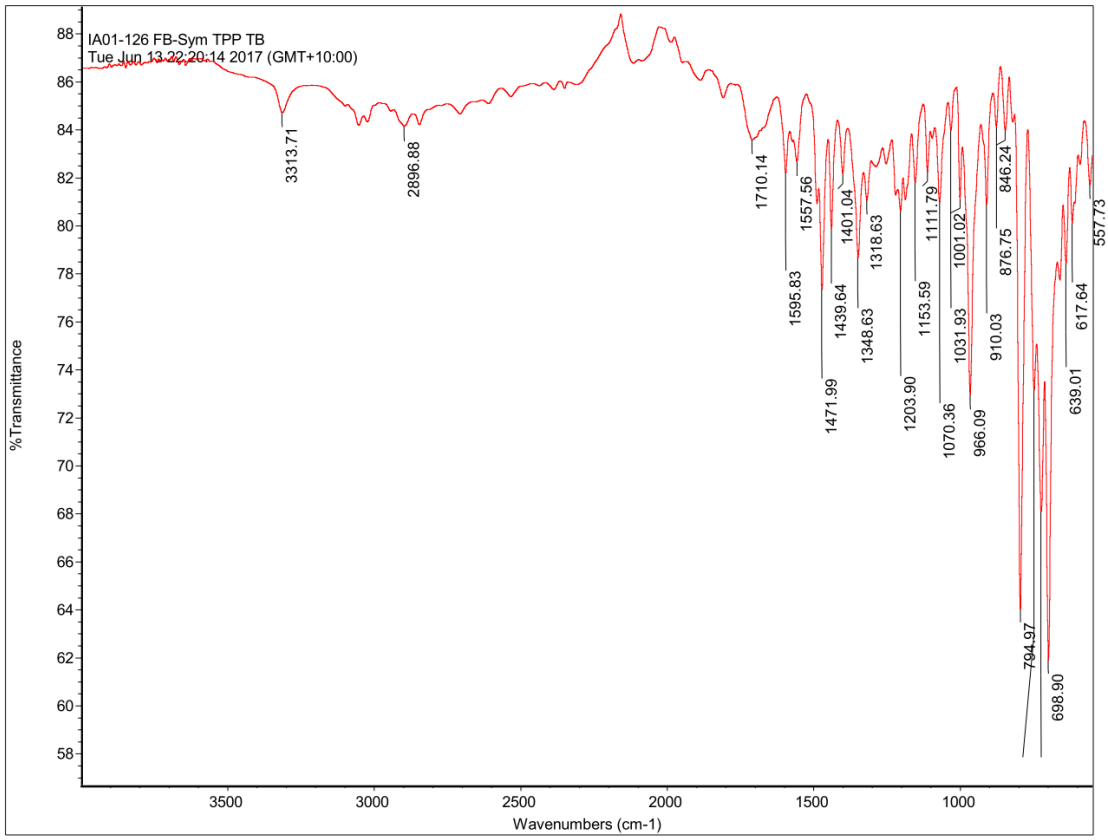

Fig. S16 Fourier transform infrared (FTIR) spectrum of free-base porphyrin dyad **8**.

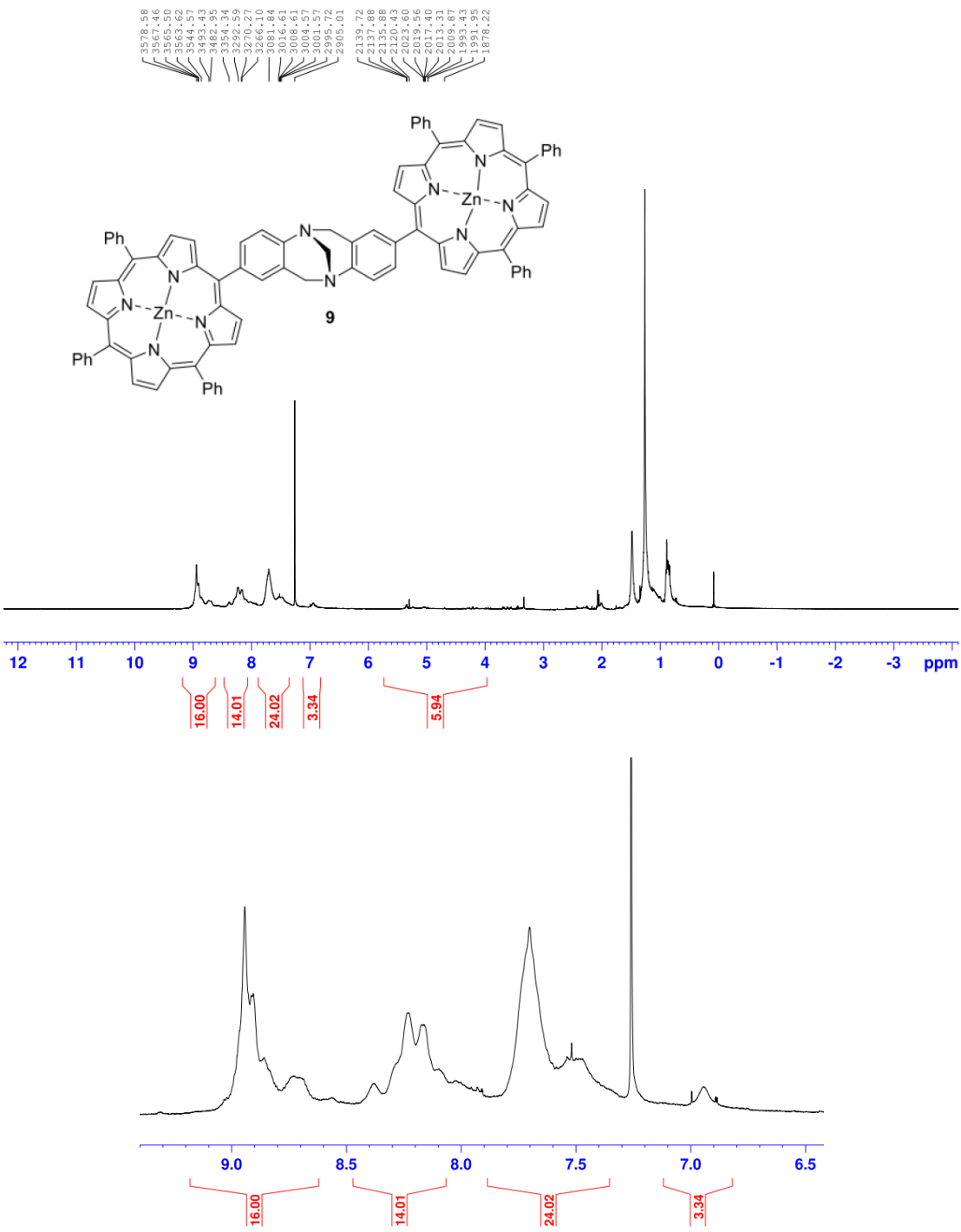

Fig. S17 ^{1}H NMR spectrum (400 MHz) of dizinc(II)porphyrin dyad **9** in $CDCl_3$.

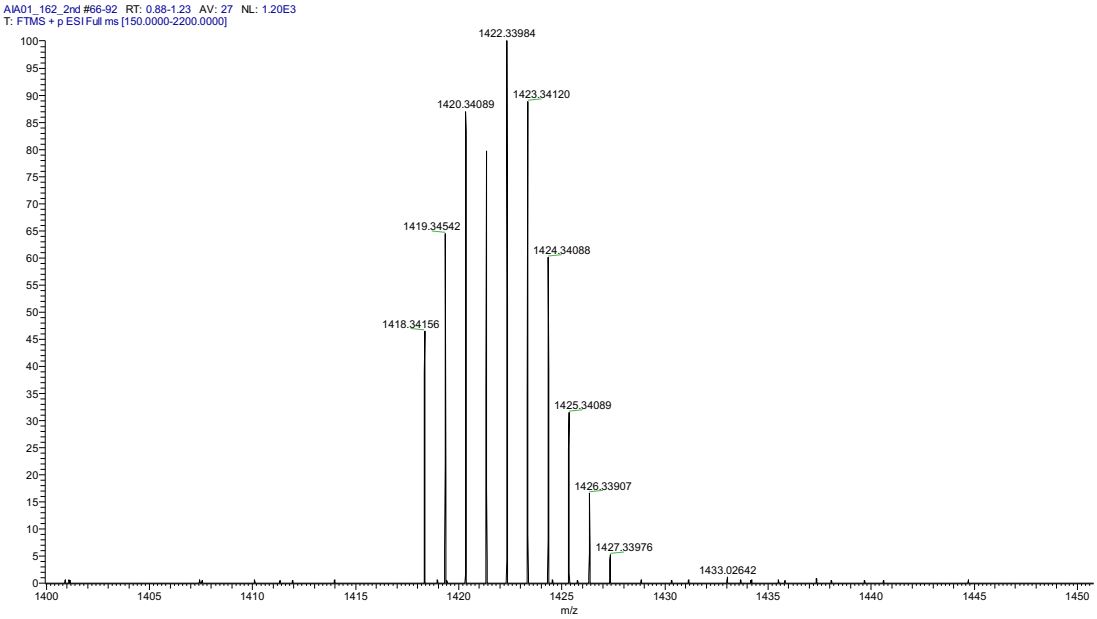

Fig. S18 High resolution mass spectrum of dizinc(II)porphyrin dyad **9**.

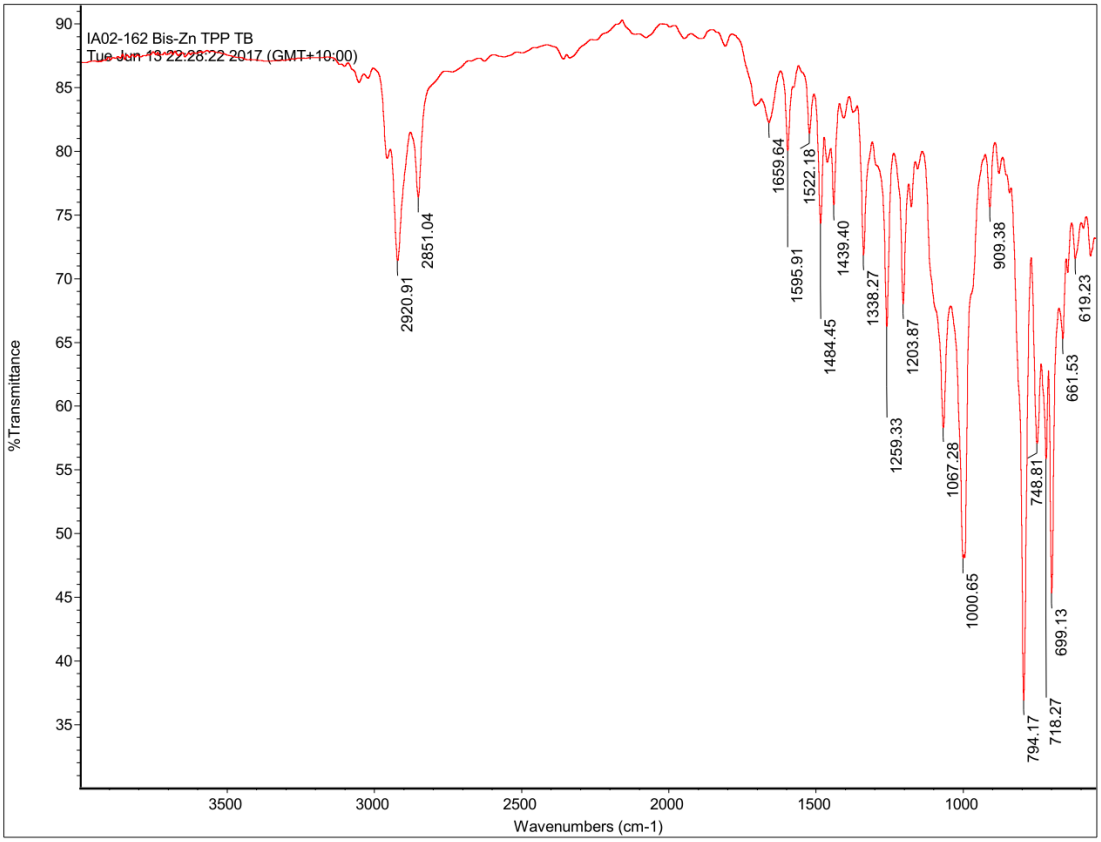

Fig. S19 Fourier transform infrared (FTIR) spectrum of dizinc(II)porphyrin dyad **9**.

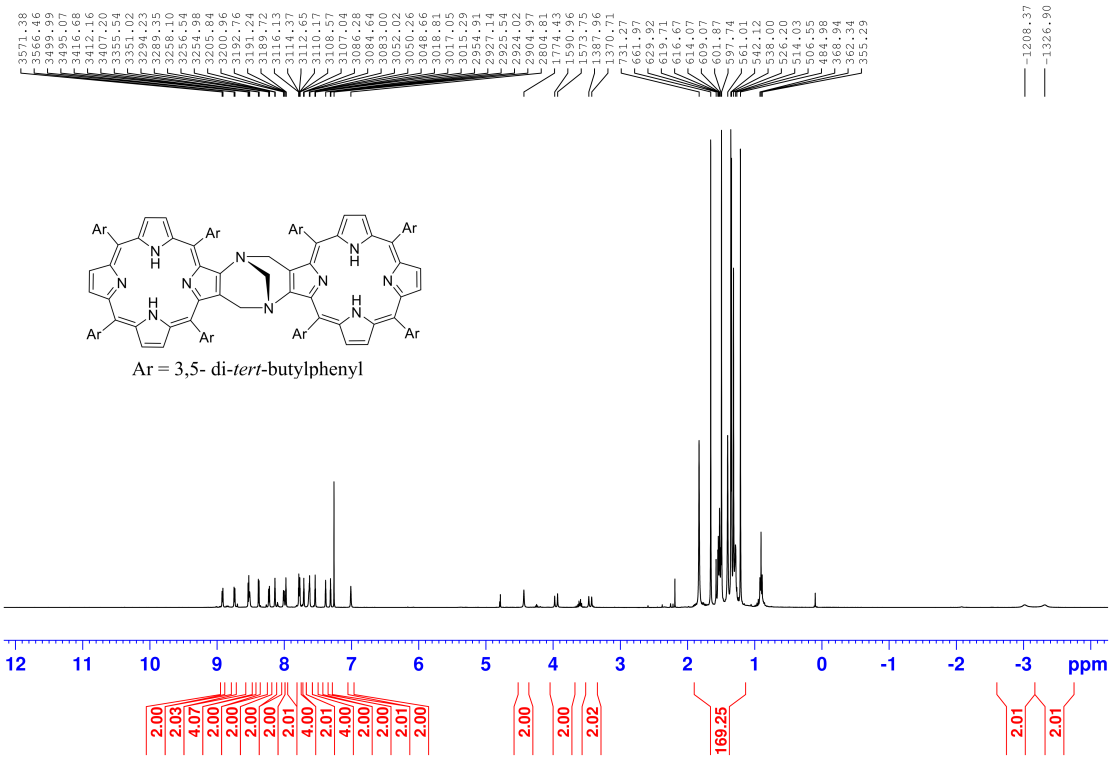

Fig. S20 ^{1}H NMR spectrum (400 MHz) of free-base fused-porphyrin dyad **11** in $CDCl_3$.

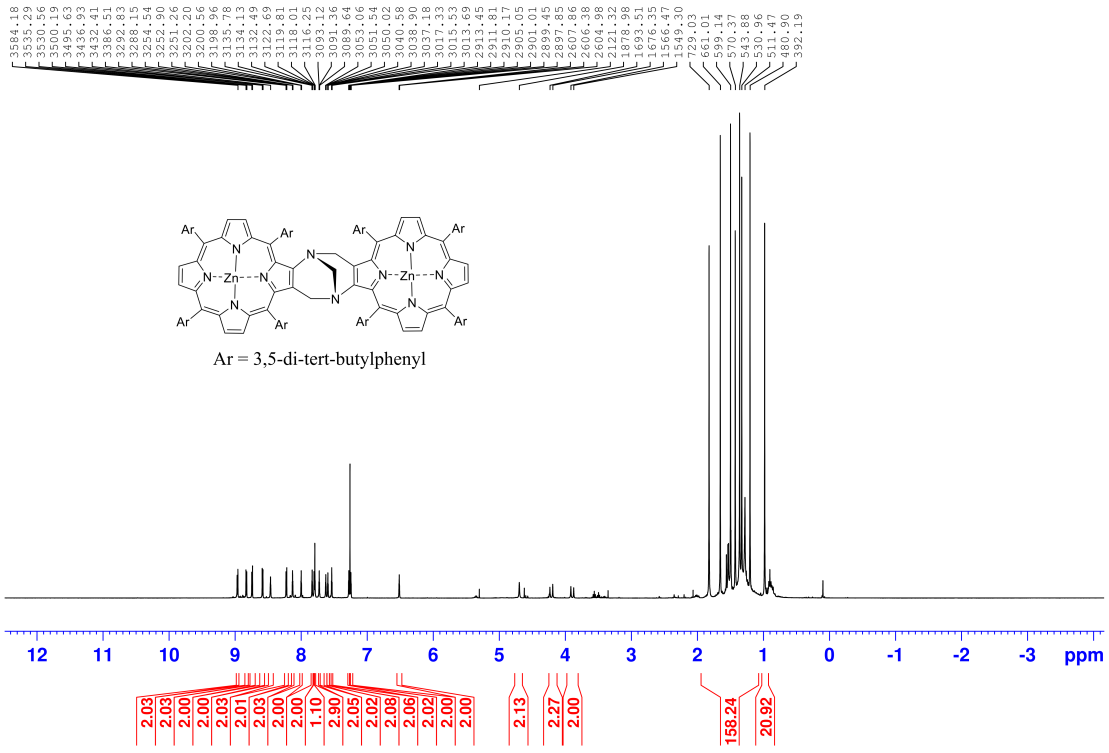

Fig. S21 ^{1}H NMR spectrum (400 MHz) of dizinc(II) fused-porphyrin dyad **12** in $CDCl_3$.

References

1. A. D. Adler, F. R. Longo, J. D. Finarelli, J. Goldmacher, J. Assour and L. Korsakoff, *J. Org. Chem.*, 1967, **32**, 476-476.
2. R. Luguya, L. Jaquinod, F. R. Fronczek, A. G. H. Vicente and K. M. Smith, *Tetrahedron*, 2004, **60**, 2757-2763.
3. L. Zamani and B. B. F. Mirjalili, *Chem. Heterocycl. Compd.*, 2015, **51**, 578-581.
4. V. Promarak and P. L. Burn, *J. Chem. Soc., Perkin Trans. 1*, 2001, 14-20.
5. H. Imahori, K. Hagiwara, M. Aoki, T. Akiyama, S. Taniguchi, T. Okada, M. Shirakawa and Y. Sakata, *J. Am. Chem. Soc.*, 1996, **118**, 11771-11782.
6. M. J. Crossley, T. W. Hambley, L. G. Mackay, A. C. Try and R. Walton, *J. Chem. Soc., Chem. Commun.*, 1995, 1077-1079.

Chapter Four

Statement of Contribution

The research presented in this manuscript is based on work done by author (M.I.A) except high-resolution mass spectra which were obtained commercially at Australian Proteome Analysis Facility (APAF), Macquarie University. DFT calculation was done by (P.K). The manuscript was written by me and it was checked and edited by the principal supervisor (P.K).

Synthesis and Photophysical Studies of β,β′-Pyrrolic Tetraaryl fused-Porphyrin Tröger's Base Fullerene—C_{60} Dyad

Md Imam Ansari, Andrew Try, and Peter Karuso*

Department of Molecular Sciences, Macquarie University, Sydney NSW 2109, Australia

* Corresponding author. Tel.: +612-9850-8290 fax: +612-9850-8313, e-mail: peter.karuso@mq.edu.au

Abstract There has been a great deal of recent attention given to the construction of porphyrin-fullerene dyads to study photoinduced electron transfer processes that mimic natural photosynthesis and to design artificial photosynthetic models. To date, porphyrin and fullerene have been linked together either through a conjugated bridge molecule or *via* a non-covalent supramolecular interaction. Herein, we report a systematic approach to link a porphyrin with C_{60} through a rigid and non-conjugated bridging molecule that allows intramolecular through-space electronic interaction to be studied. The rigid V-type geometry of Tröger's base, holds two chromophores in close proximity at a fixed distance. Preliminary photophysical investigation of porphyrin-TB-C_{60} dyads reveals the existence of an energy transfer from porphyrin to the C_{60}. Additionally, six novel porphyrin TBs were prepared in this work as a synthetic tool bearing ester, alcohol and aldehyde functional groups. The aldehyde porphyrin TB was used in a Prato reaction to append C_{60} chromophore onto the porphyrin TB system.

Introduction

Mimicry of electron and energy transfer processes of photosynthesis have attracted a great deal of attention recently for the construction of light harvesting complexes (LHCs), electron donor-acceptor dyads and artificial photosynthetic models.[1-3] Porphyrins as an electron donor component are commonly used in the construction of donor-acceptor dyads or LHCs.[2, 4-5] The highly delocalised π-system of porphyrins is suitable for efficient electron transfer reactions. Moreover, porphyrins strong and extensive absorption in the visible region and established synthetic methods with the choice of central metal ion, are appealing features for the construction of LHCs and electron transfer units. On the other hand, fullerene-C_{60} is a popular choice as an electron acceptor due to its small reorganization energy[6] and its facile reduction potential.[7] Indeed, the remarkable features of porphyrins and fullerenes have been

widely utilised to construct porphyrin-fullerene dyads in the quest for efficient electron and energy transfer architectures.[8-13] For Instance, Crossley, Reimers and Fukuzumi reported on giant photosynthetic reaction centre models based on porphyrin/Tröger's base with extensive photochemical studies.[11] They also investigated the mechanism of electron transfer reactions using femtosecond and nanosecond transient absorption spectroscopy, revealing picosecond-timescale charge-separations.[11] These chromophores are potentially useful in organic photovoltaics, light-energy harvesting systems and artificial photosynthesis.[1-2, 14-15] Traditionally, covalently linked conjugated porphyrin-fullerene dyads, and triads have been developed to study the photoinduced electron transfer process of natural photosynthesis.[1-3, 12, 16] However, the development of through-space interacting porphyrin arrays or donor-acceptor dyads has rarely been achieved due to the lack of efficient scaffolding materials.[17] Tröger's base (TB) is rigid non-conjugated and V-shaped molecule that can accommodate two chromophores at well-defined distances (Fig. 1).[18-19] Employing a TB framework as a bridge between two chromophores is an approach to constructing donor-acceptor assemblies with not only defined spatial orientations but without hyperconjugation.

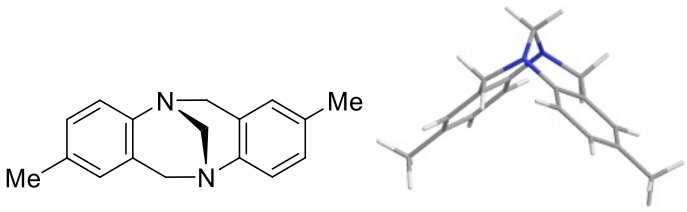

Fig. 1 Structural formula and optimised geometry of Tröger's base.

In previous studies, two porphyrins have been assembled, separated by a TB bridge. For example, Crossley and co-workers synthesised porphyrin analogues of Tröger's base in which the methanodiazocine ring was fused to two tetraarylporphyrins, forming a well-defined chiral cleft molecule.[18] In 2000, Crossley and Ghiggino reported

photoinduced energy and electron transfer in bisporphyrins with quinoxaline Tröger's base or biquinoxalinyl spacers.[19] However, the construction of rigid, but non-conjugated, porphyrin-fullerene dyads with precise spatial orientations remains a challenge due to the lack of efficient building blocks and the difficulty of positioning porphyrins close to one another, especially at well-defined distances with a fixed orientation.[17] We envisioned the construction of a porphyrin-fullerene dyad bridged with TB, so that the two chromophores are held at well-defined distances and in close proximity to each other. In order to append different chromophores, we tested a mixed condensation approach (2-aminoporphyrin **1** and ethyl 4-amino-3-methylbenzoate) with paraformaldehyde in the presence of TFA to synthesise hybrid porphyrin TB **2**.

Moreover, we have devised a new synthetic procedure, by which several issues associated with the synthesis of a rigid and non-conjugated bridged donor-acceptor complexes involving porphyrins and fullerenes may be circumvented. Application of this procedure provides a facile synthesis of such donor-acceptor complexes that, as far as we are aware, have not been synthesised previously.

Results and discussion

Synthesis and characterisation of porphyrin TBs

5,10,15,20-Tetrakis(3',5'-di-*tert*-butylphenyl)porphyrin was chosen for this work as the 3,5-di-*tert*-butylphenyl *meso*-substituents afford good solubility to the porphyrin. Accordingly, 2-aminoporphyrin **1** was synthesised by the method of Burn and co-workers[20] *via* multistep synthesis procedure, using 3,5-di-*tert*-butylbenzaldehyde and freshly distilled pyrrole to give 5,10,15,20-tetrakis(3,5-di-*tert*-butylphenyl)porphyrin. Mononitration was achieved with a solution of nitrogen dioxide in hexane with the reaction followed closely by thin-layer chromatography and reduction of the nitro

group with mixture of tin(II) chloride in concentrated hydrochloric acid afforded the desired 2-aminoporphyrin **1**. Compound **1** was used to prepare the target hybrid ester porphyrin TB **2** *via* the mixed condensation approach by reacting **1** with ethyl 4-amino-3-methylbenzoate and paraformaldehyde in the presence of TFA (Scheme 1).

We expected two more symmetric TB products (**3** and **4**) from this reaction, however, the crude material after workup, showed only one major porphyrinic band on TLC. The only other isolatable compound was traces of **3**. We optimised this procedure on a gram scale, obtaining the hybrid product **3** in good yields (50-60%).

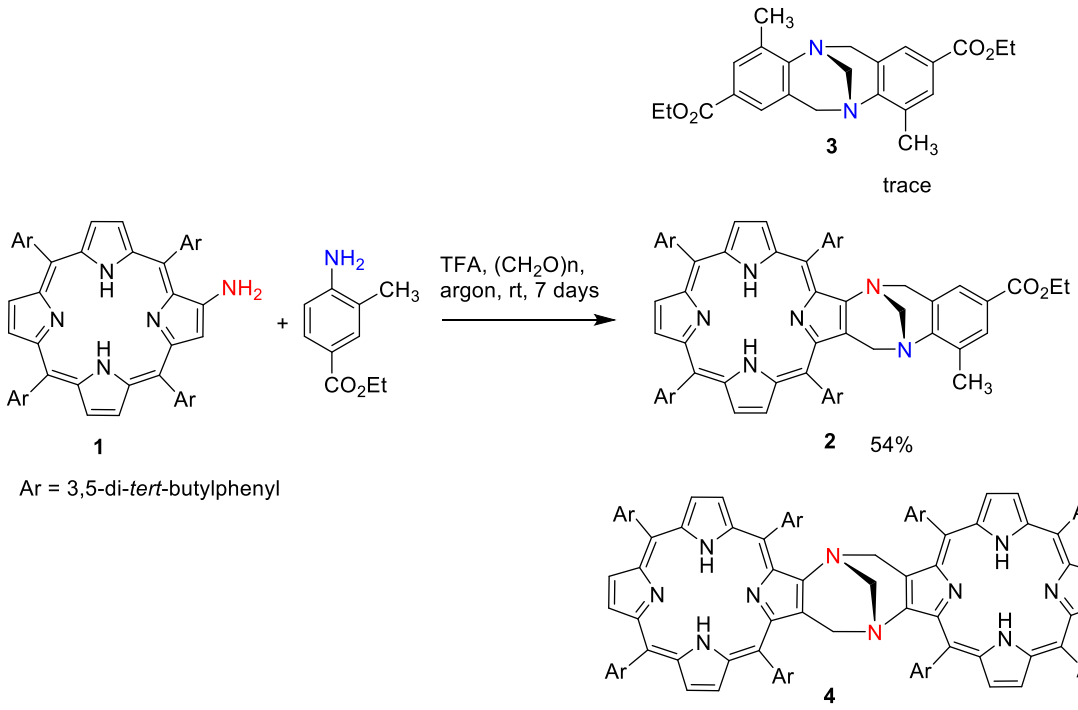

Scheme 1 Synthesis of hybrid ester porphyrin Tröger's base **2** *via* mixed condensation approach.

Our attempts to prepare **4** by reacting **1** with paraformaldehyde, in the presence of TFA were unsuccessful. This could be due to the bulky *tert*-butyl groups hindering the formation of **4**. In this case, although the porphyrin TB **4** was not formed in the reaction, isolation of the desired porphyrin TB **2** was convenient by using column

chromatography. In any case, compound **2** was converted to the aldehyde **6** by a two-step process involving reduction of the ethyl ester to the alcohol ($LiAlH_4$) and oxidation back up to the aldehyde with MnO_2 (Scheme 2a). The zinc complex of each of these compound was made using $Zn(OAc)_2$ (Scheme 2b) and characterised by NMR techniques and UV/Vis spectroscopy, zinc was selected as the metal because of its diamagnetism.

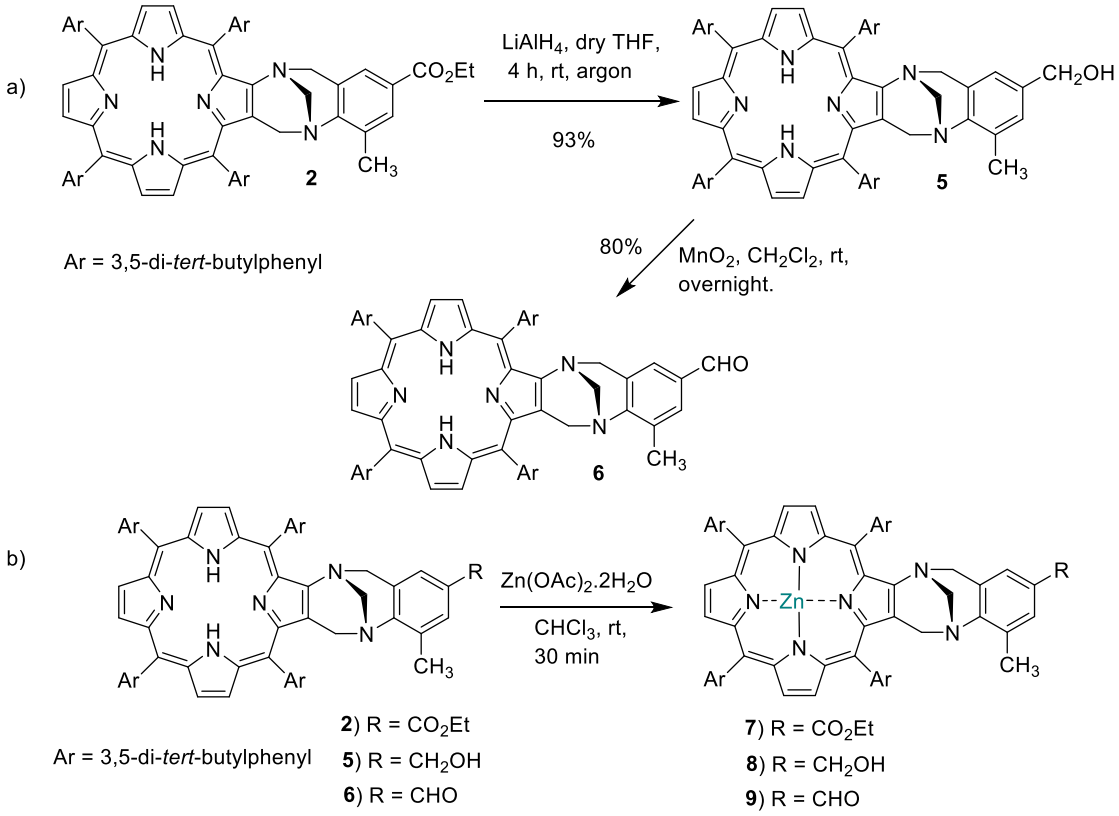

Scheme 2 a) Synthetic route of aldehyde functionalised porphyrin Tröger's base 6 b) Synthesis of zinc derivatives of porphyrin Tröger's base.

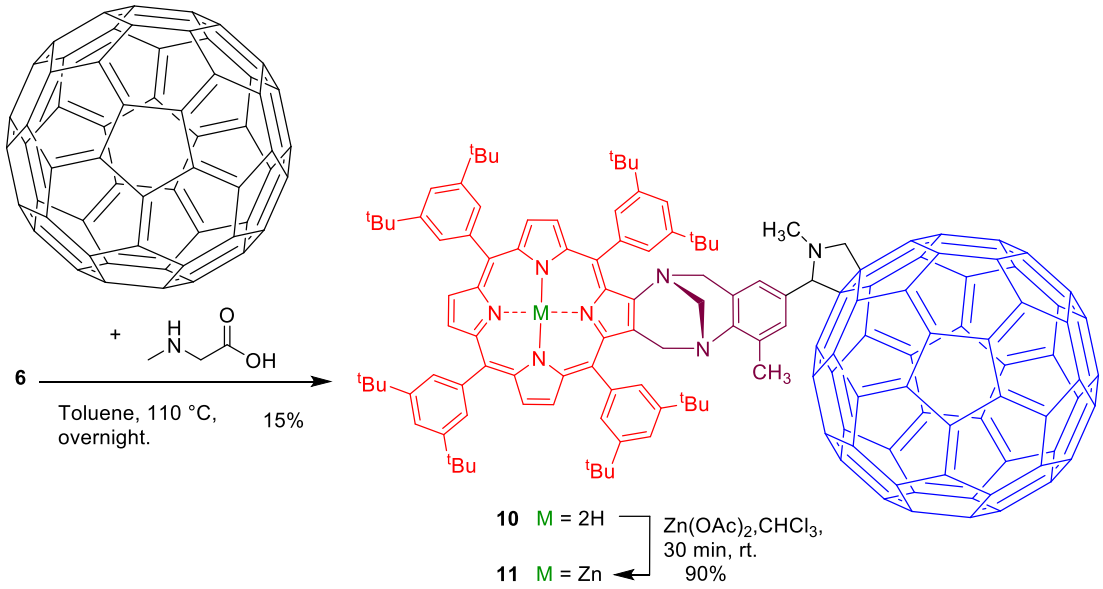

Scheme 3 Synthesis of porphyrin-TB-fullerene-C_{60} dyads.

The most successful approach for the functionalisation of fullerene-C_{60} has been the reaction between an aryl aldehyde, sarcosine and fullerene-C_{60} introduced by Prato *et al*.[21] Thus, compound **6** was condensed with sarcosine and fullerene-C_{60} to give dyad **10** (Scheme 3). Zinc(II)porphyrin-TB-C_{60} dyad **11** was prepared by metallation of **10** using the same condition developed for **7-9** (Scheme 3).

Fullerene-C_{60} insolubility in common organic solvents[22] often makes the purification process more challenging. However, the solubility of dyads **10** and **11** was drastically enhanced compared to C_{60} due to the presence of eight *tert*-butyl groups on the porphyrin macrocycle. This facilitated easy purification by column chromatography. Moreover, NMR sample preparation was convenient in $CDCl_3$ without the need for carbon disulphide. The molecular formula of **10** ($C_{149}H_{110}N_7$) was confirmed by high-resolution electron-spray ionization (HR-ESI) mass spectrometry of the $[M+H]^+$ ion (Δmmu −0.29). The structure was also supported by ^{1}H NMR spectroscopy (Fig. 2). The pyrrolidine protons were also clearly visible with the methylene seen as an AB system (J = 9.5 Hz).[21, 23] Appearance of pyrrolidine protons was evidence that the

fullerene molecule was successfully incorporated into the porphyrin TB system. The Tröger's base system was evident from the diazocine bridge protons which appeared as six geminally coupled doublets (Fig. 2). The broad peak at δ_H −2.91 ppm (2H) is indicative of the NH protons of a porphyrin macrocycle (Fig. S18).

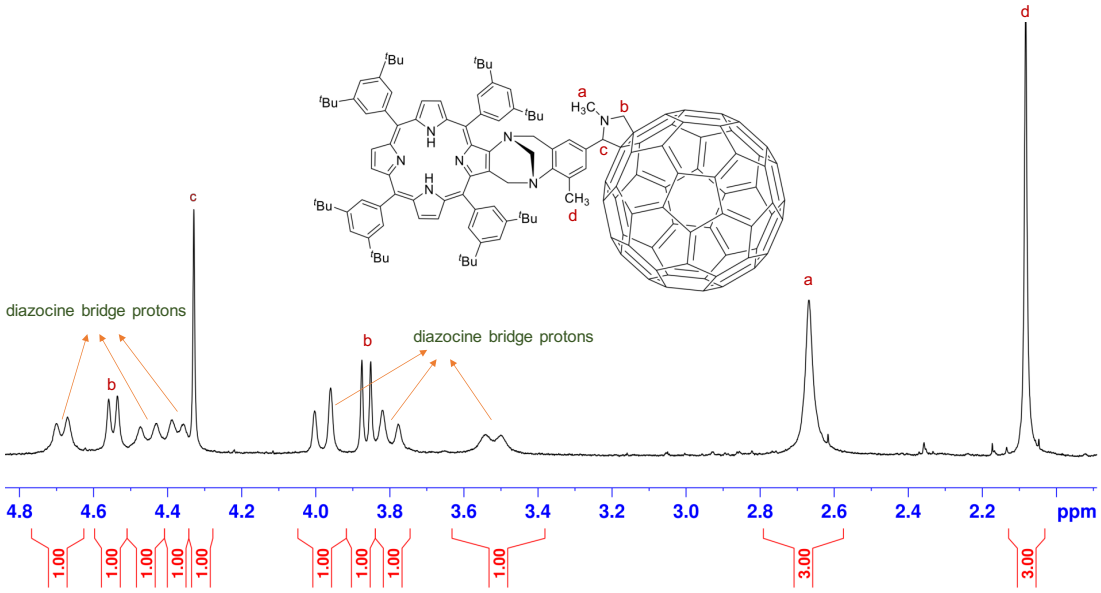

Fig. 2 Expansion of 400 MHz ^{1}H NMR (298 K, $CDCl_3$) spectra of **10** showing important features of Tröger's base region and pyrrolidine functionalised fullerene-C_{60}. The peaks marked with ***a***, ***b*** and ***c*** display the protons for *N*-methylpyrrolidine and ***d*** represents aromatic

Interestingly, dyad **10** at room temperature showed much-simpler ^{1}H NMR spectra than expected owing to restricted rotation of the fused-porphyrin macrocycle with the diazocine bridge at room temperature. Compound **11** showed a very similar NMR spectrum (Fig. S19) except with less signal overlap and minus the NH protons at −3 ppm. The high-resolution electron-spray ionization (HR-ESI) mass spectrometry gave an isotopic pattern consistent with one zinc atom (Fig. S27) and a molecular formula of $C_{149}H_{108}N_7Zn$ (Δ −0.33).

DFT//bp86/SV(P) calculation of porphyrin-TB-C_{60} dyad **11** show that the *exo*-conformer is slightly more stable than the *endo*-conformer (Fig. 3, 4). The energy difference between the *endo*- and *exo*- forms is less than 1 kcal/mol at this level of theory (neglecting zero point energies and any basis set superposition errors) suggesting, because only one set of NMR signals is seen that rotation about the TB aryl-pyrrolidine bond is fast on the NMR timescale.

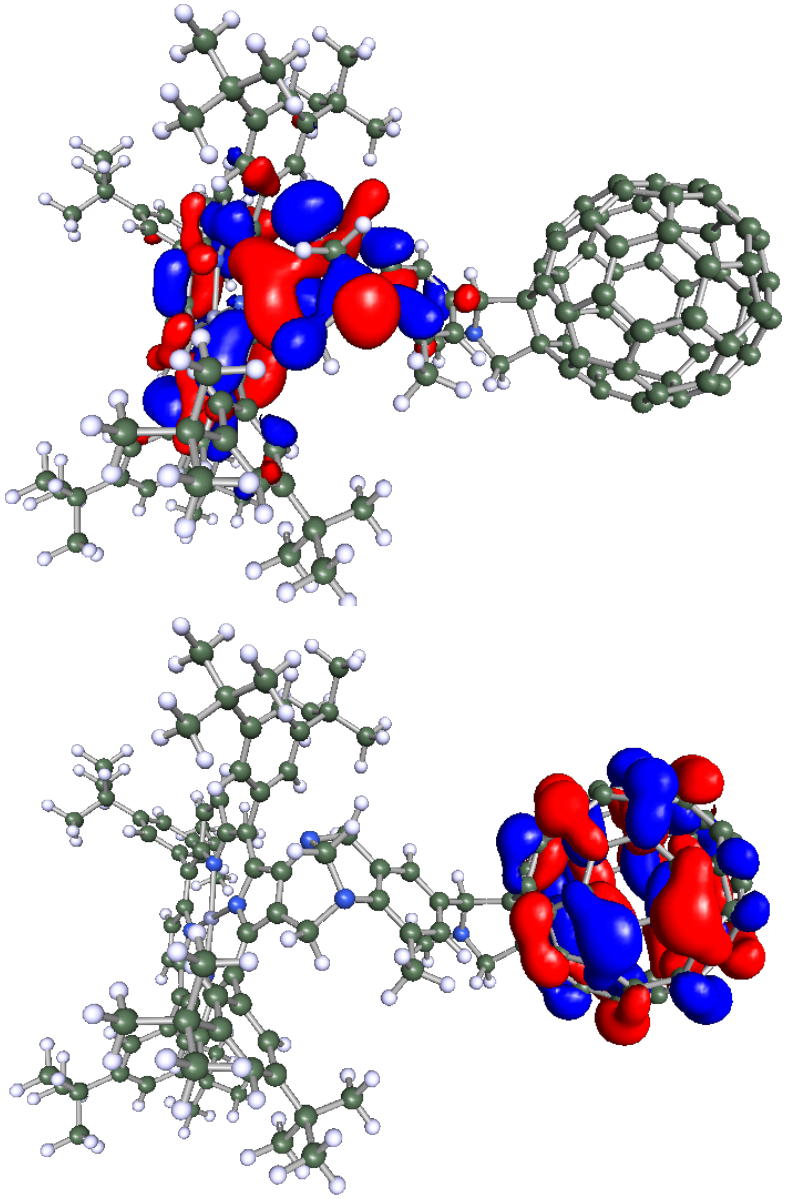

Fig. 3 *exo*-porphyrin-TB-C_{60} dyad **11** from DFT//bp86/SV(P) geometry optimisation. The HOMO (upper panel) is centred on the porphyrin and the LUMO (bottom panel) is centred on the fullerene indicative of an ICT in the excited state.

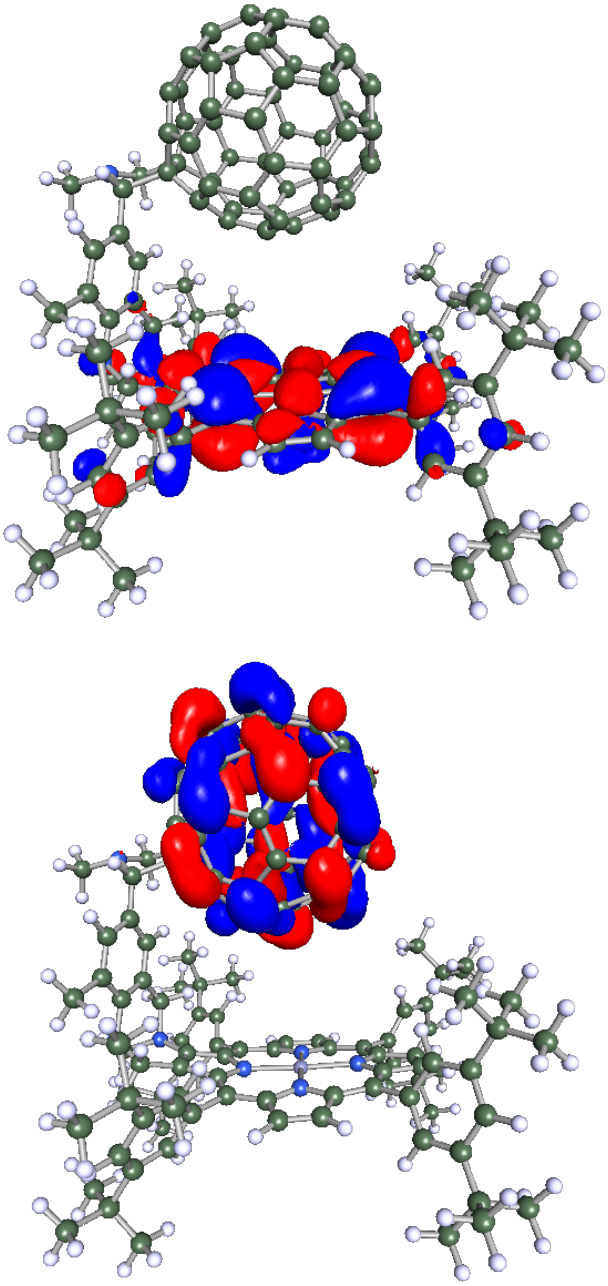

Fig. 4 *endo*-porphyrin-TB-C_{60} dyad **11** from DFT//bp86/SV(P) geometry optimisation. The HOMO (upper panel) is centred on the porphyrin and the LUMO (bottom panel) is centred on the fullerene indicative of an ICT in the excited state.

Photophysical Studies

Spectroscopic analysis was carried out in $CHCl_3$ on dyads **10** and **11**, and with their control samples **6** and **9**, respectively (Fig. 5). Electronic spectroscopy (UV/Vis) of **10** and **11** was compared to the non-fullerene analogues of **6** and **9** respectively. The zinc

porphyrins (**9** and **11**) had quite similar UV spectra but the non-metallated analogues (**6** and **10**) were quite different (Fig. 5). The Soret band was red-shifted by 25 nm in the fullerene dyad **10** compared to **6** whereas it was only shifted 10 nm between **9** and **11**. Upon zinc metallation, dyad **11** exhibited a decrease in intensity and fewer Q-bands which is attributed to the increase in symmetry of the porphyrin upon metalltion. The absorption spectra of **2**, **5**, **7**, and **8** (Fig. S1) showed similar absorption profiles compared to **6** and **9** (Fig. 5).

In general, all free-base porphyrin TBs (**2**, **5** and **6**) exhibited the Soret band around 424 nm arising from the transition of a_{1u} (π)—$e_{g.}$*(π) and due to which the intensity was very high. The other four maxima around (526, 564, 599 and 672 nm) were attributed to the Q bands corresponding to the a_{2u} (π)—$e_{g.}$*(π) transition.[24] All zinc porphyrin TBs (**7-9**), upon metallation, collapsed their Q-bands into one or two bands due to an increase in D_{4h} symmetry of the porphyrin. In contrast, the effect on the Soret band was insignificant.

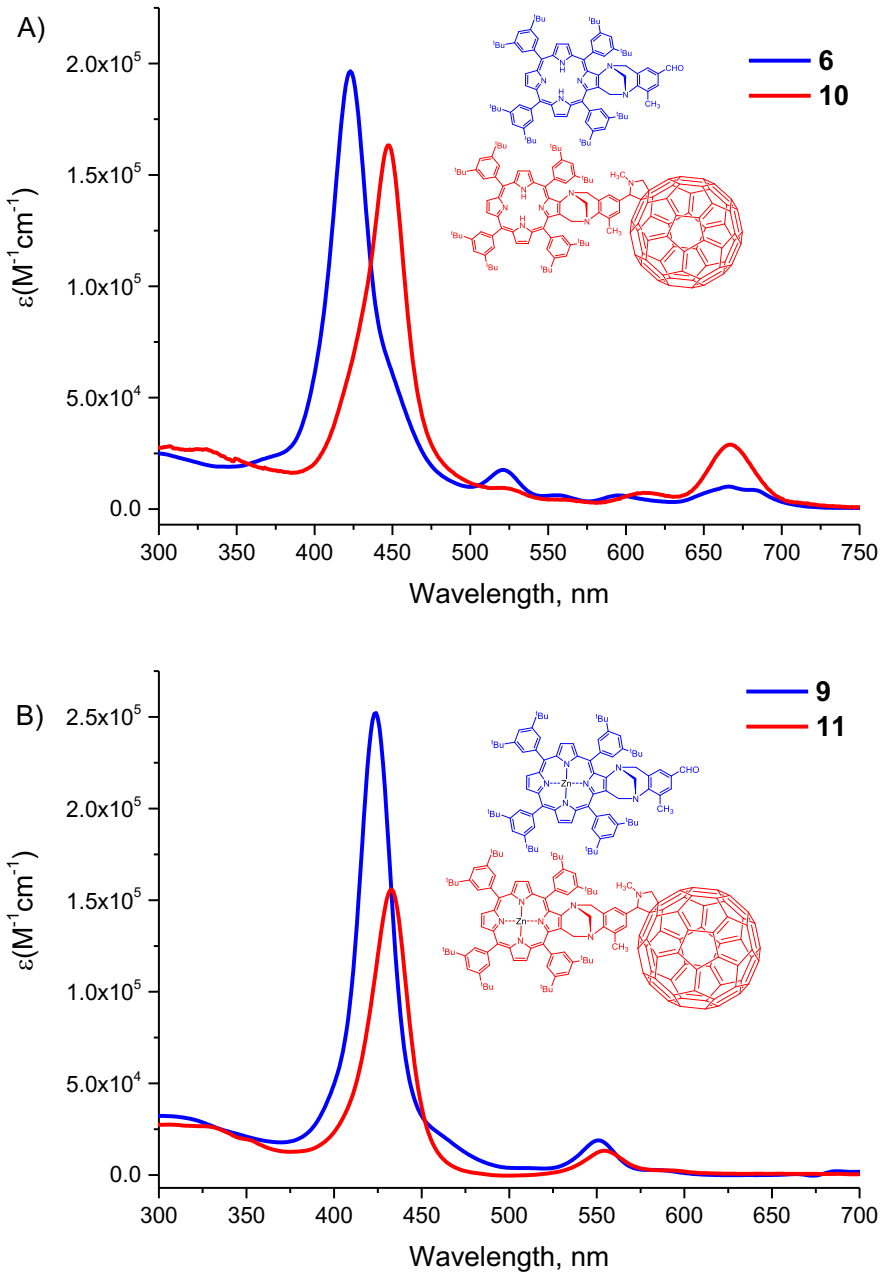

Fig. 5 UV/Vis spectra A) **6** (blue), **10** (red) top, B) **9** (blue) and **11** (red) bottom. The concentration of each compound was 2.5×10^{-6} M in $CHCl_3$.

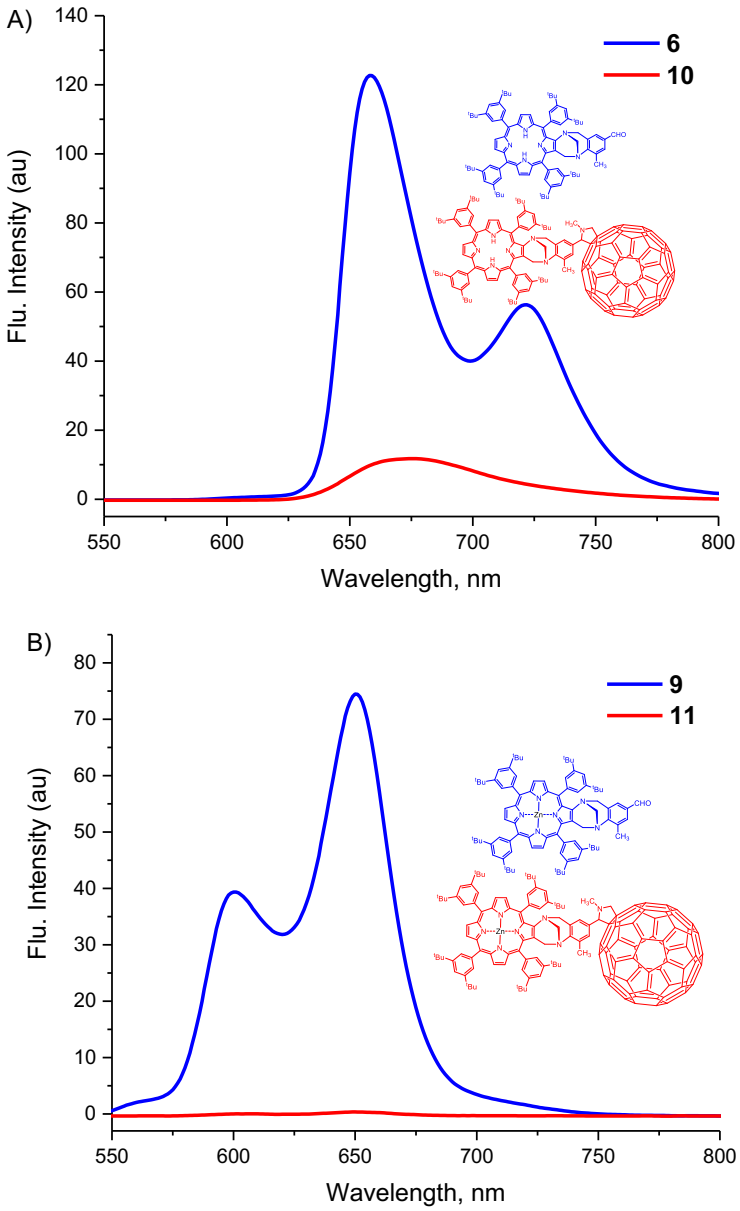

Fig. 6 Normalised Fluorescence emission spectra A) **6** (blue), **10** (red) top, B) **9** (blue) and **11** (red) bottom at λ_{ex} = 423 nm, λ_{abs} = 423 nm. The concentration of each compound was 2.5×10^{-6} M in $CHCl_3$.

Porphyrin TB **6** has emission maxima at 650 and 725 nm which were blue shifted by 50 and 75 nm, respectively, compared to the corresponding zinc derivative **9** and their intensities have undergone like mirror image (Fig. 6). The fluorescence is strongly quenched for both dyads **10** and **11** with respect to their controls **6** and **9**

respectively. For instance, the emission bands of free-base dyad **10**, were strongly quenched (>90%), whereas in the case of zinc(II) dyad **11** this quenching was over 98%, suggesting the occurrence of excited state events in both dyads **10** and **11** (Fig. 6).[25] These results infer that quenching of porphyrin singlet state is due to exclusively singlet-singlet energy transfer from the zinc quenching mechanism.[25-26]

We monitored the fluorescence excitation spectra of dyads **10** and **11** with their controls **6** and **9**, respectively, to investigate preliminary information regarding energy transfer phenomena (Fig. 7). Fluorescence spectra (Fig.6) were normalised and adjusted to the same absorption value (λ_{abs} = 423 nm). At the emission wavelength (λ_{em} 650 nm) of dyad **6** showed a strong excitation spectrum with the three Q bands peaks. However, upon appending fullerene-C_{60} chromophore to **6**, dyad **10** showed a drastic decrease in excitation, suggesting an energy transfer from the porphyrin to the fullerene-C_{60} entity. Similarly, excitation of zinc dyad **11** was strongly quenched, revealing energy transfer from zinc porphyrin to fullerene-C_{60} chromophore (Fig. 7).[17, 26]

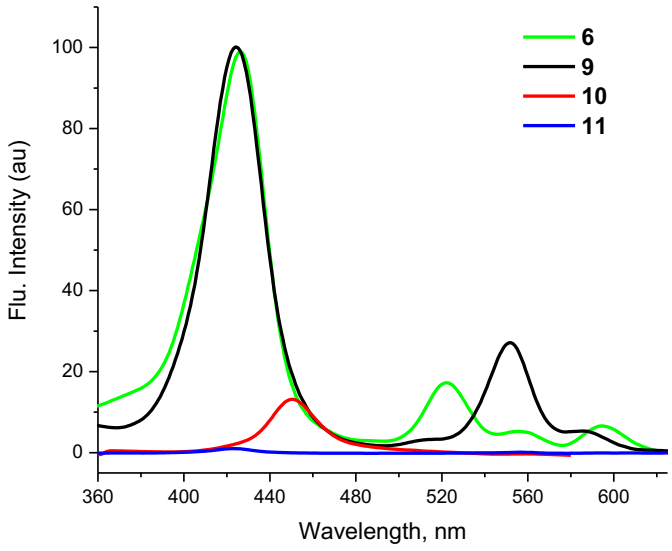

Fig. 7 Fluorescence excitation spectra of **6**, **9**, **10** and **11** at λ_{em} = 650 nm in $CHCl_3$. The concentration of each compound was 2.5×10^{-6} M.

We deconvolute the fluorescence spectra and fullerene molecule shows zero absorption near 445 nm. Overall, these results suggest strong electronic communication between the porphyrin and the fullerene chromophore and such dyads may be useful as components in artificial photosynthetic models or light harvesting complexes.

Conclusions

In summary, novel dyads featuring porphyrin, Tröger's base and fullerene-C_{60} linked by way of a non-conjugated bridge molecule (Tröger's base) have been synthesised and characterised. Ester, alcohol and aldehyde functionalised hybrid porphyrin TBs synthesised for the first time *via* mixed amine condensation. The aldehyde porphyrin TB was utilised to append the C_{60} *via* the Prato's method. The dyads presented in this work are sufficiently rigid, well-structured and due to the V-type configuration maintaining a close proximity between porphyrin and fullerene chromophores. The preliminary photophysical investigation was evident on through-space intramolecular charge transfer from porphyrin to the fullerene entity. For instance, the emission bands of free-base dyad **10**, were strongly quenched (>90%) compared to the non-fullerene counterpart, whereas in the case of zinc(II) dyad **11** this quenching was over 98%, compared to the non-fullerene counterpart. These results suggesting the occurrence of excited state events in both dyads **10** and **11**. Moreover, in the quest for electron and energy transfer through-space between donor-acceptor chromophores, a rigid dyad could supersede the non-covalent and supramolecular dyads owing to the precise distance between donor and acceptor unit and the better stability of rigid linkage even at variable temperatures. In particular, the synthetic strategy presented in this effort to assemble porphyrin and fullerene chromophores with a non-conjugated bridging molecule will overcome some of the limitations that hinder the construction of porphyrin-fullerene dyads where studies focused on through-space interactions

Acknowledgements

This work was supported by Macquarie University (Sydney, Australia). We would also like to thank India@75 and Macquarie University for the award of an iMQRES PhD scholarship to MIA.

References

1. D'Souza, F.; Ito, O., *Coord. Chem. Rev.* **2005**, *249*, 1410-1422.
2. Wasielewski, M. R., *Chem. Rev.* **1992**, *92*, 435-461.
3. Takano, Y.; Numata, T.; Fujishima, K.; Miyake, K.; Nakao, K.; Grove, W. D.; Inoue, R.; Kengaku, M.; Sakaki, S.; Mori, Y.; Murakami, T.; Imahori, H., *Chem. Sci.* **2016**, *7*, 3331-3337.
4. Smith, K. M., *Porphyrins and metalloporphyrins*. Elsevier Amsterdam: 1975; Vol. 9.
5. Latos-Grazynski, L.; Kadish, K.; Smith, K.; Guilard, R., *The porphyrin handbook*. 2000; p 361-416.
6. Hiroshi, I.; Kiyoshi, H.; Tsuyoshi, A.; Masanori, A.; Seiji, T.; Tadashi, O.; Masahiro, S.; Yoshiteru, S., *Chem. Phys. Lett.* **1996**, *263*, 545-550.
7. Xie, Q.; Perez-Cordero, E.; Echegoyen, L., *J. Am. Chem. Soc.* **1992**, *114*, 3978-3980.
8. Moreira, L.; Calbo, J.; Aragó, J.; Illescas, B. M.; Nierengarten, I.; Delavaux-Nicot, B.; Ortí, E.; Martín, N.; Nierengarten, J.-F., *J. Am. Chem. Soc.* **2016**, *138*, 15359-15367.
9. Fukuzumi, S.; Ohkubo, K.; Imahori, H.; Shao, J.; Ou, Z.; Zheng, G.; Chen, Y.; Pandey, R. K.; Fujitsuka, M.; Ito, O., *J. Am. Chem. Soc.* **2001**, *123*, 10676-10683.

10. Fukuzumi, S.; Saito, K.; Ohkubo, K.; Khoury, T.; Kashiwagi, Y.; Absalom, M. A.; Gadde, S.; D'Souza, F.; Araki, Y.; Ito, O.; Crossley, M. J., *Chem. Commun.* **2011**, *47*, 7980-7982.

11. Lee, S. H.; Blake, I. M.; Larsen, A. G.; McDonald, J. A.; Ohkubo, K.; Fukuzumi, S.; Reimers, J. R.; Crossley, M. J., *Chem. Sci.* **2016**, *7*, 6534-6550.

12. Guldi, D. M., *Chem. Soc. Rev.* **2002**, *31*, 22-36.

13. Maligaspe, E.; Tkachenko, N. V.; Subbaiyan, N. K.; Chitta, R.; Zandler, M. E.; Lemmetyinen, H.; D'Souza, F., *J. Phys. Chem. A* **2009**, *113*, 8478-8489.

14. Imahori, H.; Yamada, H.; Guldi, D. M.; Endo, Y.; Shimomura, A.; Kundu, S.; Yamada, K.; Okada, T.; Sakata, Y.; Fukuzumi, S., *Angew. Chem., Int. Ed.* **2002**, *41*, 2344-2347.

15. Fukuzumi, S.; Ohkubo, K.; Imahori, H.; Guldi, D. M., *Chem. Eur. J.* **2003**, *9*, 1585-1593.

16. Sukegawa, J.; Schubert, C.; Zhu, X.; Tsuji, H.; Guldi, D. M.; Nakamura, E., *Nat. Chem.* **2014**, *6*, 899-905.

17. Kang, B.; Yang, W.; Lee, S.; Mukherjee, S.; Forstater, J.; Kim, H.; Goh, B.; Kim, T.-Y.; Voelz, V. A.; Pang, Y., *Sci. Rep.* **2017**, *7*.

18. Crossley, M. J.; Hambley, T. W.; Mackay, L. G.; Try, A. C.; Walton, R., *J. Chem. Soc., Chem. Commun.* **1995**, 1077-1079.

19. Yeow, E. K. L.; Sintic, P. J.; Cabral, N. M.; Reek, J. N. H.; Crossley, M. J.; Ghiggino, K. P., *Phys. Chem. Chem. Phys.* **2000**, *2*, 4281-4291.

20. Promarak, V.; Burn, P. L., *J. Chem. Soc., Perkin Trans. 1* **2001**, 14-20.

21. Maggini, M.; Scorrano, G.; Prato, M., *J. Am. Chem. Soc.* **1993,** *115*, 9798-9799.

22. Ruoff, R. S.; Tse, D. S.; Malhotra, R.; Lorents, D. C., *J. Phys. Chem.* **1993**, *97*, 3379-3383.

23. Zhang, J.; Morton, J. J. L.; Sambrook, M. R.; Porfyrakis, K.; Ardavan, A.; Briggs, G. A. D., *Chem. Phys. Lett.* **2006**, *432*, 523-527.

24. Zheng, W.; Shan, N.; Yu, L.; Wang, X., *Dyes Pigm.* **2008**, *77*, 153-157.

25. Lackowicz, J. R., *Principle of Fluorescence Spectroscopy, 2006*. Vol. 13, p 978.

26. Kuciauskas, D.; Lin, S.; Seely, G. R.; Moore, A. L.; Moore, T. A.; Gust, D.; Drovetskaya, T.; Reed, C. A.; Boyd, P. D. W., *J. Phys. Chem.* **1996**, *100*, 15926-15932.

SUPPORTING INFORMATION

Synthesis and Photophysical Studies of β,β′-Pyrrolic Tetraaryl fused-Porphyrin Tröger's Base-Fullerene—C_{60} Dyad

Md Imam Ansari, Andrew Try, and Peter Karuso*

Department of Molecular Sciences, Macquarie University, Sydney NSW 2109, Australia

* Corresponding author. Tel.: +612-9850-8290 fax: +612-9850-8313, e-mail: peter.karuso@mq.edu.au

Table of Contents

General Information:

Reagents were purchased from Sigma Aldrich and Alfa Aesar and used without purification unless otherwise stated.

^{1}H NMR and ^{13}C NMR spectra were recorded in Aldrich 5 mm tubes on a Bruker DRX 400 spectrometer (400 MHz) at 300 K unless otherwise stated, processed using Topspin 3.5, and referenced to residual solvent peak ($CDCl_3$ δ_H 7.26 and δ_C 77.01 ppm, DMSO-d_6 δ_H 2.49 and δ_C 39.5 ppm) Signals were recorded in terms of chemical shifts, multiplicity, coupling constants (in Hz). The following abbreviations for multiplicity are used: s, singlet; d, doublet; t, triplet; m, multiplet; dd, doublet of doublets. Column chromatography was routinely carried out using the gravity feed column techniques on Merck silica gel type 9385 (230-400 mesh) with the stated solvent systems. Analytical thin layer chromatography (TLC) analyses were performed on Merck silica gel 60 F254 protected sheets (0.2 mm). Visualisation of compounds was achieved by illumination under ultraviolet light (254 nm). Charcoal and celite were pre-washed with MeOH and water before used. HR-ESIMS were performed at the Australian Proteome Analysis Facility (APAF), Macquarie University, Australia using a Q Exactive Plus hybrid quadrupole-

orbitrap mass spectrometer (Thermo Scientific, Bremen, Germany). ESI-MS spectra were recorded using an Agilent 6130 single quadrupole mass spectrometer (Agilent Corp.). The IR spectra were taken on a Thermo Scientific Nicolet iS10 ATR FTIR spectrometer at 298 K. UV-visible absorbances were recorded on a Varian Cary 1Bio UV-visible spectrophotometer. Fluorescence emission spectra were recorded on a Cary Eclipse Fluorescence Spectrofluorometer (Agilent Technologies). All commercial solvents were HPLC grade and used without further purification. Where solvent mixtures are used, the portions are given by volume. Pyrrole was freshly distilled before use. Chloroform used for photophysical experiments were HPLC grade purchased from Sigma-Aldrich (amylene stabilised).

Experimental Section

General Preparation of Zinc(II) Porphyrin Tröger's Base 7-9

The free-base porphyrin Tröger's (20 mg) was dissolved in chloroform (5 mL) and stirred at room temperature. Zinc acetate dihydrate (2.5 equiv) was separately dissolved in methanol (3 mL) and then added dropwise to the reaction mixture. After 30 min, the colour of the reaction changed from red to pink. The organic layers were washed with water (2 × 20 mL) and brine (20 mL), dried over anhydrous magnesium sulfate, filtered and evaporated to dryness under vacuum. The crude product did not require further purification.

Ester functionalised free-base porphyrin Tröger's base 2

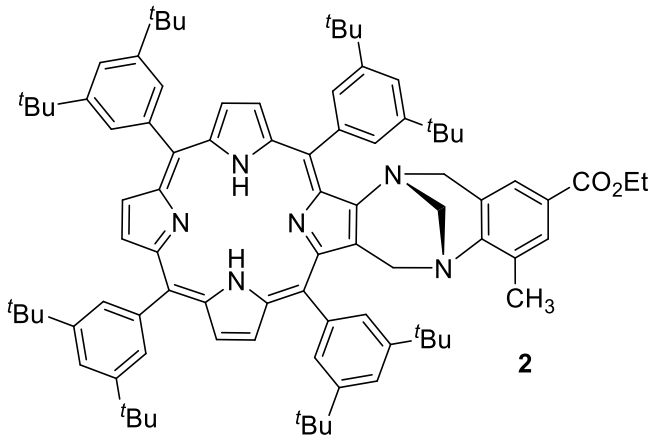

2

Ester functionalised free-base porphyrin Tröger's base **2**. A mixture of **1** (1.80 g, 1.67 mmol) and ethyl 4-amino-3-methylbenzoate (254 mg, 1.67 mmol) with paraformaldehyde (161 mg, 5.4 mmol) were dissolved in trifluoroacetic acid (60 mL) under an argon atmosphere. The reaction mixture was stirred in the dark for 7 days. The reaction progress was monitored by TLC (20% ethyl acetate/80% hexane). Upon consumption of the starting material, the reaction was stopped and then basified with a solution of concentrated ammonia (75 mL) in water (100 mL). A saturated solution of sodium bicarbonate (1 × 150 mL) was added to the reaction mixture and then extracted with ethyl acetate (3 × 150 mL). The combined organic layers were washed with brine, dried over anhydrous magnesium sulfate, filtered and evaporated to dryness under vacuum to give dark-brown solid. The crude was chromatographed (silica gel; 50% dichloromethane/50% hexane) to afford **2** (1.30 g, 62%) as a reddish brown solid. UV/Vis ($CHCl_3$) λ_{max} (log ε) 669 (4.13), 521 (4.27), 423 (5.31), 240 (4.47), 238 (4.47) nm; FTIR (neat) ν_{max} 3299, 2958, 1715, 1592, 1474, 1424, 1392, 1362, 1303, 1246, 1200, 1139, 1120, 1028, 988, 919, 899, 880, 800, 770, 715 cm^{-1}; ^1H NMR (400 MHz, $CDCl_3$) δ 8.77-8.88 (m, 5H, β-pyrrolic H), 8.63 (d, J = 4.7 Hz, 1H, β-pyrrolic H), 8.11-8.19 (m, 2H, ArH), 8.27 (s, 1H, ArH), 8.05 (s, 1H, ArH),

7.98 (s, 1H, ArH), 7.91 (s, 1H, ArH), 7.83-7.89 (m, 2H, ArH), 7.74-7.80 (m, 3H, ArH), 7.49 (s, 1H, ArH), 7.04 (s, 1H, ArH), 4.55-4.67 (m, 2H), 4.16-4.23 (m, 1H), 4.04-4.15 (m, 3H), 3.81-3.90 (m, 1H), 3.67-3.77 (m, 1H), 1.46-1.62 (m, 72H, *tert*-butyl H), 2.20 (3H, s, CH_3), 1.15 (t, J = 7.0 Hz, 3H), −2.80 (br s, 2H, NH); ^{13}C NMR (100 MHz, $CDCl_3$) δ 166.3, 150.9, 149.7, 149.5, 148.6, 147.9, 141.5, 141.3, 141.1, 139.8, 132.5, 130.7, 130.5, 129.7, 129.6, 129.5, 129.3, 128.6, 127.7, 125.9, 124.9, 121.8, 121.6, 121.5, 120.9, 120.2119.1, 118.8, 67.7, 60.4, 59.5, 55.5, 53.5, 35.2, 35.1, 34.9, 31.9, 31.8, 31.7, 31.6, 31.2, 29.7, 22.6, 17.4, 14.1; HRMS (ESI) *m/z*: 1293.8623 $[M+H]^+$ (calcd for $C_{89}H_{109}N_6O_2$, 1293.8612).

Alcohol functionalised free-base porphyrin Tröger's base 5

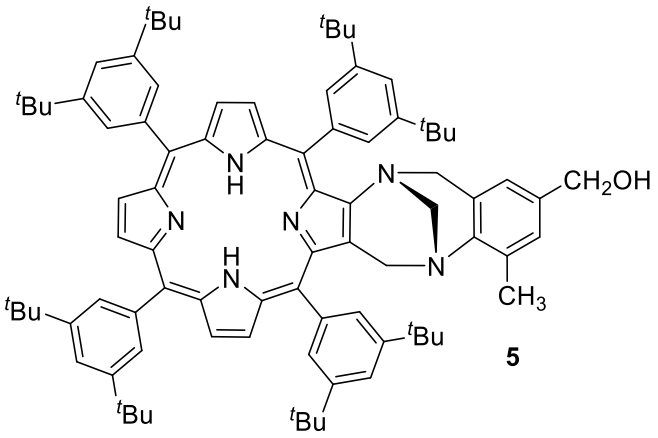

5

Alcohol functionalised free-base porphyrin Tröger's base **5**. Ester porphyrin TB **2** (20 mg, 0.02 mmol) was dissolved in dry tetrahydrofuran (10 mL). Lithium aluminium hydride (10 mg, 0.26 mmol, 17 equiv with respect to total mmol of ester) was added to the reaction mixture and stirred at 0 °C for 2 h (on ice bath) under an argon atmosphere. Water (1 mL) and 15% sodium hydroxide solution (2 mL) were added dropwise to the reaction mixture. Then again, water (3 mL) added to provide an inorganic precipitate. The reaction mixture was then rinsed with ethyl acetate (2 × 50 mL). The combined organic layers were washed

with brine (50 mL), dried over anhydrous magnesium sulfate, filtered and evaporated to dryness to afford **5** as a dark purple solid (15 mg, 80%); UV/Vis ($CHCl_3$) λ_{max} (log ε) 669 (4.28), 447 (5.02), 423 (5.11), 242 (4.48), 240 (4.47) nm; FTIR (neat) ν_{max} 3645, 3300, 2959, 2901, 1590, 1526, 1474, 1423, 1392, 1361, 1296, 1246, 1211, 1038, 914, 898, 879, 800, 728, 714, 648 cm^{-1}; ^1H NMR (400 MHz, $CDCl_3$) δ 8.78-8.91 (m, 5H, β-pyrrolic H), 8.61-8.68 (m, 2H, β-pyrrolic H), 8.29 (s, 1H, ArH), 8.13-8.22 (m, 2H, ArH), 7.93-8.11 (m, 4H, ArH), 7.87 (s, 2H, ArH), 7.75-7.83 (m, 3H, ArH), 7.24 (m, 1H, ArH), 6.84 (s, 1H, ArH), 6.32 (s, 1H, ArH), 4.54-4.74 (m, 3H), 4.16-4.31 (m, 3H), 4.06 (d, *J* = 7.4 Hz, 1H), 3.80-3.92 (m, 1H), 3.71 (d, *J* = 7.4 Hz, 1H), 2.20 (s, 3H, CH_3), 1.45-1.66 (m, 72H, *tert*-butyl H), −2.76 (br s, 2H, NH); ^{13}C NMR (100 MHz, $CDCl_3$) δ 151.2, 150.8, 149.7, 149.3, 148.6, 148.5, 147.8, 145.7, 145.4, 143.1, 141.5, 141.3, 141.2, 140.1, 139.8, 135.5, 132.8, 130.8, 130.4, 129.7, 129.6, 129.5, 129.4, 128.8, 127.7, 127.5, 126.8, 126.1, 124.6, 123.4, 123.3, 123.1, 121.8, 121.7, 121.5, 121.4, 121.3, 120.9, 120.1, 119.1, 118.8, 69.7, 67.8, 66.1, 65.1, 55.8, 55.3, 53.5, 43.9, 35.3, 35.2, 35.1, 35.0, 34.9, 31.8, 31.5, 31.4, 31.0, 31.9, 29.7, 29.4, 29.3, 27.5, 17.5, 14.1; HRMS (ESI) *m/z*: 1251.8526 $[M+H]^+$ (calcd for $C_{87}H_{107}N_6O$, 1251.8506).

Aldehyde functionalised free-base porphyrin Tröger's base 6

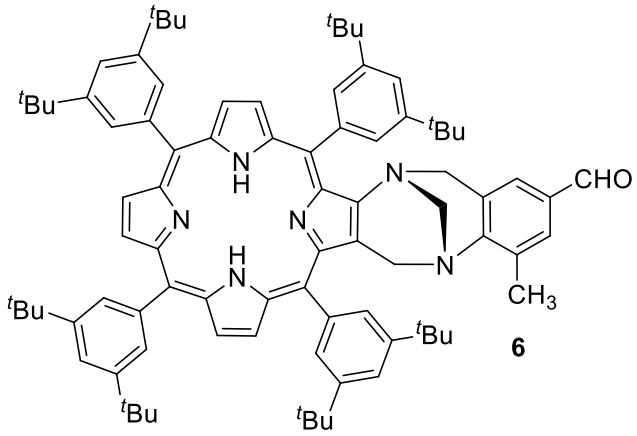

6

Aldehyde functionalised free-base porphyrin Tröger's base **6**. Manganese dioxide (2.01 g, 23 mmol) was added to a solution of porphyrin TB **5** (500 mg, 0.40 mmol) in dichloromethane (150 mL) at 0 °C (ice bath) and stirred for 30 min with a drying tube attached. The reaction progress was checked by TLC (20% ethyl acetate/80% hexane). The reaction mixture was allowed to warm to a room temperature overnight. The mixture was filtered through celite and the solvent was evaporated to dryness to afford purple crude as purple solid which was then purified by column chromatography (20% ethyl acetate/80% hexane) to afford **6** as a purple microcrystalline solid (400 mg, 80 %). UV/Vis ($CHCl_3$) λ_{max} (log ε) 671 (4.62), 448 (5.27), 262 (3.92), 225 (4.09), 213 (4.18), 204 (4.24) nm; FTIR (neat) ν_{max} 3299, 2956, 2903, 1695, 1591, 1472, 1424, 1392, 1362, 1292, 1246, 1211, 1123, 986, 919, 899, 879, 798, 715 cm^{-1}; ^1H NMR (400 MHz, $CDCl_3$) δ 8.78-8.91 (m, 5H, β-pyrrolic H), 8.61-8.68 (m, 2H, β-pyrrolic H), 8.29 (s, 1H, ArH), 8.13-8.22 (m, 2H, ArH), 7.93-8.11 (m, 4H, ArH), 7.87 (s, 2H, ArH), 7.75-7.83 (m, 3H, ArH), 7.24 (m, 1H, ArH), 6.84 (s, 1H, ArH), 6.32 (s, 1H, ArH), 4.54-4.74 (m, 3H), 4.16-4.31 (m, 3H), 4.06 (d, *J* = 7.4 Hz, 1H), 3.80-3.92 (m, 1H), 3.71 (d, *J* = 7.4 Hz, 1H), 1.45-1.66 (m, 72H, *tert*-butyl H),

2.20 (s, 3H, CH_3), −2.75 (br s, 2H, NH); ^{13}C NMR (100 MHz, $CDCl_3$) δ 191.3, 152.9, 149.8, 149.5, 148.6, 148.1, 141.5, 141.3, 141.1, 139.8, 133.5, 131.5, 130.8, 130.3, 129.7, 129.6, 129.4, 129.3,129.2, 129.1, 128.9, 128.2, 127.8, 126.8, 124.2, 121.8, 121.6, 121.5, 120.9, 120.3, 119.2, 118.8, 67.5, 55.6, 55.5, 35.2, 35.2, 35.1, 35.0, 31.9, 31.8, 31.7, 31.6, 31.4, 31.3, 29.7, 29.4, 22.7, 22.6, 17.6; HRMS (ESI) *m/z*: 1249.8370 $[M+H]^+$ (calcd for $C_{87}H_{105}N_6O$, 1249.8350).

Ester functionalised zinc(II)porphyrin Tröger's base 7

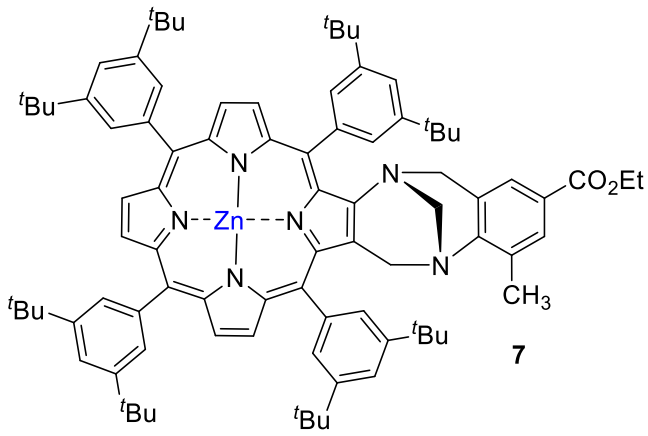

7

Ester functionalised zinc(II)porphyrin Tröger's base **7**. Starting with **2** (50 mg, 0.04 mmol) and porphyrin TB, **7** (51 mg, 98%) was obtained as a purple microcrystalline solid. UV/Vis ($CHCl_3$) λ_{max} (log ε) 551 (4.11), 423 (5.21), 240 (4.41), 238 (4.38) nm; FTIR (neat) ν_{max} 2957, 2359, 1715, 1591, 1474, 1425, 1391, 1362, 1302, 1246, 1199, 1136, 1030, 917, 900, 879, 797, 714 cm^{-1}; ^1H NMR (400 MHz, $CDCl_3$) δ 8.99 (d, *J* = 4.7 Hz, 1H, β-pyrrolic H), 8.91-8.97 (m, 4H, β-pyrrolic H), 8.70 (d, *J* = 4.7 Hz, 1H, β-pyrrolic H), 8.24 (t, *J* = 1.6 Hz, 1H, ArH), 8.16 (t, *J* = 1.7 Hz, 1H, ArH), 8.15 (t, *J* = 1.7 Hz, 1H, ArH), 8.08 (t, *J* = 1.6 Hz, 1H, ArH), 8.06 (t, *J* = 1.7 Hz, 1H, ArH), 8.04 (t, *J* = 1.7 Hz, 1H, ArH), 7.90 (t, *J* = 1.7 Hz, 1H, ArH), 7.87 (t, *J* = 1.8 Hz, 1H, ArH), 7.85 (t, *J* = 1.7 Hz, 1H, ArH), 7.79 (t, *J* = 1.8 Hz, 1H, ArH), 7.76-7.78 (m, 2H, ArH), 7.55 (d, *J* = 1.4 Hz, 1H, ArH), 7.13 (d, *J* = 1.4 Hz, 1H,

ArH), 4.75 (m, 1H), 4.64 (m, 1H), 4.07-4.28 (m, 4H), 3.92 (d, J = 17.5 Hz, 1H, ArH), 3.75 (d, J = 17.5 Hz, 1H, ArH), 2.24 (s, 3H, CH_3), 1.47-1.67 (m, 72H, *tert*-butyl H); ^{13}C NMR (100 MHz, $CDCl_3$) δ 166.4, 152.5, 151.7, 151.3, 151.2, 150.2, 150.1, 149.6, 149.5, 149.3, 148.5, 148.4, 148.3, 147.7, 145.5, 142.1, 142.0, 141.9, 141.8, 140.5, 132.7, 132.3, 131.8, 131.7, 130.6, 130.5, 130.1, 129.6, 129.5, 128.9, 128.7, 127.6, 126.1, 124.9, 123.0, 122.7, 121.5, 120.8, 120.2, 120.0, 119.8, 67.6, 60.4, 55.5, 54.0, 35.3, 35.2, 35.1, 35.08, 35.06, 31.81, 31.79, 31.75, 31.71, 31.5, 29.7, 17.6, 14.1; HRMS (ESI) *m/z*: 1355.7764 $[M+H]^+$ (calcd for $C_{89}H_{107}N_6O_2Zn$, 1355.7747).

Alcohol functionalised zinc(II)porphyrin Tröger's base 8

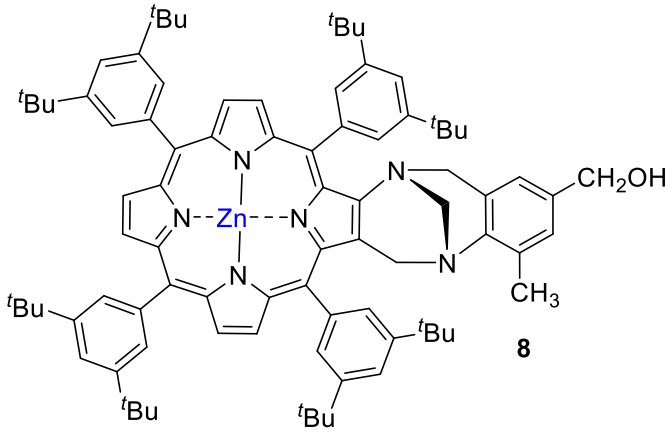

Alcohol functionalised zinc(II)porphyrin Tröger's base **8**. Starting with **5** (20 mg, 0.02 mmol) and porphyrin TB **8** (19 mg, 91%) was obtained as a purple microcrystalline solid. UV/Vis ($CHCl_3$) λ_{max} (log ε) 551 (4.27), 423 (5.42), 240 (4.44), 238 (4.46) nm; FTIR (neat) ν_{max} 3645, 2958, 1591, 1475, 1425, 1391, 1361, 1292, 1247, 1207, 1128, 1069, 1004, 936, 899, 879, 821, 795, 714 cm^{-1}; ^{1}H NMR (400 MHz, $CDCl_3$) δ 9.02 (d, J = 4.7 Hz, 1H, β-pyrrolic H), 8.94-9.00 (m, 4H, β-pyrrolic H), 8.73 (d, J = 4.7 Hz, 1H, β-pyrrolic H), 8.24 (t, J = 1.6 Hz, 1H, ArH), 8.19 (t, J = 1.7 Hz, 1H, ArH), 8.11 (t, J = 1.6 Hz, 1H, ArH), 8.08 (t, J = 1.7 Hz, 1H, ArH), 8.06 (t, J = 1.7 Hz, 1H, ArH), 7.87-7.92 (m, 3H, ArH),

7.82 (t, *J* = 1.8 Hz, 1H, ArH), 7.80 (t, *J* = 1.8 Hz, 1H, ArH), 7.78 (t, *J* = 1.8 Hz, 1H, ArH), 6.78 (s, 1H, ArH), 6.33 (s, 1H, ArH), 4.73 (m, 1H), 4.65 (m, 1H), 3.99-4.33 (m, 5H), 3.91 (d, *J* = 17.6 Hz, 1H), 3.73 (d, *J* = 17.6 Hz, 1H), 2.23 (s ,3H), 1.50-1.68 (m, 72H, *tert*-butyl H); ^{13}C NMR (100 MHz, $CDCl_3$) δ 151.7, 150.6, 150.2, 149.1, 148.9, 148.5, 148.4, 148.3, 148.1, 147.4, 147.2, 146.5, 145.1, 144.8, 141.1, 140.9, 140.8, 139.4, 131.8, 131.1, 130.7, 130.6, 130.5, 129.7, 129.3, 129.1, 128.7, 128.6, 128.5, ;128.4, 127.9, 127.8, 126.5, 123.1, 122.0, 121.8, 121.5, 120.3, 119.6, 119.1, 118.8, 118.7, 66.7, 63.8, 54.7, 52.9, 35.3, 34.1, 34.05, 34.04, 34.0, 33.98, 33.95, 33.77, 30.88, 30.75, 30.73, 30.68, 30.63, 30.4, 30.2, 28.7, 28.6, 28.3, 27.8, 21.9, 21.6, 16.4, 13.1, 12.9; HRMS (ESI) *m/z*: 1313.7659 $[M+H]^+$ (calcd for $C_{87}H_{105}N_6OZn$, 1313.7641).

Aldehyde functionalised zinc(II)porphyrin Tröger's base 9

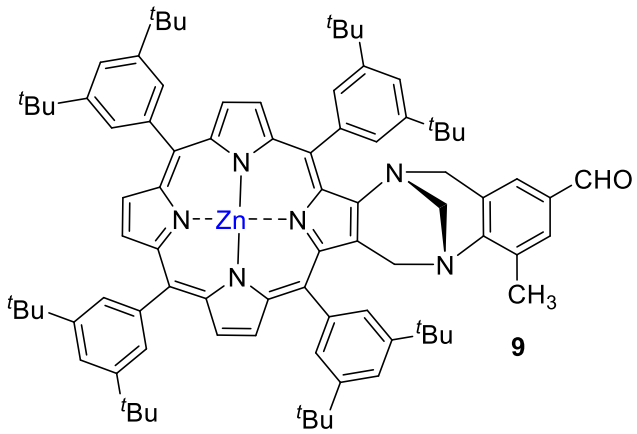

9

Aldehyde functionalised zinc(II)porphyrin Tröger's base **9**. Starting with **6** (20 mg, 0.02) and porphyrin TB **9** (20 mg, 95%) was obtained as a purple microcrystalline solid. UV/Vis ($CHCl_3$) λ_{max} (log ε) 552 (4.29), 424 (5.42), 240 (4.56), 238 (4.55) nm; FTIR (neat) ν_{max} 2956, 2868, 1695, 1592, 1475, 1426, 1391, 1361, 1290, 1246, 1210, 1068, 1004, 937, 922, 898, 879, 823, 795, 714 cm^{-1}; ^{1}H NMR (400 MHz, $CDCl_3$) δ 9.59 (s, 1H, CHO), 8.98 (d, *J* = 4.7 Hz, 1H, β-pyrrolic H), 8.91-8.96 (m, 4H, β-pyrrolic H), 8.69 (d, *J* = 4.7 Hz, 1H, β-

pyrrolic H), 8.22 (s, 1H, ArH), 8.15 (s, 2H, ArH), 8.03-8.08 (m, 2H, ArH), 8.02 (s, 1H, ArH), 7.90 (app s, 1H, ArH), 7.87 (t, J = 1.6 Hz, 1H, ArH), 7.83 (app s, 1H, ArH), 7.75-7.80 (m, 3H, ArH), 7.40 (s, 1H, ArH), 6.92 (s, 1H, ArH), 4.78 (m, 1H), 4.66 (m, 1H), 4.18-4.29 (m, 2H), 3.92 (d, J = 17.5 Hz, 1H), 3.78 (d, J = 17.5 Hz, 1H), 2.26 (s, 3H), 1.45-1.66 (m, 72H, *tert*-butyl H); ^{13}C NMR (100 MHz, $CDCl_3$) δ 191.4, 153.2, 152.3, 151.7, 151.2, 150.2, 150.1, 149.7, 149.6, 149.5, 149.3, 148.5, 148.4, 148.3, 147.7, 145.3, 141.9, 141.8, 141.7, 140.4, 133.6, 132.3, 131.8, 131.7, 131.5, 130.6, 130.2, 129.9, 129.6, 129.5, 129.4, 129.3, 128.6, 127.6, 127.0, 123.1, 122.7, 121.5, 120.7, 120.2, 120.1, 119.7, 67.5, 55.6, 53.9, 35.20, 35.12, 35.07, 35.05, 35.02, 34.99, 31.8, 31.77, 31.71, 31.66, 31.5, 31.3, 29.7, 29.4, 22.7, 17.7; HRMS (ESI) *m/z*: 1311.7514 $[M+H]^+$ (calcd for $C_{87}H_{103}N_6OZn$, 1311.7485).

Free-base porphyrin Tröger's base-fullerene-C_{60} dyad 10

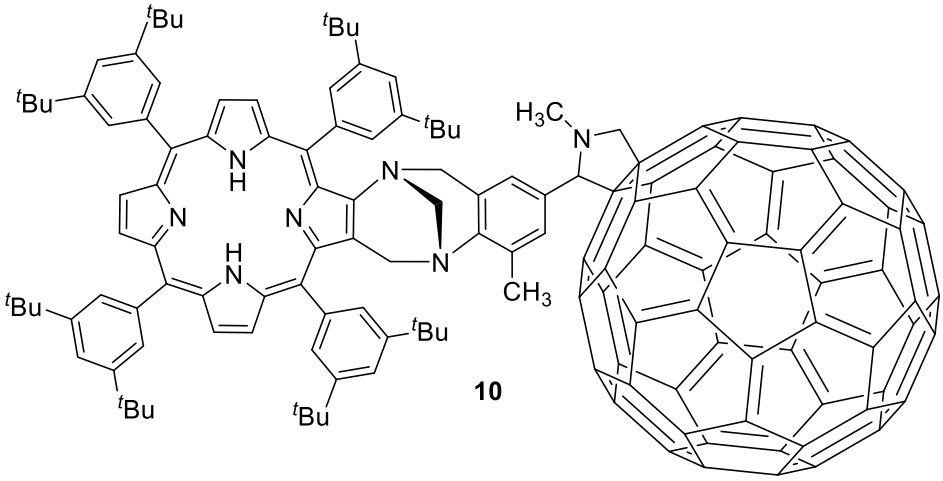

10

Free-base porphyrin Tröger's base fullerene-C_{60} dyad **10**. A solution of C_{60} (22 mg, 0.03 mmol), porphyrin TB **6** (40 mg, 0.03 mmol), and *N*-methylglycne (11 mg, 0.13 mol) in toluene (200 mL) was refluxed under an argon atmosphere in the dark for 15 h. The reaction mixture was allowed to cool to room temperature and then solvent was removed under reduced pressure. Flash column chromatography on silica (90% toluene/10% ethyl

acetate) was performed to afford free-base porphyrin TB-C_{60} **10** as a dark brown solid. (24mg, 37%). UV/Vis ($CHCl_3$) λ_{max} (log ε) 668 (4.46), 447 (5.21), 256 (5.03), 234 (4.93), 205 (4.77) nm; FTIR (neat) ν_{max} 2961, 2359, 1591, 1461, 1361, 1259, 1204, 1081, 1025, 922, 877, 797, 714 cm^{-1}; ^1H NMR (400 MHz, $CDCl_3$) δ 8.90 (d, 2H, *J* = 4.6 Hz, β-pyrrolic H), 8.56 (d, 2H, *J* = 4.6 Hz, β-pyrolic H), 8.76 (d, 1H, *J* = 4.6 Hz, β-pyrrolic H), 8.66 (d, 1H, *J* = 4.4 Hz, β-pyrrolic H), 8.27-8.40 (m, 2H, ArH), 8.16-8.26 (m, 2H, ArH), 8.09 (br s, 1H, ArH), 7.90-8.04 (m, 2H, ArH), 7.81 (t, *J* = 1.8 Hz, ArH), 7.76 (t, *J* = 1.8 Hz, ArH), 7.71-7.76 (m, 2H, ArH), 7.21 (br s, 1H, ArH), 6.87 (d, *J* = 17.5 Hz, 1H, ArH), 4.68 (d, *J* = 11.9 Hz, 1H,) 4.55 (d, *J* = 9.4 Hz, 1H pyrrolidine), 4.45 (d, *J* = 17.6 Hz, 1H), 4.37 (d, *J* = 12.3 Hz, 1H), 4.33 (s, 1H, pyrrolidine), 3.98 (d, *J* = 17.2 Hz, 1H), 3.86 (d, *J* = 9.4 Hz, 1H pyrrolidine), 3.79 (d, *J* = 17.2 Hz, 1H), 3.51 (d, *J* = 16.2 Hz, 1H) 2.66 (s, 3H, N-CH_3 pyrrolidine), 2.08 (s, CH_3), 1.70 (d, *J* = 13.3 Hz, 18H, *tert*-butyl H), 1.32-1.57 (m, 54H, *tert*-butyl H), −2.92 (s, br, 2H, NH); HRMS (ESI) *m/z*: 1996.88169 $[M+H]^+$ (calcd for $C_{149}H_{110}N_7$, 1996.88226).

Zinc(II)porphyrin Tröger's base fullerene-C_{60} dyad 11

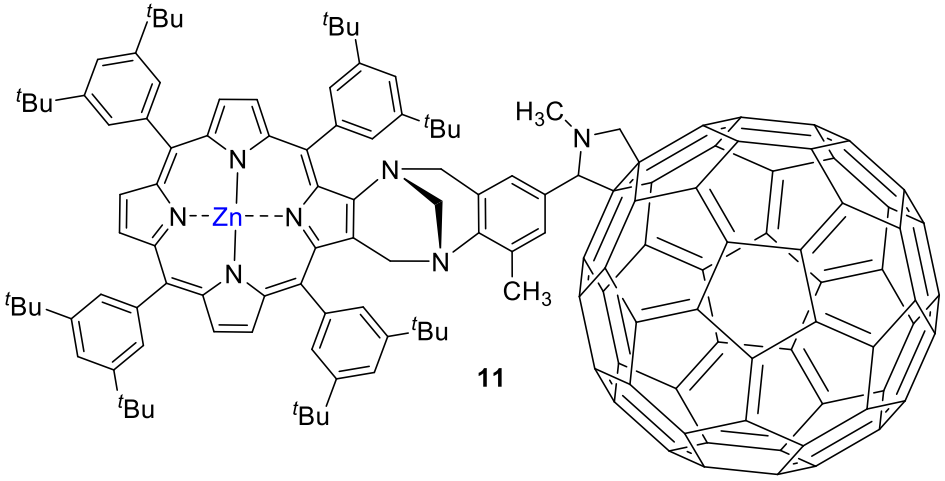

11

Zinc(II)porphyrin Tröger's base fullerene-C_{60} dyad **11**. Free-base porphyrin TB-C_{60} **10** (5 mg, 2.5 μmol) was dissolved in chloroform (5 mL) and stirred in the dark at room temperature. Zinc acetate dihydrate (2 mg, 9.1 μmol, 2.5 equiv) was separately dissolved in methanol (2 mL) and then added dropwise to the reaction mixture. After 30 min, a red colour solution was observed. The reaction progress was monitored by TLC (30% ethyl acetate/70% hexane) and upon consumption of all the starting material the reaction was stopped. Chloroform (5 mL) was added to the reaction mixture then washed with water (2 × 10 mL), dried over magnesium sulfate and filtered. The solvent was evaporated to dryness to afford zinc(II) porphyrin TB-C_{60} **11** as dark-purple solid (5 mg, 94%) that did not require further purification. UV/Vis ($CHCl_3$) λ_{max} (log ε) 555 (4.12), 433 (5.20), 257 (4.97), 235 (4.88) nm; FTIR (neat) ν_{max} 2919, 2359, 2339, 2113, 1792, 1591, 1460, 1361, 1293, 1247, 1217, 1130, 1073, 1007, 937, 899, 879, 823, 795, 714 cm^{-1}; ^1H NMR (400 MHz, $CDCl_3$) δ 8.98 (d, *J* = 4.7 Hz, 1H, β-pyrrolic H), 8.98 (t, *J* = 4.7 Hz, 3H, β-pyrrolic H), 8.88 (d, *J* = 4.7 Hz, 1H, β-pyrrolic H), 8.76 (d, *J* = 4.3 Hz, 1H, β-pyrrolic H), 8.37 (br s, 1H, ArH), 8.32 (br s, 1H, ArH), 8.11 (s, 1H, ArH), 8.03 (t, *J* = 1.7 Hz, 1H, ArH), 7.98

(br s, 1H, ArH), 7.91 (t, J = 1.7 Hz, 1H, ArH), 7.80 (t, J = 1.8 Hz, 1H, ArH), 7.76 (t, J = 1.8 Hz, 1H, ArH), 7.70-7.75 (m, 2H, ArH), 7.18 (br s, 1H, ArH), 6.88 (d, J = 9.1 Hz, 2H, ArH), 4.68 (d, J = 12.3 Hz, 1H), 4.54 (d, J = 9.5 Hz, 1H, pyrrolidine), 4.45 (d, J = 17.7 Hz, 1H) 4.38 (d, J = 12.3 Hz, 1H), 4.33 (s, 1H, pyrrolidine), 3.98 (d, J = 17.7 Hz, 1H), 3.86 (d, J = 9.5 Hz, 1H, pyrrolidine), 3.79 (d, J = 16.8 Hz, 1H), 3.58 (d, J = 16.8 Hz, 1H), 2.67 (s, 3H, CH_3, pyrrolidine), 2.09 (s, 3H, CH_3), 1.70 (d, J = 13.3 Hz, 18H, *t*-butyl H), 1.32-1.57 (m, 54H, *tert*-butyl H); HRMS (ESI) *m/z*: 2058.79508 $[M+H]^+$ (calcd for $C_{149}H_{108}N_7Zn$, 2058.79576).

UV/Vis and Fluorescence Spectra

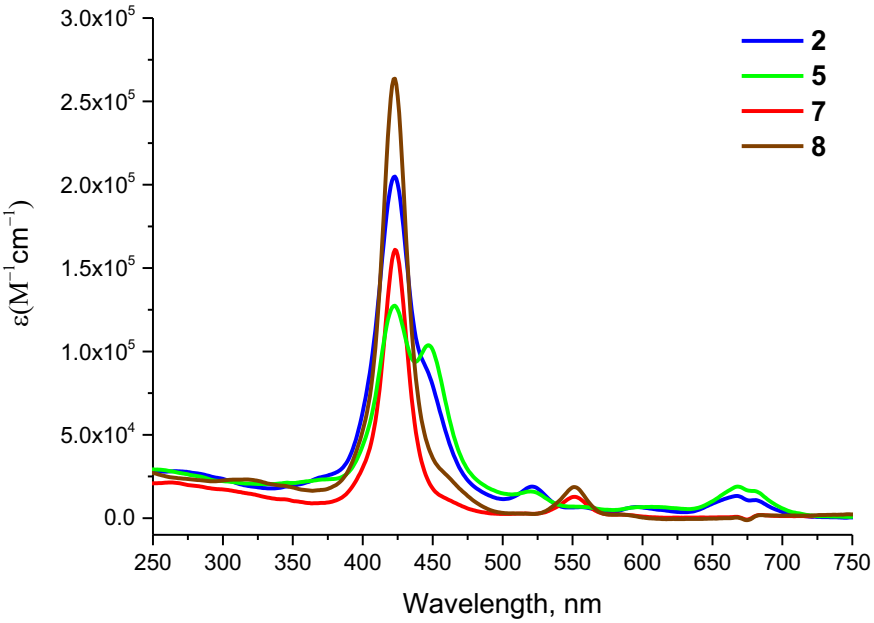

Fig. S1 UV/Vis spectra of **2** (blue), **5** (green), **7** (red), and **8** (brown). The concentration of each compound was 2.5×10^{-6} M in $CHCl_3$.

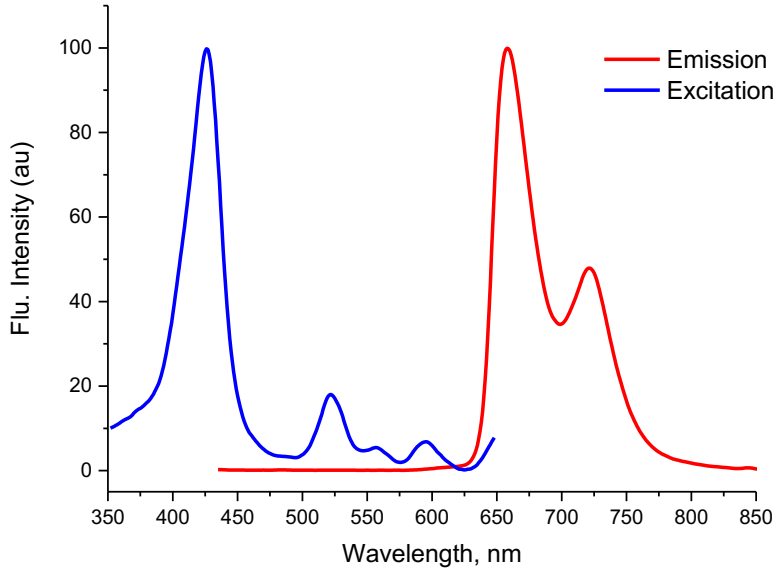

Fig. S2 Fluorescence excitation (blue) and emission (red) spectra of **2** (2.5×10^{-6} M) in $CHCl_3$.

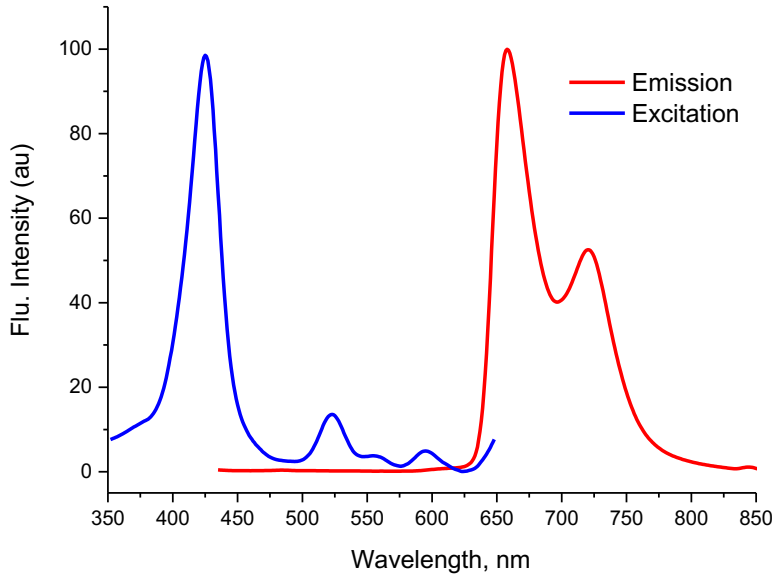

Fig. S3 Fluorescence excitation (blue) and emission (red) spectra of **5** (2.5×10^{-6} M) in $CHCl_3$.

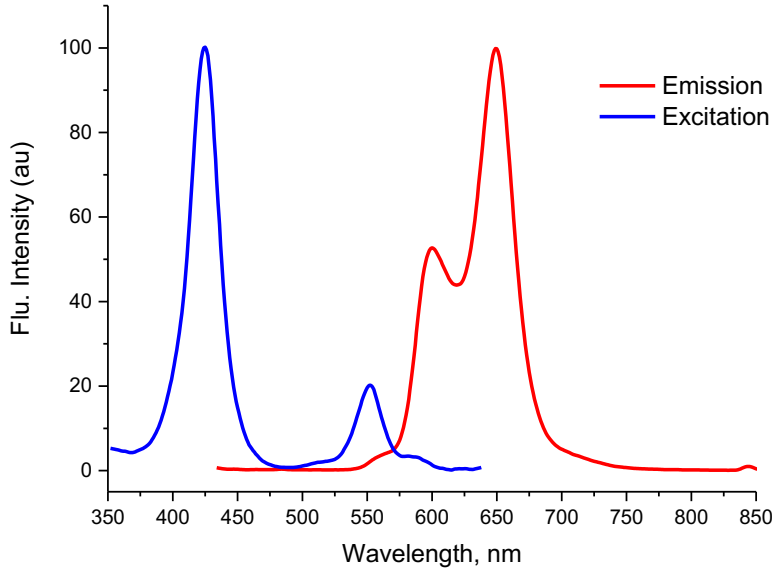

Fig. S4 Fluorescence excitation (blue) and emission (red) spectra of **7** (2.5×10^{-6} M) in $CHCl_3$.

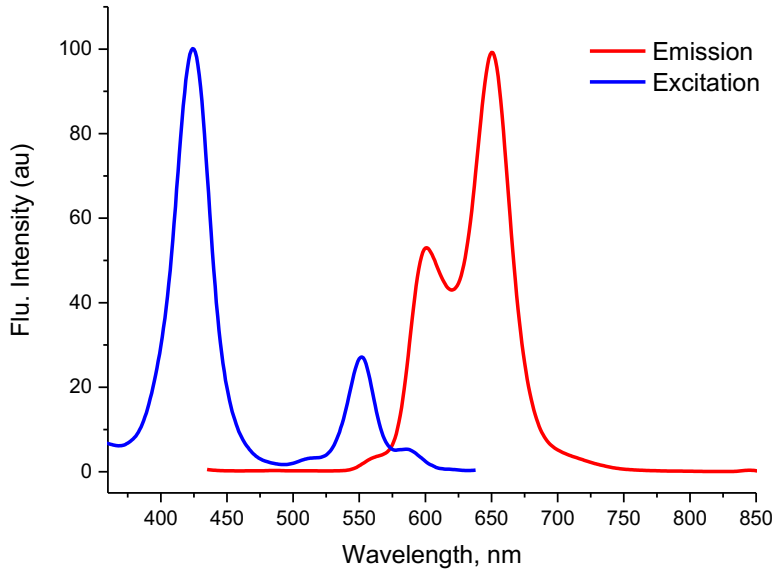

Fig. S5 Fluorescence excitation (blue) and emission (red) spectra of **8** (2.5×10^{-6} M) in $CHCl_3$.

NMR Spectra

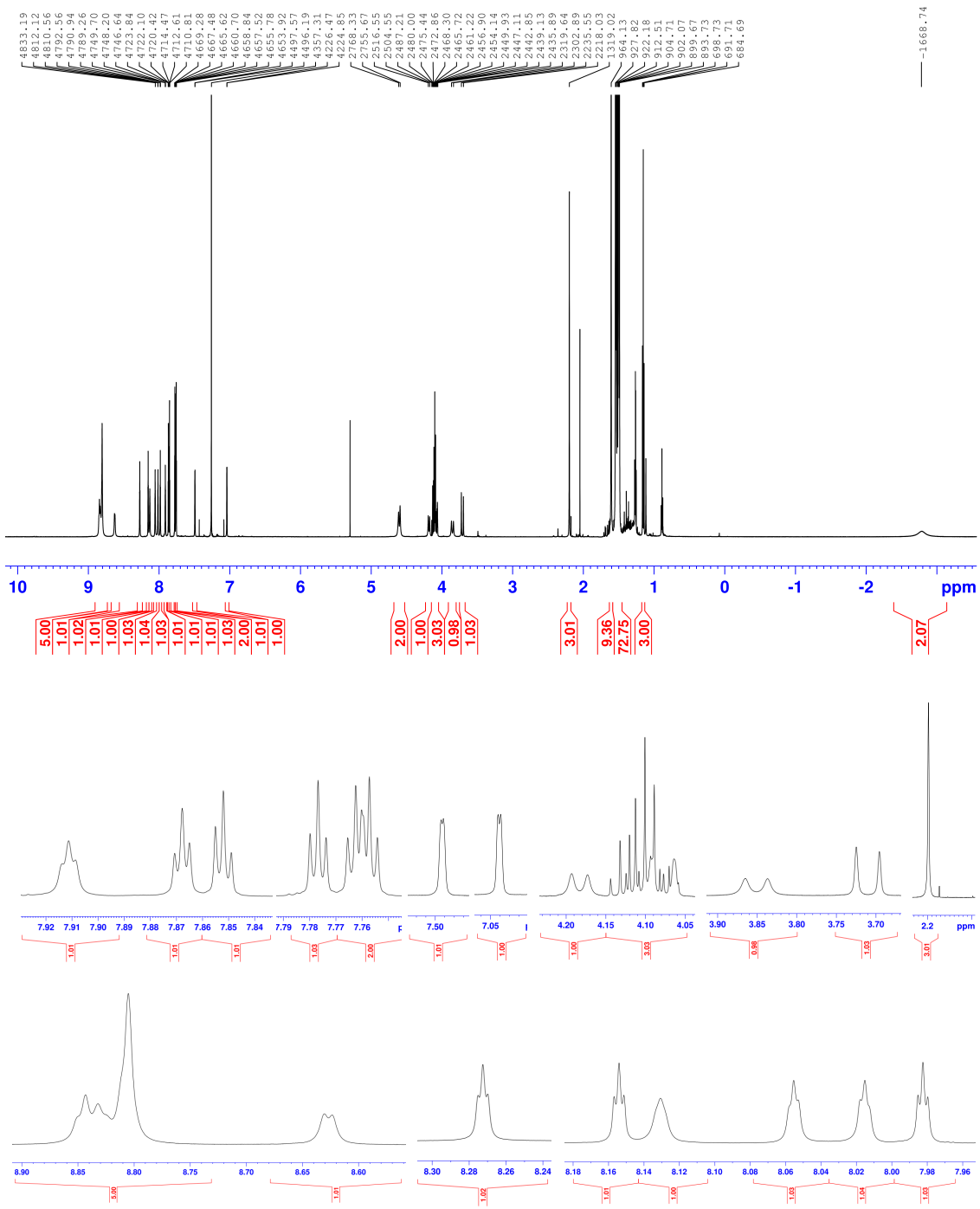

Fig. S6 ^{1}H NMR spectrum (400 MHz) of **2** in $CDCl_3$.

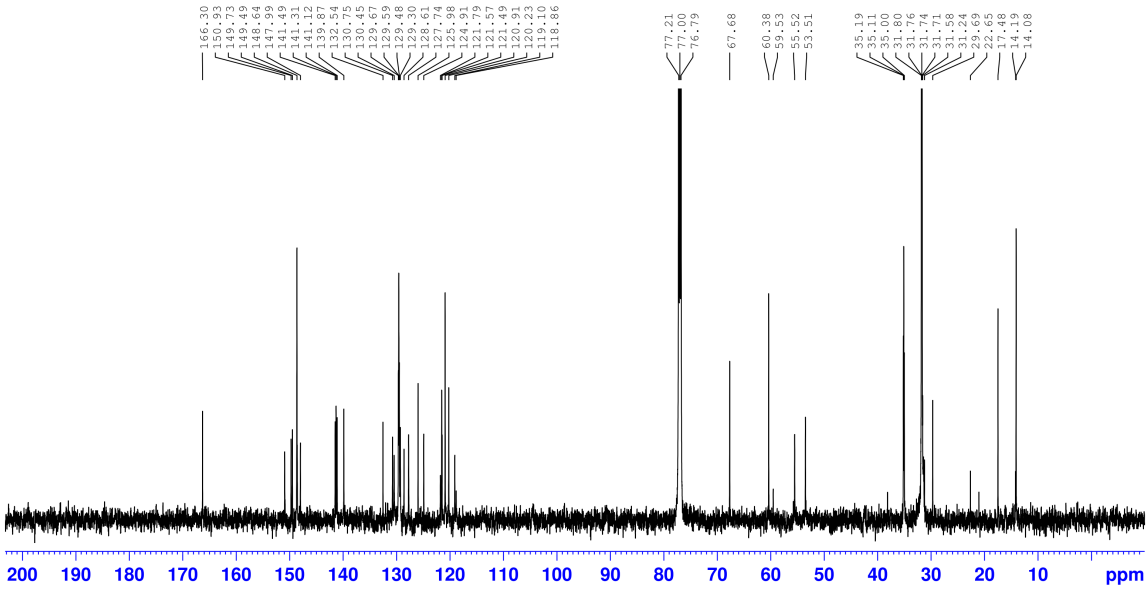

Fig. S7 ^{13}C NMR spectrum (125 MHz) of **2** in $CDCl_3$.

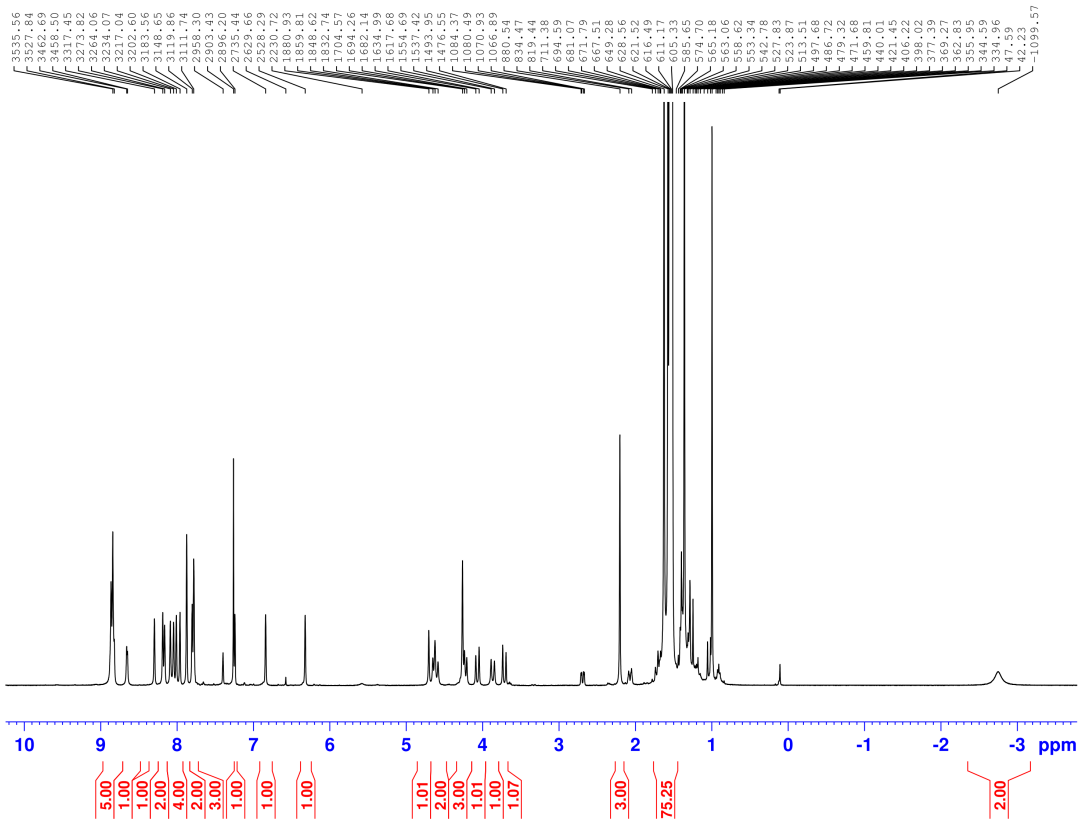

Fig. S8 ^{1}H NMR spectrum (400 MHz) of **5** in $CDCl_3$.

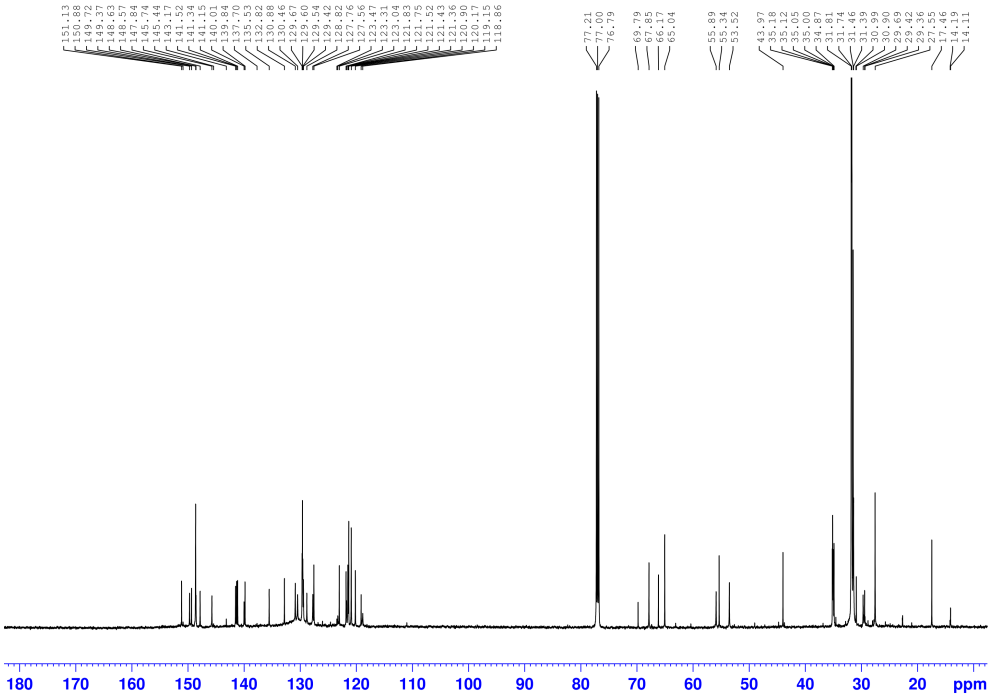

Fig. S9 ^{13}C NMR spectrum (125 MHz) of **5** in $CDCl_3$.

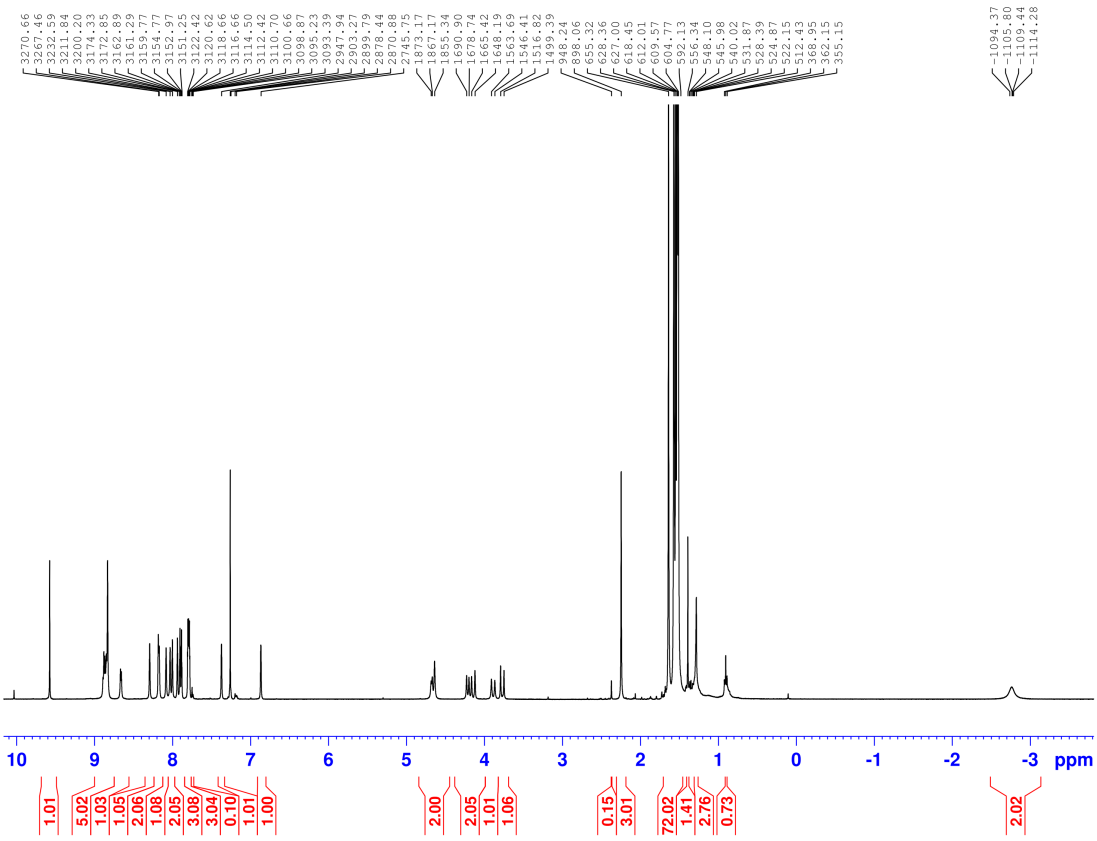

Fig. S10 ^{1}H NMR spectrum (400 MHz) of **6** in $CDCl_3$.

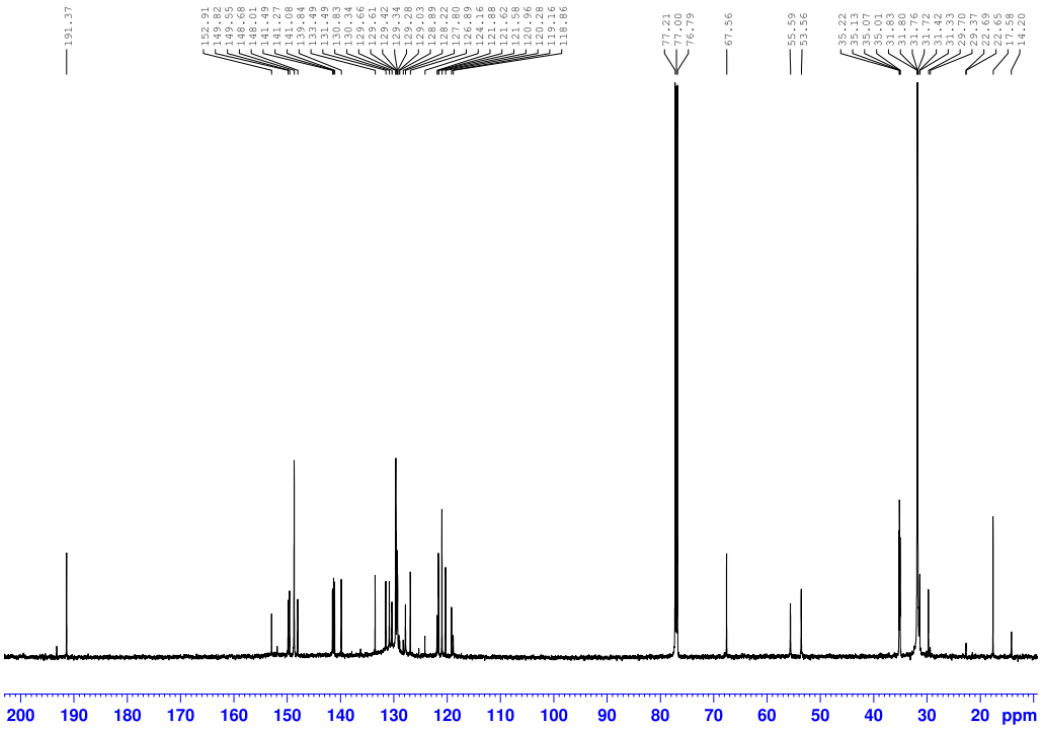

Fig. S11 ^{13}C NMR spectrum (125 MHz) of **6** in $CDCl_3$.

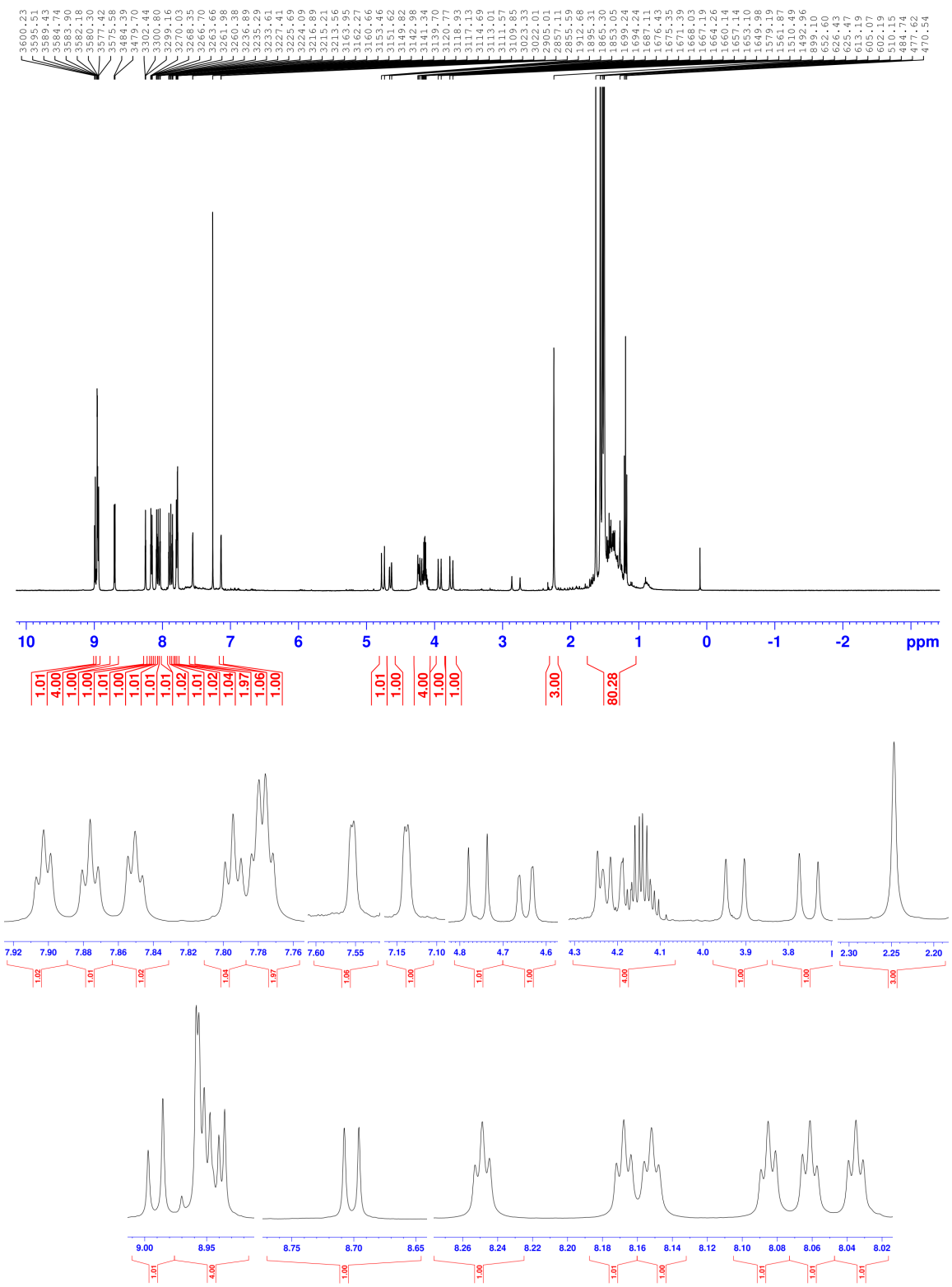

Fig. S12 ^{1}H NMR spectrum (400 MHz) of **7** in $CDCl_3$.

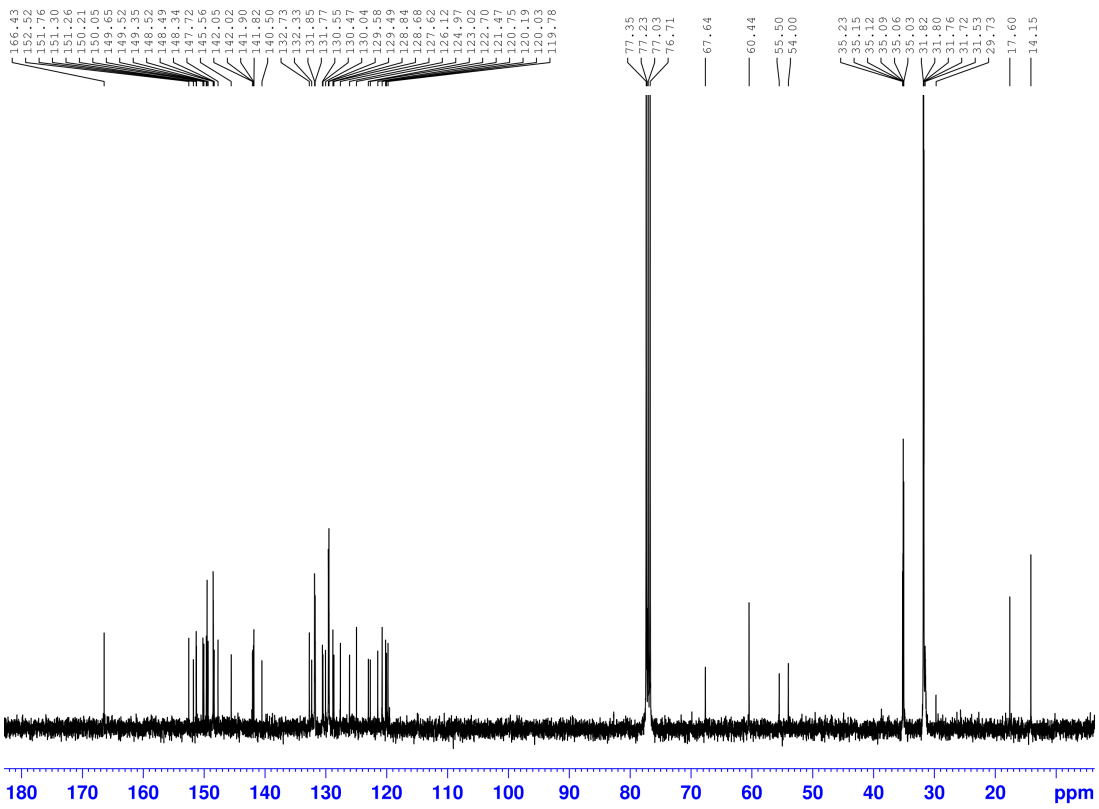

Fig. S13 ^{13}C NMR spectrum (125 MHz) of **7** in $CDCl_3$.

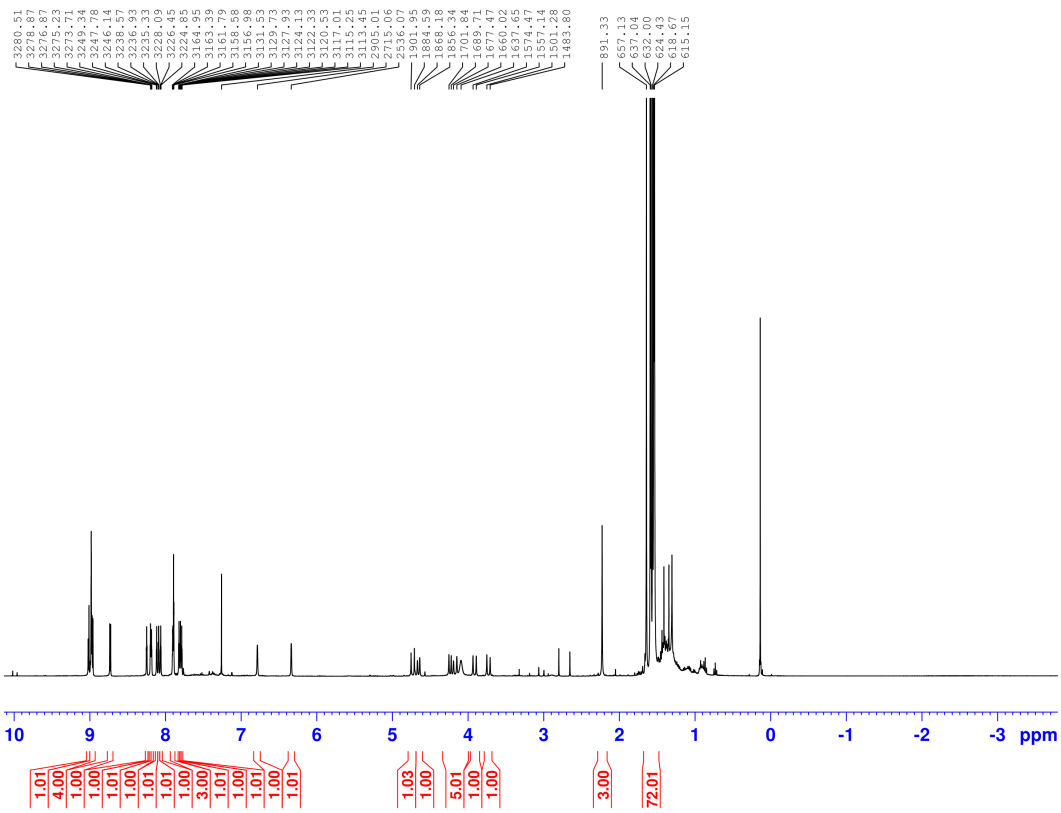

Fig. S14 ^{1}H NMR spectrum (400 MHz) of **8** in $CDCl_3$.

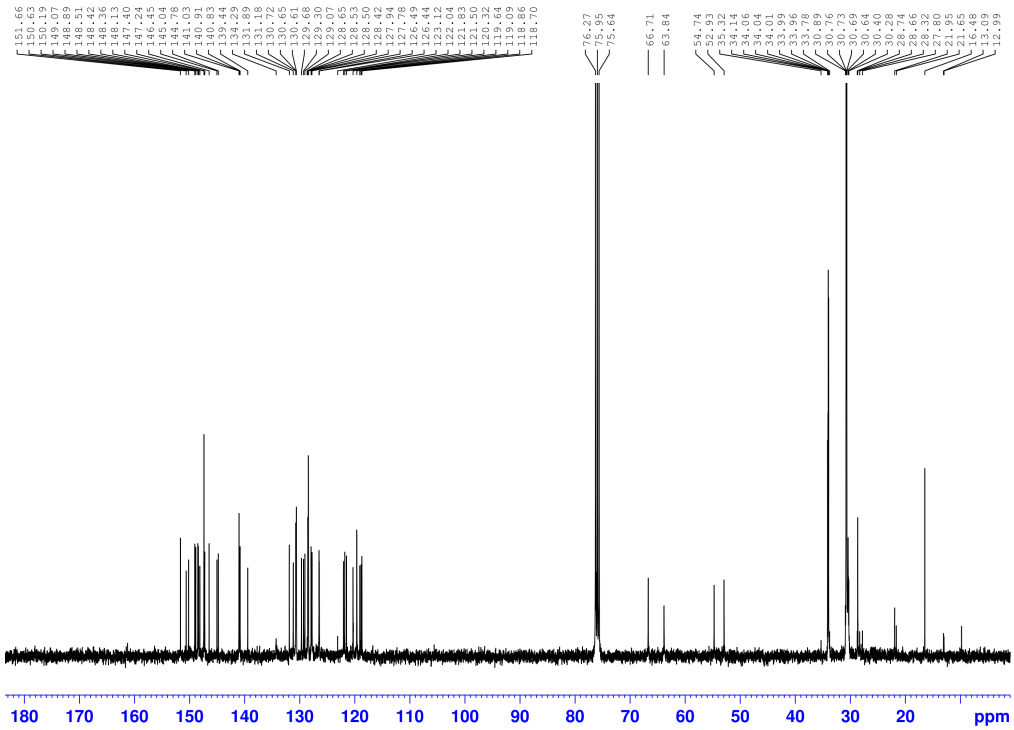

Fig. S15 ^{13}C NMR spectrum (125 MHz) of **8** in $CDCl_3$.

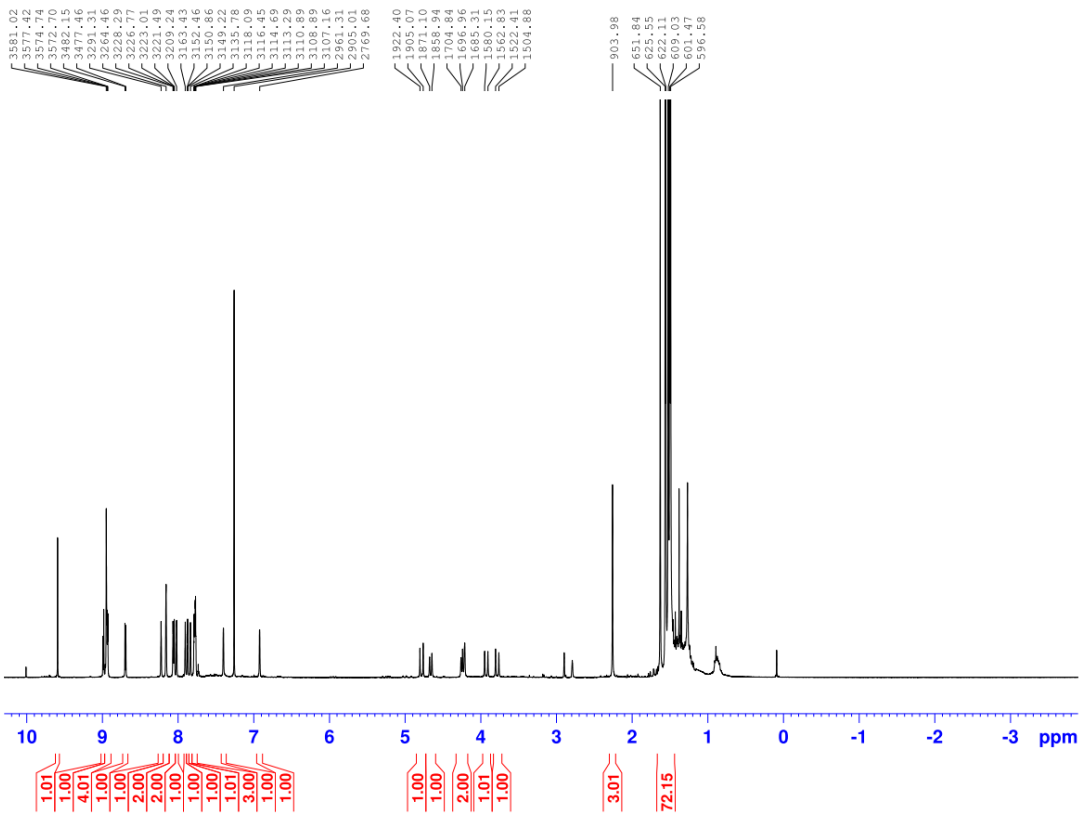

Fig. S16 ^{1}H NMR spectrum (400 MHz) of **9** in $CDCl_3$.

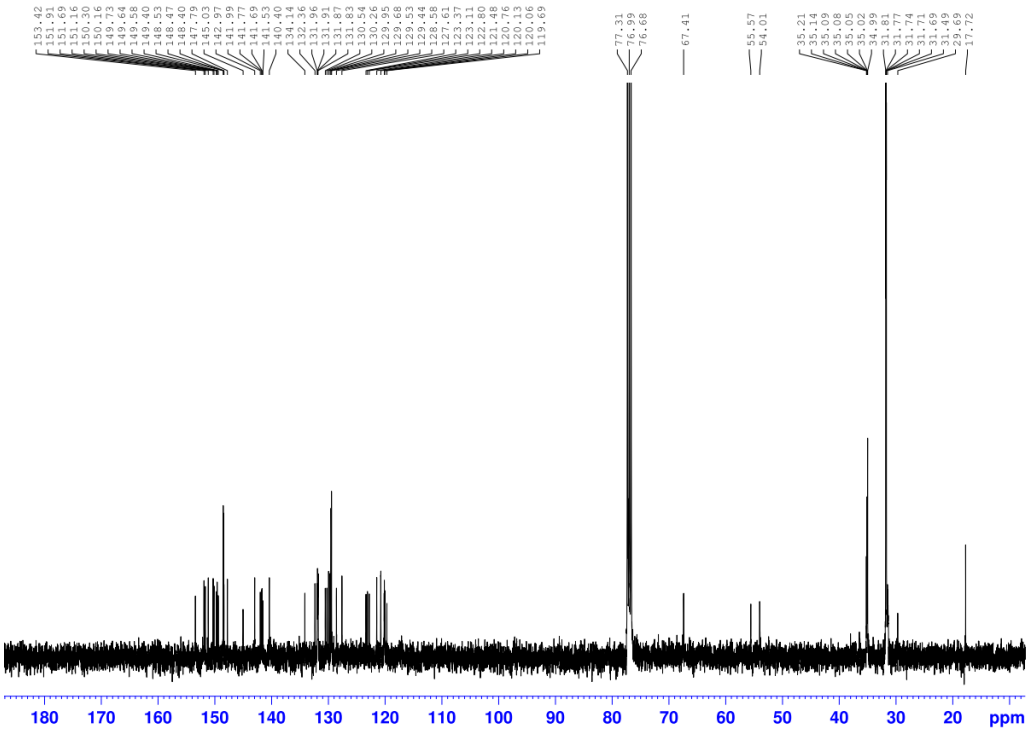

Fig. S17 ^{13}C NMR spectrum (125 MHz) of **9** in $CDCl_3$.

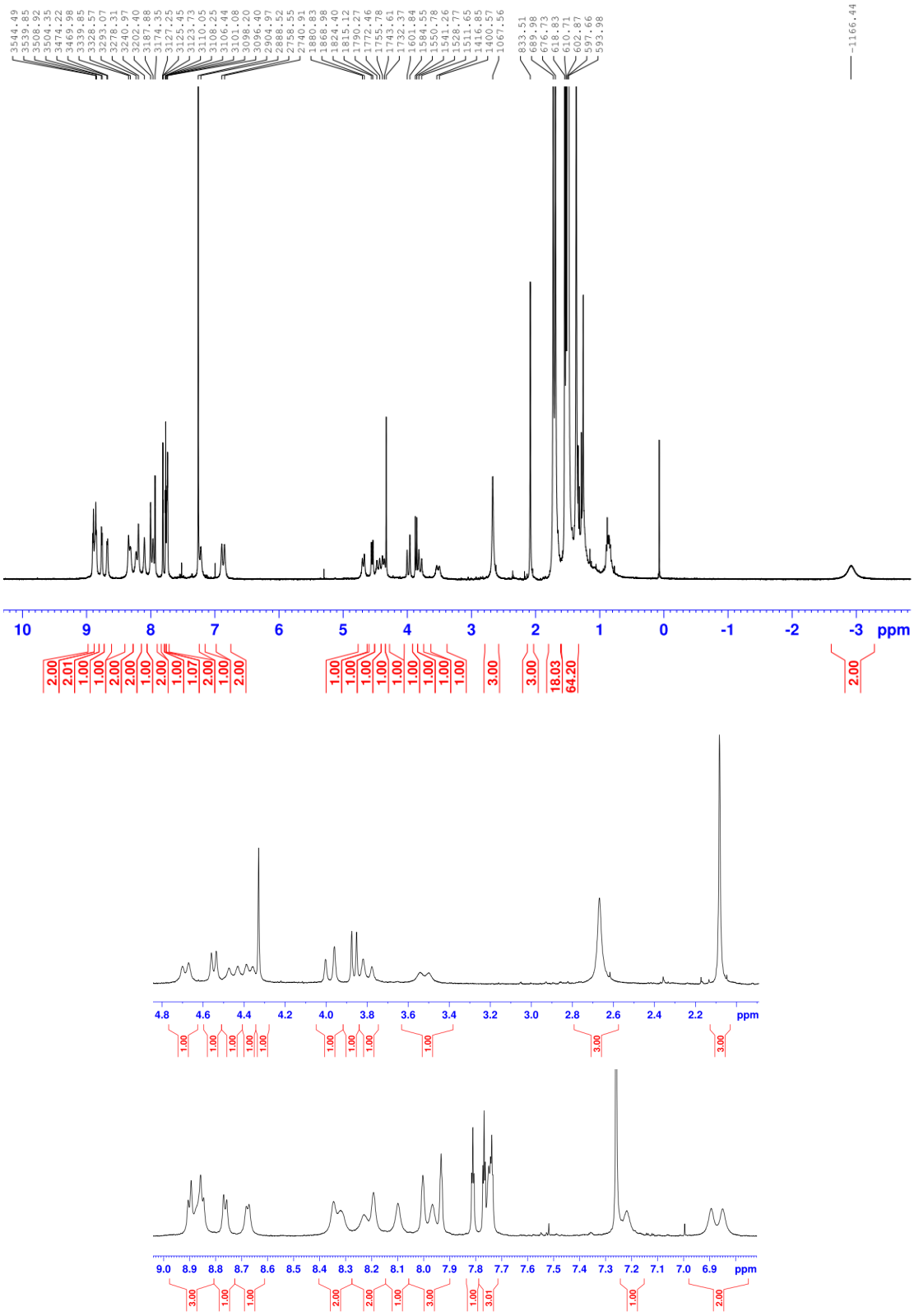

Fig. S18 ^{1}H NMR spectrum (400 MHz) of **10** in $CDCl_3$.

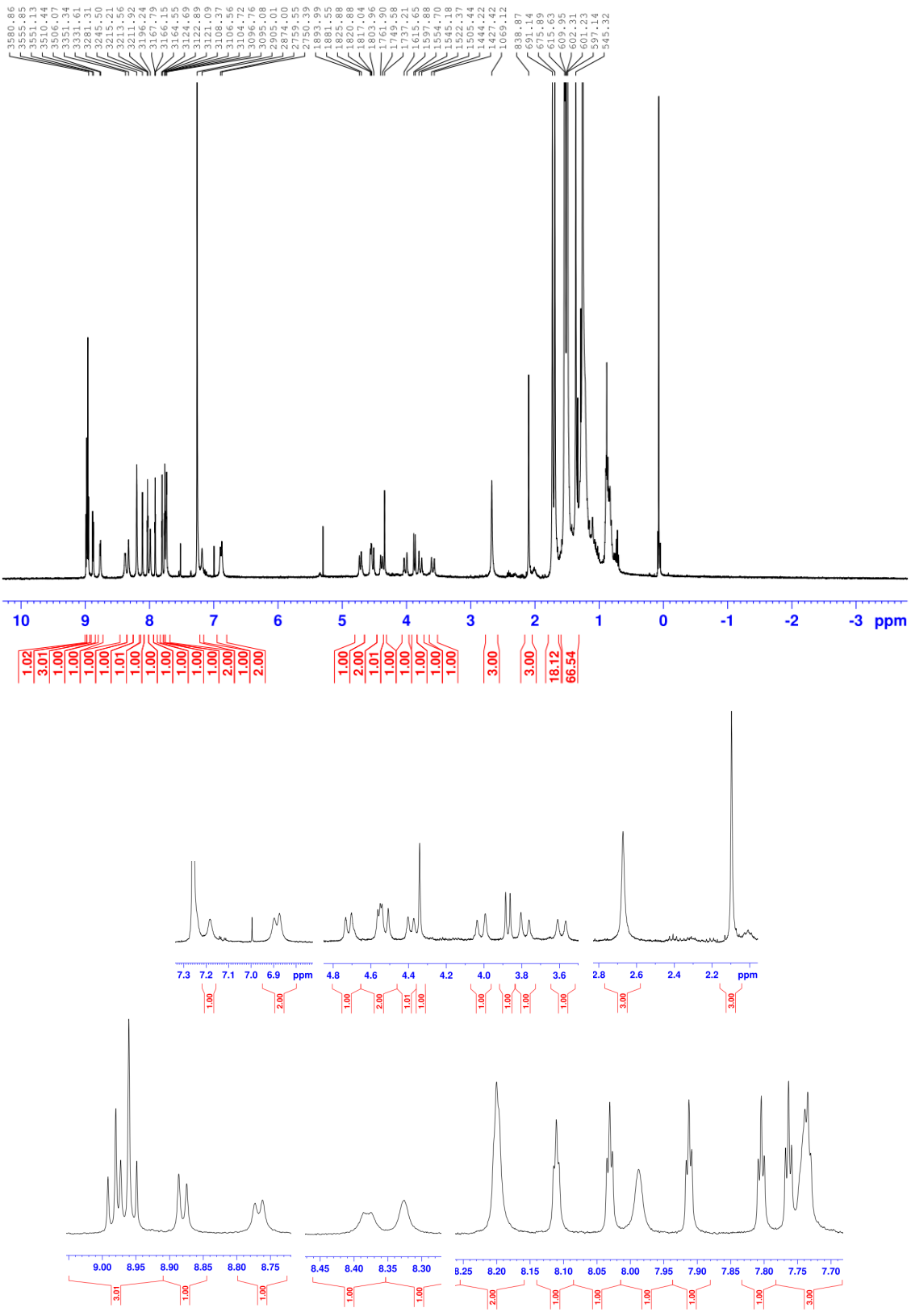

Fig. S19 ^{1}H NMR spectrum (400 MHz) of **11** in $CDCl_3$.

HRMS (ESI) Data

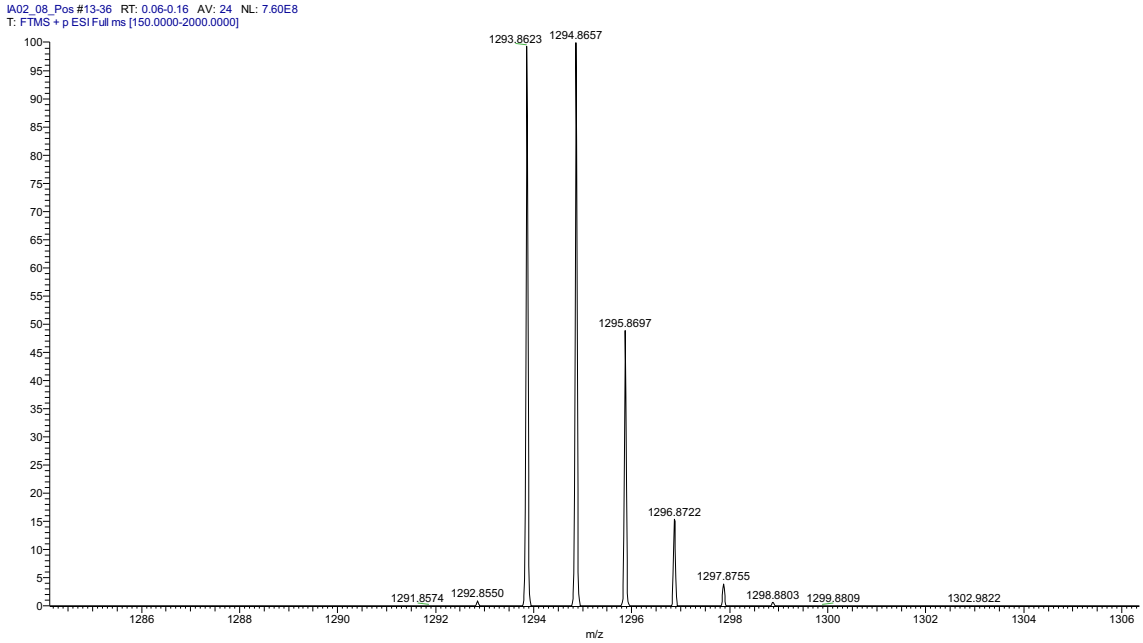

Fig. S20 High resolution mass spectrum of porphyrin TB **2**.

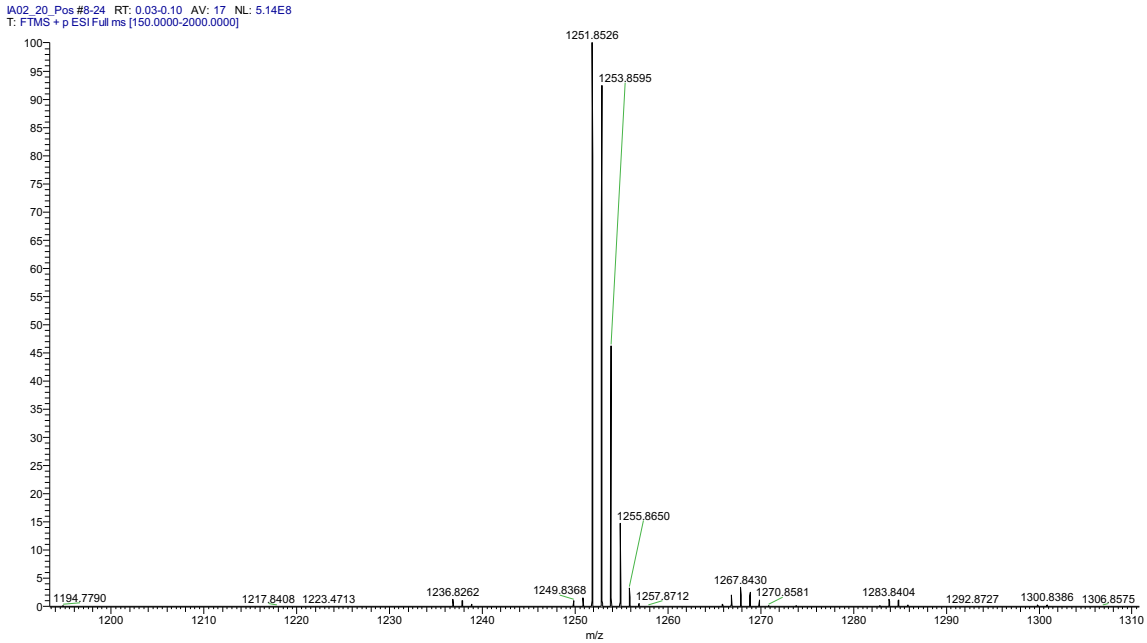

Fig. S21 High resolution mass spectrum of porphyrin TB **5**.

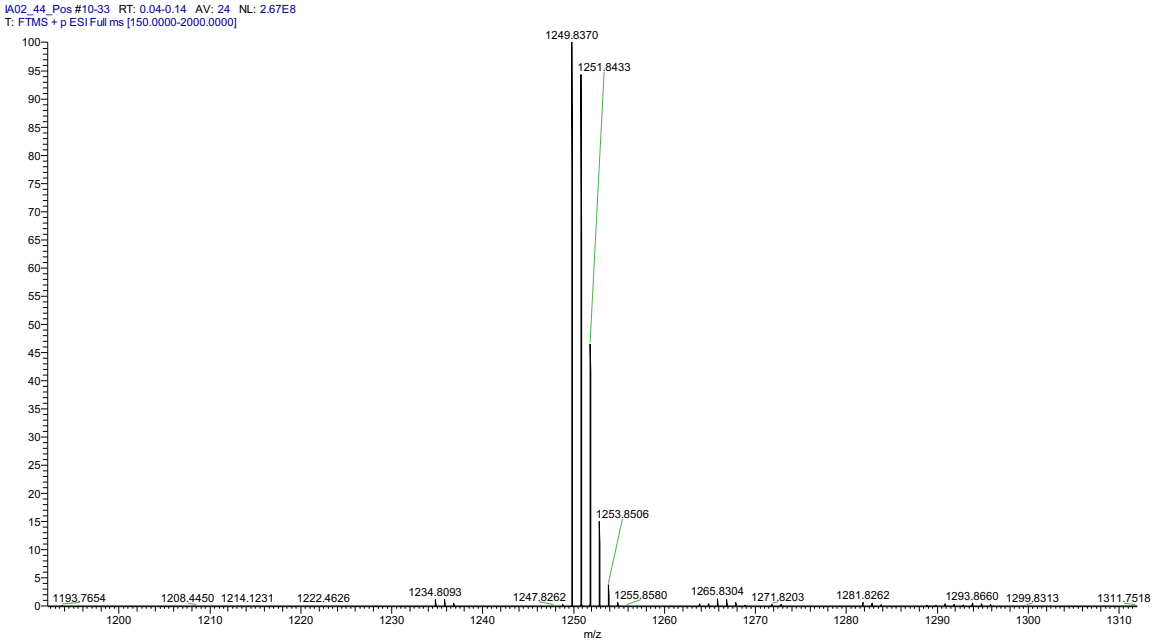

Fig. S22 High resolution mass spectrum of porphyrin TB **6**.

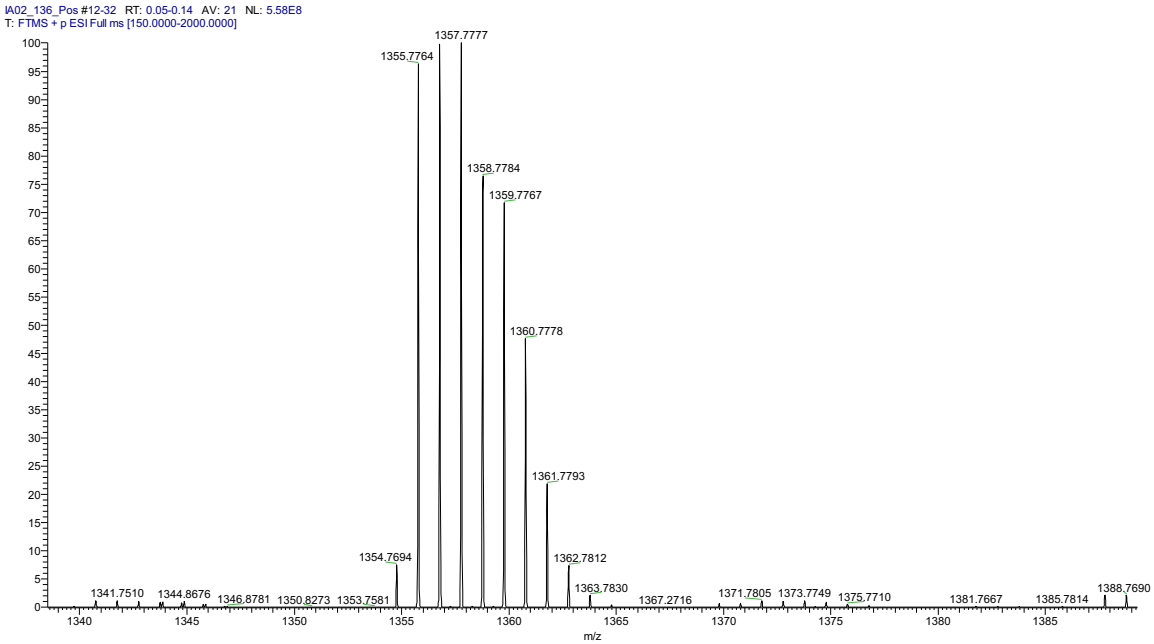

Fig. S23 High resolution mass spectrum of porphyrin TB **7**.

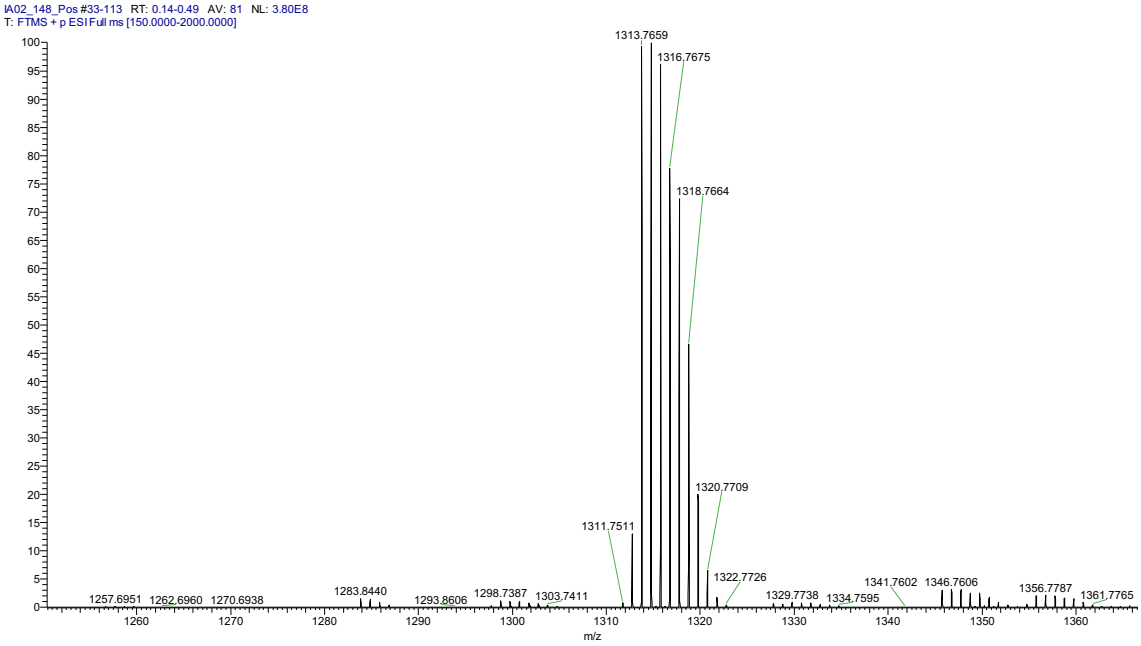

Fig. S24 High resolution mass spectrum of porphyrin TB **8**.

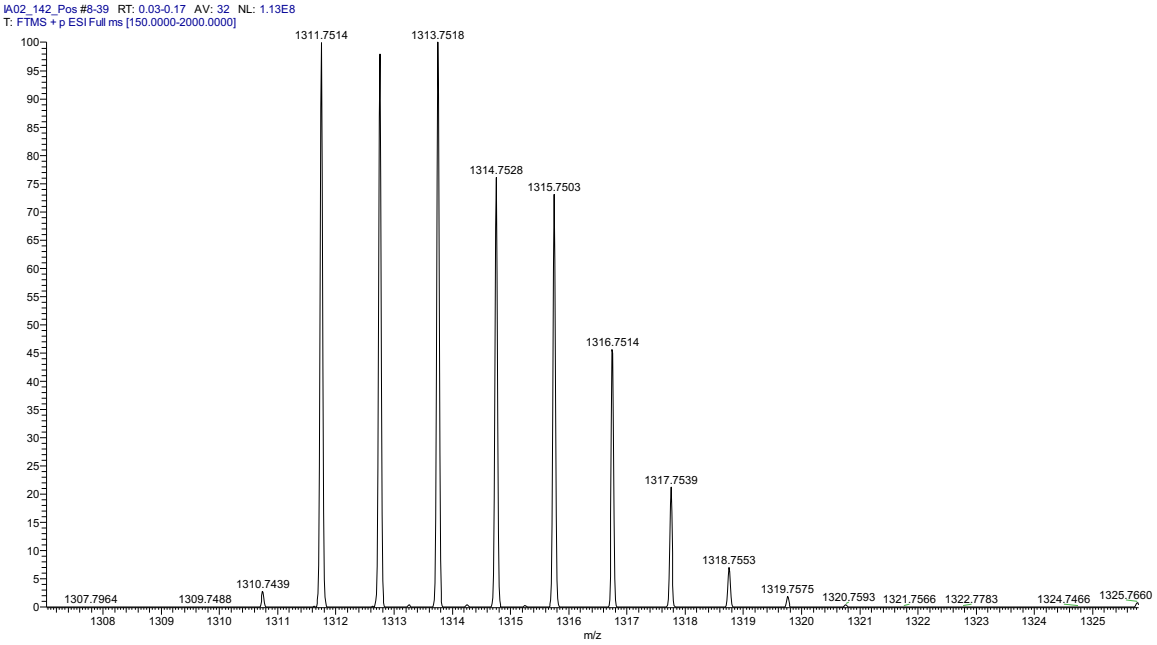

Fig. S25 High resolution mass spectrum of porphyrin TB **9**.

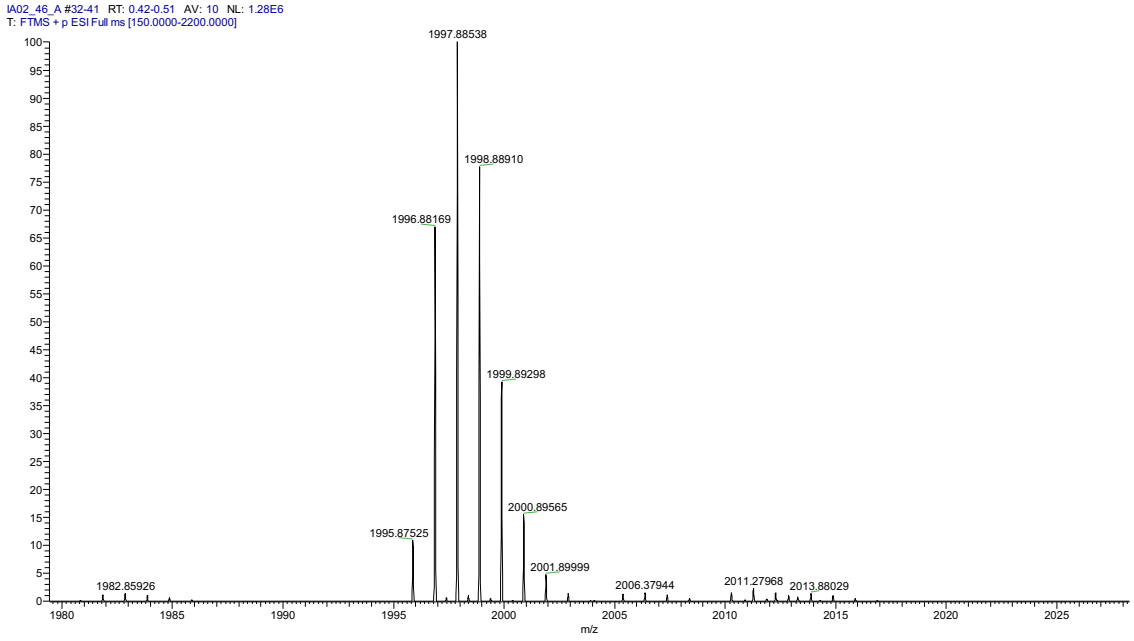

Fig. S26 High resolution mass spectrum of porphyrin-TB-fullerene dyad **10**.

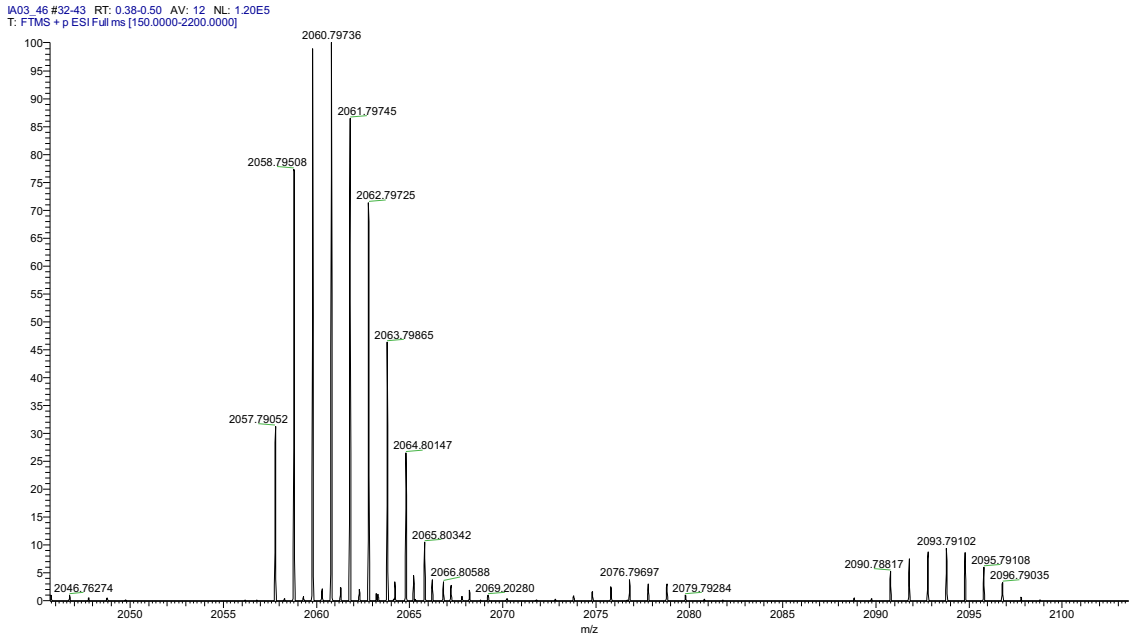

Fig. S27 High resolution mass spectrum of porphyrin-TB-fullerene dyad **11**.

FTIR Spectra

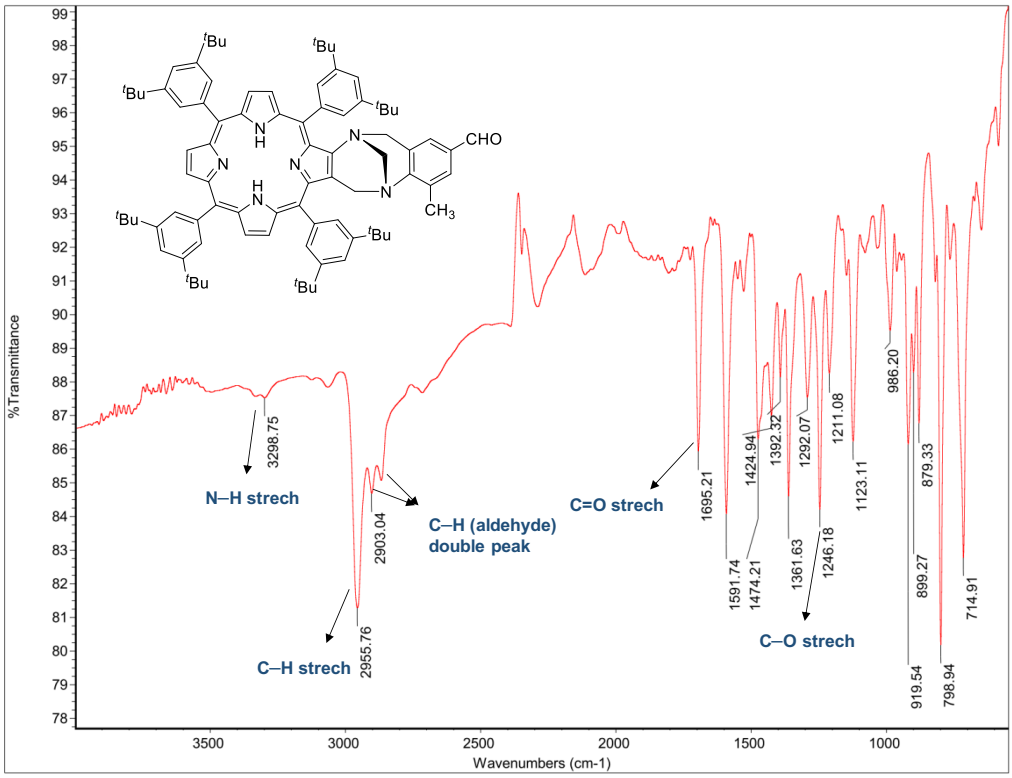

Fig. S28 Fourier transform infrared (FTIR) spectrum of porphyrin Tröger's base **6**.

DFT calculations

Molecular Modelling was performed in MOE (Molecular Operating Environment).[1] Low mode molecular dynamics with a RMSD of 0.25 Å and a 7 kcal/mol energy window was used to generate a database of conformations of all possible stereoisomers of **11**. Structures were minimized to an RMS gradient of <0.001 kcal/mol using the PFROSST forcefield and ranked by energy. The two lowest energy *endo*- and *exo*- conformers were further geometry optimized using density functional theory (DFT).

DFT calculations were carried out using Turbomole 7.1.1 (Cosmologic GmbH).[2] Structures were energy minimized (DFT//bp86/SV(P)) *in vacuo*. HOMO and LUMO orbital geometries were calculated within Turbomole.

Coordinates (XYZ format) of optimized (DFT//bp86/SV(P)) ground state structures of the exo- and endo- conformers of **11**.

Porphyrin-TB-C_{60} (**11**).xyz

```
264

C -3.462340 -3.279084 1.057698
C -3.341778 -4.483554 1.855952
H -3.807582 -5.447847 1.621547
C -2.552441 -4.170585 2.935461
H -2.267832 -4.827997 3.764465
C -2.147377 -2.783281 2.777478
N -2.735819 -2.257445 1.644318
C -4.207181 -3.190582 -0.143684
C -1.241555 -2.110454 3.641410
C -0.803985 -0.768474 3.483573
C 0.299448 -0.150493 4.207279
C 0.361384 1.161278 3.760482
C -0.714788 1.354323 2.786295
N -1.357143 0.143996 2.599107
C -1.093411 2.585011 2.188277
C -2.046777 2.711284 1.139668
C -2.438612 3.975683 0.539193
H -2.102927 4.965927 0.865403
C -3.284732 3.680587 -0.501772
H -3.759285 4.379954 -1.200154
C -3.443784 2.239406 -0.521019
N -2.694000 1.674693 0.496246
C -4.226019 1.537379 -1.470971
C -4.418122 0.133748 -1.480991
C -5.269765 -0.571265 -2.422816
H -5.825938 -0.105441 -3.245005
C -5.257775 -1.895212 -2.055978
H -5.802091 -2.727092 -2.518394
C -4.402962 -1.999447 -0.886385
N -3.893607 -0.757141 -0.565424
C -4.914157 2.338183 -2.539417
C -0.528244 3.875152 2.717147
C -0.749596 -2.889160 4.826133
C -4.858884 -4.441842 -0.659556
C 3.449340 0.216063 4.154676
C 3.448228 1.237618 3.165792
C 1.375052 -0.708304 5.121282
H 1.753905 -1.677412 4.741385
H 0.988960 -0.910524 6.145544
N 2.506765 0.247360 5.231523
C 2.401565 2.351534 3.206144
H 1.940223 2.477549 2.206061
H 2.880586 3.326869 3.457153
N 1.338499 2.086962 4.190582
C 1.969411 1.595530 5.420735
H 2.788939 2.288900 5.702311
H 1.218674 1.570831 6.237801
C 4.427341 -0.815682 4.102016
C 5.366610 -0.796342 3.055831
H 6.137431 -1.587647 3.028297
C 5.381273 0.201164 2.058674
C 4.408097 1.217925 2.139650
H 4.355799 2.007395 1.370885
C 4.484562 -1.877655 5.173189
H 3.780440 -2.718464 4.972617
H 4.195521 -1.449313 6.157382
```

H 5.502722 -2.315756 5.249476
C 6.466539 0.144836 0.979983
H 7.090427 -0.745086 1.222734
C -4.359454 -5.072901 -1.812759
H -3.481575 -4.627857 -2.308326
C -4.950827 -6.249959 -2.327241
C -6.066155 -6.770062 -1.643279
H -6.544062 -7.683796 -2.025328
C -6.603498 -6.165101 -0.480570
C -5.981401 -4.996930 -0.002747
H -6.362363 -4.482533 0.891211
C -1.135697 -2.502267 6.125928
H -1.769607 -1.606519 6.230341
C -0.748898 -3.240384 7.263773
C 0.042569 -4.392589 7.061619
H 0.346865 -4.983395 7.934293
C 0.449940 -4.819076 5.777977
C 0.047831 -4.043120 4.670290
H 0.343529 -4.334460 3.649283
C 0.279358 4.704639 1.918689
H 0.535946 4.361604 0.903038
C 0.749789 5.954910 2.386032
C 0.377741 6.345198 3.685877
H 0.726186 7.314403 4.070884
C -0.439277 5.543059 4.521203
C -0.878684 4.308494 4.016446
H -1.518414 3.649383 4.620315
C -4.462560 2.282338 -3.873309
H -3.591581 1.646250 -4.099802
C -5.093157 3.021045 -4.896543
C -6.201255 3.821183 -4.541558
H -6.704879 4.400814 -5.325346
C -6.687045 3.903473 -3.217904
C -6.023000 3.150197 -2.227095
H -6.368855 3.176240 -1.180910
C 6.805703 2.270826 -0.035301
H 7.600344 2.959604 -0.401020
H 6.002016 2.917286 0.411365
N 7.361541 1.295031 0.871217
C 7.985545 1.788533 2.081956
H 8.466665 0.945003 2.624203
H 8.779428 2.521097 1.815269
H 7.272491 2.288716 2.790151
C 3.431399 0.271861 -1.061309
C 3.679495 1.592943 -1.685047
C 4.980346 2.057123 -1.855739
C 5.942157 -0.021590 -0.517254
C 4.493589 -0.517332 -0.633495
C 2.690710 1.777405 -2.735318
C 5.344841 2.682663 -3.105638
C 6.676879 -1.188309 -1.195371
C 4.468545 -1.933529 -0.916251
C 2.294102 -0.327173 -1.738705
C 7.697351 -1.042617 -2.127983
C 7.947704 0.275698 -2.753590
C 3.034522 2.430224 -3.938513
C 6.696608 2.259397 -3.445196
C 4.394761 2.894430 -4.128127
C 5.821226 -2.349612 -1.259585
C 3.363307 -2.541472 -1.549950
C 2.247684 -1.718138 -1.971449
C 1.838063 0.595912 -2.770221
C 3.579520 -3.572916 -2.559886
C 1.765706 -2.228565 -3.247631
C 1.357188 0.104829 -3.998172
C 6.030131 -3.363900 -2.218885
C 4.764575 2.674260 -5.522583
C 2.589761 -3.378032 -3.612753
C 1.327849 -1.333837 -4.244674
C 1.727840 0.771652 -5.242975
C 1.939680 -0.254369 -6.253576
C 6.288064 1.242485 -6.861698
C 1.692740 -1.556271 -5.636157
C 2.487747 -2.665129 -5.988783
C 3.560751 -2.511042 -6.965268
C 2.944489 -3.591116 -4.959176
C 7.099330 -3.214828 -3.186836
C 5.185800 0.651642 -7.509634
C 4.886907 -3.976547 -2.887733
C 5.255140 -4.200390 -4.280777
C 3.828856 1.070763 -7.170134
C 7.410789 0.414644 -6.429058
C 7.388355 -0.975211 -6.661243
C 2.972917 -0.109139 -7.200633
C 3.798687 -1.256830 -7.560240
C 4.301181 -4.009609 -5.299217
C 4.681466 -3.341888 -6.538651
C 5.166300 -0.786355 -7.750254
C 6.624989 -3.727401 -4.464776
C 7.841485 -1.896192 -5.622919
C 6.249987 -1.584467 -7.333253
C 6.989048 -3.080602 -5.662902
C 6.003075 -2.886344 -6.715924
C 6.071973 2.269916 -5.849500
C 7.061297 2.069906 -4.795595
C 7.886278 0.932645 -5.153557
C 2.551602 1.914731 -5.212582
C 3.622338 2.065729 -6.194356
C 6.212521 1.413910 -1.202658
C 7.165617 1.371308 -2.407727
C 8.310502 0.043457 -4.142487
C 7.910599 -2.060408 -3.144594
C 8.286669 -1.393824 -4.385240
Zn -2.666413 -0.299776 1.042432
C -7.903788 4.775480 -2.830071
C -8.508074 5.517127 -4.041734
H -9.377856 6.128169 -3.713273
H -8.871757 4.812335 -4.821459
H -7.776507 6.209404 -4.513899
C -7.461970 5.834455 -1.786346
H -6.675977 6.502117 -2.204866
H -7.050569 5.364682 -0.866705
H -8.326534 6.468168 -1.484704
C -9.007330 3.875263 -2.216059
H -9.890959 4.487488 -1.924519
H -8.652426 3.342720 -1.306966

```
H -9.346151 3.106623 -2.945708
C -4.559008 2.933457 -6.344764
C -3.082784 3.407768 -6.377514
H -2.677143 3.347981 -7.413189
H -2.431417 2.786557 -5.725452
H -2.995782 4.462765 -6.034634
C -5.367406 3.810029 -7.325241
H -5.327049 4.887137 -7.050856
H -6.435482 3.503474 -7.374477
H -4.946691 3.712923 -8.350490
C -4.639378 1.463461 -6.832527
H -4.247819 1.376007 -7.871532
H -5.691053 1.099539 -6.830140
H -4.043704 0.778950 -6.190166
C -0.818839 6.049016 5.931800
C -1.590512 7.388813 5.810079
H -0.983487 8.174500 5.309670
H -2.524741 7.258222 5.220102
H -1.870436 7.770419 6.818315
C -1.714088 5.046724 6.691399
H -2.674302 4.863683 6.161189
H -1.960754 5.449292 7.698923
H -1.208903 4.066658 6.837095
C 0.471308 6.270344 6.763036
H 1.145982 7.019457 6.293683
H 0.219977 6.638158 7.784115
H 1.042215 5.321364 6.869056
C 1.624790 6.837990 1.466305
C 2.045237 8.159393 2.145037
H 1.167119 8.784872 2.419157
H 2.645557 7.982462 3.064711
H 2.672946 8.757532 1.447823
C 0.828060 7.187244 0.182390
H -0.098746 7.750559 0.431293
H 1.442507 7.819153 -0.498367
H 0.528392 6.277912 -0.382978
C 2.911841 6.065585 1.077968
H 2.682436 5.118146 0.543380
H 3.549800 6.683537 0.406090
H 3.511069 5.810943 1.980898
C -1.208718 -2.781871 8.667213
C -0.687298 -3.704479 9.789803
H 0.423999 -3.733694 9.822694
H -1.039779 -3.331050 10.776637
H -1.058251 -4.747072 9.678376
C -2.758692 -2.779709 8.723807
H -3.201388 -2.097065 7.966329
H -3.111134 -2.445484 9.725986
H -3.165361 -3.798573 8.537859
C -0.681475 -1.348735 8.938111
H -1.010592 -0.996198 9.941914
H -1.056566 -0.619581 8.187151
H 0.430862 -1.321621 8.912897
C 1.274860 -6.107900 5.553818
C 2.577741 -5.774193 4.784528
H 3.168800 -6.699906 4.600180
H 3.214911 -5.072786 5.367302
H 2.372896 -5.307400 3.796664
C 1.664603 -6.796991 6.879174
H 0.773238 -7.116225 7.462772
H 2.263487 -7.709987 6.665778
H 2.283552 -6.135689 7.525043
C 0.428672 -7.106323 4.720033
H 0.999513 -8.045538 4.540071
H 0.148791 -6.686362 3.729371
H -0.511476 -7.372577 5.252457
C -7.836270 -6.793260 0.209436
C -8.275270 -6.000140 1.459150
H -8.565403 -4.956053 1.208717
H -9.160238 -6.489563 1.922951
H -7.474573 -5.959239 2.230493
C -7.497780 -8.241015 0.650504
H -6.649669 -8.250345 1.370955
H -7.215029 -8.884101 -0.211349
H -8.376336 -8.712166 1.146987
C -9.024570 -6.821652 -0.786587
H -9.922794 -7.274903 -0.309092
H -8.790920 -7.417985 -1.695684
H -9.292294 -5.793321 -1.116547
C -4.360516 -6.913097 -3.592748
C -2.888357 -7.317299 -3.319261
H -2.258711 -6.440207 -3.054348
H -2.824012 -8.044658 -2.479488
H -2.441141 -7.792262 -4.221832
C -5.137813 -8.179620 -4.010932
H -6.201425 -7.956924 -4.249259
H -5.116821 -8.962651 -3.220675
H -4.677596 -8.617608 -4.924128
C -4.408831 -5.905450 -4.770436
H -3.978816 -6.361118 -5.691014
H -3.829870 -4.981694 -4.551974
H -5.456328 -5.603243 -4.993569
```

Bucky_dyad2.xyz

```
264

C -3.404432 -3.265675 1.072846
C -3.309635 -4.464945 1.881899
H -3.766848 -5.430746 1.636502
C -2.561401 -4.142571 2.987844
H -2.304885 -4.793426 3.831129
C -2.159485 -2.752900 2.838665
N -2.708542 -2.236082 1.682001
C -4.099734 -3.189444 -0.157772
C -1.292504 -2.068882 3.733202
C -0.868914 -0.720204 3.591191
C 0.199265 -0.086715 4.353067
C 0.263351 1.224460 3.903760
C -0.779932 1.402179 2.890869
N -1.401154 0.183651 2.684896
C -1.153596 2.626869 2.277161
C -2.078366 2.739993 1.201436
C -2.476802 3.999426 0.594440
```

H -2.168790 4.994273 0.933843
C -3.290043 3.692937 -0.469462
H -3.761470 4.385870 -1.176470
C -3.419220 2.249046 -0.499790
N -2.688432 1.694343 0.536794
C -4.154592 1.536217 -1.478300
C -4.314204 0.129032 -1.502804
C -5.103558 -0.592154 -2.486207
H -5.627573 -0.136187 -3.334725
C -5.078708 -1.916921 -2.121898
H -5.577273 -2.761272 -2.612801
C -4.280815 -2.004138 -0.911551
N -3.811965 -0.752590 -0.566400
C -4.829038 2.329159 -2.561855
C -0.614689 3.924797 2.814023
C -0.823379 -2.846441 4.927842
C -4.718280 -4.451871 -0.690325
C 3.338437 0.312090 4.414760
C 3.363045 1.327364 3.422922
C 1.243458 -0.627279 5.312764
H 1.645904 -1.595937 4.956745
H 0.819073 -0.825051 6.322665
N 2.360273 0.339883 5.459586
C 2.309962 2.434835 3.421635
H 1.884762 2.558058 2.405253
H 2.772526 3.413445 3.689810
N 1.213057 2.162360 4.366296
C 1.803166 1.683260 5.621970
H 2.604863 2.386155 5.929546
H 1.023035 1.655187 6.410943
C 4.329856 -0.710892 4.404877
C 5.306330 -0.699082 3.394170
H 6.083399 -1.480016 3.430340
C 5.342936 0.294773 2.389133
C 4.362710 1.302482 2.434672
H 4.362754 2.089298 1.657570
C 4.363444 -1.755416 5.494364
H 3.669843 -2.603701 5.288548
H 4.044295 -1.313024 6.462726
H 5.381916 -2.184378 5.606793
C 6.341486 0.295330 1.229306
H 6.125149 1.215542 0.640985
C -4.105066 -5.148889 -1.745957
H -3.166612 -4.745017 -2.158924
C -4.660963 -6.341158 -2.265847
C -5.860091 -6.804447 -1.691322
H -6.312314 -7.728328 -2.079807
C -6.513879 -6.129764 -0.631203
C -5.921575 -4.950808 -0.141375
H -6.387987 -4.385149 0.677948
C -1.248485 -2.474032 6.219494
H -1.899735 -1.589612 6.313461
C -0.876622 -3.212047 7.362539
C -0.059280 -4.348359 7.173983
H 0.235254 -4.937755 8.050900
C 0.386318 -4.760939 5.898509
C -0.003295 -3.986350 4.785537
H 0.321081 -4.267331 3.770360
C 0.207336 4.755118 2.031308
H 0.490157 4.408540 1.023804
C 0.660136 6.009930 2.503788
C 0.254639 6.403891 3.792401
H 0.589644 7.376186 4.181513
C -0.578624 5.601516 4.611421
C -0.999484 4.362380 4.102029
H -1.649850 3.702664 4.693744
C -4.311597 2.331673 -3.872516
H -3.397914 1.747870 -4.070637
C -4.931150 3.063147 -4.907821
C -6.096727 3.793944 -4.589191
H -6.593125 4.366104 -5.383016
C -6.649073 3.815985 -3.289501
C -5.993060 3.073676 -2.285030
H -6.388840 3.055128 -1.256545
C 7.119722 -1.905912 0.799740
H 7.351103 -2.627066 -0.015490
H 6.672137 -2.500817 1.641059
N 6.278069 -0.840865 0.309263
C 4.982032 -1.211266 -0.223523
H 4.486197 -0.314922 -0.656515
H 5.119649 -1.953916 -1.040673
H 4.286561 -1.653806 0.538054
C 8.627639 -0.046627 4.075207
C 9.102232 -1.417152 3.768879
C 9.109584 -1.882377 2.457293
C 7.884529 0.319843 1.625733
C 8.176230 0.789233 3.058873
C 10.217304 -1.705887 4.656614
C 10.258908 -2.615043 1.978503
C 8.597351 1.427182 0.834422
C 8.589517 2.173262 3.059954
C 9.458154 0.476632 5.146459
C 9.415301 1.207229 -0.267826
C 9.892497 -0.159642 -0.576660
C 11.319631 -2.461813 4.202450
C 10.511269 -2.210300 0.602190
C 11.340659 -2.928109 2.830024
C 8.844872 2.569593 1.682112
C 9.374928 2.710079 4.103239
C 9.820110 1.840396 5.173733
C 10.438283 -0.540929 5.504240
C 10.451472 3.647215 3.796589
C 11.176631 2.227563 5.536836
C 11.745057 -0.168384 5.870994
C 9.869908 3.494623 1.387303
C 12.709740 -2.832045 2.333713
C 11.568280 3.347369 4.684710
C 12.123580 1.241506 5.879403
C 12.884631 -0.941998 5.386594
C 13.961035 -0.009850 5.084209
C 14.029615 -1.512760 0.695547
C 13.490242 1.340006 5.388660
C 13.868488 2.420027 4.566341
C 14.724356 2.188645 3.407770
C 12.890514 3.440428 4.207894
C 10.718392 3.268399 0.233535

C 14.826683 -0.994112 1.734650
C 10.694037 4.032209 2.465178
C 12.062101 4.131882 1.970552
C 14.576068 -1.394347 3.116329
C 13.573414 -0.637738 -0.381328
C 13.932391 0.725193 -0.378035
C 14.792374 -0.230389 3.967882
C 15.177592 0.887967 3.114069
C 13.142036 3.839995 2.826416
C 14.275041 3.066101 2.332666
C 15.197873 0.415798 1.734317
C 12.075826 3.657673 0.589024
C 12.945608 1.741086 -0.732217
C 14.758337 1.259364 0.694943
C 13.171537 2.908340 0.114976
C 14.288135 2.609540 0.999695
C 12.951471 -2.445973 1.002392
C 11.834202 -2.140912 0.114799
C 12.217612 -1.032763 -0.737880
C 12.674284 -2.069272 4.566952
C 13.536333 -2.298792 3.410314
C 8.409186 -1.169642 1.291408
C 9.521282 -1.226565 0.232649
C 11.257463 -0.051118 -1.065479
C 10.496595 2.130505 -0.572303
C 11.631547 1.357727 -1.062288
Zn -2.652166 -0.277455 1.086399
C -7.929625 4.610044 -2.942291
C -8.512816 5.352733 -4.163515
H -9.429817 5.906980 -3.863709
H -8.799223 4.652430 -4.978815
H -7.797652 6.096295 -4.579452
C -7.600716 5.660819 -1.849649
H -6.833312 6.382112 -2.208904
H -7.210993 5.187496 -0.922583
H -8.513642 6.237255 -1.576597
C -9.010670 3.633651 -2.409386
H -9.940794 4.187886 -2.147677
H -8.672307 3.095624 -1.497138
H -9.268770 2.869162 -3.175156
C -4.323152 3.043860 -6.329463
C -2.877638 3.603811 -6.276418
H -2.417986 3.593411 -7.290885
H -2.224659 3.004869 -5.605081
H -2.871123 4.652791 -5.905766
C -5.133123 3.897356 -7.328861
H -5.169186 4.967747 -7.028588
H -6.177926 3.531607 -7.437626
H -4.658518 3.850545 -8.333890
C -4.292098 1.584867 -6.854903
H -3.845582 1.548335 -7.874501
H -5.319060 1.160275 -6.913436
H -3.688882 0.919629 -6.199515
C -0.991930 6.110415 6.011332
C -1.763009 7.448402 5.868766
H -1.146291 8.234113 5.380408
H -2.683597 7.314723 5.258383
H -2.066142 7.831971 6.869495
C -1.902482 5.108124 6.752544
H -2.849548 4.921347 6.200407
H -2.173547 5.512943 7.752804
H -1.398606 4.129713 6.913115
C 0.278617 6.336079 6.871210
H 0.962390 7.085613 6.415939
H 0.003175 6.705379 7.885422
H 0.849069 5.388615 6.992321
C 1.552674 6.893407 1.601470
C 1.957604 8.215706 2.287772
H 1.073587 8.841244 2.542000
H 2.537982 8.039861 3.220329
H 2.600217 8.813343 1.603908
C 0.780795 7.240475 0.301819
H -0.151338 7.803143 0.531641
H 1.407832 7.872207 -0.367579
H 0.492801 6.329859 -0.267803
C 2.848443 6.123007 1.239344
H 2.630808 5.174826 0.700670
H 3.498998 6.741432 0.580173
H 3.430459 5.868993 2.153465
C -1.378927 -2.770462 8.756836
C -0.869340 -3.691140 9.886489
H 0.241099 -3.700988 9.947133
H -1.252728 -3.330234 10.866445
H -1.218742 -4.739383 9.759552
C -2.929560 -2.795838 8.774384
H -3.365106 -2.116205 8.010117
H -3.312734 -2.474184 9.769390
H -3.313262 -3.820486 8.572217
C -0.883878 -1.330101 9.049770
H -1.243571 -0.990345 10.047384
H -1.253644 -0.602467 8.294721
H 0.228015 -1.283155 9.052015
C 1.239338 -6.033844 5.688064
C 2.550213 -5.675392 4.943802
H 3.161931 -6.589816 4.770865
H 3.163034 -4.962338 5.538259
H 2.355334 -5.212275 3.952139
C 1.616972 -6.717710 7.019654
H 0.721096 -7.056233 7.585084
H 2.238284 -7.617947 6.816628
H 2.209685 -6.045291 7.678489
C 0.427755 -7.046074 4.836716
H 1.019699 -7.973802 4.665703
H 0.158383 -6.628654 3.841984
H -0.516965 -7.331396 5.350738
C -7.835905 -6.695339 -0.063032
C -8.391491 -5.835343 1.092750
H -8.619642 -4.797076 0.766186
H -9.338059 -6.280871 1.471045
H -7.683377 -5.780305 1.948773
C -7.595843 -8.129885 0.475130
H -6.838582 -8.128272 1.290749
H -7.235488 -8.819070 -0.319536
H -8.540426 -8.554425 0.884550
C -8.901531 -6.737728 -1.189270
H -9.861841 -7.146887 -0.801308

```
H -8.581827 -7.378555 -2.039824
H -9.098544 -5.718260 -1.589027
C -3.944529 -7.081277 -3.418654
C -2.519543 -7.486749 -2.959819
H -1.907705 -6.603450 -2.674261
H -2.562765 -8.165451 -2.079208
H -1.983115 -8.017410 -3.779004
C -4.692482 -8.360426 -3.851816
H -5.717615 -8.138529 -4.222488
H -4.776571 -9.096279 -3.021655
H -4.139830 -8.856008 -4.680478
C -3.843135 -6.140773 -4.647388
H -3.319499 -6.651586 -5.487155
H -3.277964 -5.211915 -4.414460
H -4.853561 -5.840501 -5.003829
```

1. *Molecular Operating Environment (MOE 2016.10)*, Chemical Computing Group Inc.: 1010 Sherbooke St. West, Suite #910, Montreal, QC, Canada, H3A 2R7, 2016.
2. *TURBOMOLE V7.1.1*, a development of the University of Karlsruhe and Forschungszentrum Karlsruhe GmbH: 2016.

Chapter Five

Statement of Contribution

The research presented in this manuscript is based on work done by author (M.I.A) except high-resolution mass spectra which were obtained commercially at Australian Proteome Analysis Facility (APAF), Macquarie University. The manuscript was written by author (M.I.A) and it was checked and edited by the principal supervisor (P.K).

Synthesis and Photophysical Studies of β,β′-Pyrrolic Tetraaryl fused-Porphyrin Tröger's Base-Naphthalene Diimide Dyad

Md Imam Ansari, Andrew Try, and Peter Karuso*

Department of Molecular Sciences, Macquarie University, Sydney NSW 2109, Australia

* Corresponding author. Tel.: +612-9850-8290 fax: +612-9850-8313, e-mail: peter.karuso@mq.edu.au

Abstract Porphyrins and naphthalene diimides (NDI) represent two well studied classes of compounds used in photovoltaics, artificial photosynthesis or solar cell applications. To date, porphyrins linked to NDI have either involved a conjugated bridge or by a supramolecular interaction. Compounds that combine two chromophores, in a single molecule, *via* a non-conjugated, V-shaped and rigid bridge molecule are not known. Herein, we report the synthesis and characterisation of a new type of closely positioned donor-acceptor system containing zinc(II)porphyrin and a naphthalene diimide molecule bridged by Tröger's base (TB). Here, a donor porphyrin is linked to Tröger's base at the β-pyrrole position and an electron acceptor NDI is connected covalently to the aryl ring of TB, enabling highly constrained, rigid and V-type conformation of donor-acceptor dyads. The dyad displayed through-space intramolecular interaction between the two chromophores.

Introduction

Porphyrins have a highly delocalised π-system that is suitable for efficient electron transfer reactions.[1, 2] Importantly, zinc and free-base porphyrins, are the most widely used chromophoric units due to their structural similarity with chlorophyll.[3-5] However, owing to the high symmetry of porphyrins, they exhibit considerably smaller excitation coefficients than chlorophyll. So, it is necessary to add other chromophores to achieve practical antennae.[6] Naphthalene diimides (NDIs) are a neutral, redox active, chemically robust and electron deficient class of chromophore that have been used in variety of applications in molecular electronics.[7] In particular, there is increasing interest in NDIs as electron acceptors in artificial photosynthetic models and donor-acceptor dyads.[7-10] Bridged donor-acceptor (D-A) systems have been used[6, 8, 10-12] to establish charge transport between donor/acceptor and get better understanding of how molecular structure and dynamics impact the charge transfer processes. More

importantly, the spatial orientation of donor-acceptor pairs provide insights into electron and energy transfer mechanisms.[13] A number of porphyrin-NDI dyads have been reported in the past decade with or without a spacer either in a conjugated or supramolecular fashion.[6, 8, 10, 11, 14-17] For example, Bhosale and Vauthey,[11] reported on triads where two tetraphenylporphyrin are linked *via* an NDI bridge. Ultrafast fluorescence and transient absorption spectroscopies revealed charge separation between the porphyrin and NDI in the excited state. The construction of a rigid and non-conjugated bridged porphyrin-NDI dyad which would have to interact through-space remains a challenge due to the general lack of functional building blocks and the difficulty in positioning the porphyrin entity in close proximity to the NDI moiety.

A simple synthetic protocol was reported by Crossley and co-workers[18, 19] to synthesise porphyrin-Tröger's base dyads where two porphyrins are connected by a diazocine bridge. This type of porphyrin-Tröger's base conjugate make a starting point for our investigation of the system. We envisioned the construction of a hybrid dyad containing a porphyrin and NDI unit bridged by a Tröger's base. To achieve this, we used a mixed amine condensation (2-aminoporphyrin and 2-methyl-4-nitroaniline) reaction to synthesise hybrid porphyrin Tröger's base (bearing nitro and amino functional group) that could be potentially utilised to append the NDI chromophore *via* post-modification of porphyrin TB. Consequently, the resultant dyad holds the two chromophores in close proximity in a rigid and V-type conformation. Herein, we report a simple and systematic synthetic route to a porphyrin-Tröger's base-NDI dyad separated by a rigid and non-conjugated bridge molecule. This, allows through-space intramolecular electronic communications between the porphyrin and the NDI chromophore owing to the V-type configuration.

Results and discussion

Synthesis and characterisation

As part of our ongoing investigation on the synthesis of donor-acceptor complexes, we were very keen to synthesise porphyrin Tröger's base with amino functional group, in order to enforce the NDI unit and thus replacing the fullerene-C_{60} as an electron acceptor. This had been achieved by the use of mixed amine condensation for TB synthesis. In the previous study, the Try lab has reported that TB hybrids can be prepared *via* a one-step reaction from the mixed condensation of two different aminoaryl units.[20] This approach yields a range of hybrid compounds in acceptable yields provided symmetric products have different R_f values. We devised a synthetic route for porphyrin **2** *via* 2-aminoporphyrin **1** where 5,10,15,20-tetrakis(3',5'-di-*tert*-butylphenyl)porphyrin was chosen because it affords good solubility to the product. 2-Methyl-4-nitroaniline was also selected to access amino functional group on the porphyrin TB. 2-aminoporphyrin **1** was synthesised by the method of Burn and co-workers[21] *via* multistep synthesis, using 3,5-di-*tert*-butylbenzaldehyde and freshly distilled pyrrole to give 5,10,15,20-tetrakis(3,5-di-*tert*-butylphenyl)porphyrin followed by nitration and reduction. The target porphyrin TB **2** was prepared by reacting **1** with 2-methyl-4-nitroaniline and paraformaldehyde in the presence of TFA to afford **2** in good yield (Scheme 1). It is noteworthy, that the reaction theoretically affords three products; two symmetric products (**3** and **4**) and a hybrid porphyrin product **2** from this reaction (Scheme 1). The crude material after workup, showed only one major porphyrinic band on TLC. The only other isolatable compound was a trace of **3**. We optimised this procedure for the synthesis of porphyrin TB **2** on a gram scale in good yields (60-66%). However, our initial attempts to prepare **4** by reacting **1** with paraformaldehyde, in the presence of TFA were also unsuccessful. This could be due to

the bulky *tert*-butyl groups hindering the formation of **4**. In any case, although the porphyrin TB **4** was not formed in the reaction, isolation of the desired porphyrin product **2** was convenient *via* column chromatography. Similar results we have obtained when ethyl 4-amino-3-methylbenzoate was used instead of 2-methyl 4-nitroaniline for the synthesis porphyrin hybrid Tröger's base.[22]

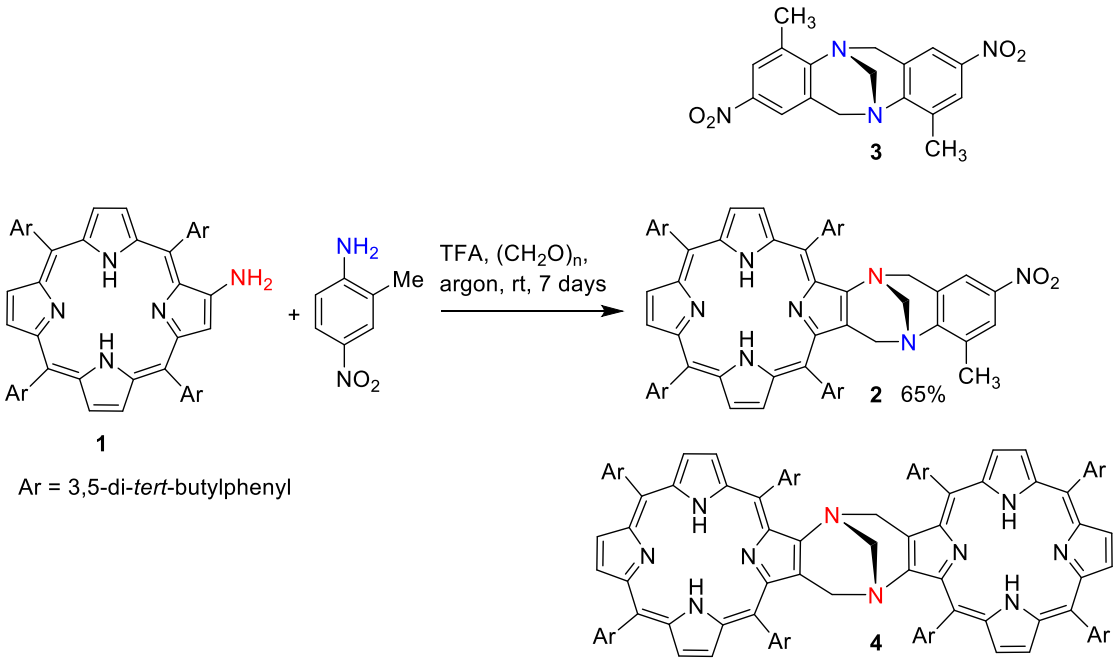

Scheme 1. Synthesis of hybrid porphyrin Tröger's base.

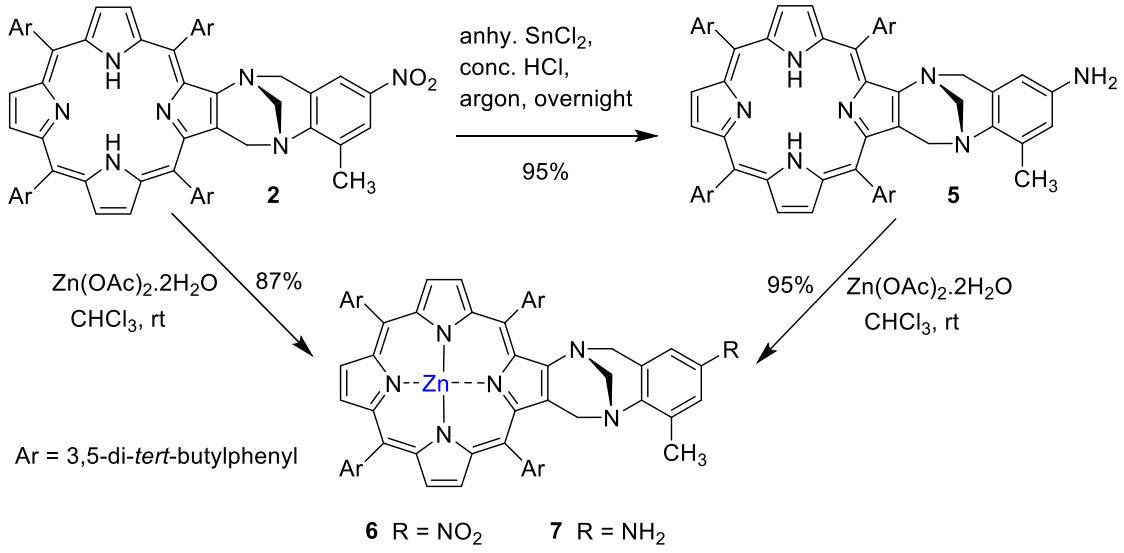

Scheme 2. Synthesis and zinc metallation of hybrid porphyrin Tröger's base.

We turned our attention to reduced **2** using 10% Pd/C under H_2 atmosphere in the dark in ethanol as a solvent. Unfortunately, this reaction led to a complex reaction mixture with several porphyrinic bands were observed on TLC. In contrast, when $SnCl_2$ was used in the presence of concentrated hydrochloric acid (Scheme 2), the reaction was successful and the desired porphyrin **5** was obtained in excellent yield without any further purification. It is worth noting that, reaction workup was done in the dark to avoid any photodegradation. Nitro and amino groups on the porphyrin TB are important synthetic tools for porphyrin derivatisation.[23, 24] We have prepared porphyrin **2** and **5** on a gram scale and our method is clean, high-yielding, and convenient. The only proviso is that the preparation of **5** should be done in the dark as light may causes formation of impurities that require column purification. Compounds **2** and **5** are important building blocks that could find utility in more complex porphyrin-based systems. ^{1}H NMR spectroscopic analysis of **2** and **5** revealed the substituent effects of the NO_2 and NH_2 on the adjacent protons of TB aryl ring (Fig. 1).

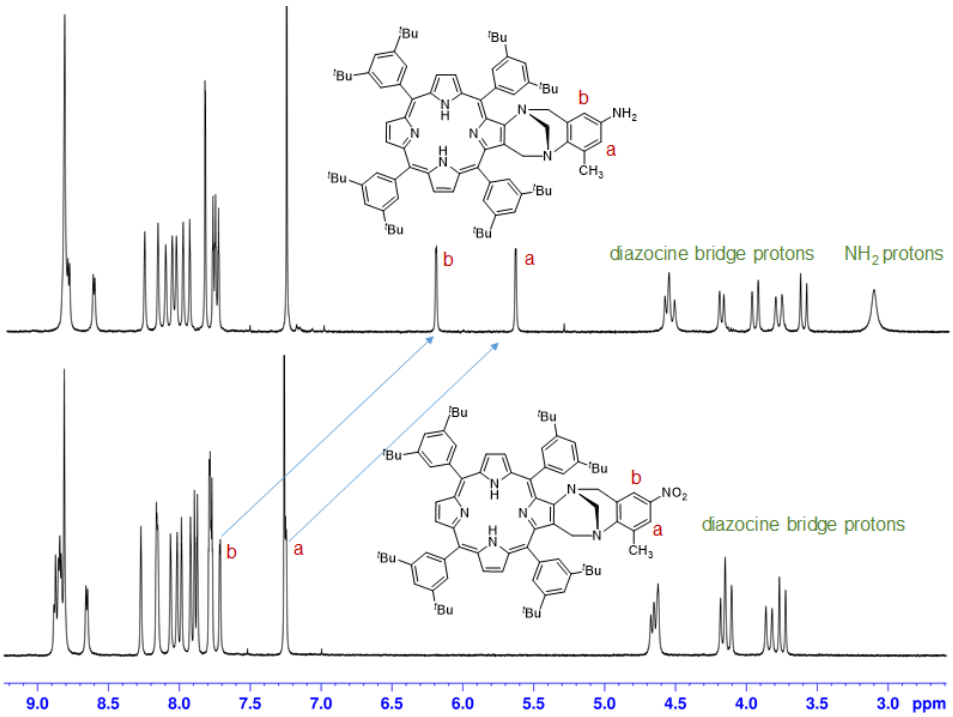

Fig. 1 Partial 400 MHz ^{1}H NMR (298 K, $CDCl_3$) comparison of **2** (bottom) and **5** (top) shows important features of nitro and amino functionalised porphyrin Tröger's base.

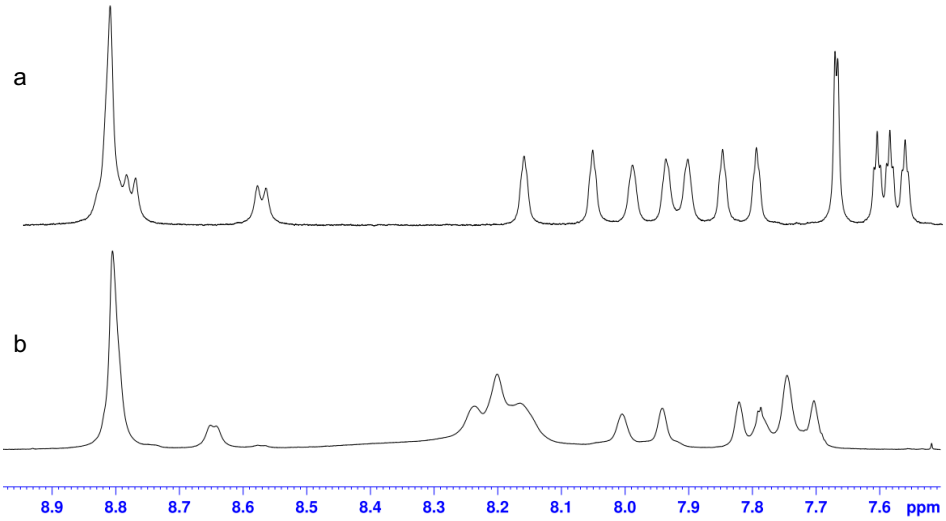

Fig. 2 Partial 400 MHz ^{1}H NMR (298 K, $CDCl_3$) spectra shows a section of aromatic region before and after appending NDI. a) aminoporphyrin TB **5**. b) porphyrin-TB-NDI dyad **9**.

Our plan for the construction of porphyrin **9** (Scheme 3), required porphyrin **5** and naphthalene monoimide **8**. In order to achieve better solubility of the target

compounds, the *n*-hexylamine analogues used. Compound **8** was prepared according to the literature method.[25] Initially, reacting **5** with **8** in DMF at 125 °C did not produce **9**. TLC analysis showed starting material **5** did not consumed in the reaction mixture, under various stoichiometric ratios. However, when the reaction was repeated in toluene with excess imidazole (Scheme 4), **9** was isolated in moderate to good yield after column purification. The zinc porphyrin dyad **10** was prepared by the same condition developed for **6** and **7** (Scheme 2). The high-resolution (ESI) mass spectrum of dyads **9** and **10** correspond to molecular formula of $C_{106}H_{121}N_8O_4$ (Δmmu −0.07) and $C_{106}H_{118}N_8O_4Zn$ (Δmmu −1.01), respectively. Both porphyrin TB-NDI dyads **9** and **10** were considerably less soluble than their parent porphyrin TB analogues **2**, **5**, **6**, and **7**.

^{1}H NMR spectroscopic analysis of **9** after appending NDI to **5**, showed distorted doublets and triplets (Fig. 2, Fig. S16). This was a clear indication that aromatic protons of porphyrin lose their equivalency owing to the presence of the NDI moiety. The identity of zinc dyad **10** was unambiguously determined due to the absence of inner NH peak at −3.01 ppm. The presence of diimides in **9** and **10** were supported by IR (ν_{max} 1667 and 1668).

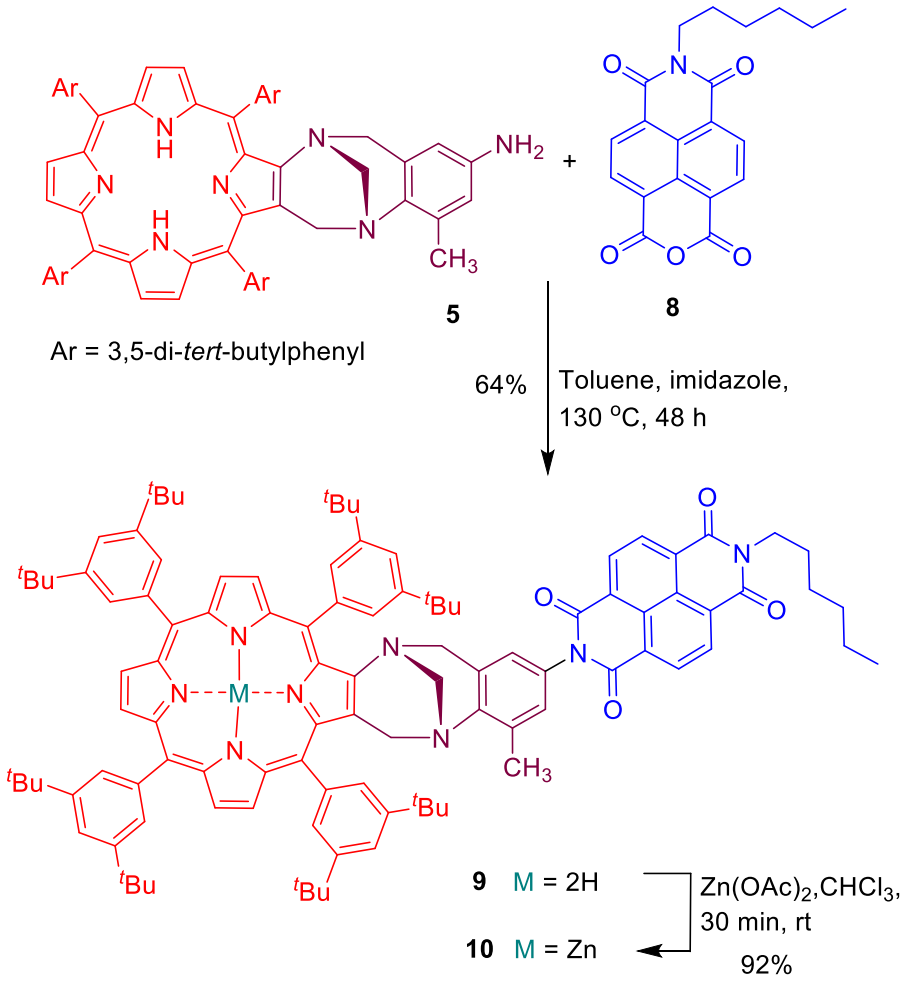

Scheme 3. Synthesis of porphyrin Tröger's base NDI dyads.

Photophysical Properties

The UV/Vis absorption spectra of free-base dyad **9** and its zinc(II) counterpart **10** along with the control compounds **5**, **8** and **7** (Figs 3, 4) shows that dyad **9** has a typical porphyrin spectrum with strong absorption at 450 and 650 nm. The weak absorption features observed at 357 and 381 nm in dyad **9** results from the NDI acceptor.[10, 26] The absorption spectra of dyads **9** and **10**, are essentially composites of their constituents suggest a minimal electronic coupling between the chromophores. For example, the NDI absorption, in dyads **9** and **10** is only red-shifted compared to **8**. This indicates a weak ground state interaction between the porphyrin and the NDI moieties (Fig. 3 and 4).

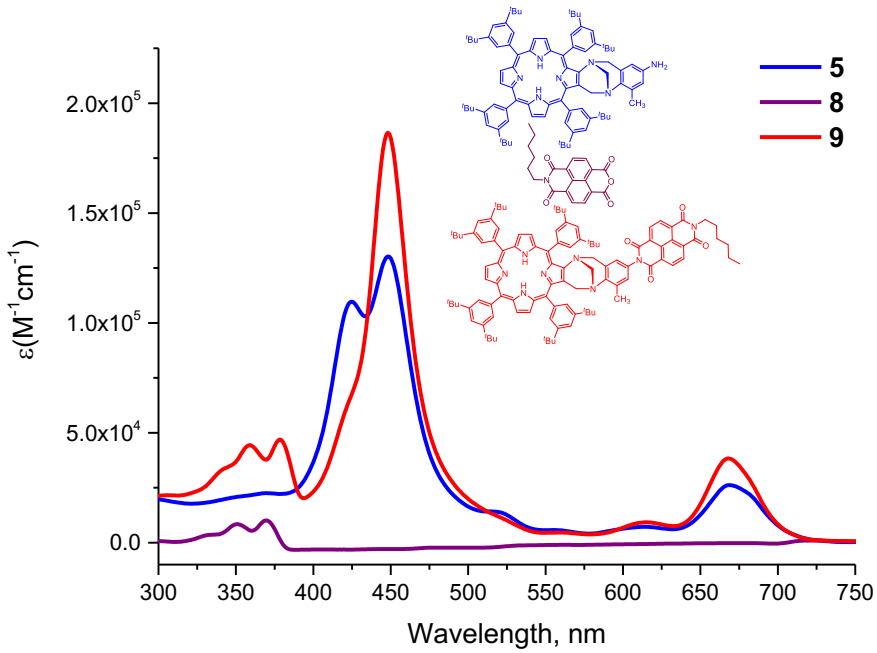

Fig. 3 UV/Vis spectra of **5** (blue), **8** (purple) and **9** (red) in $CHCl_3$. The concentration of each compound was 2.5×10^{-6} M in $CHCl_3$.

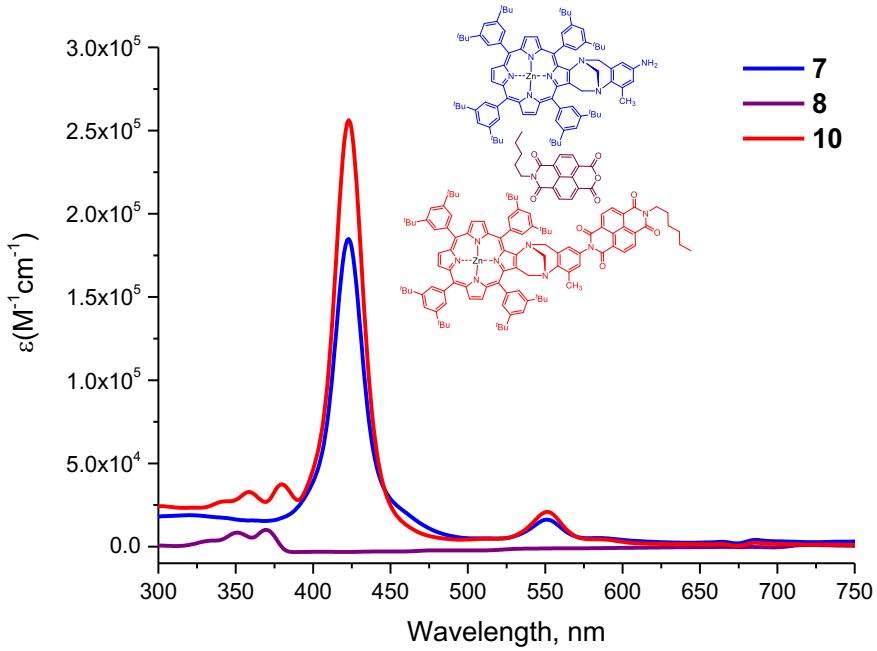

Fig. 4 UV/Vis spectra of **7** (blue), **8** (purple) and **10** (red). The concentration of each compound was 2.5×10^{-6} M in $CHCl_3$.

To investigate the excited state interactions, we measured the fluorescence emission and excitation of dyads **9** and **10** compared to controls **5** and **7** (Figs 5, 6 and 7). The naphthalene **8** is weakly fluorescent and exhibits some stationary fluorescence emission. No quenching was observed upon appending the NDI moiety onto the porphyrin TB **5**, in fact relative intensity of dyad **9** was increased, which indicated that there was efficient S_1-T_1 intramolecular energy transfer (Fig. 5).[27] In contrast, the fluorescence was strongly quenched for zinc dyad **10** compare to **9** with the emission intensity for **10** reduced by >90% with respect to **9** (Fig. 6). This fluorescence quenching was indicative of coupling between the porphyrin excited state and the NDI unit in **10**, suggesting an efficient energy transfer.[28] It is noteworthy that, although the fluorescence is always quenched for **10** compare to **9**, the relative intensity and the position of emission band around 650 nm was also detected. Moreover, the emission spectra were recorded for the free-base compound **2**, showed two peaks observed at 659 and 725 nm which was blue shifted by 57 and 75 nm respectively compared to the corresponding zinc compound **6** (Figs S24, S25).

Fluorescence excitation spectra of **5**, **7**, **9** and **10** were recorded at λ_{em} 650 nm. Zinc porphyrin TB **7**, showed a strong excitation spectrum with two Q-band peaks (Fig. 7). The zinc dyad **10** mirrored the quenching seen in the emission spectrum. Indirect information regarding the degree of energy transfer was obtained from the decreased peak intensity (which indicates an increase in the energy transfer) from donor porphyrin to the acceptor NDI (Fig. 7).

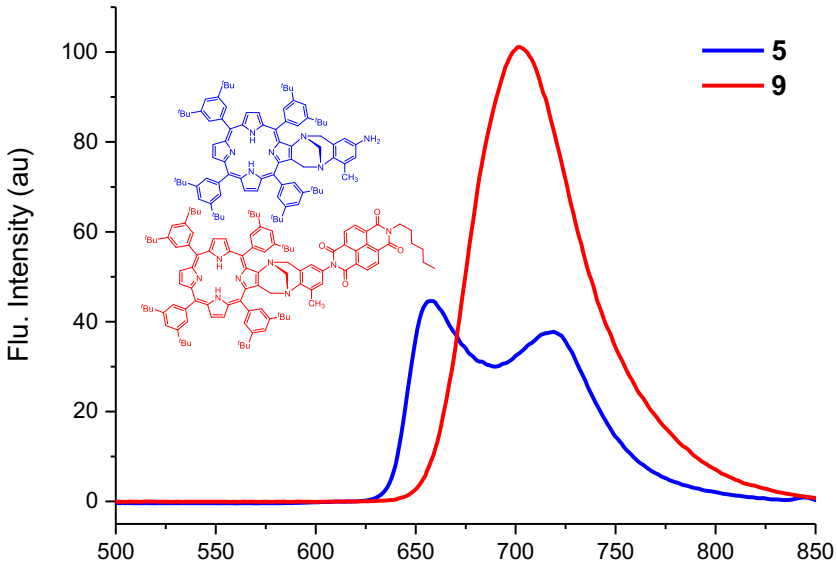

Fig. 5 Fluorescence emission spectra of **5** (blue) and **9** (red) in $CHCl_3$. Max λ_{ex} = 424 nm. The concentration of each compound was 2.5 × 10^{-6} M.

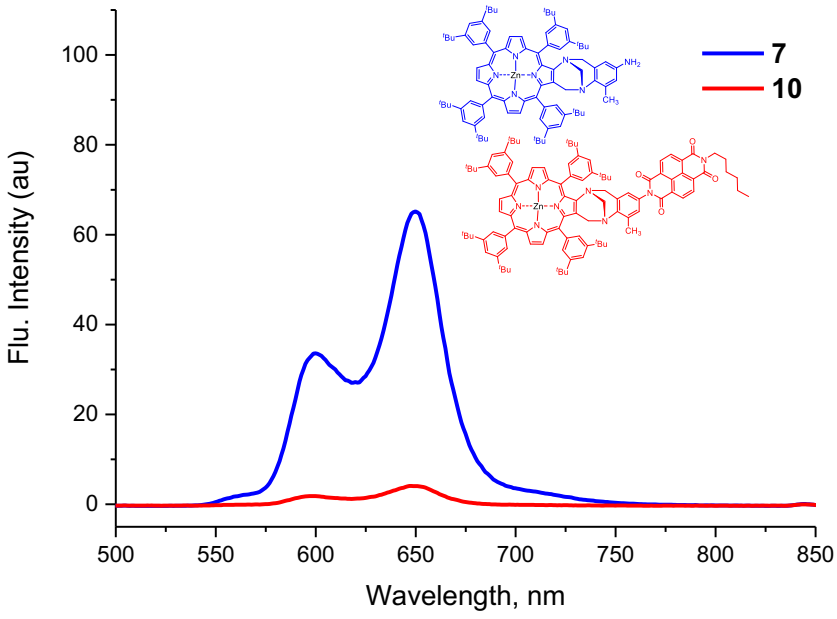

Fig. 6 Fluorescence emission spectra of **7** (blue) and **10** (red) in $CHCl_3$. Max λ_{ex} = 424 nm. The concentration of each compound was 2.5 × 10^{-6} M.

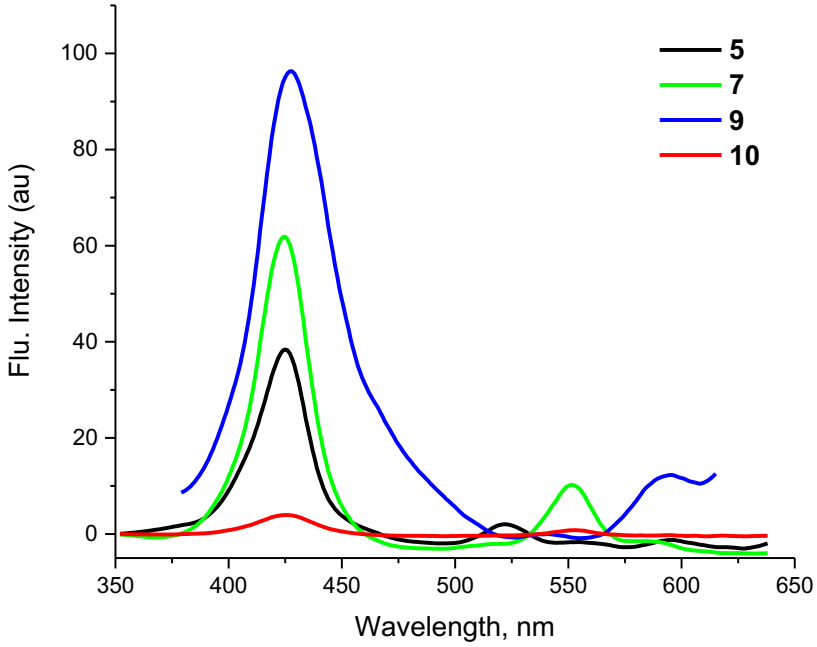

Fig. 7 Fluorescence excitation spectra of **5**, **7**, **9** and **10** (λ_{em} 650 nm) in $CHCl_3$. The concentration of each compound was 2.5×10^{-6} M.

Conclusions

Herein, we present our results on the design, synthesis and photophysical properties of a rigid, non-conjugated and V-shaped dyads featuring porphyrin and naphthalene diimide. Simple synthetic protocol allows easy access to dyad separated by a rigid Tröger's base that holds the two chromophores in close proximity. The electronic communication between the donor-acceptor was evidenced by UV/Vis and fluorescence spectroscopy. The previous approaches to prepare through-space interacting donor-acceptor dyad where non-trivial synthesis and supramolecular assemblies of dyad can limit the interactions between the two chromophores (due to weaker and reversible interactions) and produce ambiguous results. In contrast, we have been able to control the rigidity with precise distance between donor and acceptor component. Additionally, the nitro and amino functionalised hybrid porphyrin TBs

synthesised *via* a mixed amine condensation reaction (2-aminoporpyrin and ethyl 2-methyl-4-nitroaniline) of Tröger's base. This could be used as a potential synthetic tool in the development of more complex porphyrin-based architectures.

Acknowledgements

This work was supported by Macquarie University (Sydney, Australia). We would also like to thank India@75 and Macquarie University for the award of an iMQRES PhD scholarship to M.I.A.

Experimental Section

General Information:

Reagents were purchased from Sigma Aldrich and Alfa Aesar and used without purification unless otherwise stated.

^{1}H NMR and ^{13}C NMR spectra were recorded in Aldrich 5 mm tubes on a Bruker DRX 400 spectrometer (400 MHz) at 300 K unless otherwise stated, processed using Topspin 3.5, and referenced to residual solvent peak ($CDCl_3$ δ_H 7.26 and δ_C 77.01 ppm, DMSO-d_6 δ_H 2.49 and δ_C 39.5 ppm) Signals were recorded in terms of chemical shifts, multiplicity, coupling constants (in Hz). The following abbreviations for multiplicity are used: s, singlet; d, doublet; t, triplet; m, multiplet; dd, doublet of doublets. Column chromatography was routinely carried out using the gravity feed column techniques on Merck silica gel type 9385 (230-400 mesh) with the stated solvent systems. Analytical thin layer chromatography (TLC) analyses were performed on Merck silica gel 60 F254 protected sheets (0.2 mm). Visualisation of compounds was achieved by illumination under ultraviolet light (254 nm). Charcoal and celite were pre-washed with MeOH and water before used. HRMS (ESI) were performed at the Australian Proteome Analysis Facility (APAF), Macquarie University, Australia using a Q Exactive Plus hybrid quadrupole-orbitrap mass spectrometer (Thermo Scientific, Bremen, Germany). ESI-

MS spectra were recorded using an Agilent 6130 single quadrupole mass spectrometer (Agilent Corp.). The IR spectra were taken on a Thermo Scientific Nicolet iS10 ATR FTIR spectrometer at 298 K. UV/Visible absorbances were recorded on a Varian Cary 1Bio UV-visible spectrophotometer. Fluorescence emission spectra were recorded on a Cary Eclipse Fluorescence Spectrofluorometer (Agilent Technologies). All commercial solvents were HPLC grade and used without further purification. Where solvent mixtures are used, the portions are given by volume. Pyrrole was freshly distilled before use.

Porphyrin Tröger's Base 2

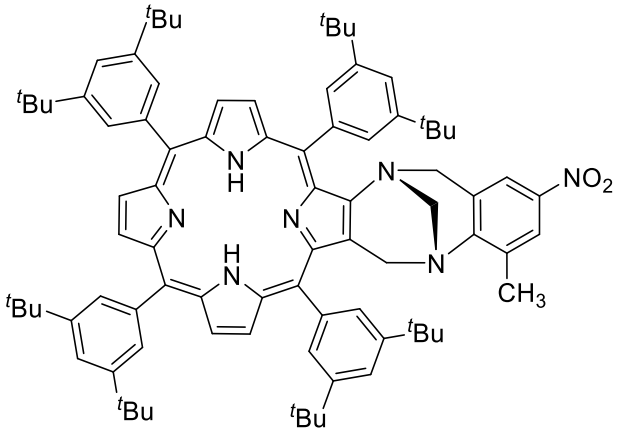

2-Amino-5,10,15,20-tetrakis(3,5-di-*tert*-butylphenyl)porphyrin **1** (600 mg, 0.56 mmol) and 2-methyl-4-nitroaniline (101 mg, 0.56 mmol) with paraformaldehyde (54 mg, 1.8 mmol) were dissolved in trifluoroacetic acid (15 mL) and the mixture was stirred in the dark for 7 days. The reaction mixture was then poured onto ice (150 g), basified by the addition of concentrated ammonia (20 mL) and water (30 mL). A saturated solution of sodium bicarbonate (50 mL) was added to the reaction mixture. To the combined layers ethyl acetate was added (300 mL) and the layers were separated, washed with brine (150 mL), dried over magnesium sulphate, filtered and evaporated to dryness to afford crude as dark brown solid. The crude compound was chromatographed (silica gel, 20% ethyl acetate/80% hexane) to afford porphyrin TB **2** in (460 mg, 65%). UV/Vis ($CHCl_3$)

λ_{max} (log ε) 668 (3.81), 520 (4.13), 424 (5.34), 229 (4.33); FTIR (neat) ν_{max} 3298, 2957, 2902, 2867, 1695, 1591, 1525, 1473, 1425, 1393, 1361, 1340, 1294, 1246, 1210, 1120, 1096, 987, 941, 987, 918, 898, 879, 819, 798, 714 cm^{-1}; ^1H NMR (400 MHz, $CDCl_3$) δ 8.76-8.92 (m, 5H, β-pyrrolic H), 8.65 (m, 1H, β-pyrrolic H), 8.27 (br s, 1H, ArH), 8.12-8.19 (m, 2H, ArH), 8.06 (br s, 1H, ArH), 8.01 (br s, 1H, ArH), 7.98 (br s, 1H, ArH), 7.92 (br s, 1H, ArH), 7.89 (br s, 1H, ArH), 7.85-7.88 (m, 1H, ArH), 7.75-7.81 (m, 3H, ArH), 7.71 (d, *J* = 2.2 Hz, 1H, ArH), 7.24 (d, *J* = 2.2 Hz, 1H, ArH), 4.55-4.73 (m, 2H), 4.07-4.24 (m, 2H), 3.79-3.90 (m, 1H), 3.69-3.79 (m, 1H), 2.24 (s, 3H, CH_3), 1.44-1.68 (m, 72H, *tert*-butyl H), −2.79 (br s, 2H, NH); ^{13}C NMR (100 MHz, $CDCl_3$) δ 149.9, 149.6, 148.7, 142.9, 141.5, 141.2, 141.1, 139.7, 134.0, 130.8, 129.8, 129.6, 129.2, 127.7, 123.4, 121.9, 121.6, 120.9, 120.3, 120.1, 119.1, 55.6, 53.6, 35.2, 35.1, 35.0, 31.8, 31.7, 31.6, 29.7, 17.6; HRMS (ESI) *m/z*: 1266.8264 $[M+H]^+$ (calcd for $C_{86}H_{104}N_7O_2$, 1266.8251).

Porphyrin Tröger's Base 5

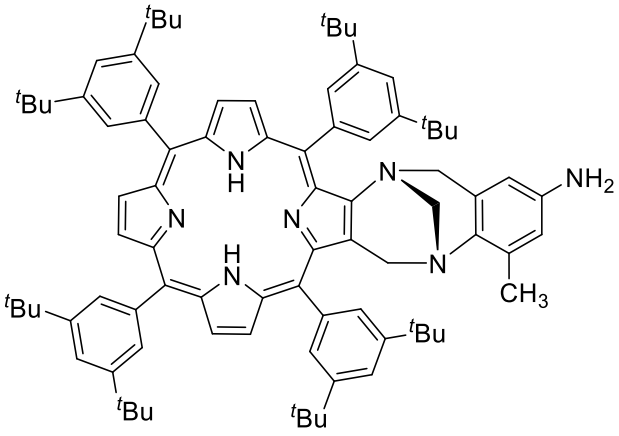

Porphyrin TB **2** (150 mg, 0.12 mmol) and anhydrous stannous chloride (180 mg, 0.95 mmol) in dichloromethane (50 mL), was added hydrochloric acid (10 M; 1 mL) under an argon atmosphere. The reaction mixture was stirred in the dark for overnight. The reaction progress was followed by TLC (30% ethyl acetate/70% hexane), upon consumption of the starting material reaction was stopped. The organic layer was

washed with water (2 × 50 mL), sodium hydroxide (3 M; 2 × 50 mL) water (50 mL), and brine (50 mL), dried over anhydrous magnesium sulfate, filtered and evaporated to dryness under vacuum to afford porphyrin TB **5** (132 mg, 90%) as a purple microcrystalline solid. The crude compound did not require further purification. UV/Vis ($CHCl_3$) λ_{max} (log ε) 669 (4.43), 448 (5.12), 425 (5.04), 259 (4.48), FTIR (neat) ν_{max} 3359, 2956, 2866, 1707, 1591, 1527, 1475, 1424, 1393, 1361, 1296, 1245, 1208, 1122, 1028, 987, 961, 916, 989, 879, 819, 799, 714, 651, 602 cm^{-1}; ^1H NMR (400 MHz, DMSO-d_6) δ 8.82 (s, 4H, β-pyrrolic H), 8.79 (d, J = 4.7 Hz, β-pyrrolic H), 8.62 (d, J = 4.7 Hz, β-pyrrolic H), 8.26 (br s, 1H, ArH), 8.16 (br s, 1H, ArH), 8.11 (br s, 1H, ArH), 8.06 (br s, 1H, ArH), 8.03 (br s, 1H, ArH), 7.99 (br s, 1H, ArH), 7.94 (br s, 1H, ArH), 7.81-7.85 (m, 2H, ArH), 7.78 (t, J = 1.7 Hz, 1H, ArH), 7.76 (t, J = 1.7 Hz, 1H, ArH), 7.74 (br s, 1H, ArH), 6.20 (d, J = 2.0 Hz, 1H, ArH), 5.64 (d, J = 2.0 Hz, 1H, ArH), 4.46-4.66 (m, 2H, CH_2), 4.13-4.26 (m, 1H, CH_2), 3.95 (d, J = 17.1 Hz, 1H, CH_2), 3.71-3.84 (m, 1H, CH_2), 3.61 (d, J = 17.1 Hz, 1H, CH_2), 3.11 (br s, 2H, NH_2), 2.11 (s, 3H, CH_3), 1.43-1.63 (m, 72H, *t*-butyl H), −2.76 (br s, 2H); ^{13}C NMR (100 MHz, $CDCl_3$) δ 149.6, 149.2, 148.6, 148.5, 147.6, 141.7, 141.5, 141.4, 141.2, 139.8, 137.7, 133.5, 130.8, 130.5, 129.7, 129.6, 129.5, 129.4, 129.3 129.1, 128.2, 127.7, 121.7, 121.5, 121.4, 120.8, 120.1, 119.1, 118.8, 116.1, 109.9, 68.1, 60.3, 55.9, 53.7, 35.2, 35.1, 35.0, 31.9, 31.8, 31.7, 31.6, 31.5, 29.7, 22.6, 21.1, 17.4, 14.2; HRMS (ESI) *m/z*: 1236.8534 $[M+H]^+$ (calcd for $C_{86}H_{106}N_7$, 1236.8510).

Porphyrin Tröger's Base 6

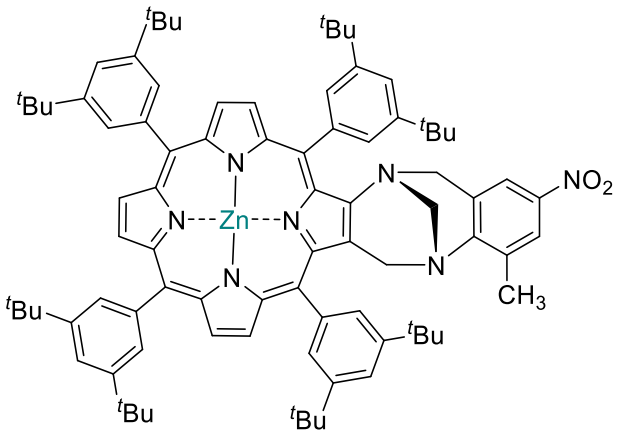

Free-base porphyrin TB **2** (50 mg, 0.04 mmol) was dissolved in chloroform (10 mL) and stirred at room temperature. Zinc acetate dihydrate (25 mg, 0.12 mmol, 2.5 equiv) was separately dissolved in methanol (3 mL) and then added dropwise to the reaction mixture. After 30 min, a pink coloured solution was observed. The reaction progress was followed by TLC (20% ethyl acetate/80% hexane) and upon consumption of all the starting material the reaction was stopped. Chloroform (20 mL) was added to the reaction mixture then washed with water (2 × 20 mL), dried over magnesium sulfate and filtered. The solvent was evaporated to dryness to afford zinc(II) porphyrin TB **6** as dark-purple microcrystals (45 mg, 87%). UV/Vis ($CHCl_3$) λ_{max} (log ε) 551 (4.19), 425 (5.36), 316 (4.33), 240 (4.33); FTIR (neat) ν_{max} 2956, 2903, 2867, 1590, 1465, 1426, 1361, 1391, 1338, 1292, 1246, 1211, 1002, 938, 897, 879, 821, 795, 714 cm^{-1}; ^1H NMR (400 MHz, $CDCl_3$) δ 8.98 (d, *J* = 4.7 Hz, 1H, β-pyrrolic H), 8.90-8.97 (m, 4H, β-pyrrolic H), 8.69 (d, *J* = 4.7 Hz, 1H, β-pyrrolic H), 8.22 (br s, 1H, ArH), 8.15 (br s, 2H, ArH), 8.03-8.11 (m, 2H, ArH), 8.01 (br s, 1H, ArH), 7.90 (br s, 1H, ArH), 7.87 (br s, 1H, ArH), 7.83 (br s, 1H, ArH), 7.71-7.81 (m, 4H, ArH), 7.31 (d, *J* = 1.6 Hz, 1H, ArH), 4.79 (d, *J* = 17.4 Hz, 1H), 4.66 (m, 1H), 4.12-4.30 (m, 2H), 3.90 (d, *J* = 17.4 Hz, 1H), 3.77 (d, *J* = 17.4 Hz, 1H), 2.27 (s, 3H), 1.45-1.70 (m, 72H, *tert*-butyl H); ^{13}C NMR (100 MHz, $CDCl_3$) δ 153.4, 151.9, 151.7, 151.1, 150.2, 150.1, 149.7, 149.6, 149.5,

149.4, 148.5, 148.4, 148.3, 147.8, 145.0, 142.9, 141.9, 141.8, 141.7, 141.5, 140.4, 134.1, 132.4, 131.95, 131.91, 131.86, 131.82, 130.5, 130.3, 129.9, 129.5, 129.4, 128.6, 127.6, 123.4, 123.1, 122.8, 121.4, 120.7, 120.2, 120.1, 119.7, 67.4, 55.5, 54.0, 35.3, 35.2, 35.1, 35.08, 35.05, 34.9, 31.8, 31.77, 31.74, 31.70, 31.68, 31.5, 29.6, 17.7; HRMS (ESI) *m/z*: 1328.7409 $[M+H]^+$ (calcd for $C_{86}H_{102}N_7O_2Zn$, 1328.7386).

Porphyrin Tröger's Base 7

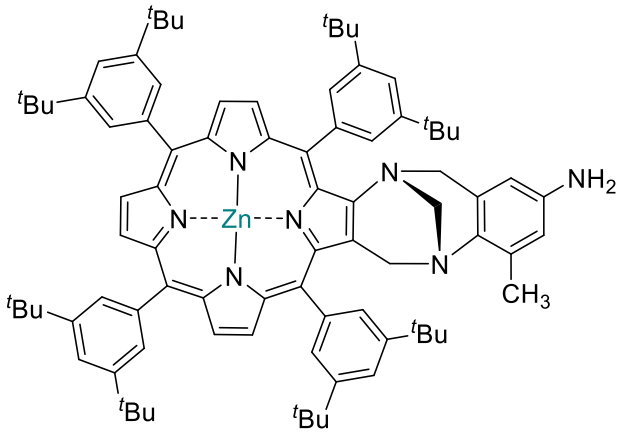

Free-base porphyrin TB **5** (10 mg, 0.01 mmol) dissolved in chloroform (5 mL) and stirred in the dark at room temperature. Zinc acetate dihydrate (5 mg, 0.02 mmol, 2.5 equiv) was separately dissolved in methanol (2 mL) and then added dropwise to the reaction mixture. After 30 min, a pink coloured solution was observed. The reaction progress was followed by TLC (30% ethyl acetate/70% hexane), upon consumption of starting material the reaction was stopped. Chloroform (10 mL) was added to the reaction mixture then washed with water (2 × 10 mL), dried over magnesium sulfate and filtered. The solvent was evaporated to dryness to afford zinc(II) porphyrin TB **7** as dark-purple microcrystals (10 mg, 95%). UV/Vis ($CHCl_3$) λ_{max} (log ε) 551 (4.21), 423 (5.28), 240 (4.26), 233 (4.33); FTIR (neat) ν_{max} 3360, 2955, 2866, 2160, 2029, 1708, 1653, 1591, 1476, 1425, 1390, 1361, 1293, 1246, 1207, 1130, 1073, 1034, 1003, 963, 920, 899, 879, 822, 797, 759, 714, 664, 601 cm^{-1}; ^1H NMR (400 MHz, $CDCl_3$) δ 8.95

(d, J = 4.7 Hz, 1H, β-pyrrolic H), 8.88-8.94 (m, 4H, β-pyrrolic H), 8.67 (d, J = 4.7 Hz, 1H, β-pyrrolic H), 8.18 (t, J = 1.6 Hz, 1H, ArH), 8.19 (t, J = 1.7 Hz, 1H, ArH), 8.09 (t, J = 1.6 Hz, 1H, ArH), 8.07 (t, J = 1.7 Hz, 1H, ArH), 8.04 (t, J = 1.7 Hz, 1H, ArH), 8.02 (t, J = 1.7 Hz, 1H, ArH), 7.81-7.86 (m, 3H, ArH), 7.77 (t, J = 1.8 Hz, 1H, ArH), 7.75 (t, J = 1.8 Hz, 1H, ArH), 7.73 (t, J = 1.8 Hz, 1H, ArH), 5.97 (d, J = 1.6 Hz, 1H, ArH), 5.45 (d, J = 1.6 Hz, 1H, ArH), 4.62 (d, J = 17.2 Hz, 1H), 4.55 (d, J = 12.2 Hz, 1H), 4.17 (d, J = 12.2 Hz, 1H), 3.97 (d, J = 17.2 Hz, 1H), 3.76 (d, J = 17.4 Hz, 1H), 3.56 (d, J = 17.4 Hz, 1H), 2.76 (br s, 2H, NH_2), 2.09 (s, 3H), 1.46-1.62 (m, 72H, *tert*-butyl H); ^{13}C NMR (100 MHz, $CDCl_3$) δ 151.6, 151.2, 150.0, 149.8, 149.5, 149.2, 149.1, 148.4, 148.2, 147.3, 146.1, 142.2, 142.1, 141.9, 141.8, 138.2, 132.1, 131.6, 131.5, 130.6, 130.4, 129.6, 129.5, 127.5, 122.8, 122.5, 121.2, 120.6, 120.1, 119.7, 119.1, 116.0, 110.2, 67.8, 61.1, 55.8, 54.1, 35.2, 35.1, 34.9, 31.8, 31.7, 31.6, 29.7, 17.4, 14.0; HRMS (ESI) *m/z*: 1298.7673 $[M+H]^+$ (calcd for $C_{86}H_{104}N_7Zn$, 1298.7645).

Porphyrin-TB-NDI dyad 9

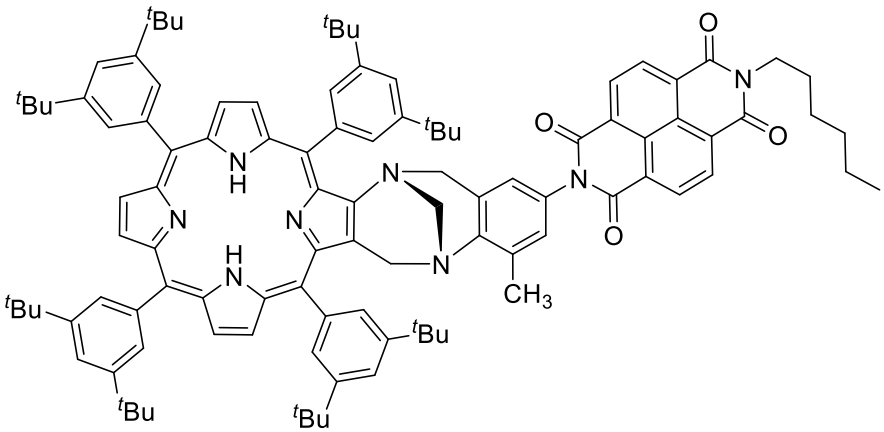

7-hexyl-1*H*-isochromeno[6,5,4-*def*]isoquinoline-1,3,6,8(7*H*)-tetraone (**8**) (5 mg, 0.014 mmol) was dissolved in toluene (10 mL) with 1.63 g imidazole and free-base porphyrin TB **5** (15 mg, 0.01 mmol) under an argon atmosphere. The reaction mixture was stirred overnight at reflux condition. The reaction progress was followed by TLC, upon consumption of starting material, the reaction was stopped. Then water (3 × 50 mL)

was added followed by dichloromethane (20 mL), The organic layers were separated, dried under reduced pressure. The crude solid was chromatographed (silica gel, 95% chloroform/5% methanol) to afford porphyrin TB NDI **9** as a dark purple solid (12 mg, 64%). UV/Vis ($CHCl_3$) λ_{max} (log ε) 669 (4.75), 448 (5.44), 380 (4.81), 360 (4.74), 240 (4.67), 227 (4.33), 212 (4.33), 201 (4.38); FTIR (neat) ν_{max} 3674, 3302, 2960, 2901, 2360, 2157, 1972, 1707, 1668, 1581, 1525, 1475, 1452, 1423, 1393, 1362, 1336, 1246, 1210, 1189, 1154, 1109, 1079, 987, 913, 879, 800, 766, 716, 669, 647,620, 527 cm^{-1}; ^1H NMR (400 MHz, $CDCl_3$) δ 8.90-8.70 (br m, 5H, β-pyrrolic H), 8.64 (d, *J* = 3.6 Hz, β-pyrrolic H), 8.20 (t, *J* = 14.4 Hz, 8H), 8.00 (br s, 1H), 7.94 (br s, 1H), 7.65-7.86 (m, 6H), 6.74 (br s, 1H), 6.37 (br s, 1H), 4.60 (d, *J* = 12.2 Hz, 1H), 4.55 (d, *J* = 17.4 Hz, 1H), 4.23 (d, *J* = 12.2 Hz, 2H), 4.02-4.15 (m, 3H), 3.78 (d, *J* = 17.4 Hz, 1H), 2.26 (s, 3H, CH_3), 1.20-1.60 (m, 80H), 0.86 (t, *J* = 7.0 Hz, 3H, CH_3), −3.02 (br s, 2H); ^{13}C NMR (100 MHz, $CDCl_3$) δ 163.0, 162.4, 150.6, 150.5, 150.4, 149.9, 148.6, 148.5, 143.8, 141.8, 141.7, 135.2, 134.0, 132.5, 132.4, 132.2, 131.8, 130.9, 130.6, 129.9, 129.7, 126.8, 126.5, 126.4, 126.3, 122.8, 122.6, 120.8, 119.3, 41.0, 35.1, 35.0, 31.8, 31.7, 31.5, 29.7, 27.9, 26.8, 26.7, 22.6, 14.0; HRMS (ESI) *m/z*: 1569.95096 $[M+H]^+$ (calcd for $C_{106}H_{121}N_8O_4$, 1569.95107).

Zinc(II)porphyrin TB-NDI dyad 10

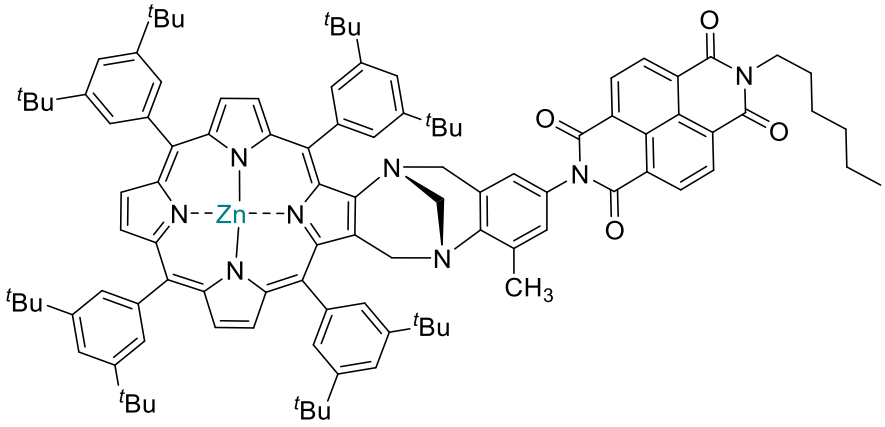

Free-base porphyrin TB NDI **9** (10 mg, 6.4 μmol) was dissolved in chloroform (5 mL) and stirred in the dark at room temperature. Zinc acetate dihydrate (4 mg, 0.02 mmol, 2.5 equiv) was separately dissolved in methanol (2 mL) and then added dropwise to the reaction mixture. After 30 min, a bright red coloured solution was observed. The reaction progress was followed by TLC (30% ethyl acetate/70% hexane), upon consumption of starting material the reaction was stopped. Chloroform (10 mL) was added to the reaction mixture then washed with water (2 × 10 mL), dried over magnesium sulfate and filtered. The solvent was evaporated to dryness to afford zinc(II) porphyrin-TB-NDI **10** as dark-purple solid (10 mg, 95%). UV/Vis ($CHCl_3$) λ_{max} (log ε) 551 (4.36), 423 (5.52), 381 (4.54), 360 (4.37), 239 (4.44), 219 (4.05), 211 (4.05), 203 (4.13); FTIR (neat) ν_{max} 3673, 2958, 2903, 2361, 1706, 1667, 1581, 1475, 1452, 1391, 1362, 1337, 1292, 1247, 1207, 1189, 1136, 1109, 1069, 1005, 967, 936, 916, 899, 879, 824, 798, 767, 716, 679, 695, 623, 584 cm^{-1}; ^1H NMR (400 MHz, $CDCl_3$) δ 8.87-8.96 (m, 5H, β-pyrrolic H), 8.71 (d, J = 4.7 Hz, 1H, β-pyrrolic H), 8.37 (br s, 3H), 8.10-8.25 (m, 5H), 7.94-8.09 (m, 3H), 7.82 (s, 2H), 7.74 (s, 2H), 7.69 (br s, 1H), 6.77 (s, 1H), 6.41 (s, 1H), 4.69 (d, J = 17.5 Hz, 1H), 4.62 (d, J = 12.3 Hz, 1H), 4.19-4.36 (m, 2H), 3.97-4.14 (m, 3H), 3.79 (d, J = 17.5 Hz, 1H), 2.27 (s, 3H, CH_3), 1.18-1.69 (m, 80H), 0.78-0.92 (m, 3H); ^{13}C NMR (100 MHz, $CDCl_3$) δ 163.1, 162.5,

152.8, 151.6, 151.2, 150.1, 149.9, 149.6, 149.4, 149.3, 148.5, 148.4, 148.3, 147.5, 147.4, 145.8, 142.1, 141.9, 141.8, 140.3, 134.5, 132.2, 131.9, 131.8, 131.7, 130.9, 130.6, 130.4, 130.0, 129.7, 129.6, 129.4, 129.0, 128.2, 128.1, 127.6, 126.4, 125.8, 125.3, 123.8, 122.9, 122.6, 121.3, 120.6, 120.2, 119.8, 67.6, 55.6, 53.7, 40.9, 35.2, 35.0, 34.9, 33.7, 31.8, 31.7, 31.4, 29.7, 29.4, 27.9, 26.7, 26.6, 22.7, 22.5, 22.5, 17.6, 14.2, 14.1, 14.0, 13.9; HRMS (ESI) *m/z*: 1630.85576 $[M+H]^+$ (calcd for $C_{106}H_{118}N_8O_4Zn$, 1630.85677).

References

1. K. M. Smith, *Porphyrins and metalloporphyrins*, Elsevier Amsterdam, 1975.
2. Y. K. Kang, P. M. Iovine, M. J. Therien; *Coord. Chem. Rev*. 2011, **255**, 804-824.
3. M. R. Wasielewski, *Chem. Rev.*, 1992, **92**, 435-461.
4. R. Purrello, S. Gurrieri and R. Lauceri, *Coord. Chem. Rev.*, 1999, **190**, 683-706.
5. K. M. Kadish, K. M. Smith and R. Guilard, *The Porphyrin Handbook: Multiporphyrins, multiphthalocyanines, and arrays*, Academic Press, 2003.
6. D. Villamaina, M. M. A. Kelson, S. V. Bhosale and E. Vauthey, *Phys. Chem. Chem. Phys.*, 2014, **16**, 5188-5200.
7. M. A. Kobaisi, S. V. Bhosale, K. Latham, A. M. Raynor and S. V. Bhosale, *Chem. Rev.*, 2016, **116**, 11685-11796.
8. M. Handayani, S. Gohda, D. Tanaka and T. Ogawa, *Chem. Eur. J.*, 2014, **20**, 7655-7664.
9. S. V. Bhosale, C. H. Jani and S. J. Langford, *Chem. Soc. Rev.*, 2008, **37**, 331-342.
10. V. L. Gunderson, A. L. Smeigh, C. H. Kim, D. T. Co and M. R. Wasielewski, *J. Am. Chem. Soc.*, 2012, **134**, 4363-4372.

11. D. Villamaina, S. V. Bhosale, S. J. Langford and E. Vauthey, *Phys. Chem. Chem. Phys.*, 2013, **15**, 1177-1187.

12. K. P. Ghiggino, J. A. Hutchison, S. J. Langford, M. J. Latter, M. A.-P. Lee and M. Takezaki, *Aust. J. Chem.*, 2006, **59**, 179-185.

13. D. Gust, T. A. Moore and A. L. Moore, *Acc. Chem. Res.*, 2001, **34**, 40-48.

14. N. Banerji, S. V. Bhosale, I. Petkova, S. J. Langford and E. Vauthey, *Phys. Chem. Chem. Phys.*, 2011, **13**, 1019-1029.

15. K. P. Ghiggino, J. A. Hutchison, S. J. Langford, M. J. Latter, M. A. P. Lee and M. Takezaki, *Aust. J. Chem.*, 2006, **59**, 179-185.

16. B. Robotham, K. A. Lastman, S. J. Langford and K. P. Ghiggino, *J Photochem. Photobiol. A Chem.*, 2013, **251**, 167-174.

17. L. H. Tong, P. Pengo, W. Clegg, J. P. Lowe, P. R. Raithby, J. K. M. Sanders and S. I. Pascu, *Dalton Trans.*, 2011, **40**, 10833-10842.

18. M. J. Crossley, T. W. Hambley, L. G. Mackay, A. C. Try and R. Walton, *J. Chem. Soc., Chem. Commun.*, 1995, 1077-1079.

19. E. K. L. Yeow, P. J. Sintic, N. M. Cabral, J. N. H. Reek, M. J. Crossley and K. P. Ghiggino, *Phys. Chem. Chem. Phys.*, 2000, **2**, 4281-4291.

20. M. Faroughi, K. X. Zhu, P. Jensen, D. C. Craig and A. C. Try, *Eur. J. Org. Chem.*, 2009, **2009**, 4266-4272.

21. V. Promarak and P. L. Burn, *J. Chem. Soc., Perkin Trans. 1*, 2001, 14-20.

22. M. I. Ansari, PhD Thesis, Macquarie University, Australia, 2017.

23. C. M. A. Alonso, M. G. P. M. S. Neves, A. C. Tomé, A. M. S. Silva and J. A. S. Cavaleiro, *Tetrahedron*, 2005, **61**, 11866-11872.

24. H. K. Hombrecher, V. M. Gherdan, S. Ohm, J. A. S. Cavaleiro, M. d. Graça, P. M. S. Neves and M. d. Fátima Condesso, *Tetrahedron*, 1993, **49**, 8569-8578.

25. A. J. Avestro, D. M. Gardner, N. A. Vermeulen, E. A. Wilson, S. T. Schneebeli, A. C. Whalley, M. E. Belowich, R. Carmieli, M. R. Wasielewski and J. F. Stoddart, *Angew. Chem., Int. Ed.*, 2014, **53**, 4442-4449.

26. R. S. Bhosale, M. Al Kobaisi, S. V. Bhosale, S. Bhargava and S. V. Bhosale, *Sci. Rep.*, 2015, **5**, 14609.

27. J. Kroon, A. M. Oliver, M. N. Paddon-Row and J. W. Verhoeven, *J. Am. Chem. Soc.*, 1990, **112**, 4868-4873.

28. B. Kang, W. Yang, S. Lee, S. Mukherjee, J. Forstater, H. Kim, B. Goh, T.-Y. Kim, V. A. Voelz and Y. Pang, *Sci. Rep.*, 2017, **7**.

SUPPORTING INFORMATION

Synthesis and Photophysical Studies of β,β′-Pyrrolic Tetraaryl fused-Porphyrin Tröger's Base-Naphthalene Diimide Dyad

Md Imam Ansari, Andrew Try, and Peter Karuso*

Department of Molecular Sciences, Macquarie University, Sydney NSW 2109, Australia

* Corresponding author. Tel.: +612-9850-8290 fax: +612-9850-8313, e-mail: peter.karuso@mq.edu.au

Porphyrin Tröger's Base 2

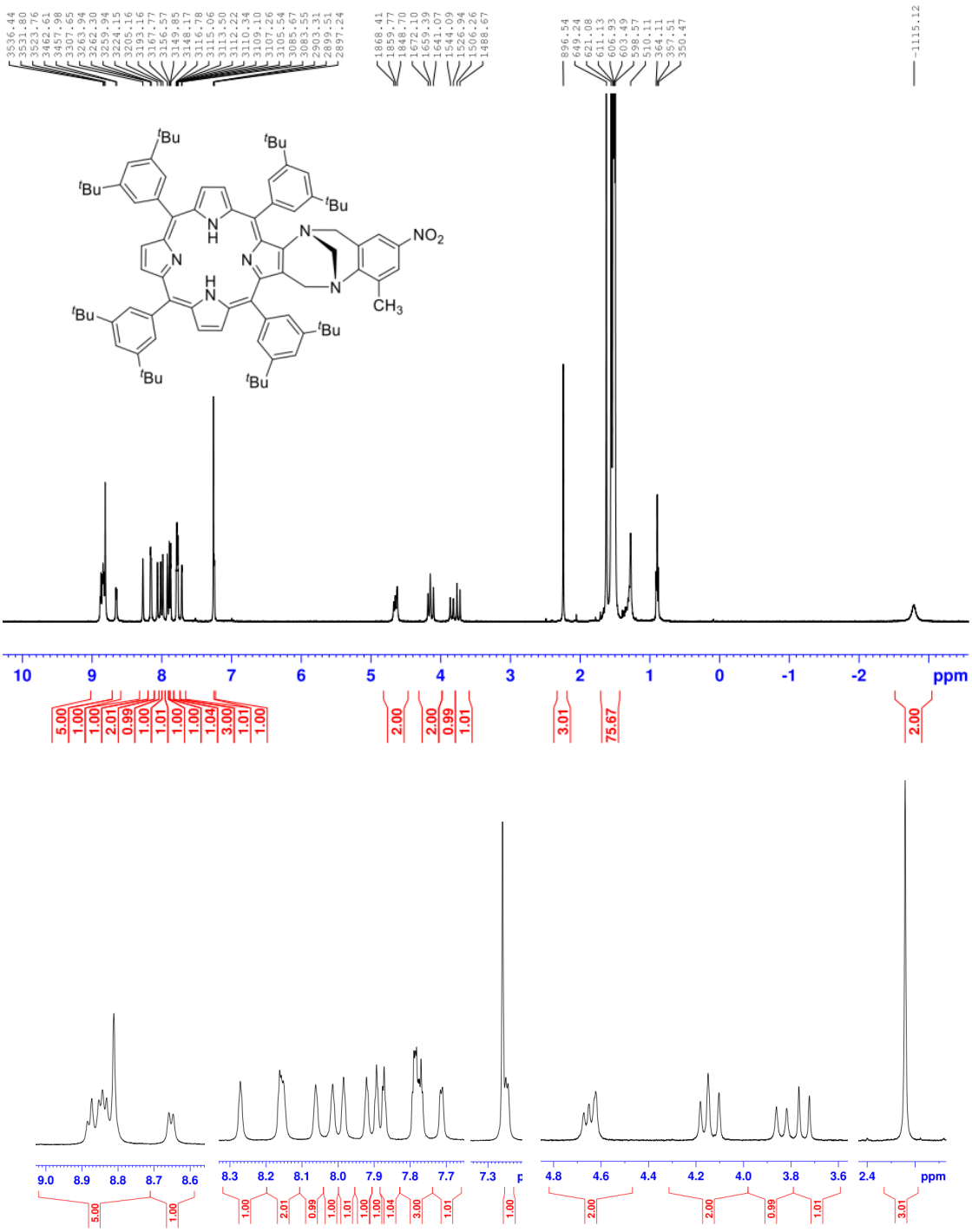

Fig. S1 ^{1}H NMR spectrum (400 MHz) of **2** in $CDCl_3$.

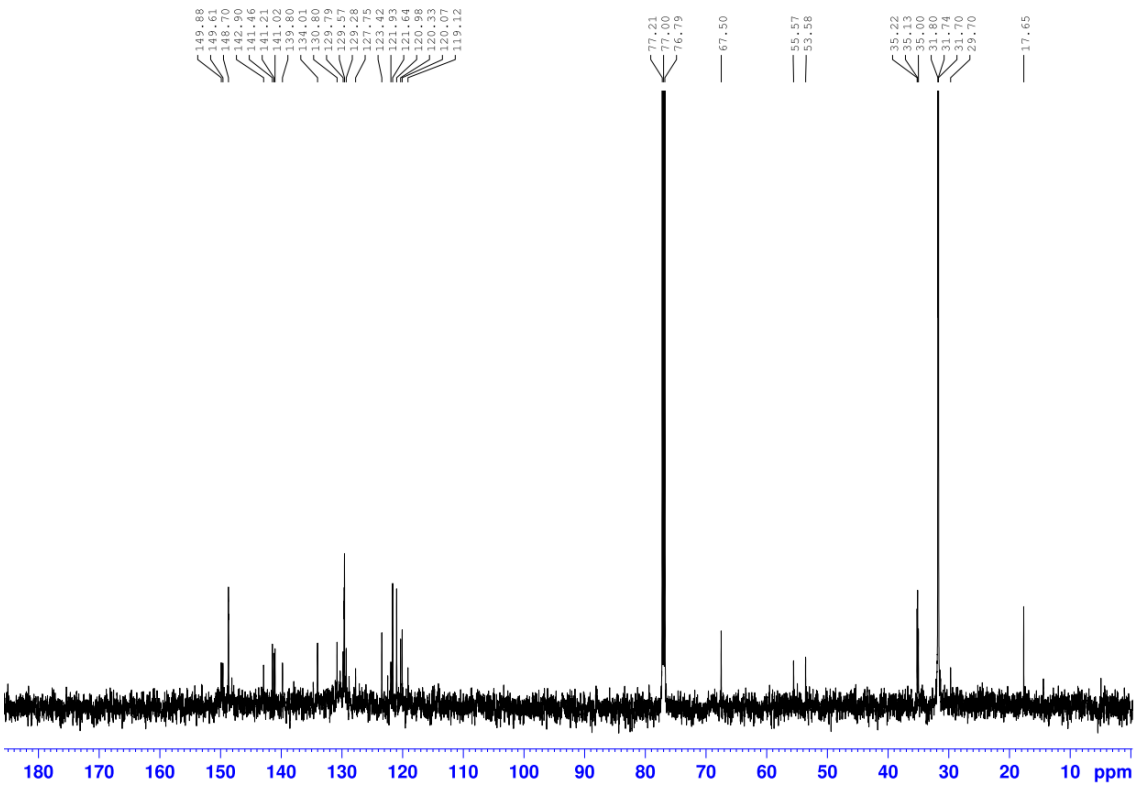

Fig. S2 ^{13}C NMR spectrum (150 MHz) of **2** in $CDCl_3$.

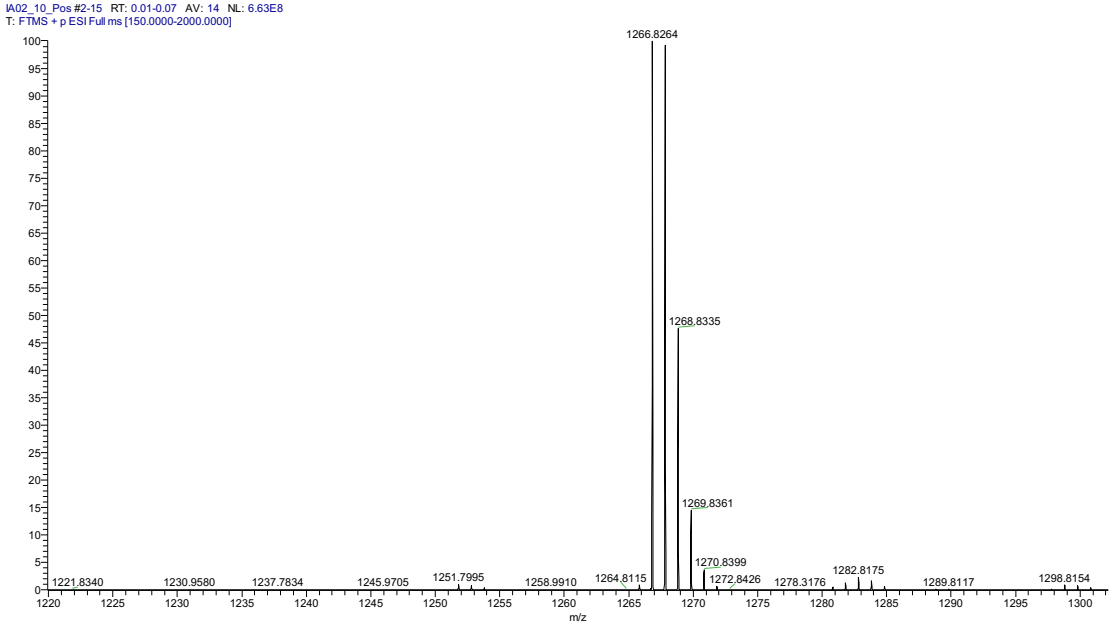

Fig. S3 High resolution mass spectrum of porphyrin TB **2**.

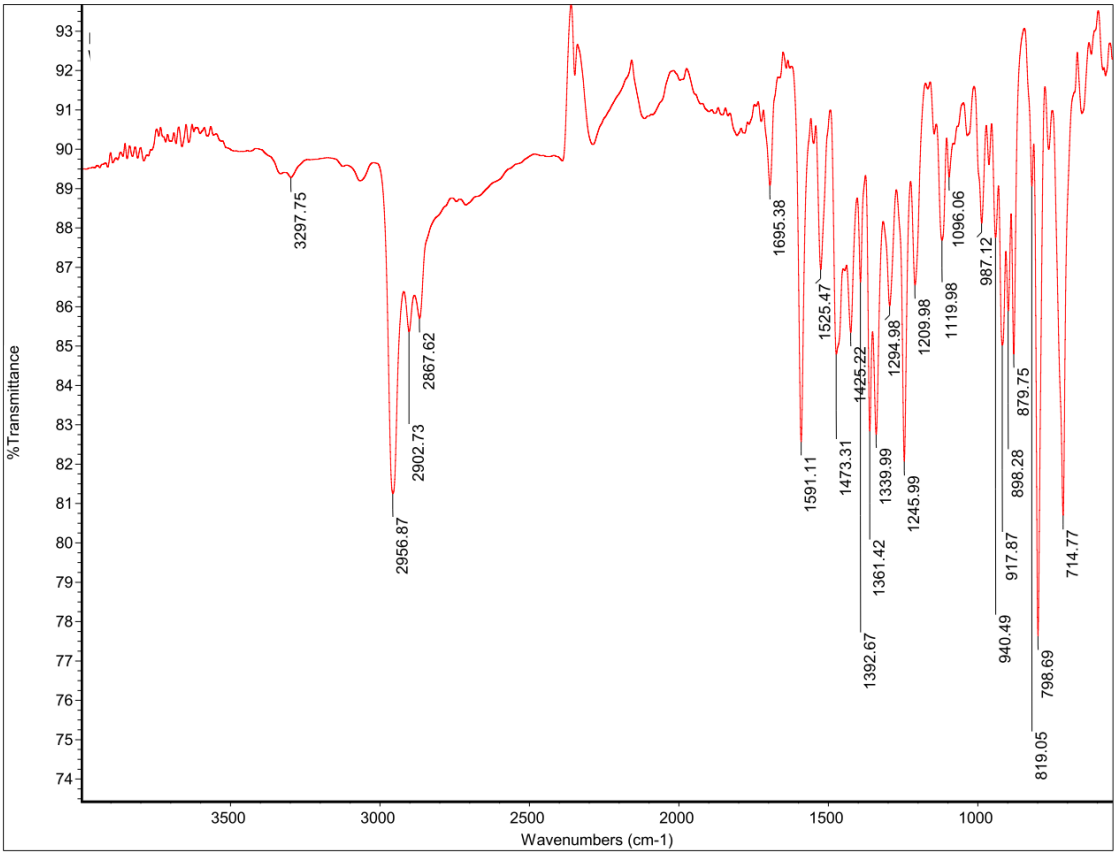

Fig. S4 Fourier transform infrared (FTIR) spectrum of porphyrin Tröger's base **2**.

Porphyrin Tröger's Base 5

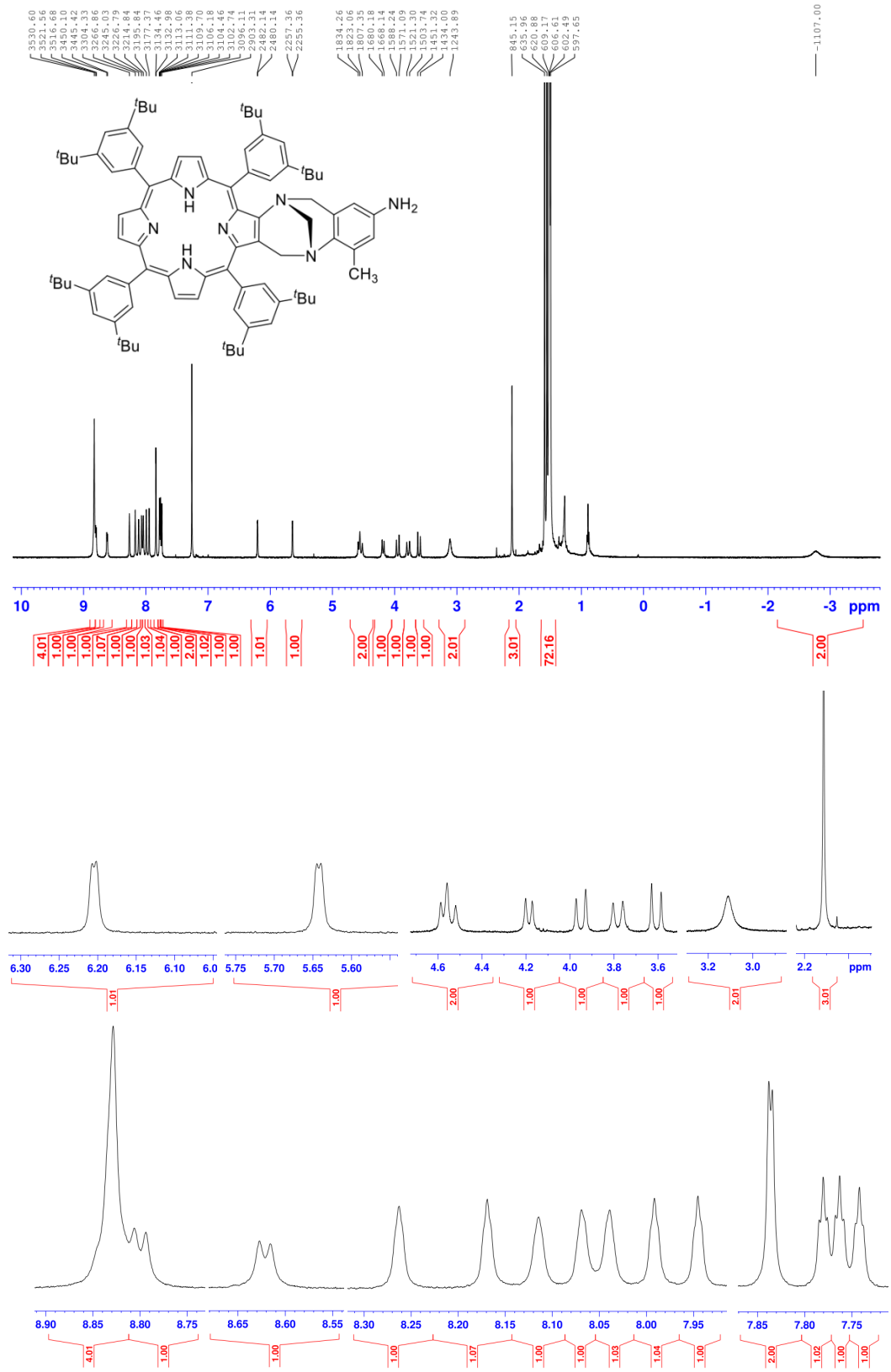

Fig. S5 ^{1}H NMR spectrum (400 MHz) of **5** in $CDCl_3$.

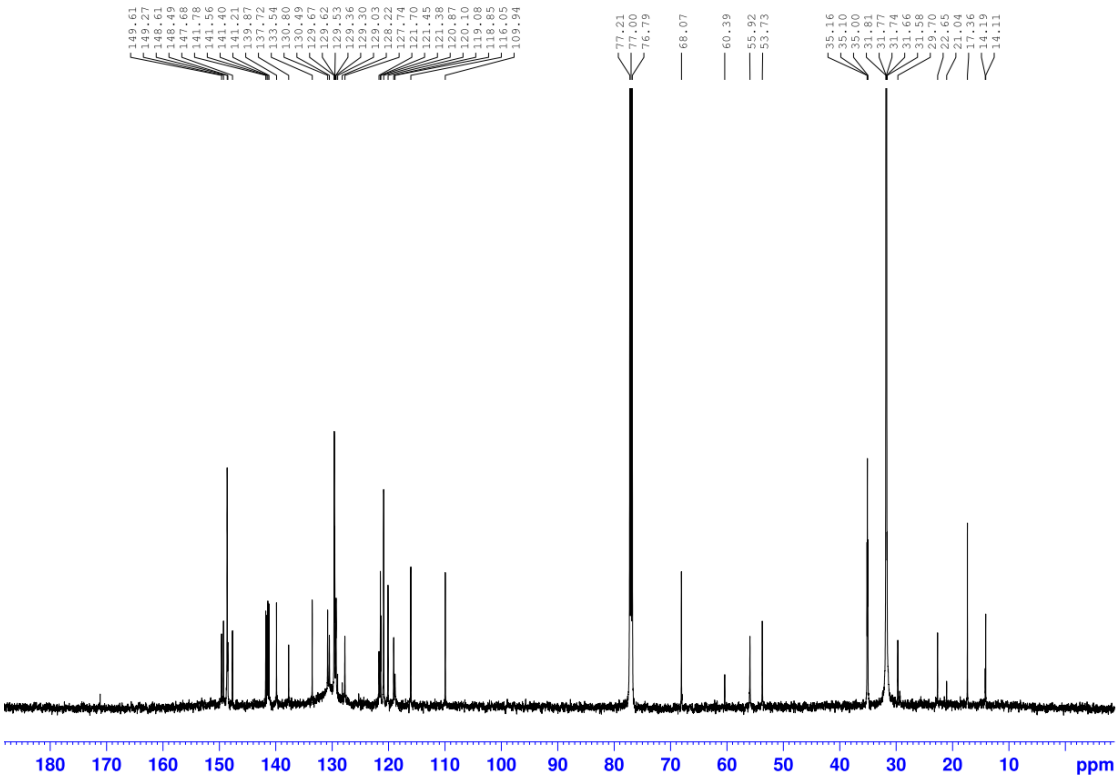

Fig. S6 ^{13}C NMR spectrum (150 MHz) of **5** in $CDCl_3$.

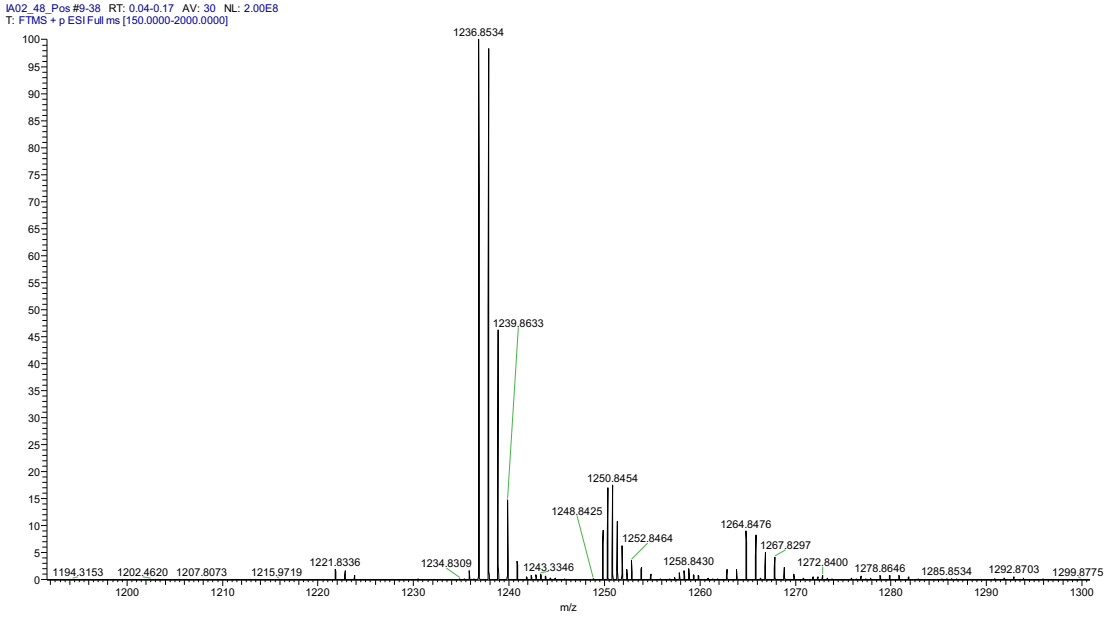

Fig. S7 High resolution mass spectrum of porphyrin TB **5**.

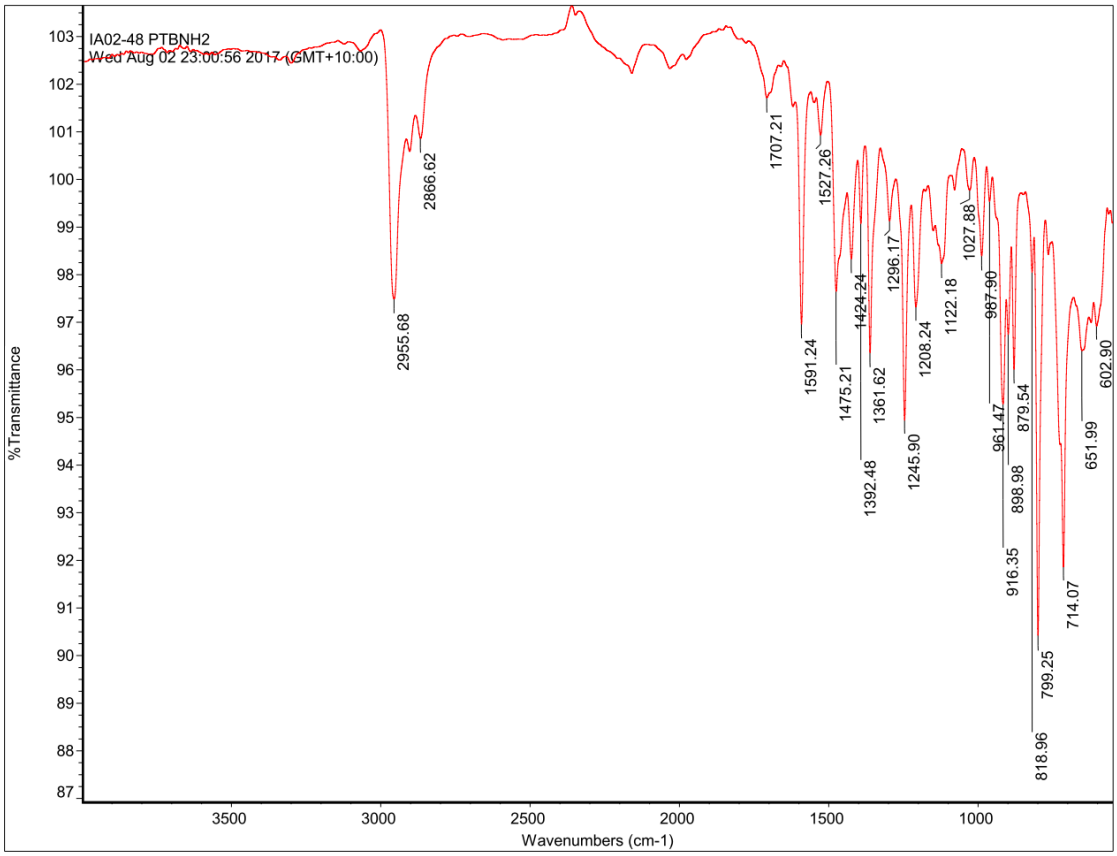

Fig. S8 Fourier transform infrared (FTIR) spectrum of porphyrin Tröger's base **5**.

Porphyrin Tröger's Base 6

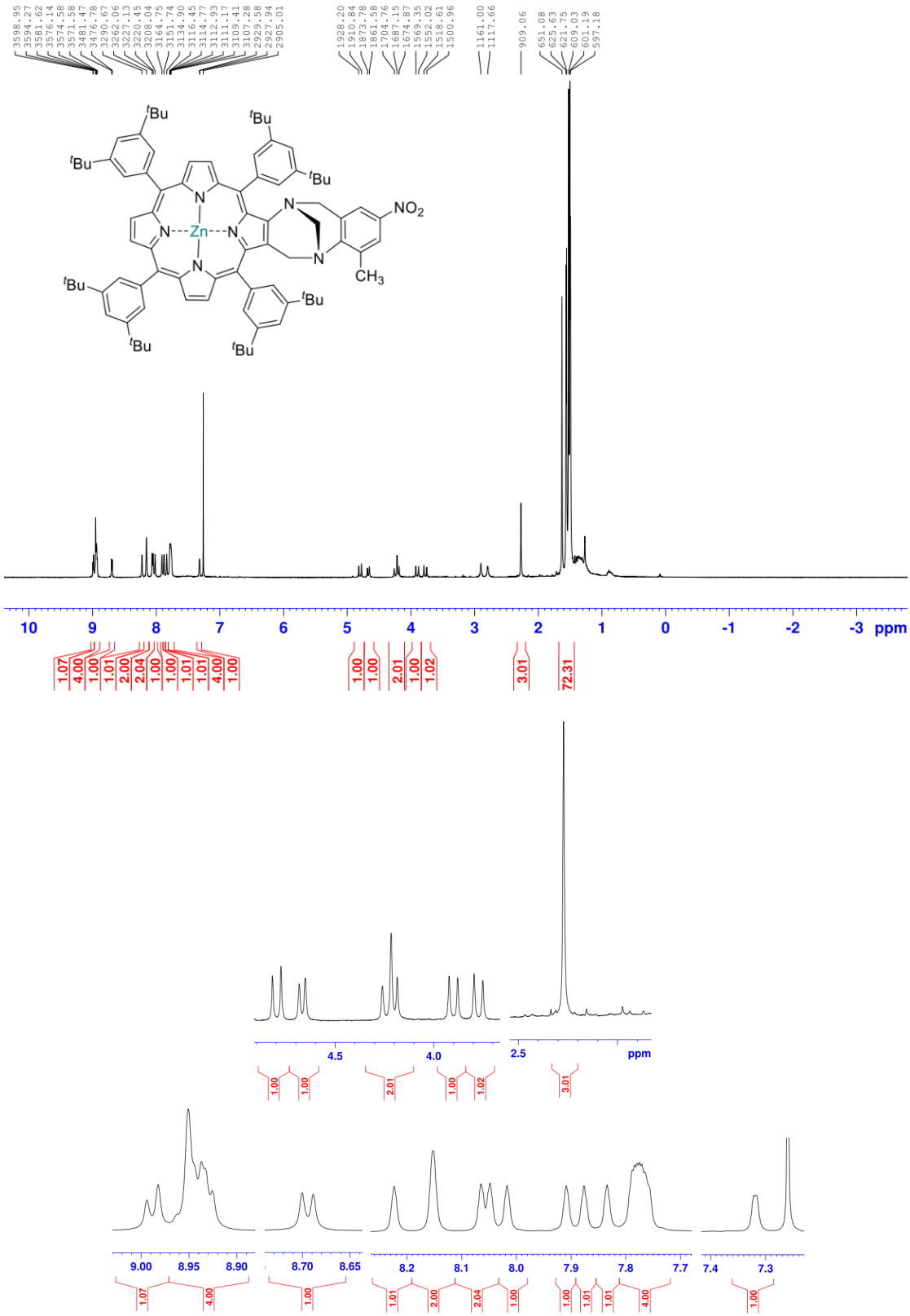

Fig. S9 ^{1}H NMR spectrum (400 MHz) of **6** in $CDCl_3$.

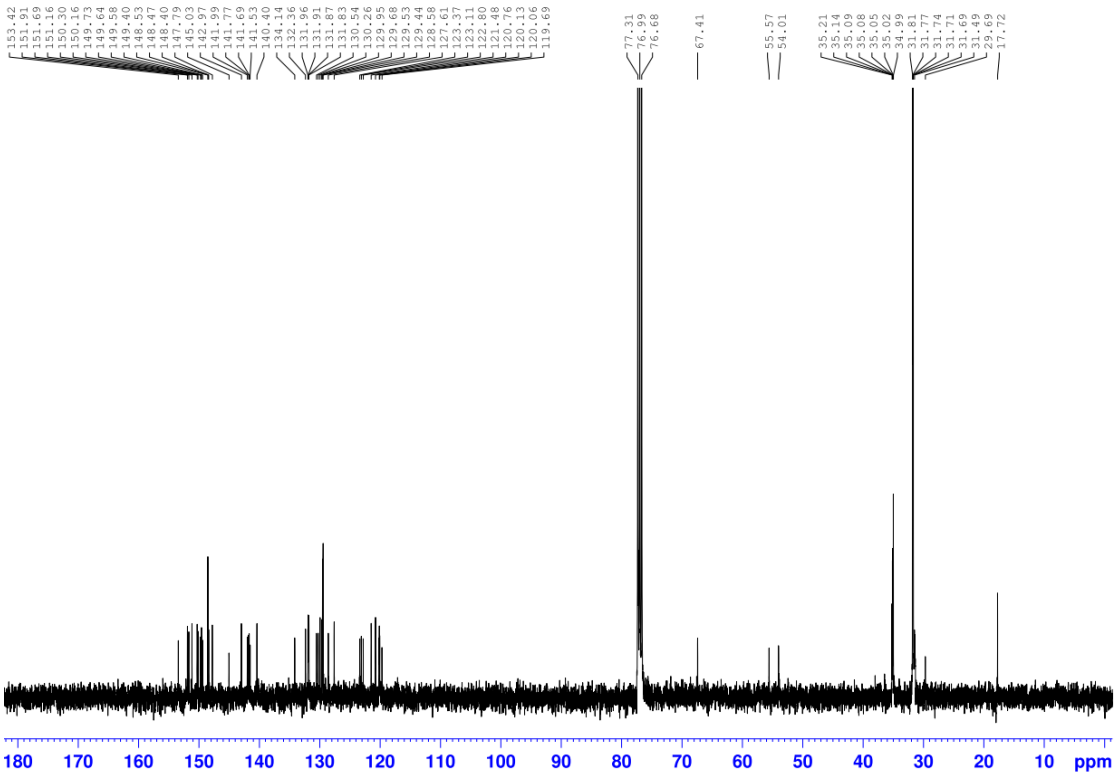

Fig. S10. ^{13}C NMR spectrum (150 MHz) of **6** in $CDCl_3$.

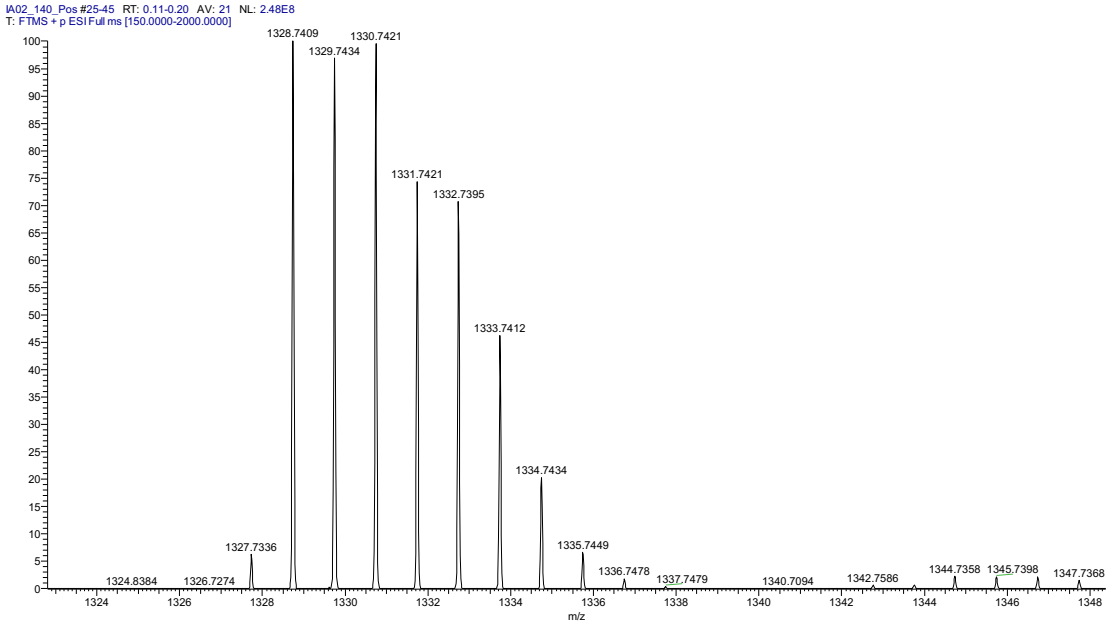

Fig. S11 High resolution mass spectrum of porphyrin TB **6**.

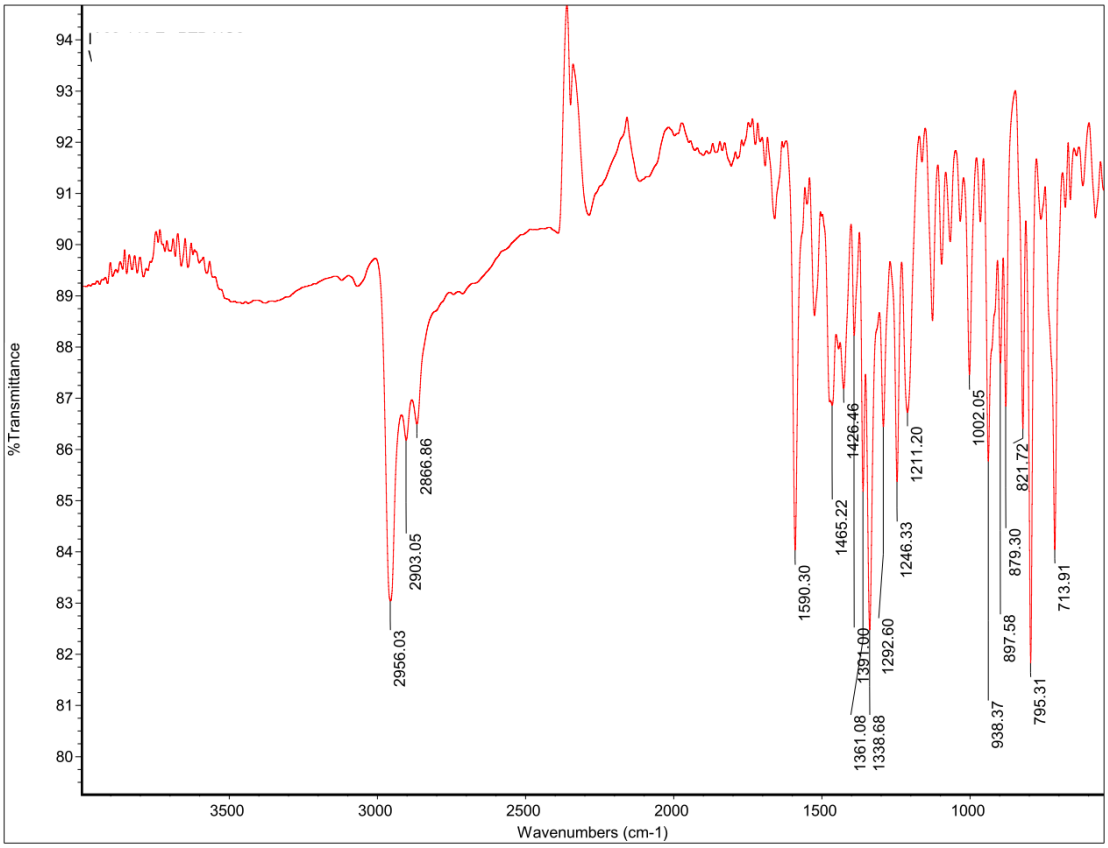

Fig. S12 Fourier transform infrared (FTIR) spectrum of porphyrin Tröger's base **6**.

Porphyrin Tröger's Base 7

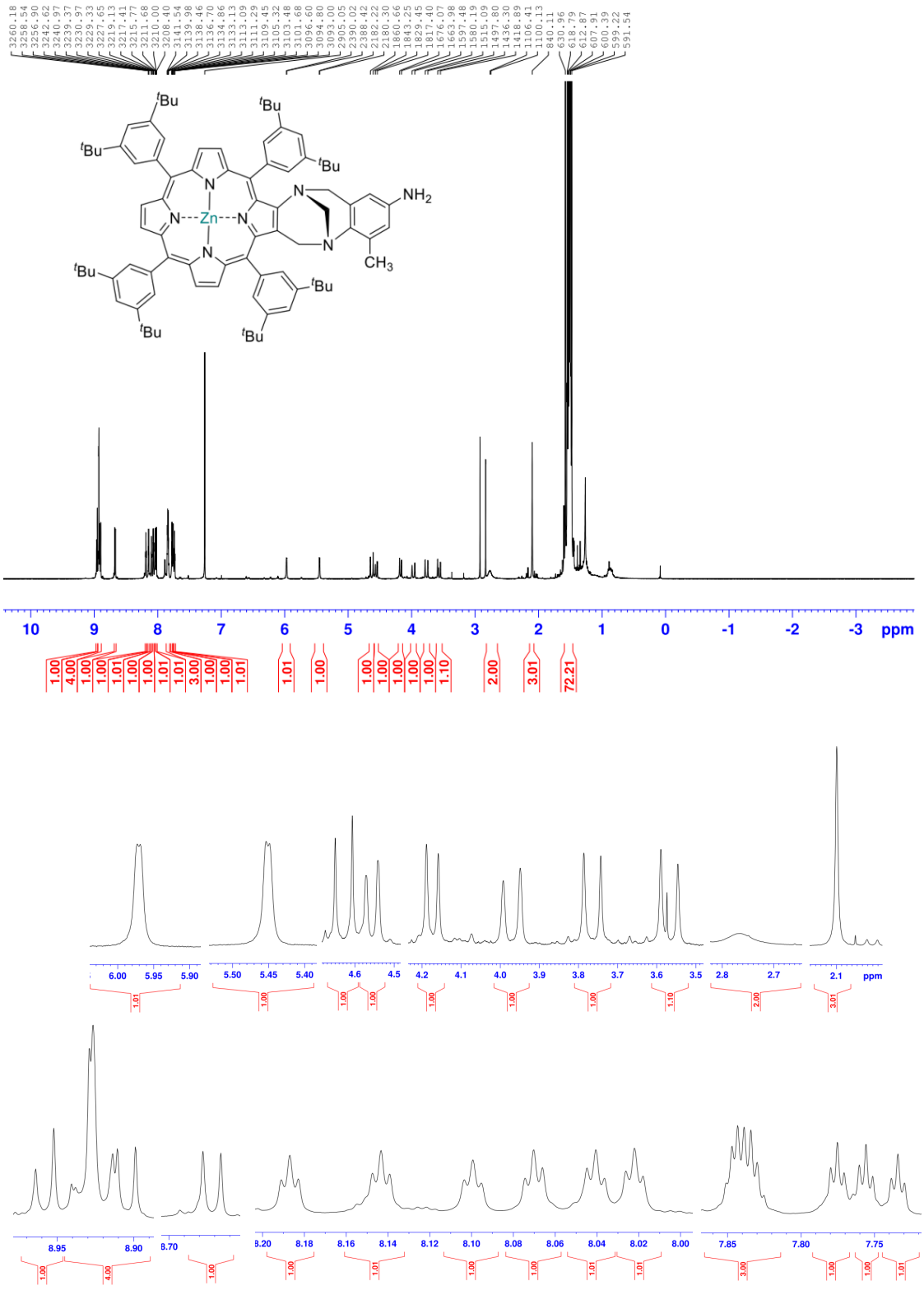

Fig. S13 ^{1}H NMR spectrum (400 MHz) of **7** in $CDCl_3$.

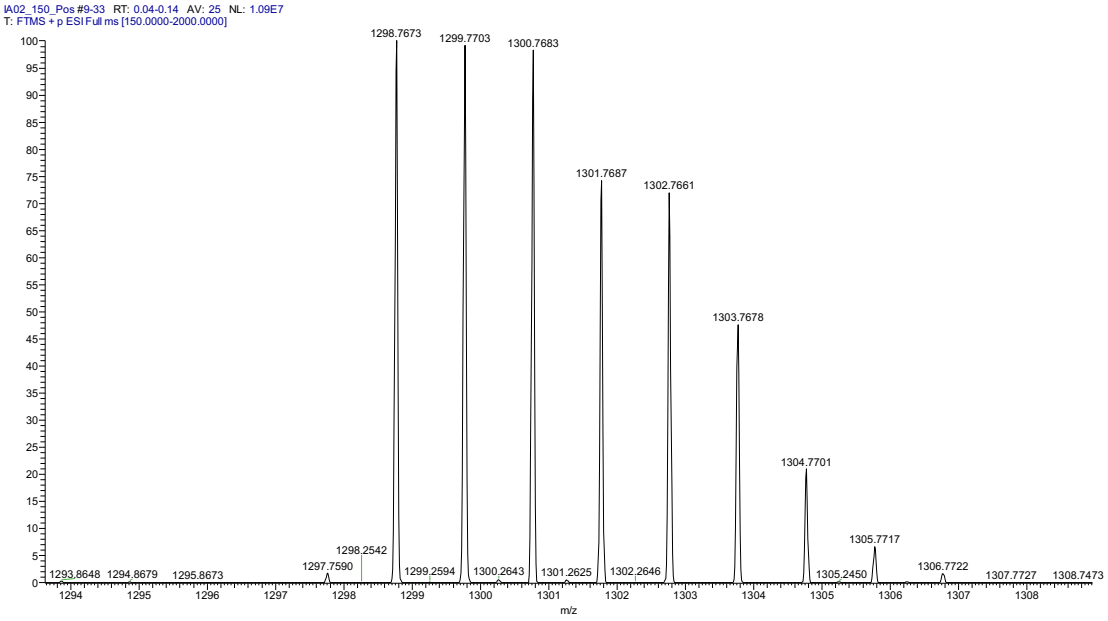

Fig. S14 High resolution mass spectrum of porphyrin TB **7**.

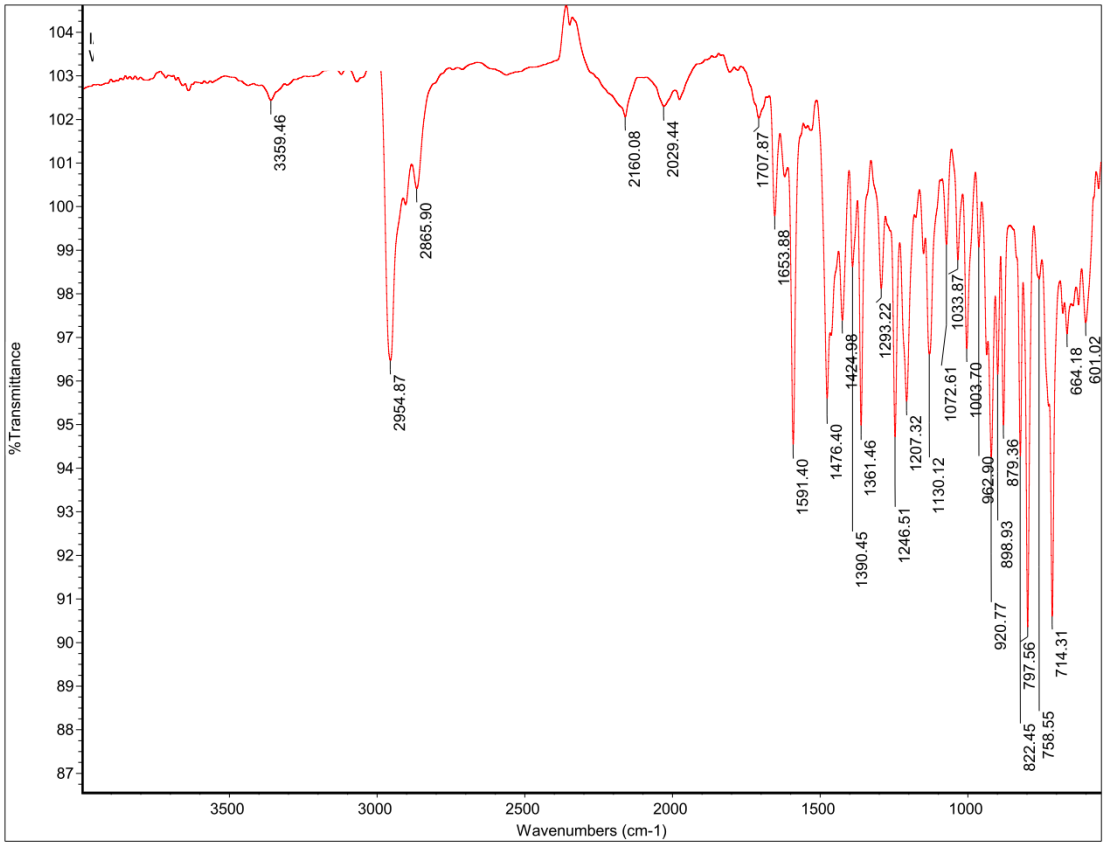

Fig. S15 Fourier transform infrared (FTIR) spectrum of porphyrin Tröger's base **7**.

Porphyrin TB naphthalene diimide dyad 9

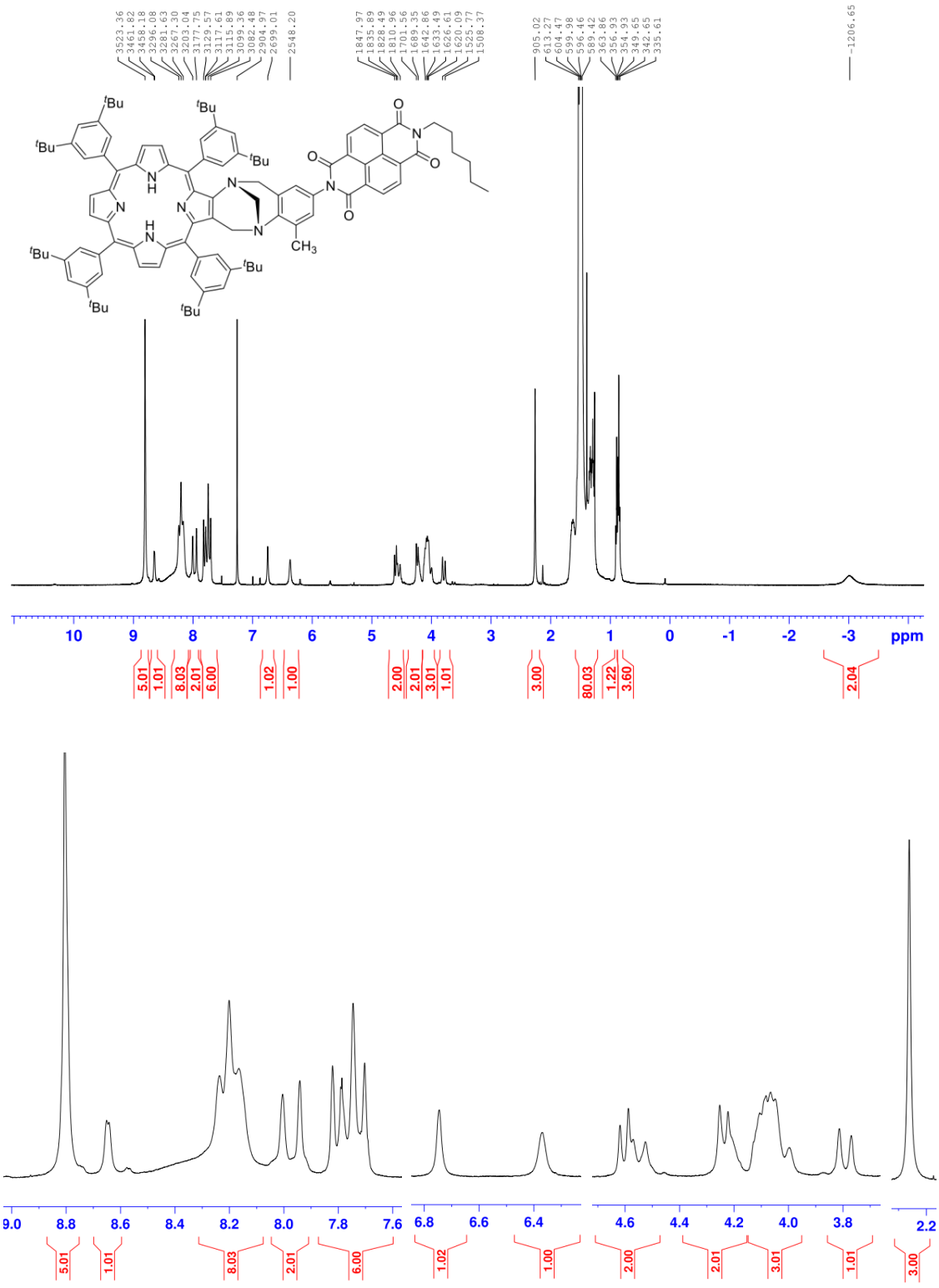

Fig. S16 ^{1}H NMR spectrum (400 MHz) of **9** in $CDCl_3$.

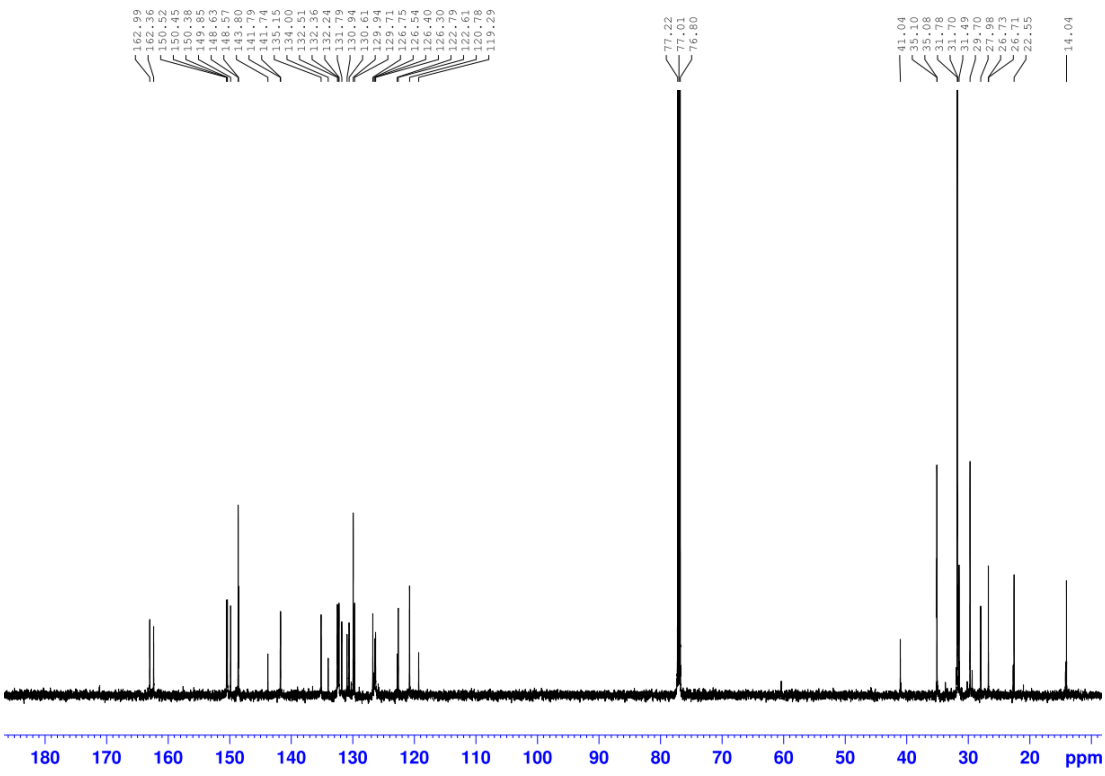

Fig. S17 ^{13}C NMR spectrum (150 MHz) of **9** in $CDCl_3$.

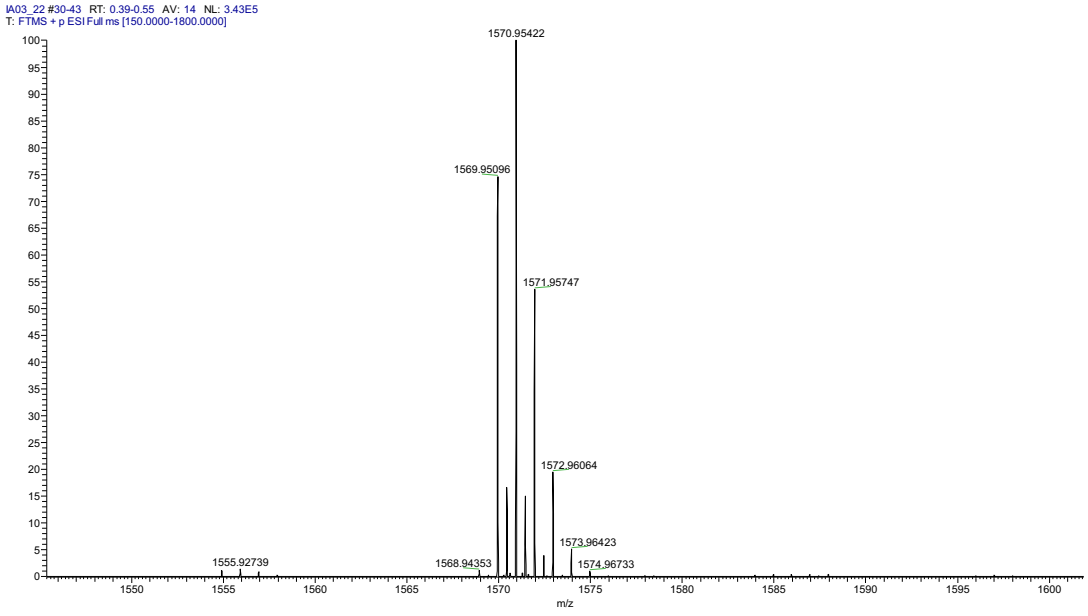

Fig. S18 High resolution mass spectrum of porphyrin TB **9**.

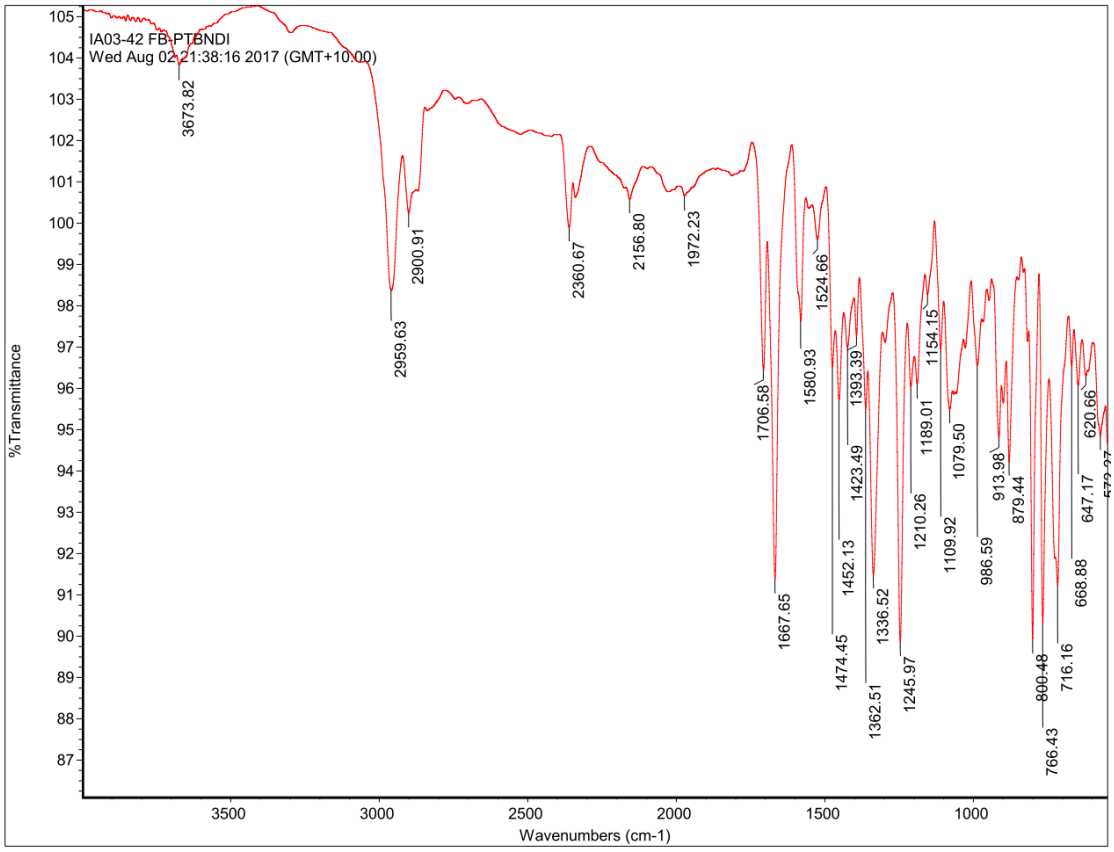

Fig. S19 Fourier transform infrared (FTIR) spectrum of porphyrin Tröger's base **9**.

Zinc(II)porphyrin TB-NDI dyad 10

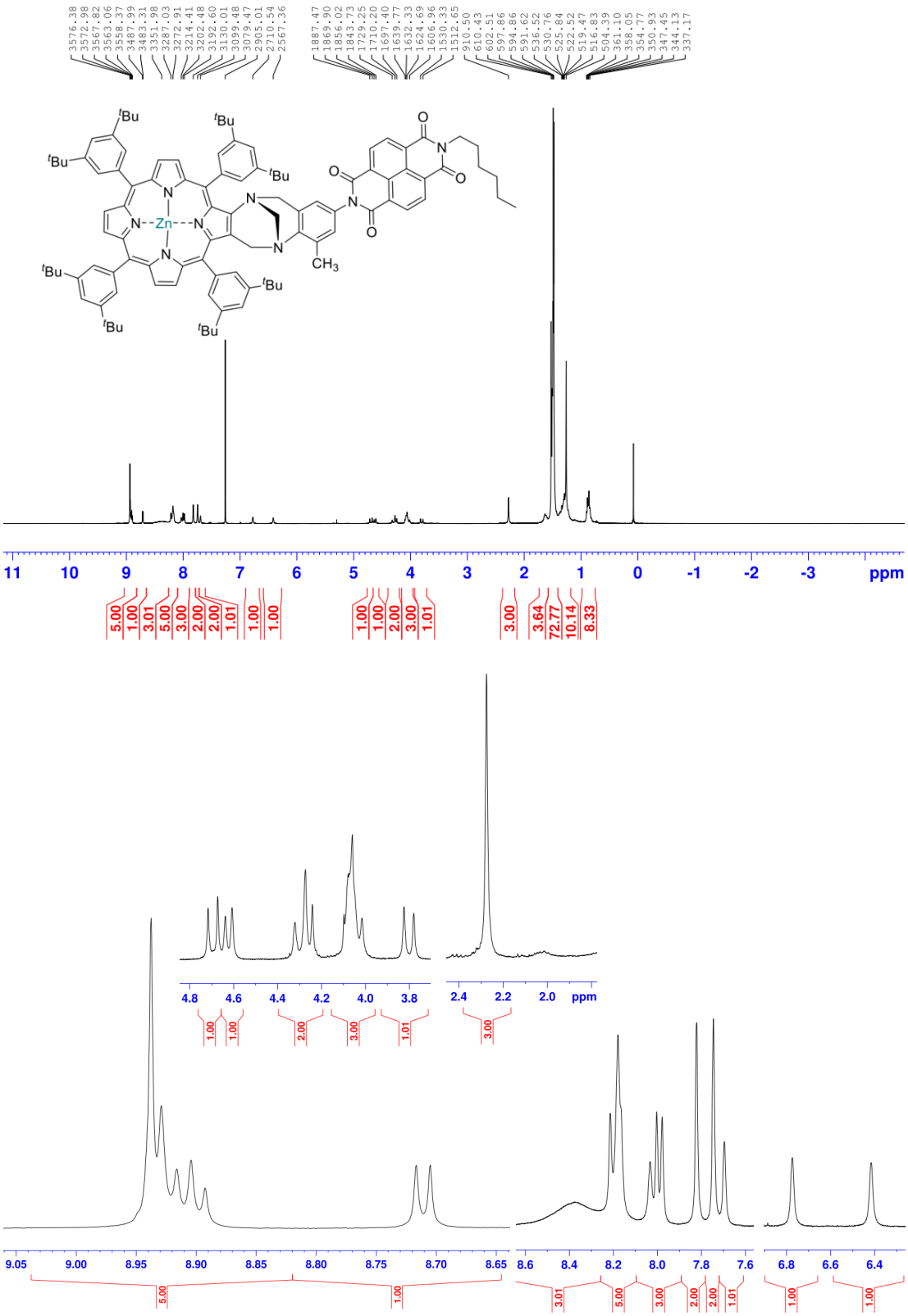

Fig. S19 ^{1}H NMR spectrum (400 MHz) of **10** in $CDCl_3$.

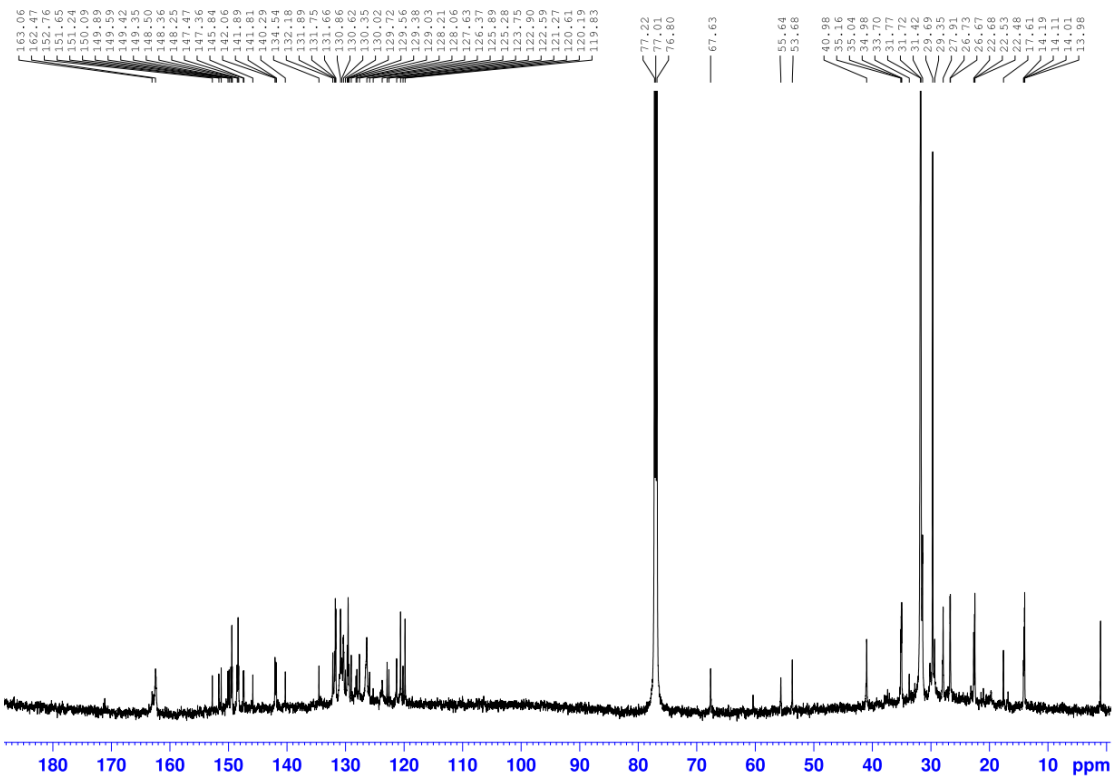

Fig. S20. ^{13}C NMR spectrum (150 MHz) of **10** in $CDCl_3$.

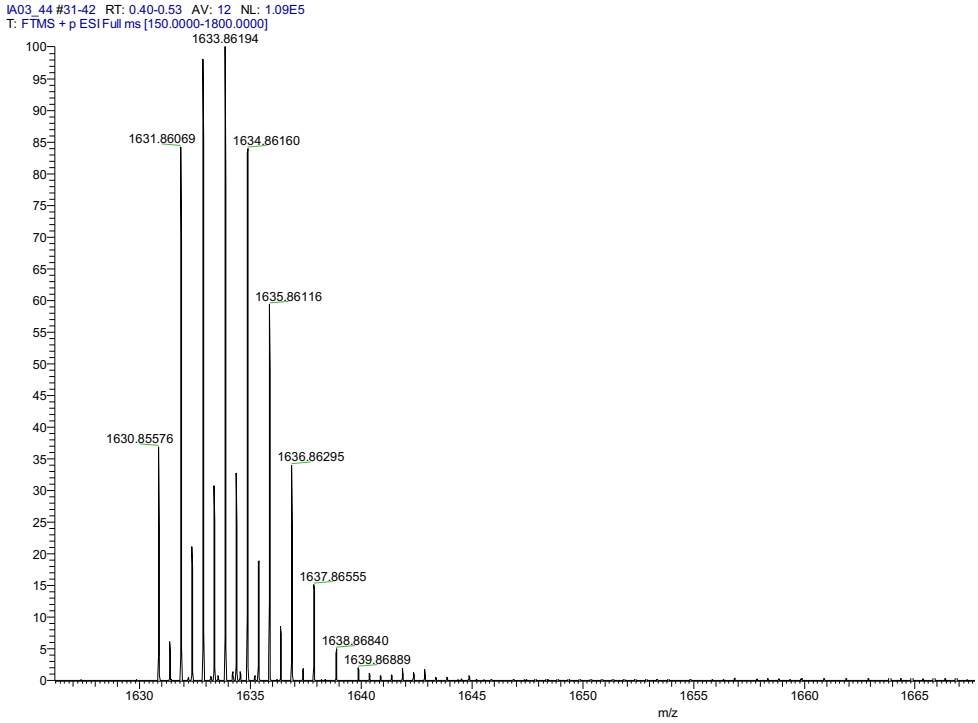

Fig. S21 High resolution mass spectrum of porphyrin TB **10**.

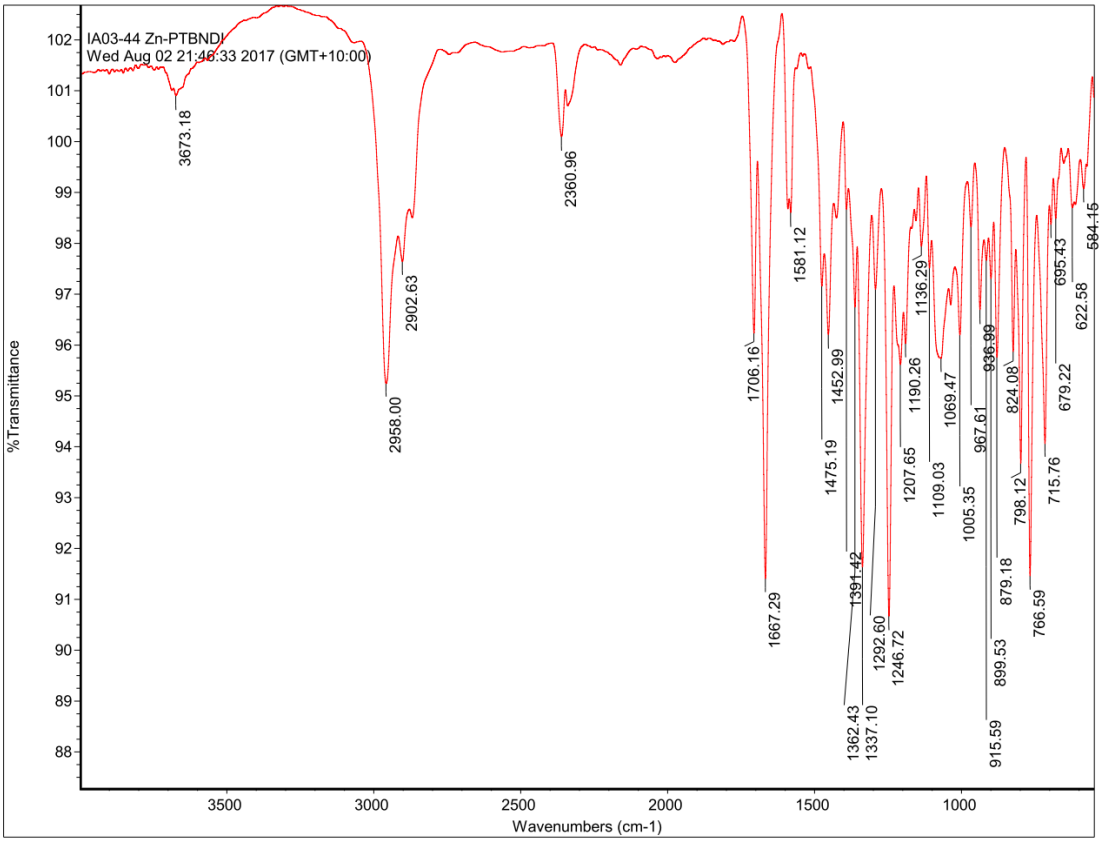

Fig. S22 Fourier transform infrared (FTIR) spectrum of porphyrin Tröger's base **10**.

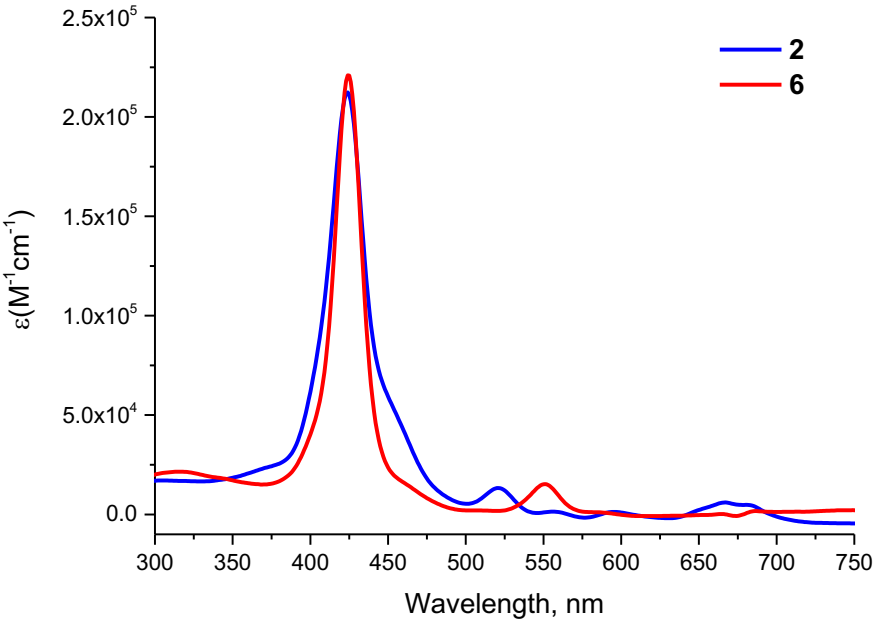

Fig. S23 UV-visible spectrum of **2** and **6** in $CHCl_3$. The concentration of each compound was 2.5×10^{-6} M.

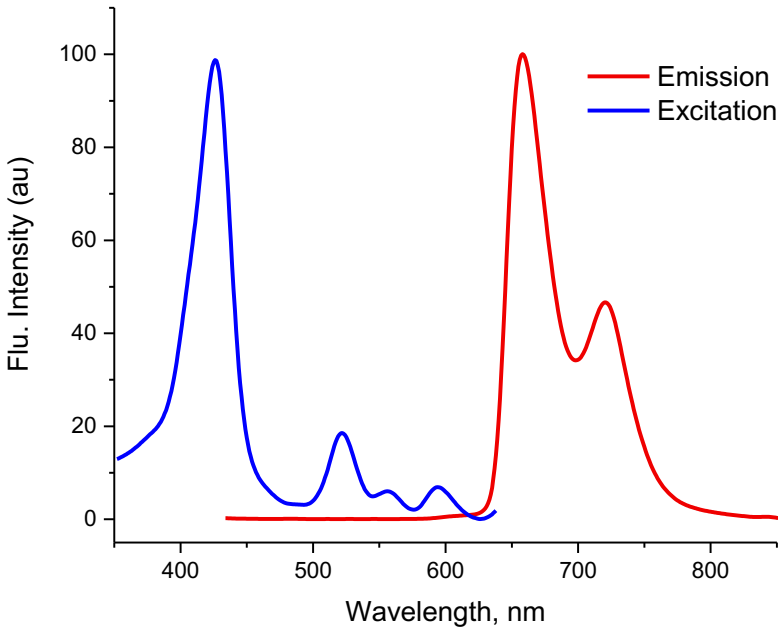

Fig. S24 Fluorescence excitation (blue) and emission (red) spectra of **2** (2.5×10^{-6} M) in $CHCl_3$.

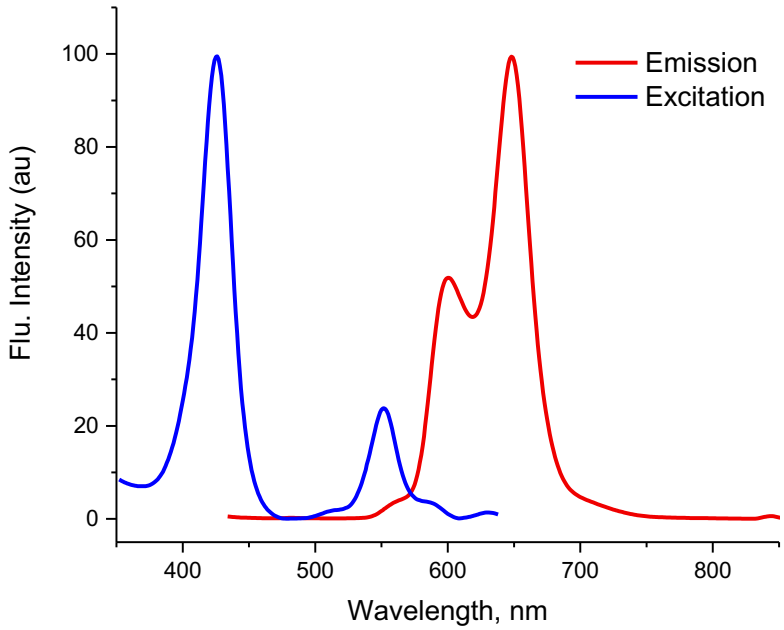

Fig. S25 Fluorescence excitation (blue) and emission (red) spectra of **6** (2.5×10^{-6} M) in $CHCl_3$.

Chapter Six

6.1 Discussion and Conclusions

The work presented in this thesis focuses on the design and synthesis of porphyrins with a Tröger's base framework, as building blocks for donor-acceptor complexes that can (potentially) be employed either for: light harvesting complexes or scaffolding materials for the construction of more complex artificial photosynthetic models.

We first investigated the synthesis of symmetric and hybrid Tröger's base (Chapter 2). Subsequently, we applied post-TB modification strategies to incorporate either naphthalene diimide or fullerene-C_{60} onto the TB framework. Hence, the novel NDI and fullerene-C_{60} appended Tröger's base compounds were made and fully characterised by ^{1}H and ^{13}C NMR spectroscopies and high-resolution electron-spray ionization (HR-ESI) mass spectrometry. At this of stage of the project we were confident that NDI and C_{60} could be easily incorporated into the TB framework. This encouraged us to investigate the synthesis of more complex porphyrin Tröger's base NDI and C_{60} dyads as electron donor-acceptor complexes.

Before we explored the hybrid porphyrin-based systems, it was necessary to investigate the synthesis of symmetric porphyrin Tröger's base systems. The synthesised symmetric porphyrin Tröger's base dyads are reported in Chapter 3. Two different types of *meso*-aryl functionalised porphyrins were synthesised: 4-(10,15,20-tris(3,5-di-*tert*-butylphenyl)porphyrin-5-yl)aniline; and 4-(10,15,20-triphenylporphyrin-5-yl)aniline to investigate their incorporation into a Tröger's base scaffold. Consequently, a series of new symmetric porphyrin Tröger's bases were synthesised and fully characterised. The dyads were shown to have a V-shaped geometry bridged by the Tröger's base. Moreover, it was demonstrated that the porphyrin anilines (3,5-di-*tert*-butylphenylporphyrins) provided easy access, in high yields, to a highly soluble

porphyrin Tröger's base dyads. Our synthetic methodology can be easily scaled up to gram quantities. The preliminary photophysical properties were studied by UV/Visible and fluorescence spectroscopy and intramolecular interaction between two porphyrin moieties was evident.

On the other hand, in Chapter 4, we prepared hybrid porphyrin Tröger's base, with different functionalities such as ester, alcohol, and aldehyde as building blocks. We optimised the reaction conditions and prepared these compounds on gram scale. These novel hybrid porphyrin TBs are valuable compounds that creates the opportunity to work further on Tröger's base chemistry and could be potentially utilised for the host-guest chemistry. The next step of this project, saw us successfully utilise our novel hybrid porphyrin TBs as building blocks to append fullerene-C_{60} chromophore to afford porphyrin-TB-fullerene dyad. The photophysical properties of the final compounds were studied by UV/Vis and fluorescence spectroscopy. They indicated evidence for some electronic interaction and charge transfer from porphyrin to fullerene chromophore. For example, the emission band of free-base porphyrin-TB-fullerene dyad was quantitatively quenched (>90%), whereas this quenching was over 98% in its zinc counterpart.

We further explored the synthesis of hybrid porphyrin Tröger's bases (Chapter 5) by introducing different anilines (e.g. 2-methyl 4-nitroaniline) into the Tröger's base reaction. Amino and nitroporphyin TBs were synthesised and then subsequently their metal counterparts were made. In this phase of the project, our objective was to replace the fullerene-C_{60} with the NDI as an electron acceptor component. We successfully synthesised the target porphyrin-TB-NDI dyads. The photophysical properties of the final compounds were studied by UV/Vis and fluorescence spectroscopy which indicated some electronic interaction between the porphyrin and NDI.

The examples of donor-acceptor pairs compounds presented in thesis are potentially useful as building blocks for efficient electron and energy transfer in organic photovoltaics, light harvesting complexes and artificial photosynthetic models.

6.2 Future Work

Research never ends! The synthesised dyads will be studied by femtosecond or nanosecond transient absorption spectroscopy in order to investigate photoinduced electron and energy transfer processes as well as femtosecond and nanosecond fluorescence decay measurements.

In addition, ab initio/ DFT calculations will be used to shed light on the charge-transfer processes and provide structural insights.

In the future: More potential dyads and triads can be made by introducing similar chromophores with varying distance of the Tröger's base framework. The more complex and multicomponent assemblies with Tröger's base bridge can be prepared (Fig. 1). For example, imidazoloporphyrin TB dyads (Scheme 1) and bis-porphyrin-fullerene and tris-porphyrin triads (Scheme 2).

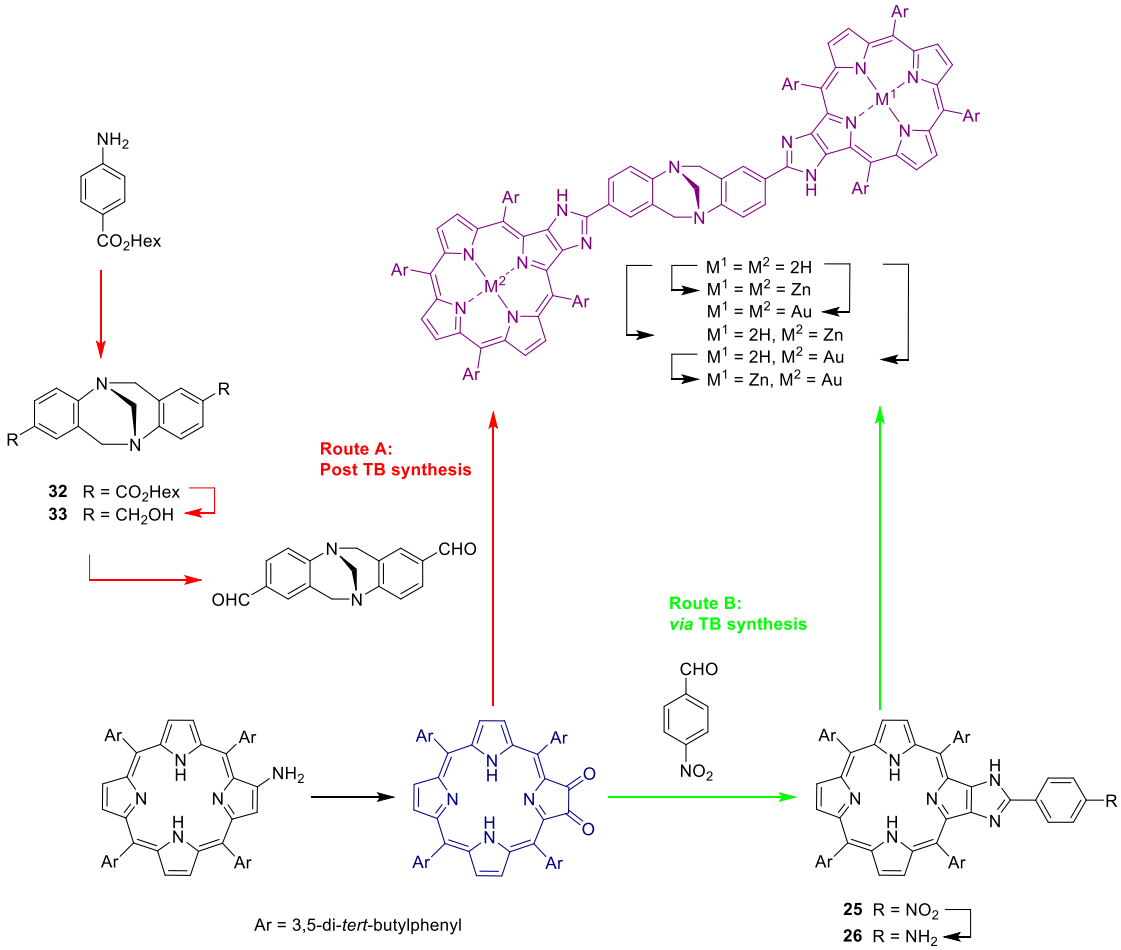

Scheme 1. Synthesis of dyads with varying distance of bridging molecule.

Increasing Complexity: Dyad to Triad

Apical Bridge Conversion: a two-step process: The synthesised dyads in this thesis could be utilised to make triads in future.

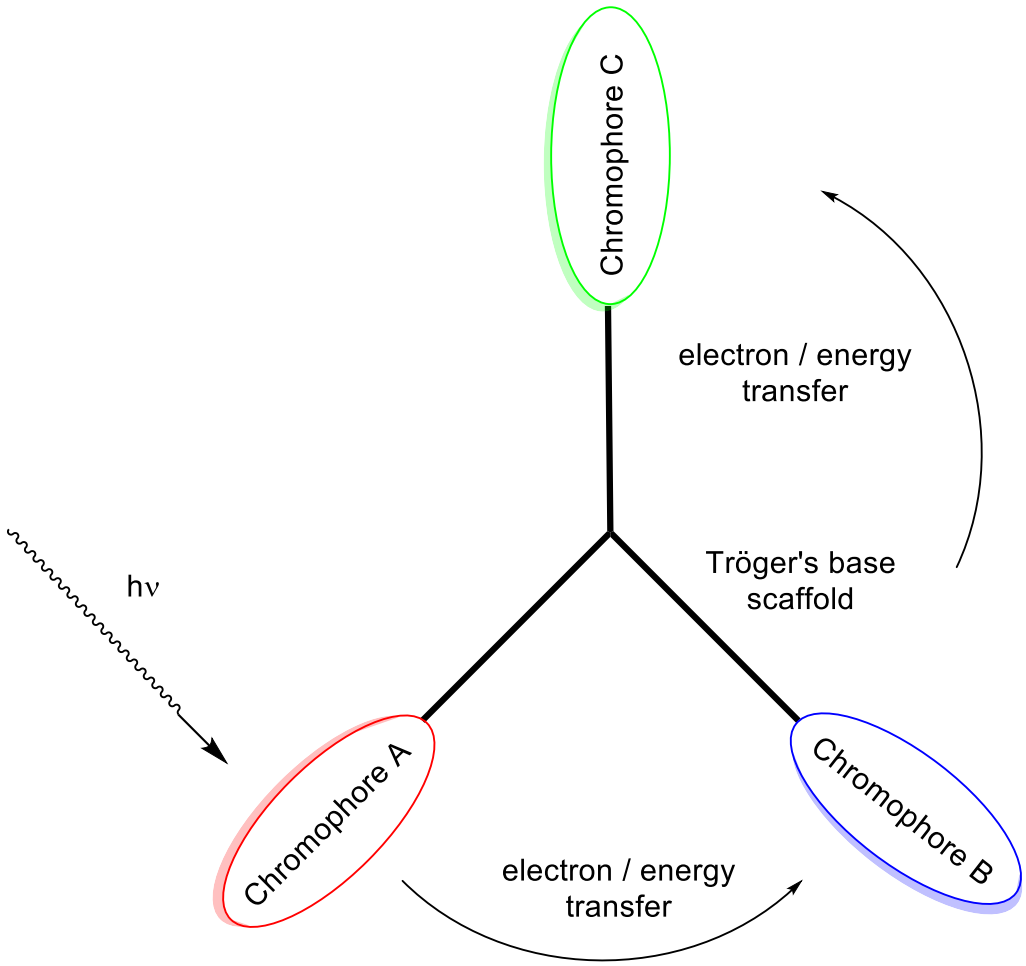

Fig. 1 Schematic view of Triad

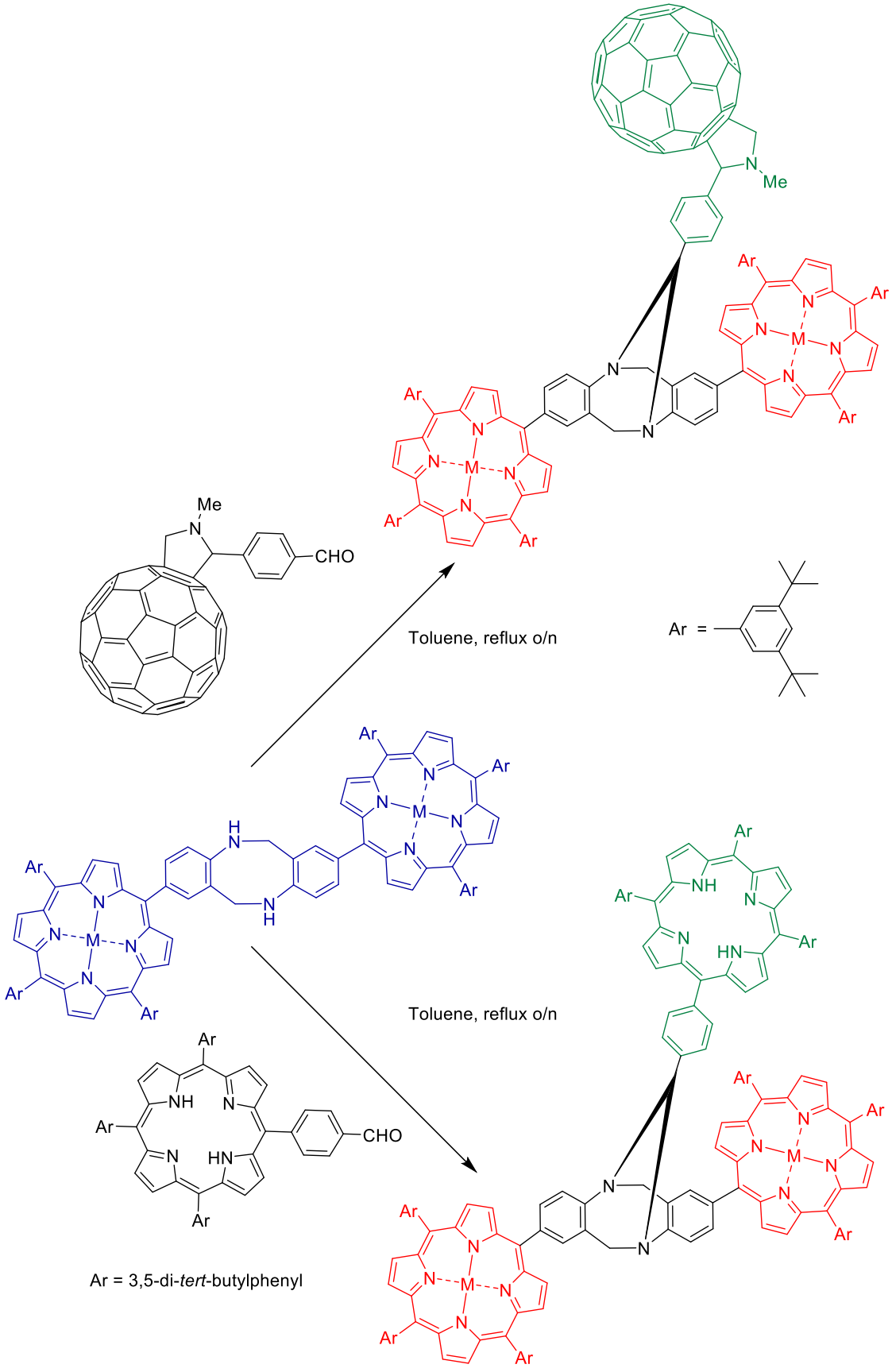

Scheme 2. Synthesis of triads as molecular switches.

APPENDIX

- Appendix contains ^{1}H NMR spectra of building blocks which were synthesised in this work.
    - Tröger's base building blocks (Appendix Section Chapter 2).
    - Porphyrin building blocks (Appendix Section Chapter 3.).

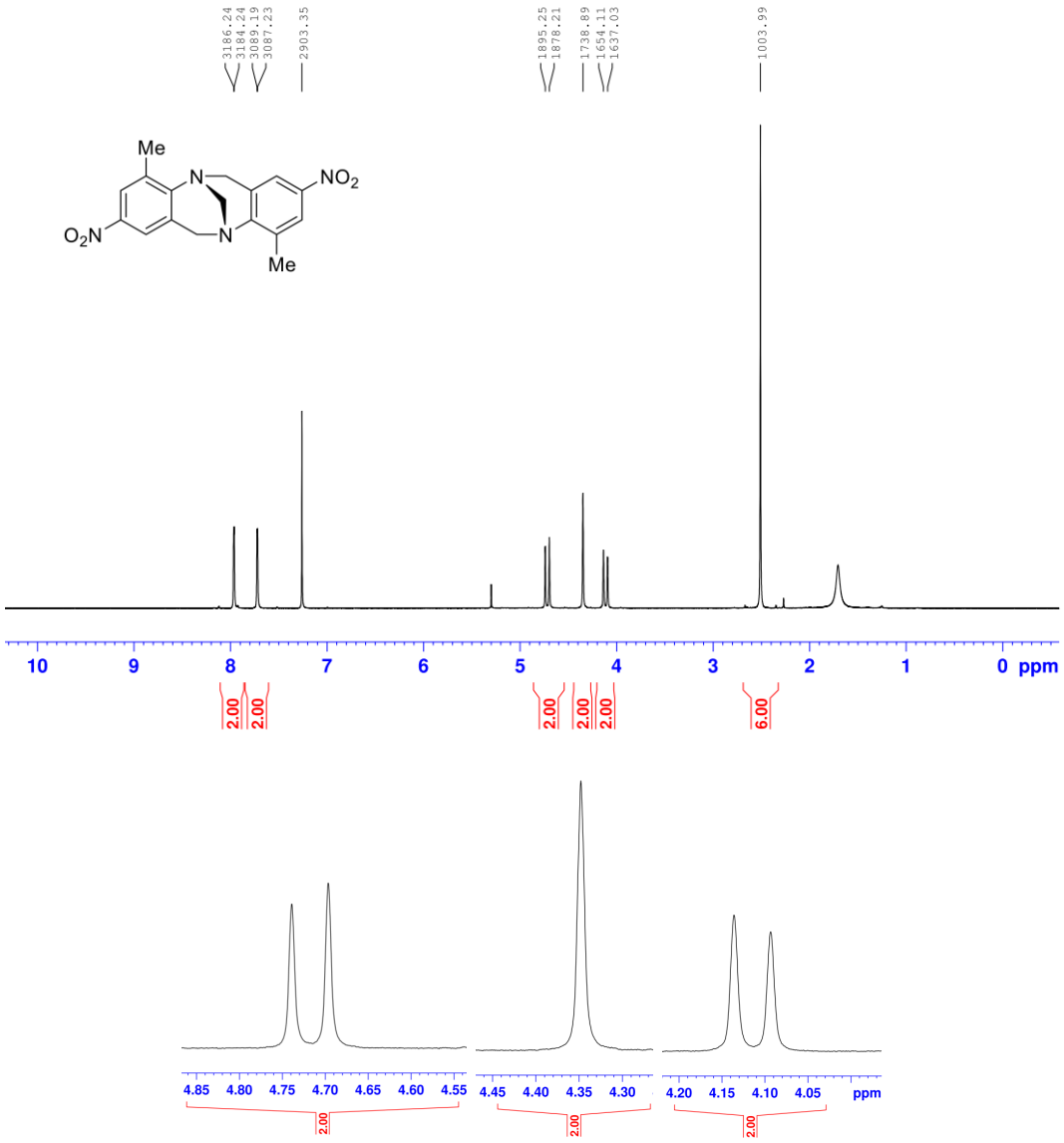

Fig. A1. ^{1}H NMR spectrum (400 MHz) of **1** in $CDCl_3$.

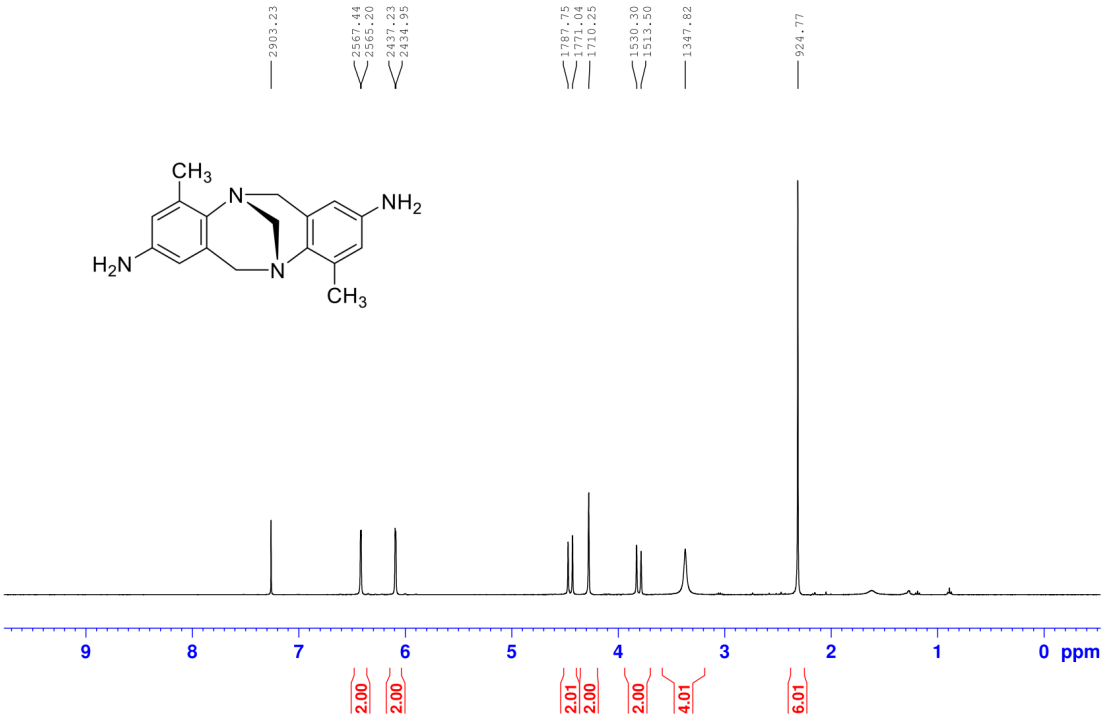

Fig. A2. ^{1}H NMR spectrum (400 MHz) of **2** in $CDCl_3$.

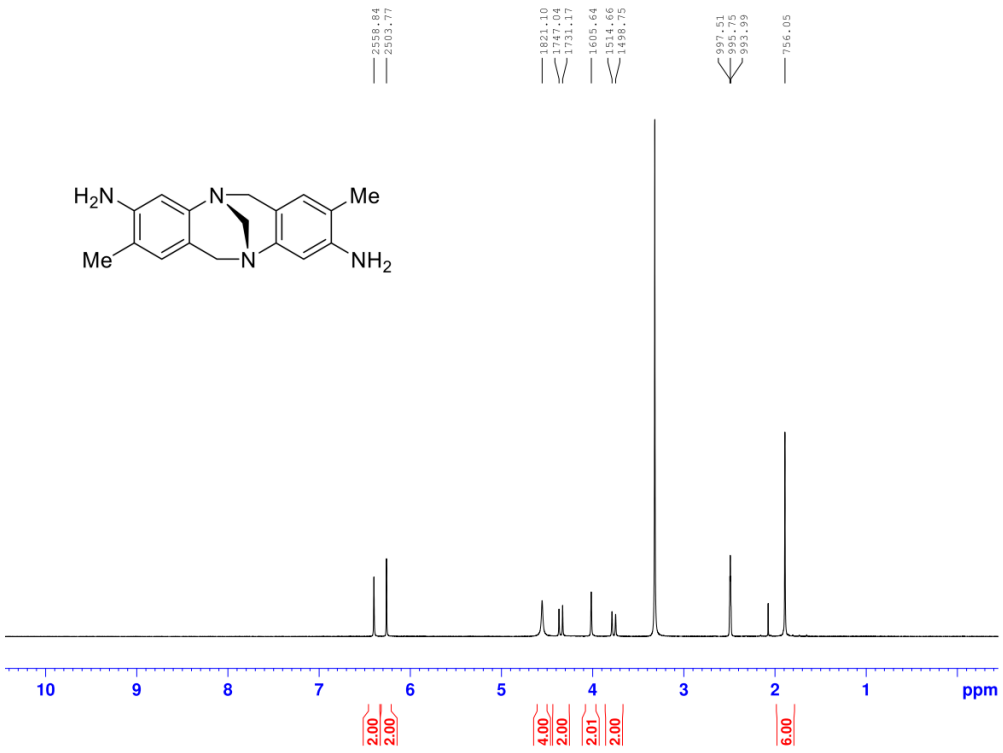

Fig. A3. ^{1}H NMR spectrum (400 MHz) of **3** in $CDCl_3$.

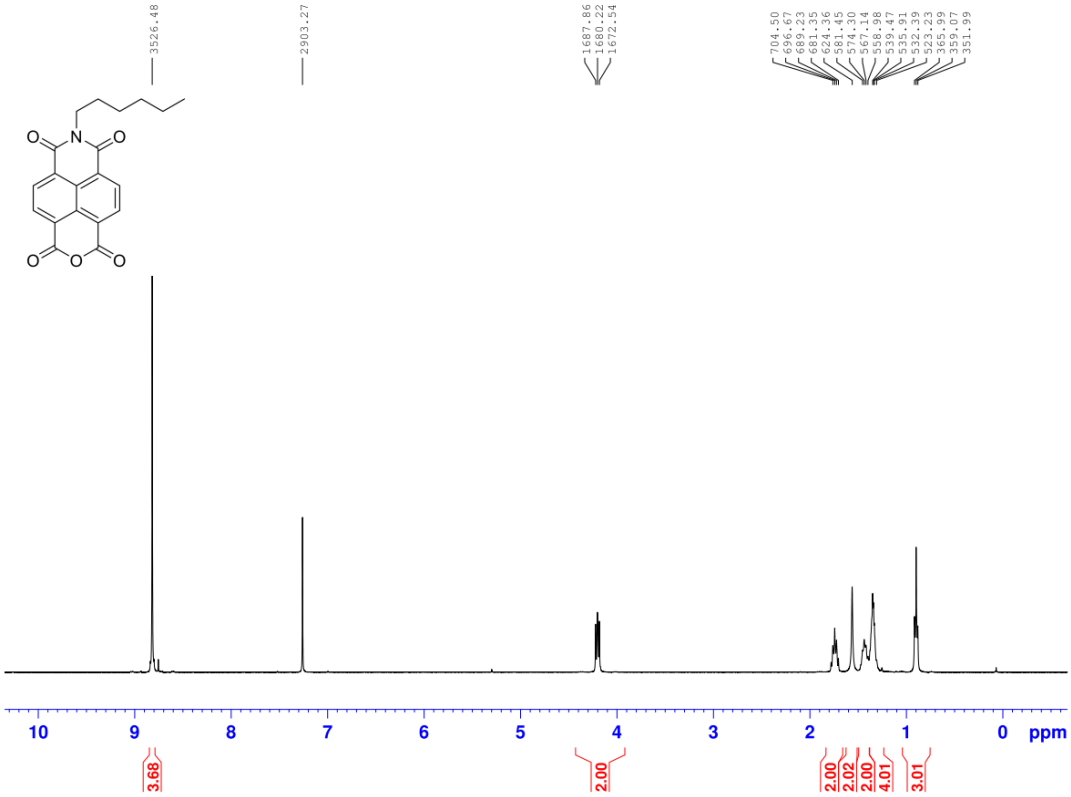

Fig. A4. ^{1}H NMR spectrum of **4** in $CDCl_3$.

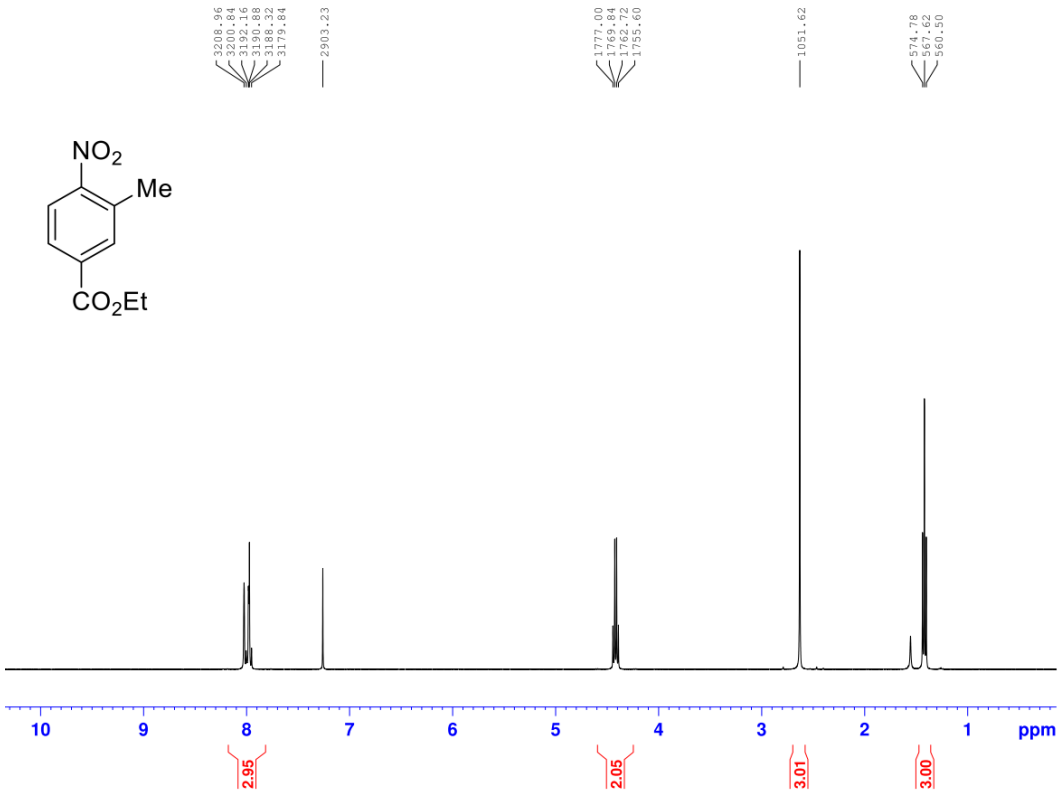

Fig. A5. ^{1}H NMR spectrum (400 MHz) of ethyl 3-methyl-4-nitrobenzoate in $CDCl_3$.

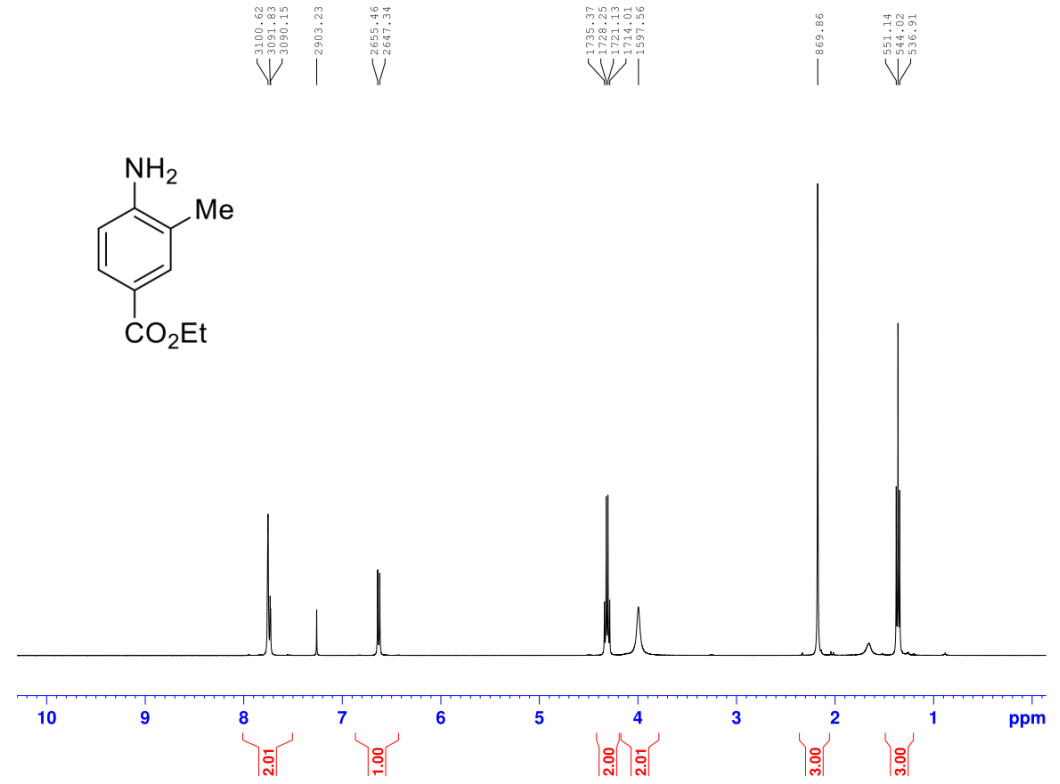

Fig. A6. ^{1}H NMR spectrum (400 MHz) of ethyl 4-amino-3-methylbenzoate in $CDCl_3$.

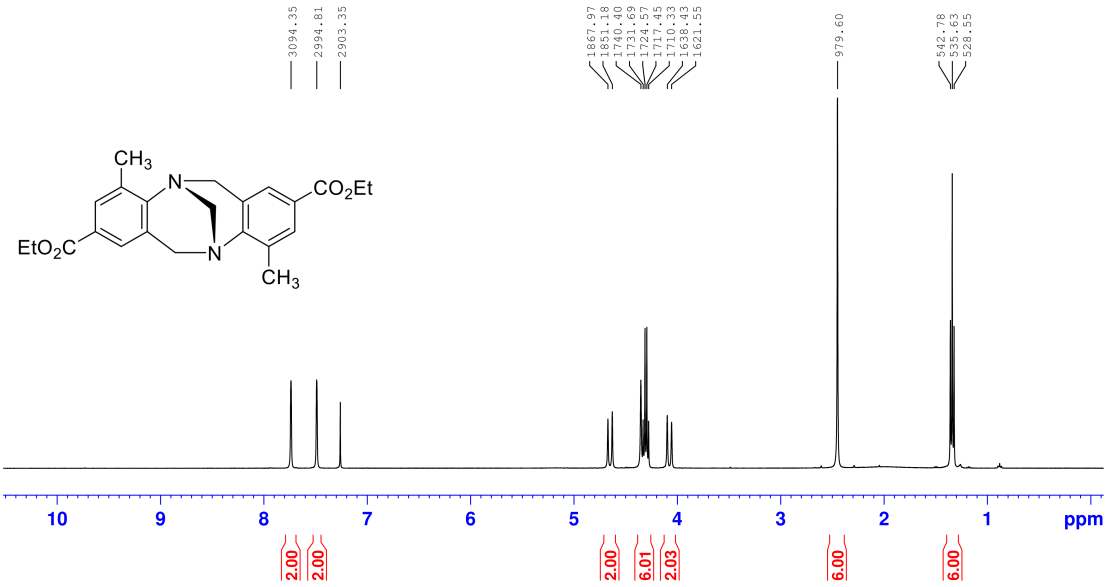

Fig. A7. ^{1}H NMR spectrum (400 MHz) of **2** in $CDCl_3$.

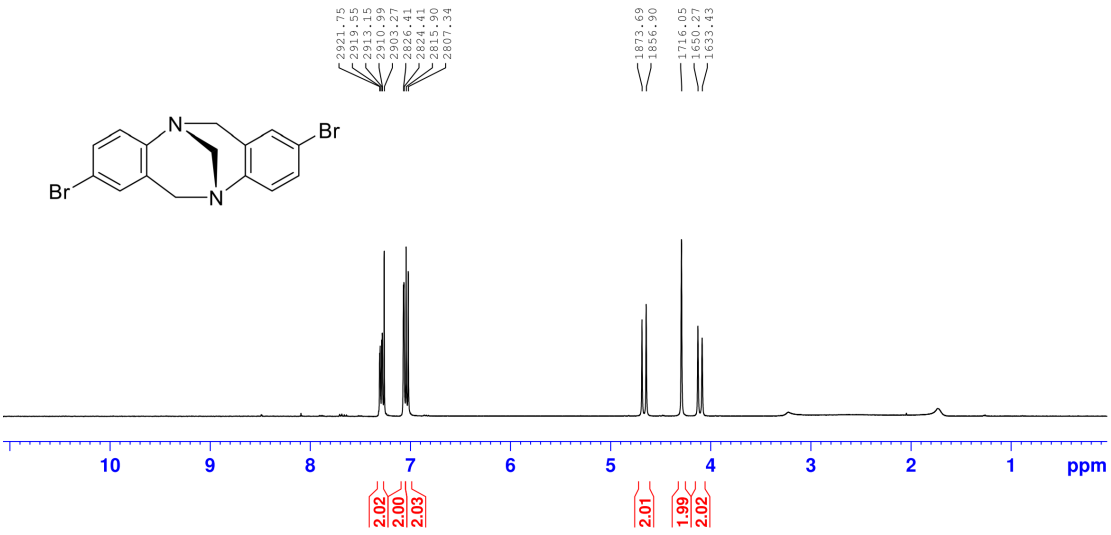

Fig. A8. ^{1}H NMR spectrum (400 MHz) of **4** in $CDCl_3$.

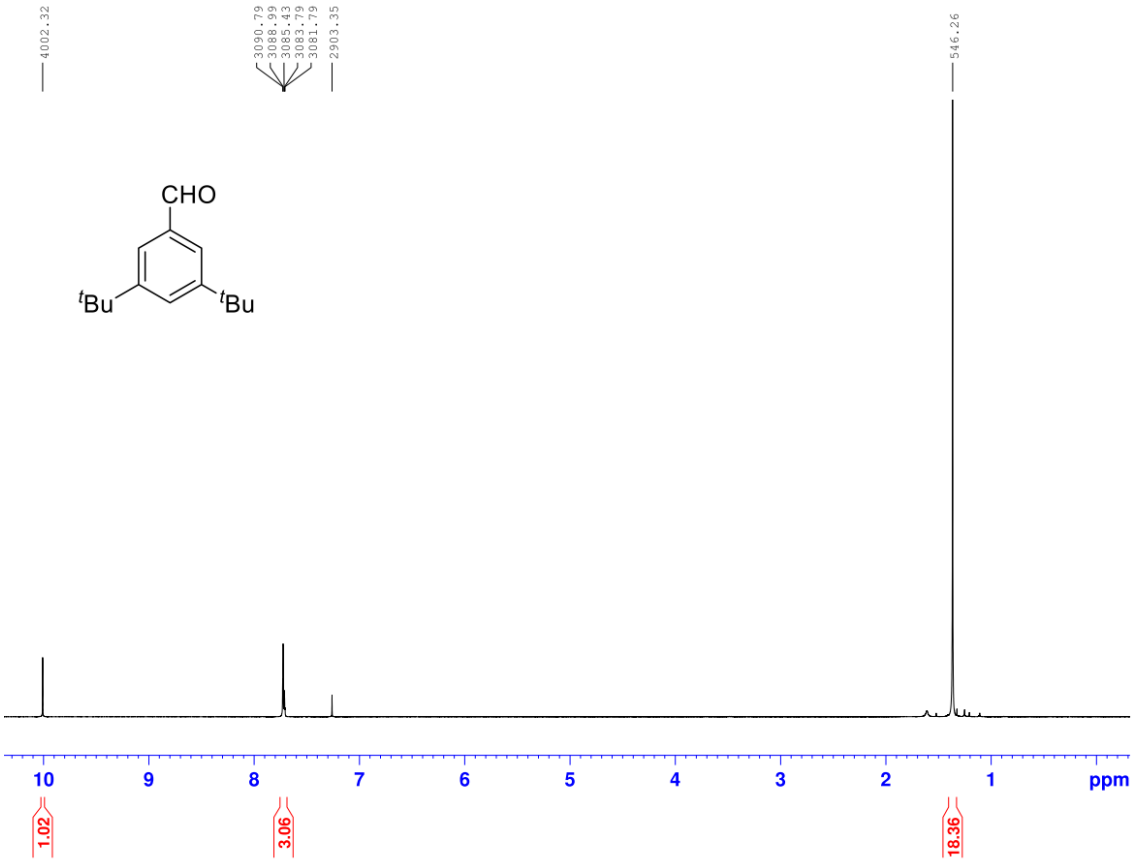

Fig. A9. ^{1}H NMR spectrum (400 MHz) of 3,5-di-*tert*-butylphenylbenzaldehyde in $CDCl_3$.

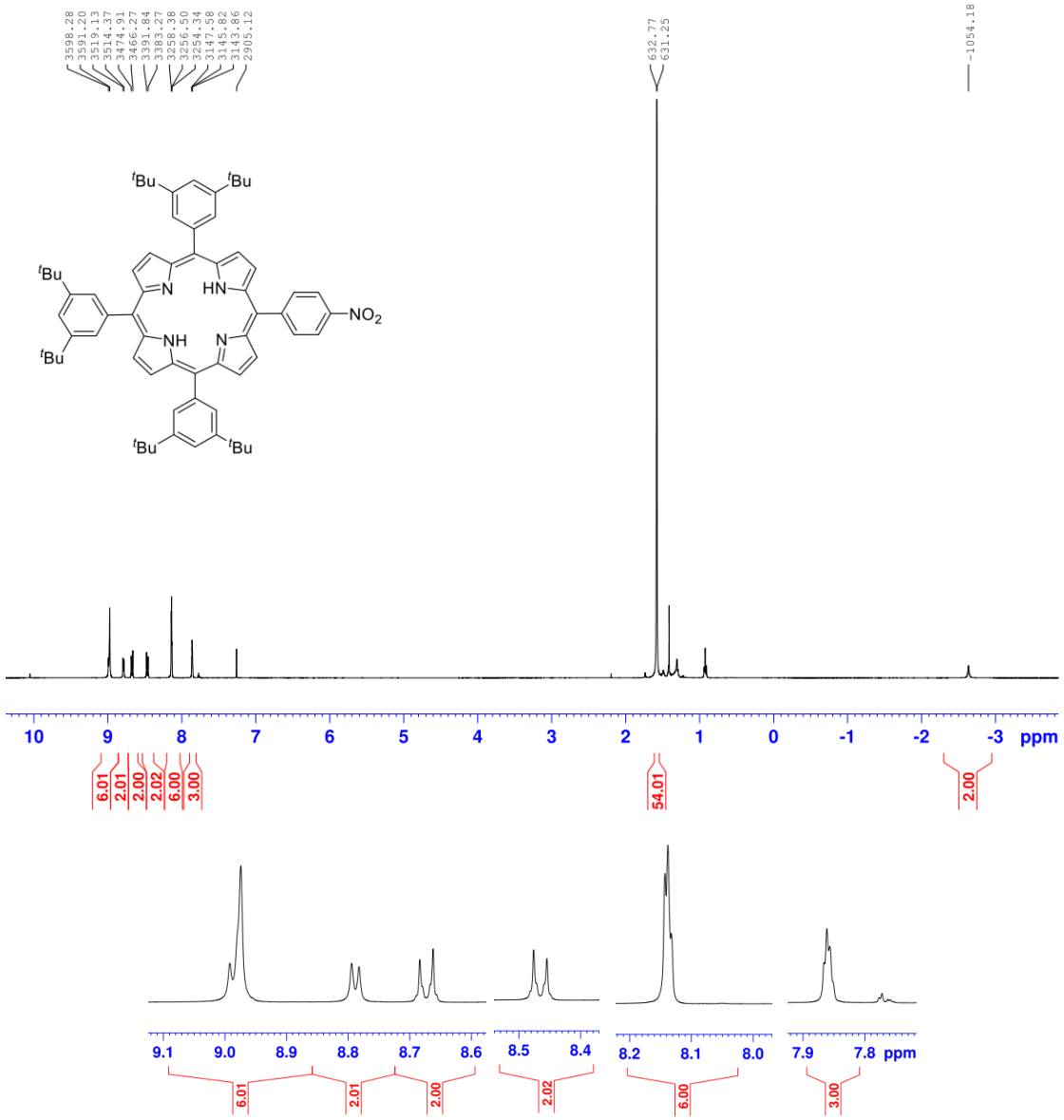

Fig. A8. ^{1}H NMR spectrum (400 MHz) of **2** in $CDCl_3$.

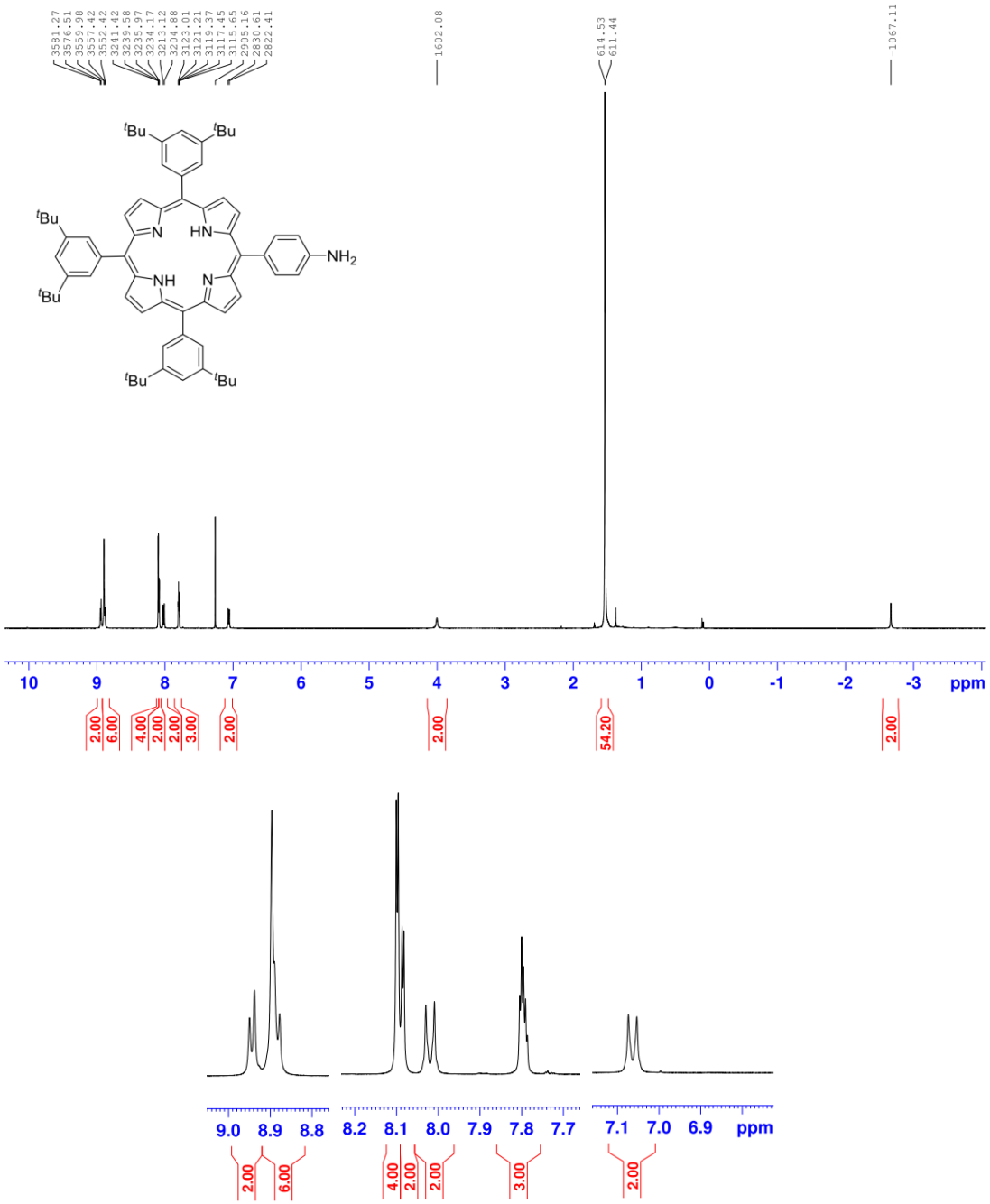

Fig. A9. ^{1}H NMR spectrum (400 MHz) of **3** in $CDCl_3$.

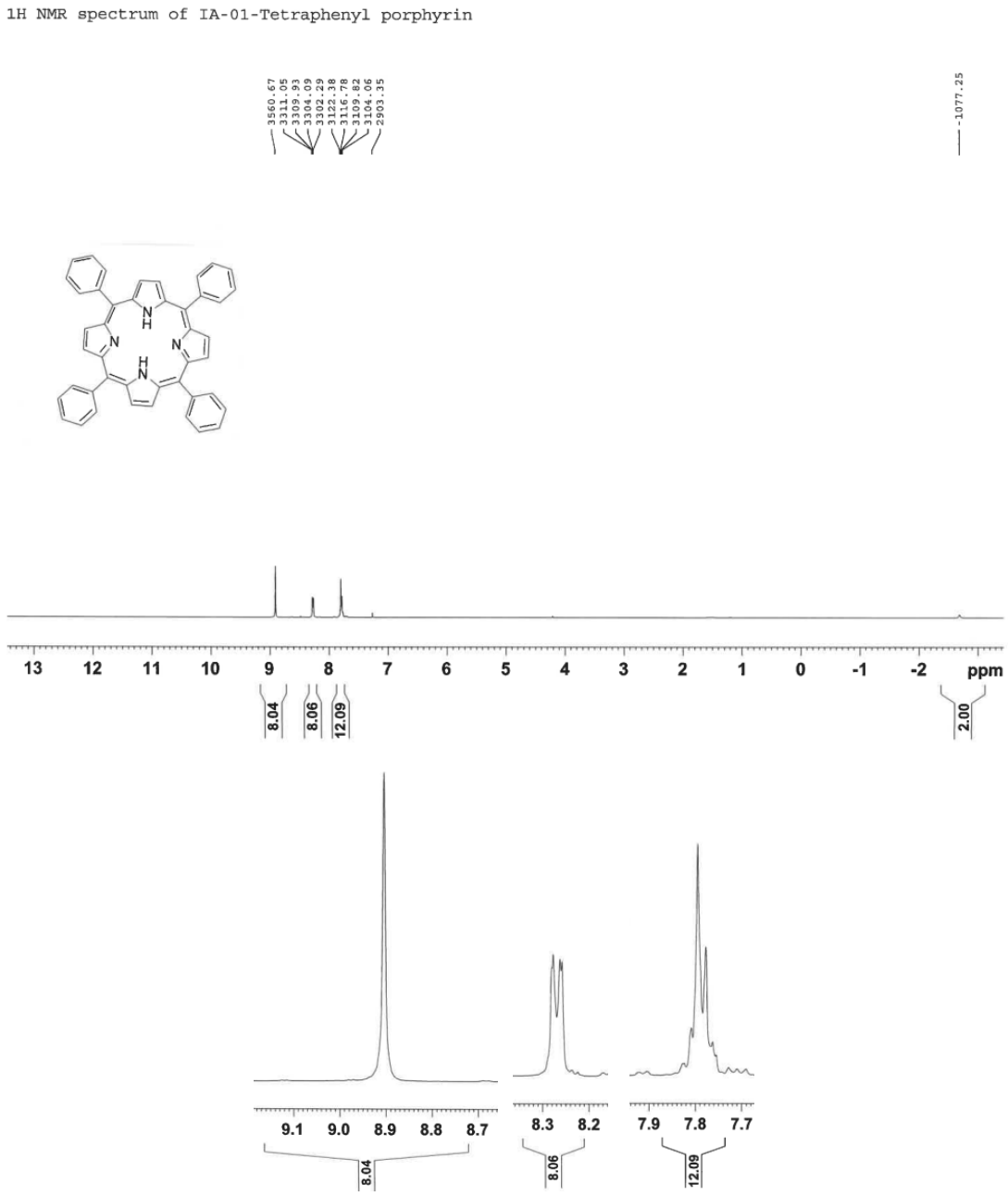

Fig. A10. ^{1}H NMR spectrum (400 MHz) of **S13** in $CDCl_3$.

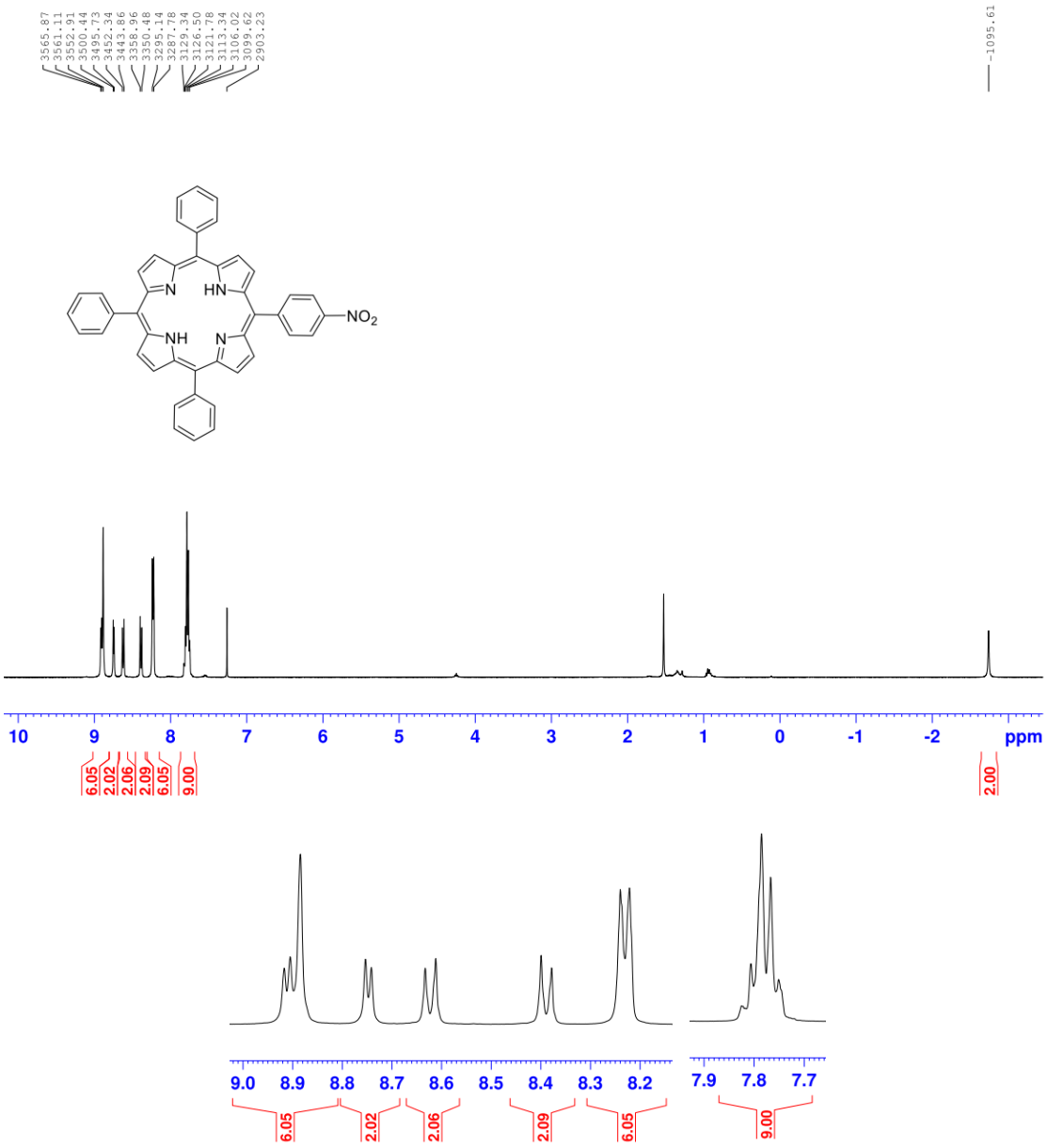

Fig. A11. ^{1}H NMR spectrum (400 MHz) of **S14**, in $CDCl_3$.

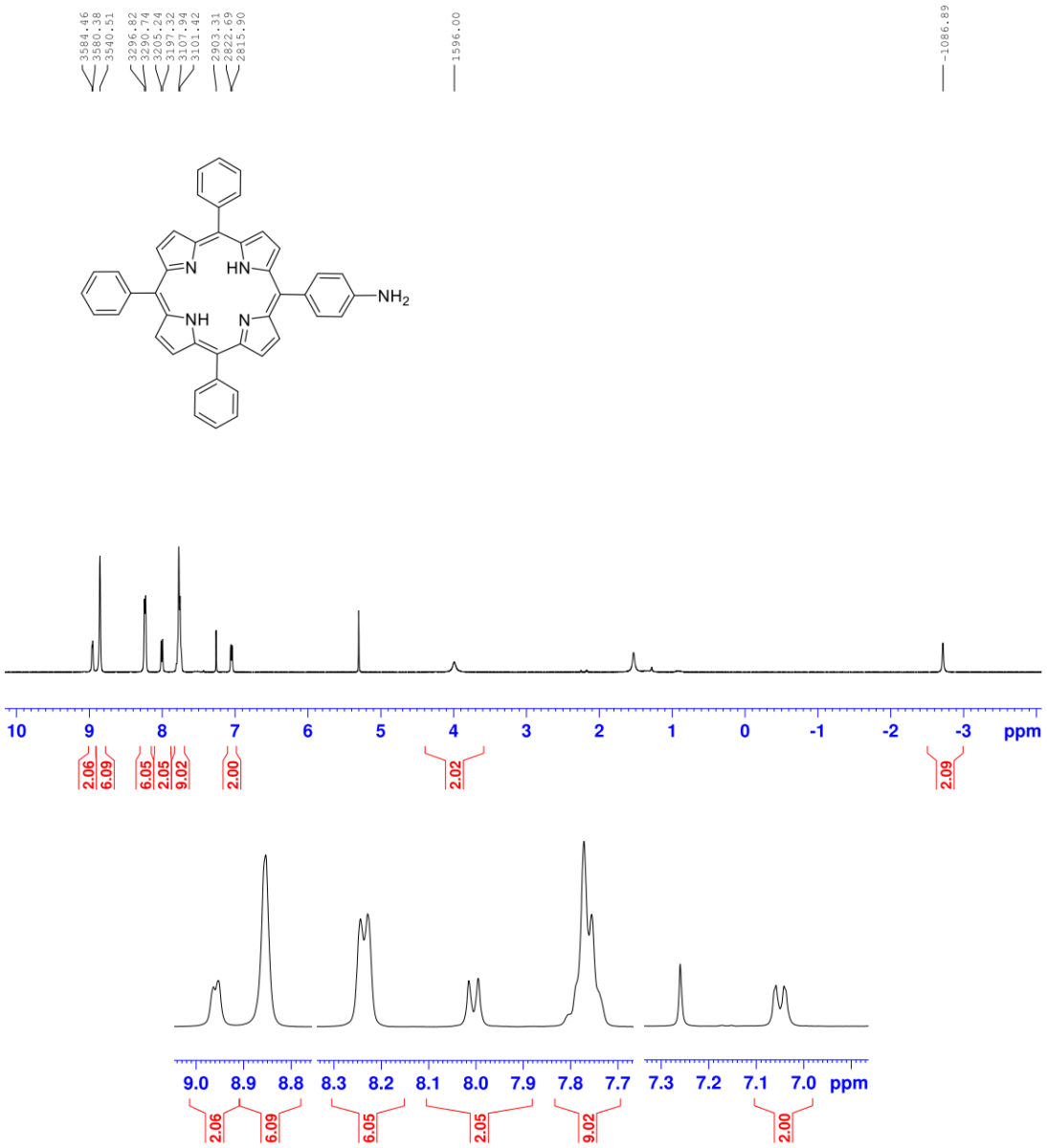

Fig. A12. ^{1}H NMR spectrum (400 MHz) of **7** in $CDCl_3$.

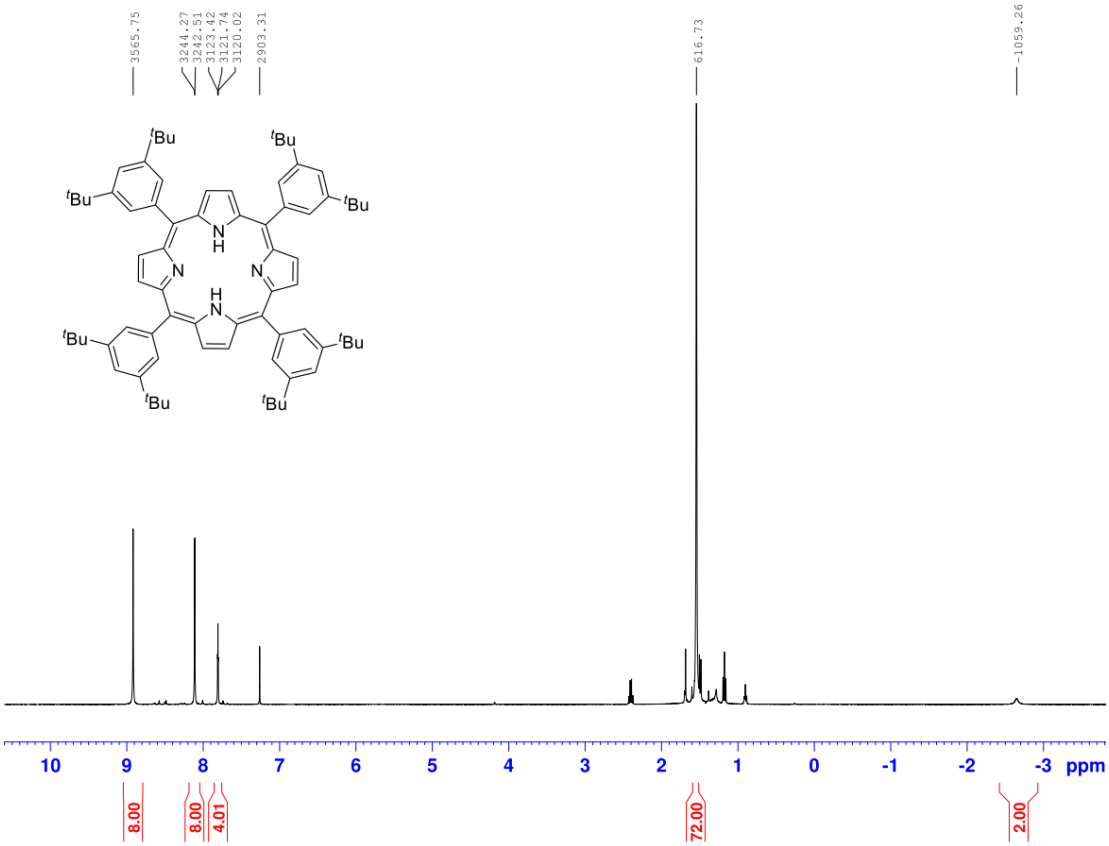

Fig. A13. ^{1}H NMR spectrum (400 MHz) of **S15** in $CDCl_3$.

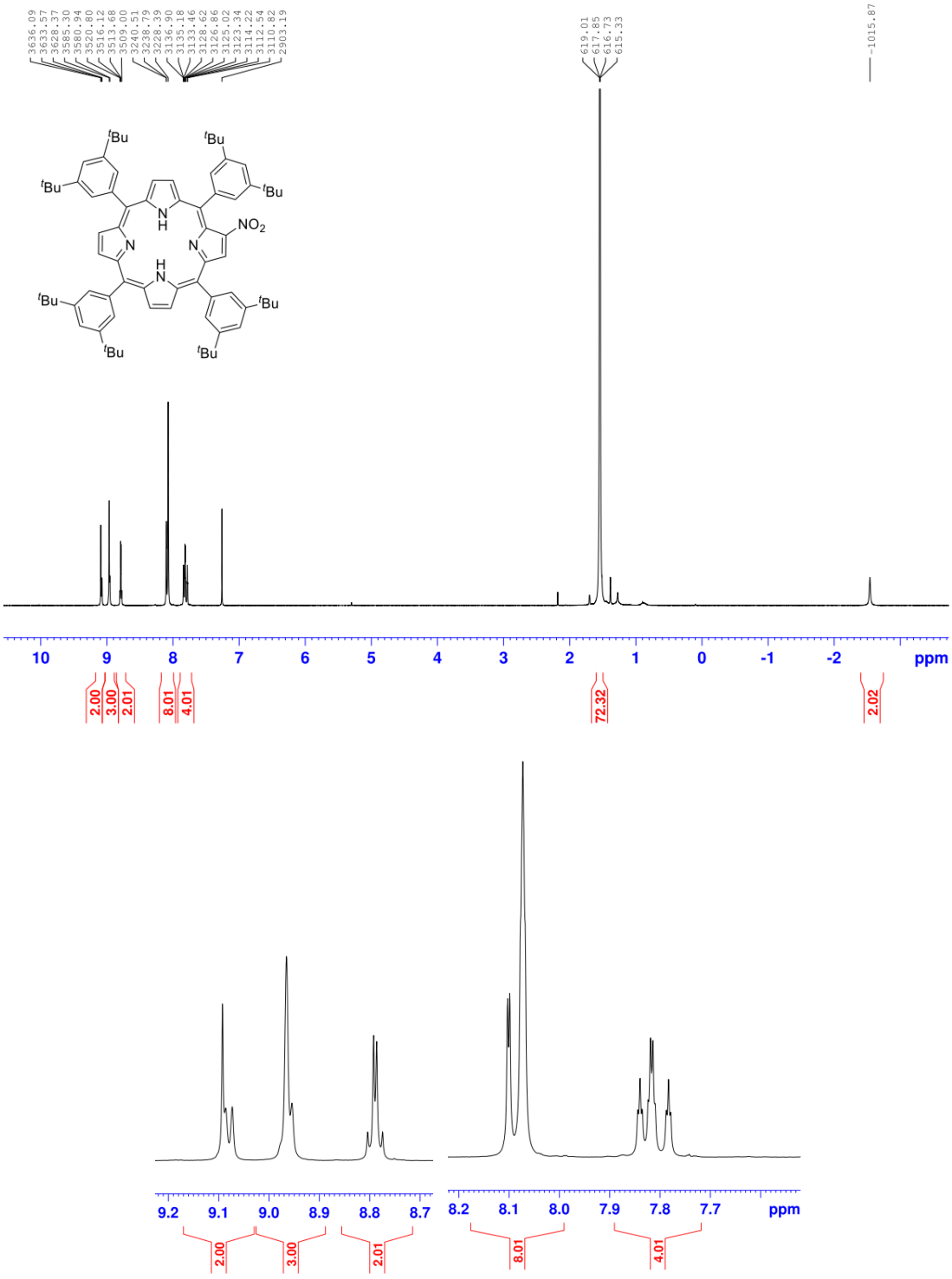

Fig. A14. ^{1}H NMR spectrum (400 MHz) of **S18** in $CDCl_3$.

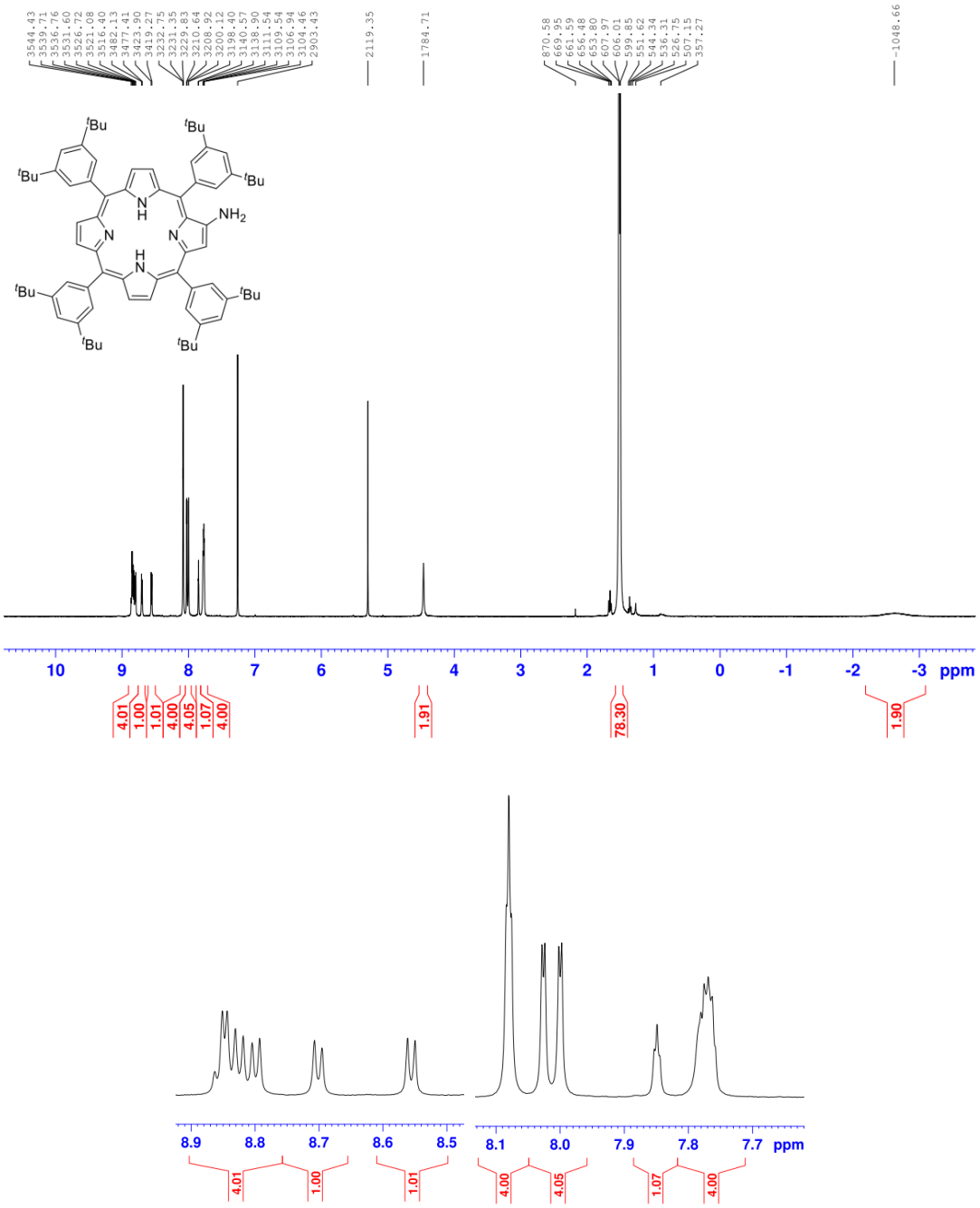

Fig. A15. ^{1}H NMR spectrum (400 MHz) of **10** in $CDCl_3$.